# SEDIMENT AND EROSION DESIGN GUIDE

Prepared for

Albuquerque Metropolitan Arroyo
Flood Control Authority
(AMAFCA)

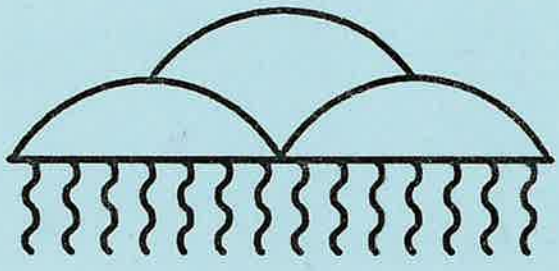

Prepared by

Robert A. Mussetter
Peter F. Lagasse
Michael D. Harvey

Resource Consultants & Engineers, Inc.
3665 John F. Kennedy Parkway
Building 2, Suite 300
P.O. Box 270460
Fort Collins, Colorado 80527

Clifford E. Anderson
Contributing Editor for AMAFCA

RCE Ref. No. 90-560

November, 1994

RCE RESOURCE CONSULTANTS & ENGINEERS, INC.
A Division of Ayres Associates

## TABLE OF CONTENTS

## LIST OF FIGURES

## LIST OF TABLES

## CONSTANTS AND CONVERSIONS

mm = ft * 304.8 = in * 25.38

Unit Weight of Water ($\gamma_w$) = 62.4 lbs/ft$^3$

Density of Water ($\rho_w$) = 1.94 slugs/ft$^3$

Specific Gravity of Sediment ($S_G$) ≈ 2.65 (Quartz)

Sediment Porosity (in-situ) ($\eta$) ≈ 0.4 at arroyo bed

Solid Unit Weight of Sediment ($\gamma_s$) $= S_G\gamma_W = 62.4S_G$

$\approx 165.36$ lb/ft$^3$ (Quartz) $= 2.65\ \gamma_w$

Bulked Unit Weight of Sediment (dry) $= (1-\eta)\ \gamma_s$

$\approx 100$ lb/ft$^3$ ($\eta = 0.395$)

Sediment Yield: 1 ac-ft/mi$^2$ (bulked) ≈ 3.4 tons/ac ($\eta = 0.395$)

Sediment Transport:

1 cfs ≈ $43.2\gamma_s$ tons/day

**Concentration by volume ($C_v$)** $= \left(\dfrac{V_s}{V_w + V_s}\right) * 10^6$

**Concentration by weight ($C_w$)** $= \left(\dfrac{W_s}{W_w + W_s}\right)10^6 = \left(\dfrac{S_g V_s}{V_w + S_G\ V_s}\right)10^6$

$$C_v = \frac{C_w}{S_G - C_W\ (S_G - 1)} \quad or \quad C_w = \frac{S_G\ C_v}{1 + C_v\ (S_G - 1)}$$

**Bulking Factor (BF)** $= \dfrac{V_w + V_s}{V_w} = 1/(1-C_v)$

**Fluid density ($\rho_m$)** $= \rho_o\ [1 + (S_G - 1)C_v]$

# 1.0 INTRODUCTION

Development in the Albuquerque metropolitan area, where arroyos are the primary conduit for passage of overland runoff and sediment derived from their watersheds, pose complex problems for planning and regulatory agencies and developers. Due to the dynamic nature of arroyos, it is imperative that appropriate steps be taken to protect adjacent structures and facilities from damage due to flooding and erosion. Lining of the arroyos with nonerosive or erosion-resistant material is a common protection method; however, the cost associated with this "hard lining," in terms of both construction and maintenance costs, as well as degradation of the natural environment, may be unacceptable. The Albuquerque Metropolitan Arroyo Flood Control Authority (AMAFCA) recognizes that some arroyos within their area of concern should remain in a natural or naturalistic condition to protect the local environment, provide safe arroyo conditions, and meet policy goals of other governmental agencies. By use of setbacks and selective stabilization, natural and naturalistic arroyos and watercourses can provide protection to adjacent property similar to that provided by lined arroyos and channels.

## 1.1 Purpose and Scope of Manual

The purpose of this manual is to provide guidance for the analysis of sediment areas and arroyos in the Albuquerque metropolitan area for use in establishing an erosion limit line. The erosion limit line would have a low possibility of being disturbed by erosion, scour, or meandering of a natural (unlined) arroyo by any storm up to and including the 100-year storm occurring at any time during a 30-year period. For purposes of this Design Guide, the erosion limit line is referred to as the Prudent Line.

The manual also contains criteria for placement of erosion barriers that may be incorporated with the Prudent Line to accomplish the dual goals of maintaining natural or naturalistic arroyos while protecting adjacent property. This Design Guide establishes simplified procedures for use by public agencies and private engineers when establishing prudent limits and erosion barriers. The Guide is accompanied by a set of computational modules (PC-based programs or spreadsheets) to support critical elements of the analyses.

## 1.2 Design Considerations

1.2.1 Hydrologic Uncertainty and Risk. The concepts of hydrologic uncertainty and risk are useful in establishing the location of the Prudent Line within which development should not occur due to erosion and flooding considerations. It is seldom practical to provide absolute protection against the maximum probable flood. It is, therefore, necessary to accept some degree of risk. The problem, then, is one of relating the Prudent Line to an acceptable degree of risk. In the hydrologic sense, risk is normally associated with the return period (or recurrence interval) of an event that may result in erosion or flooding within a given arroyo or watercourse.

The National Flood Insurance Program (NFIP) establishes the 100-year flood as the minimum level of risk that is acceptable when considering potential impacts due to flooding. With reference to **Figure 1.1**, the use of the 100-year event as the level of acceptable risk implies an approximately 74 percent chance that the event will not occur in a 30-year period. Conversely, this implies a risk of about 26 percent that the event will occur within a 30-year period.

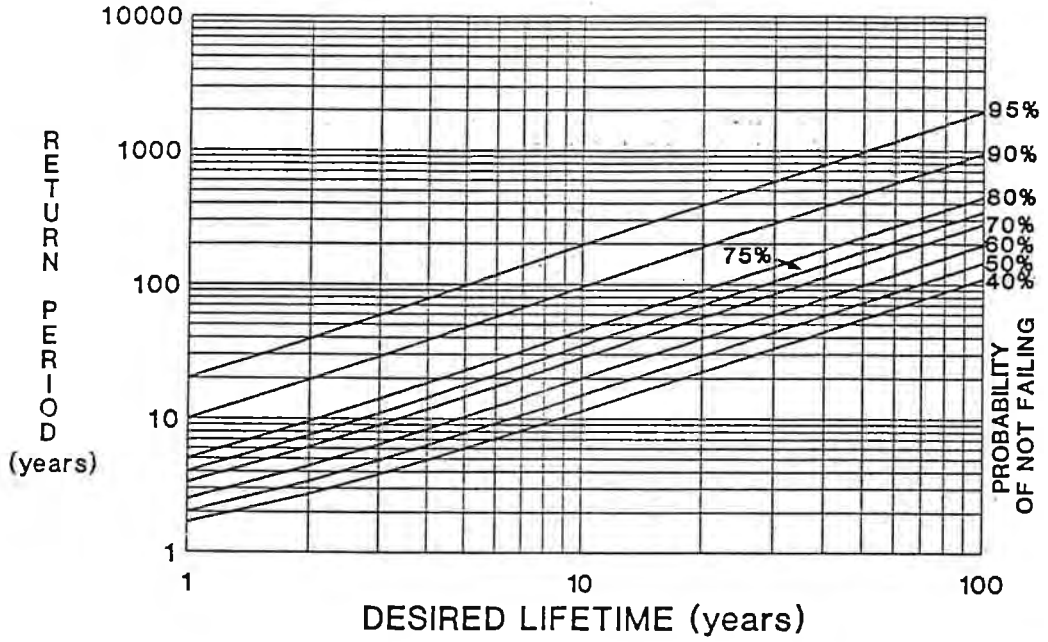


Figure 1.1. Calculated risk diagram.

While damages due to flooding are generally associated with a single, short-term event, the impacts of erosion can also be cumulative over the long term. Consequently, one must assess the erosion potential not only of a single event, such as a 100-year flood, but also the cumulative impact of a series of smaller flows. One approach to evaluating long-term erosion impacts is to develop a representative annual storm and extrapolate the effect of that storm through time. This concept is similar to the geomorphic concept of the dominant or channel-forming discharge. For adjusted perennial streams the dominant discharge is commonly assumed to be approximately the mean annual flood (Wolman and Miller, 1960). The dominant discharge for ephemeral streams, such as those in the Albuquerque area can be substantially larger. For purposes of analyzing the long-term erosion potential, the representative annual event can be more accurately defined by considering individual storm events independently and weighting the effect of each based on their probability of occurrence. This is accomplished by integrating the flow duration curve over discrete intervals resulting in the following equation;

$$Y_m = .015Y_{100} + .015Y_{50} + .04Y_{25} + .08Y_{10} + .2Y_5 + .4Y_2 \quad (1.1)$$

where $Y_m$ is the magnitude of the average annual event (i.e., runoff volume, sediment yield) and $Y_i$ is the magnitude of the event for the 2-, 5-, 10-, 25-, 50-, and 100-year return period flood. (This relationship is discussed in more detail in Chapter 4). The representative annual event, thus defined, is then used as the basis for estimating the long-term erosion potential.

1.2.2 Arroyo Processes - A General Statement of the Problem. Arroyos (or gullies) are ephemeral flow stream channels characterized by steeply sloping or vertical banks of fine sedimentary material and flat, generally sandy beds (Fairbridge, 1968). The American Geological Institute Glossary (1972) defines an arroyo as "a term applied in the arid and semiarid regions of southwestern U.S. to the deep, flat-floored channel or gully of an ephemeral stream or of an intermittent stream usually with vertical or steeply cut banks of unconsolidated material at least 60 centimeters high, that is usually dry, but may be transformed into a temporary water course or short lived torrent after heavy rains." This definition contains most of the elements of the arroyo problem in the southwest;

1. Arroyos occur at many different scales and range in size from small, gully-like features to major channels such as the Rio Puerco (Schumm et al., 1984).

2. Arroyos are incised channels and as such their morphologic, erosional (vertical and lateral), depositional and sediment transport characteristics are temporally and spatially variable and will change (evolve) systematically through time (Schumm et al., 1984).

3. Arroyo processes are episodic; therefore, the evolution of an arroyo system to an equilibrium form will take longer than is the case for channels in more humid regions. This is because arroyos are dependent on the stochastic distribution of runoff-producing events (Schumm and Gellis, 1989; Gellis et al., 1991).

4. Arroyos may never develop an equilibrium form (Thornes, 1976). In an ephemeral flow system, the channel-forming processes are not the product of continuous interaction between relatively frequent flows and channel boundary sediments (Wolman and Miller, 1960); rather, channel form and process are driven by relatively infrequent flood flows (Baker, 1977).

The causes for arroyo development were reviewed by Cooke and Reeves (1976). They concluded that for many arroyos, the initial cause of erosion was the development of roads and trails or other activities that confined the flows and permitted incision to occur. However, cycles of arroyo incision and backfilling have occurred in the past, perhaps as a result of climate change (Love, 1979) or the exceedance of geomorphic thresholds (Schumm and Hadley, 1957; Schumm, 1973; 1977).

The evolution of most arroyos follows a trend that eventually leads to the development of a relatively stable condition. During the development of this relatively stable condition, lateral and vertical erosion can occur very rapidly in response to either a single large storm event or a series of smaller storms, endangering adjacent property and delivering large quantities of sediment to downstream reaches. Even after development of the relatively stable condition, bank erosion and lateral migration may continue. The stages of evolution include: initiation, headward migration, channel widening, channel slope reduction, reduction of bank angles, deposition of sediment, and establishment of vegetation. Small arroyos may eventually be filled and obliterated. Large arroyos tend to form a new floodplain at a lower elevation than the pre-incision level (Harvey et al., 1985). The typical evolutionary sequence is illustrated in **Figures 1.2 and 1.3**.

The consequences of arroyo development and evolution can be severe. Incision can lead to the failure and loss of bridge crossings and damage to utility crossings (Shen et al., 1981). Incision-induced channel widening leads to land loss and damage to channel-margin structures. Channel erosion as a result of incision and widening of the primary arroyo, and erosion of tributaries as a result of base level lowering, both cause increased sediment delivery downstream that can lead to increased flooding frequency or loss of reservoir capacity (Schumm et al., 1984; Harvey and Watson, 1986). Arroyo incision leads to lowering of the water table and in turn threatens the survival of floodplain vegetation that might otherwise increase the resistance of the channel to lateral erosion (Gellis et al., 1991). A beneficial consequence of arroyo incision and development is the reduction in frequency of overbank flooding (Wilson, 1973).

Drainageways within AMAFCA's area of concern include examples of the entire range of the evolutionary cycle from small natural drainageways where the arroyo processes have not been initiated to large arroyos that have developed a new floodplain within the incised banks (e.g., Arroyo Calabacillas). The arroyo evolution process has not been initiated in many drainageways in undeveloped or sparsely developed areas. Because of the combined effects of land surface disturbance during construction and increased runoff and reduced sediment delivery from the watershed resulting from urbanization, it must be assumed for design purposes that the development process will create conditions where the threshold for arroyo incision will be exceeded. The evolutionary cycle illustrated in Figures 1.2 and 1.3 will thus be initiated. As this process occurs, significant deposition of material and loss of channel capacity can also be expected in local areas downstream resulting from the overload of sediment created by upstream erosion. In either the incision or aggrading condition, the potential for lateral instability of the arroyo channel may increase. Definition of the Prudent Line and design of protection measures must, therefore, consider the existing stage of the drainageway in the evolutionary cycle and the likely effect of the proposed development.

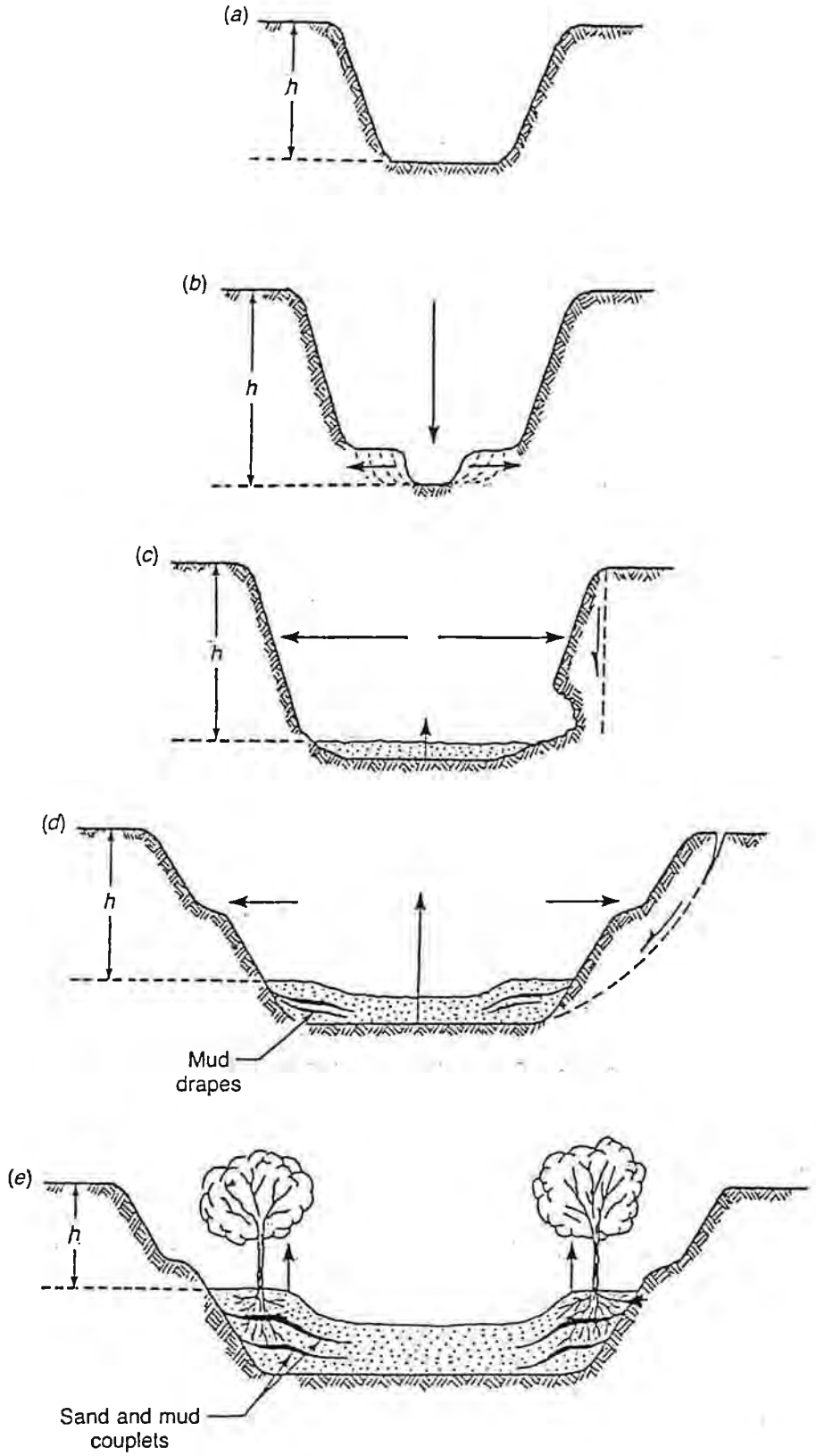


Figure 1.2. Five-stage arroyo evolution model (Schumm et al., 1984).

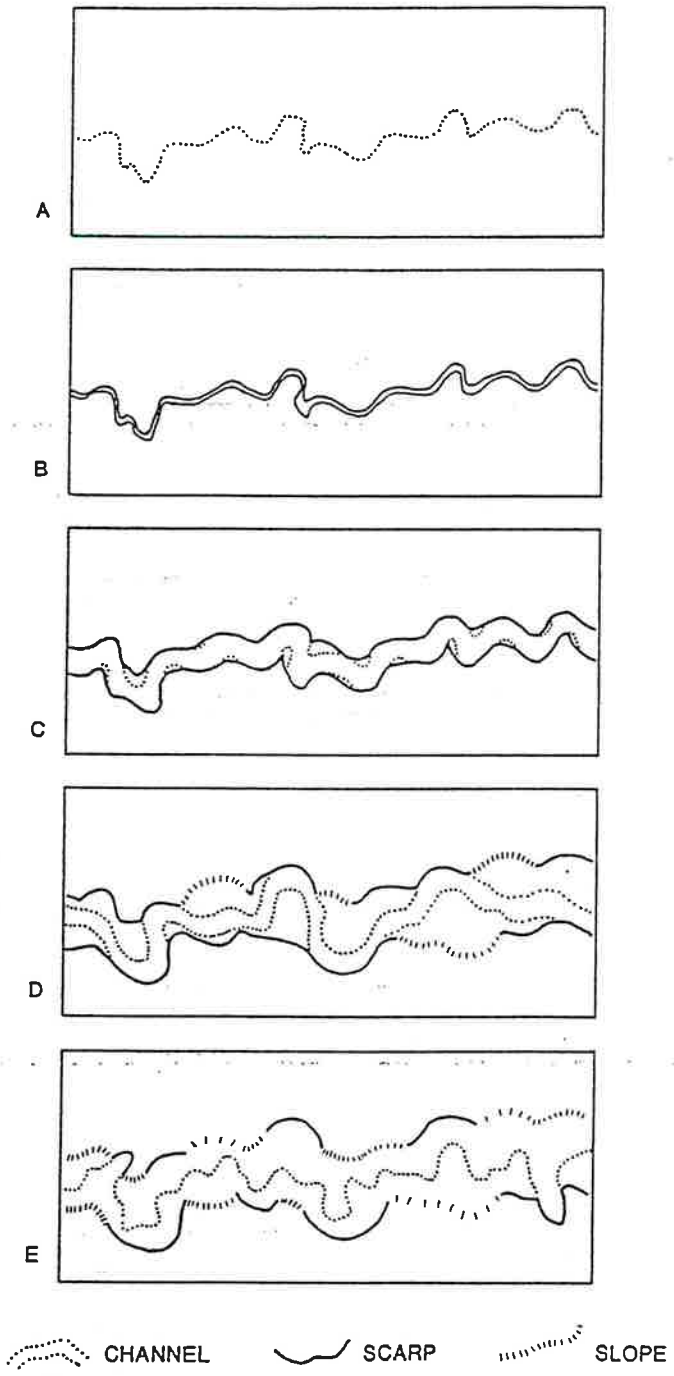


Figure 1.3. Hypothetical sequence of arroyo plan geometry evolution (Eilliott, 1979).

This Design Guide provides guidelines for evaluating the stage of existing arroyos within the evolutionary process and determining the impact of future development plans on the threshold conditions that may lead to arroyo development for those drainageways that are currently below the threshold. It also presents analysis techniques and guidelines for establishing the Prudent Line. Criteria are also presented for design of erosion control barriers (countermeasures) that may reduce the amount of land area required within the Prudent Line while maintaining the objective of a natural or naturalistic arroyo.

# 2.0 GEOMORPHOLOGY AND WATERSHED PROCESSES OF THE ALBUQUERQUE AREA

## 2.1 Geomorphology of the Albuquerque Basin

2.1.1 Albuquerque Basin Landforms. Within the Albuquerque Basin there are a number of landforms that have a bearing on channel stability and sediment yield. The landforms include: alluvial fans, pediments, alluvial terraces, floodplains of the major channels, caliche-capped mesa, and volcanic plateau.

### Alluvial Fans

Bull (1977) defined an alluvial fan as "a deposit whose surface forms a segment of a cone that radiates downslope from the point where the stream leaves the source area." Smaller fans with slopes in excess of 20 degrees have been referred to as alluvial cones, but they in fact fall within Bull's primary definition. In general, the fans are constructed by fluvial and mass-wasting processes (Lecce, 1990), and they occur in a very wide range of climatic zones; arid/semi-arid, humid-glacial, humid-temperate and humid-tropical (Kochel and Johnson, 1984). Alluvial fans are generally located along mountain fronts, and they may be coalesced and form bajadas (Eckis, 1928). Deposition on the fan is the result of rapid flow expansion rather than reduced slope (Reading, 1978). The thickness of fan deposits is variable and generally related to the type of base-level control; local control results in thin fans; whereas, tectonic control results in thick fans (Bull, 1977). Fans may be distinguished from other piedmont geomorphic features, such as pediments, by their thickness-length ratio (Doehring, 1970).

### Pediments

Pediments are defined as broad, flat or gently sloping, rock-floored erosion surfaces that are typically formed by fluvial processes in an arid or semiarid region. They are typically located at the base of an abrupt and receding mountain front or plateau escarpment, and underlain by bedrock that is generally mantled with a thin veneer of alluvial sediments that are derived from upslope erosion. The longitudinal profile of a pediment is generally slightly concave upward. The development of multiple pediment surfaces is generally the result of base-level lowering. Within the Albuquerque Basin, the best defined pediment surface is the Ortiz pediment of early Pleistocene age that has developed on the surface of the Santa Fe formation south of Tijeras Arroyo. High level pediment surfaces have been identified east of Tramway Road north of Tijeras Arroyo.

### Alluvial Terraces

Alluvial terraces are abandoned floodplains that were formed when the Rio Grande flowed at a higher elevation than at present. The surface of the terrace is no longer related to the modern hydrology of the river in that it is no longer inundated as frequently

as the active floodplain of the river. Topographically, the terrace consists of two parts: a tread which is the flat surface that represents the level of the former floodplain, and the scarp that is the steep slope that connects the tread to any surface standing at a lower elevation. The presence of a terrace always indicates that the river has downcut. The tread surface is generally underlain by alluvium of variable thickness. Well-developed terraces border the Rio Grande on both the east and west sides. The highest terrace is approximately 200 feet higher than the floodplain, an intermediate terrace is located about 100 feet above the floodplain, and a lower terrace is located about 50 feet above the floodplain.

Floodplains of the Major Channels

A floodplain is the surface of relatively smooth land adjacent to the river which has been constructed by the present river in its existing regimen and covered by water when the river overflows its banks. The floodplain is constructed of alluvium that is transported by the river. A river can only have one floodplain, but a number of former floodplain surfaces (terraces) can border the channel. Floodplains are located along the Rio Grande and along the floor of Tijeras Arroyo and the larger arroyos within the basin.

Caliche-Capped Mesa

The western margin of the Albuquerque Basin is composed of the Ceja Mesa. The mesa, a relatively flat-topped erosional landform, is underlain by sediments of the Santa Fe formation. The surface layers of the mesa are cemented with caliche that has formed a relatively erosion-resistent caprock.

Volcanic Plateau

Basalt sheets of Pleistocene age overlie sediments of the Santa Fe formation on the eastern margin of the Ceja Mesa. The basalt forms a very erosion-resistant caprock. Erosion of the plateau margins is due to sapping processes that are related to groundwater seepage. (Sapping is the process of erosion along the base of a cliff, wearing away the softer layers and allowing the rocks above to fall in large blocks.)

2.1.2 Four Quadrants in the Albuquerque Basin. The Albuquerque Basin can be divided informally into four quadrants on the basis of landscape components, channel characteristics and underlying geology. A convenient north-south dividing line is the Rio Grande, and an east-west dividing line is defined by I-40 to the west and Tijeras Arroyo to the east of the river (**Figure 2.1**). The four quadrants are discussed in the following sections.

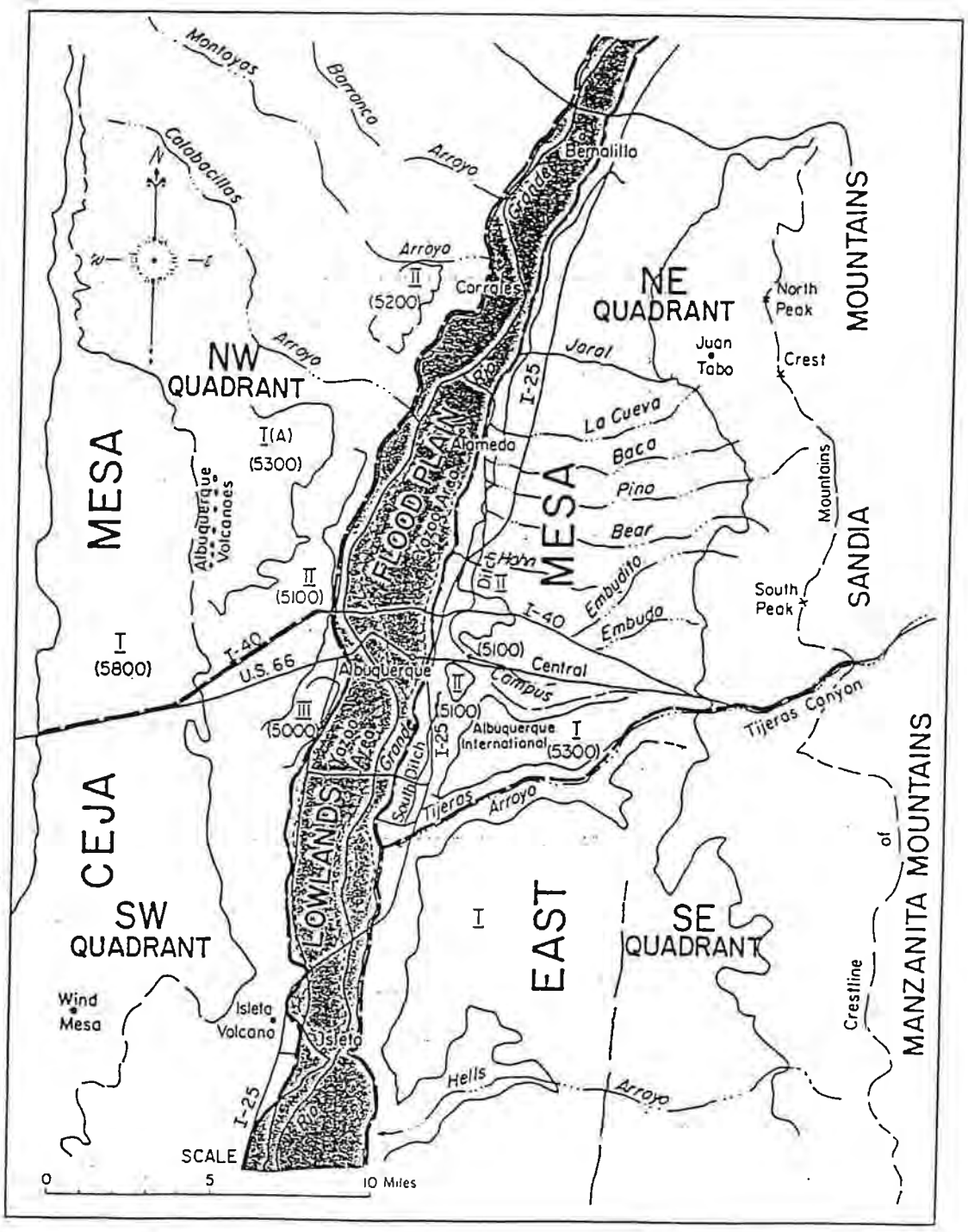


Figure 2.1. Physiographic map showing lowlands, mesas, and mountains.

Southeast Quadrant

The area of the southeast quadrant is that encompassed by Tijeras Arroyo in the north, Manzanita Mountains to the east, Rio Grande to the west, and Hell's Arroyo to the south. The quadrant lies within what has been termed the East Mesa (**Figure 2.1**), and is primarily underlain by the Santa Fe formation. Much of the surface of the mesa (locally referred to as the airport surface), especially above an elevation of about 5200 feet, is underlain by the caliche-cemented upper member of the Santa Fe formation that is generally referred to as the Ceja Member. The Ortiz pediment surface that is mantled with a relatively thin layer of sands and gravels is located in this quadrant as well (Kelley, 1977). A number of fluvial terraces ranging in elevation up to about 200 feet above the modern floodplain of the Rio Grande are located parallel to the river. These terraces are composed of fluvial sands and gravels.

The similarity in sediment composition among the Santa Fe formation, the Ortiz pediment gravels, and the fluvial terraces sometimes makes it difficult to distinguish among the sedimentary units. Topographic expression does help to distinguish the surfaces. Small, coarse-grained, steep alluvial fans (cones) have formed at the base of the Manzanita (a.k.a. Manzano) mountains. The fans grade into the mesa surfaces. Extensive areas of wind-deposited and wind-transported sand dunes are located within the quadrant. Some of the dunes may locally exceed 40 feet in height.

Within the AMAFCA area of interest, most of the channels that drain the Manzanita Mountains traverse the urbanized area of the mesa. As part of the development of the area, the channels have been converted into concrete-lined conduits. The smaller drainages that are associated with the small alluvial fans (cones) are generally located in areas that have yet to be targeted for development.

Northeast Quadrant

The northeast quadrant is bounded to the north by La Cueva Arroyo, to the east by the Sandia Mountains, to the west by the Rio Grande, and to the south by Tijeras Arroyo. The quadrant can be further subdivided into three roughly-parallel north or south trending units on the basis of geomorphic characteristics of the landscape, even though the entire quadrant is shown as part of the East Mesa (**Figure 2.1**). West of the Sandia Mountain front, the entire quadrant is underlain by the Santa Fe formation. The major geologic difference between the southeast and northeast quadrants is the absence of the caliche unit at the top of the Ceja Member in the latter quadrant (Hawley, 1978). The absence of the caliche layer may explain why the drainage density in the northeast quadrant is higher than that of the southeast quadrant (**Figure 2.1**).

The subdivisions of the quadrant from the mountain front to the west are:

1. Alluvial fan zone
2. Incised pediment zone
3. Depositional zone

The alluvial fan zone is located at the immediate mountain front. It is characterized by the presence of steep, relatively small alluvial fans that have built out onto the upper elevation areas of the mesa. The fans are composed of relatively coarse-grained sediments that are derived from weathering of the porphyritic granite. Sediment delivery to the fans is governed by the frequency of runoff-producing events on the hillslopes. However, sediment delivery to the mesa areas below the fans is dependent on the generation of flows on the fans because there is an almost unlimited reservoir of sediment within the fans. In general, the fans are located above the upper elevation of land development, but the developed areas have been subjected to flooding and sedimentation as a result of fan activity. For example, a series of small coalescing alluvial fans located in the vicinity of Villa Sandia Drive (Embudo Arroyo drainage basin) delivered significant quantities of sediment and water to developed land in the 1988 event. The discharges from the fans were intended to be conveyed to the head of a concrete-lined channel section by an earthen collector ditch that had been constructed to traverse the base of the fans. Significant sediment delivery during the runoff event led to the loss of channel capacity and overtopping of the earthen ditch prior to the flows reaching the concrete-lined section. Sediment delivery from the fans is an episodic process, but significant delivery can be expected in almost any event because of both the steepness of the fans and the considerable volume of sediment that is stored within the fans.

The incised pediment zone comprises the upper elevation areas of the Mesa and is located approximately between the mountain front and Tramway Road, the major north-south highway that traverses the East Mesa. The upper reaches of the major drainages, Embudo, Bear, Pino, and Domingo Baco Arroyos, are located within the zone. The major drainages have incised into the pediment surfaces. At the mountain front, the beds and lower banks of some of the channels are armored with large granitic boulders that represent lag deposits that are unlikely to be moved by anything less than the most extreme flows (e.g., PMF). In the downstream direction, the size of the bed sediments diminishes and the presence of lower bank armor becomes less frequent. Channel banks can be as high as 10 feet. There is abundant evidence of tension cracks in the banks and recent slab failures which indicate that bank erosion is occurring and a setback distance will be required for development. Within this zone, both channel incision and aggradation are prevalent in local areas. Aggradation occurs in low-energy zones (e.g., expansions, channel bends) downstream of significant sediment sources.

The depositional zone is located west of Tramway Road. Sediments derived from the upper watersheds and from channel erosion upstream of Tramway Road are

deposited in this zone. In many ways, the boundary between the two zones is similar to the intersection point on a fan-head trenched alluvial fan. Deposition of sediment as a result of the lack of flow confinement within well-defined channels leads to the formation of a braided or distributary type of channel network. Development of the zone has historically involved construction of a grid of roads that are oriented both across and down the topographic gradient. This pattern has the net effect of concentrating the flows, which leads to the development of incised channels. The development of the incised channels will lead eventually to the downslope displacement of the intersection point, thereby transferring the sedimentation zone towards the lower slopes. Older developments that are located on the terraces that border the Rio Grande may be adversely impacted by the downslope displacement of the intersection point.

Southwest Quadrant

The southwest quadrant is bounded to the north by I-40, to the south by the Isleta volcanic center, to the west by the eastern margin of the Ceja Mesa, and to the east by the Rio Grande. The surface of the Ceja Mesa slopes gently to the west, but the Santa Fe formation that underlies the mesa dips gently to the east (Kelley, 1977). The mesa surface is comprised of the Ceja Member, which is cemented with pedogenic caliche. Unlike the area around Tijeras Arroyo on the east side of the river, the Ceja Member in the southwest quadrant is composed primarily of sands and fine gravels. However, finer-grained facies (or layers) underlie the sandy gravels and are responsible for the relatively low permeability of the formation that has been responsible in part for the development of a badlands type of topography.

Base-level lowering as a result of Rio Grande incision has led to dissection of the Ceja Mesa perimeter and the development of a relatively high drainage density. The high drainage density implies that sediment yield should also be high (Schumm, 1977).

The dissected badland topography delivers discharges of sediment and water onto two major alluvial terraces that flank the Rio Grande. The higher terrace (Rio Rancho) is located at an elevation of about 200 feet above the floodplain of the modern river, and the lower terrace (Segundo Alto) is located at an elevation between 100 and 130 feet above the modern floodplain. A third narrow terrace (Primer Alto) is located about 60 feet above the modern floodplain and extends southward for about 6 miles. The terraces are composed of alluvial sediments that are easily eroded if flows become concentrated by development.

Northwest Quadrant

The northwest quadrant includes the drainage basin of the Blacks and Calabacillas Arroyos on the north, and is bounded to the south by I-40, to the west by the Albuquerque Volcanic field and Rio Puerco escarpment, and to the east by the Rio Grande. The quadrant is primarily underlain by the Santa Fe formation. However,

southeast of the Calabacillas Arroyo the Santa Fe formation is overlain by the late Pleistocene basaltic sheets that emanated from the seven volcanic centers and form what is referred to as the Volcanic Escarpment. The basalt acts as a caprock that overlies the erodible sediments of the Santa Fe formation.

The large arroyos, such as Calabacillas and its tributary Black Arroyo, drain areas of Santa Fe formation that are unaffected by the volcanic field. They are incised, and as such have eroding banks. Grade-control structures are being emplaced in the channels to prevent further incision that may occur as a result of the construction of flood detention structures. Significant quantities of wind-transported sediment have accumulated in the bed of the arroyos.

To the south of Calabacillas Arroyo are a number of channels (Piedras Marcadas, Boca Negra) that drain the volcanic field. The channels on the volcanic field are relatively poorly defined. They traverse and erode areas of wind-blown sediments. Where the discharges traverse the Volcano Cliffs, the channels are armored with very large angular blocks of basalt. Erosion of the jointed basalt is probably due to the sapping processes. The less resistant underlying sediments of the Santa Fe formation are eroded by seepage forces, thereby leaving the more competent basalt cantilevered. Failure of the basalt takes place along the vertical joints. The presence of petroglyphs on the failed blocks indicates that cliff retreat occurs slowly. Downstream of the Volcano Cliffs, the channels traverse more erodible materials and wherever there is flow concentration in this area, the channels have incised and are widening as a result of the incision. The channels traverse the same major terraces that were described for the southwest quadrant. The lower elevation Primer Alto terrace is not present in the northwest quadrant.

## 2.2 Rainfall-Runoff Processes

Arroyos in the Albuquerque area are ephemeral, flowing only in response to specific storm events. Analysis of arroyo stability must therefore consider the runoff characteristics of the individual storms. Applications of the analysis procedures discussed in this Design Guide require estimates of the hydrographs associated with a range of return period storm events. Since the lateral and vertical response of the arroyo channels to these storm events is related to the volume of sediment that can be carried by the flows, estimates of the duration of the flows as well as their magnitude are required.

Section 22.2, Hydrology, of the Development Process Manual (DPM 22.2) for the City of Albuquerque (City of Albuquerque, 1993) describes acceptable procedures and current policy of the local agencies regarding estimation of storm runoff hydrographs for streams and arroyos in the Albuquerque area. Prior to initiating a Prudent Line analysis, hydrographs for a range of return period storms including the 2-, 5-, 10-, 25-, 50-, and 100-year events must be developed using the procedures in DPM 22.2. The hydrograph analysis should consider watershed conditions applicable to the time period over which the Prudent Line protection is desired. Input values for the hydrograph analysis must therefore reflect changes in impervious area and runoff patterns associated with anticipated development in the watershed during that time period.

## 2.3 Sediment Yield

The total sediment yield at a specific location along an arroyo consists of sediment delivered to the channel from overland areas and sediment eroded from the arroyo boundaries by the flowing water. The most accurate method of estimating the quantity of sediment eroded from the channel boundary involves bed material transport capacity computations. Appropriate procedures for performing these computations are presented in Chapter 3. The amount of sediment derived from overland areas is estimated using empirical relationships involving various parameters describing the characteristics and condition of the watershed. **For purposes of this Design Guide, watershed sediment yield computations are performed primarily to estimate the fine sediment (or wash load) component of the total sediment yield.** (See Section 3.3 for a discussion of the various modes of sediment transport.)

As discussed in Chapter 1, the design criteria for a Prudent Line analysis considers the potential effect of a single 100-year storm event occurring at any time during a 30-year period. The effects of the 100-year storm can be evaluated using the 100-year storm hydrograph and the hydraulic and sediment transport analysis procedures presented in the remainder of the Design Guide. The cumulative effects of storms occurring over a 30-year period are estimated by evaluating the effects of the range of return period storms from the 2-year through the 100-year and weighting the individual storm effects based on the probability of occurrence of each storm. The details of the probability weighting procedure are discussed in Chapter 4.

2.3.1 Relationship of Sediment Yield to Other Analysis. Delivery of sediment from overland areas to the arroyo channels can be a significant consideration in planning and designing erosion and flood protection measures. Urbanization tends to increase runoff and decrease sediment yield which increases the tendency of arroyos to incise and erode laterally. This potentially destabilizing influence can result in a net increase in the amount of sediment delivered to downstream reaches. Conversely, disturbance of the land surface during construction or the absence of natural erosion protection in the watershed area can significantly increase the quantity of sediment reaching the arroyo compared to natural conditions. In either case, the capacity and effectiveness of flood detention structures can be substantially reduced and the lateral erosion potential of the arroyo can increase.

2.3.2 Description of Sediment Yield Processes. Watershed sediment yield in arid regions such as the Albuquerque metropolitan area, results primarily from two processes: sheet wash (which includes rilling) and gullying.

Sheet wash is largely a function of raindrop detachment and transport by overland flow. The susceptibility of an area to erosion by these processes is directly related to the type of soil, amount of protection by vegetation or other types of surface cover and the steepness of the land slope. Overland erosion usually results in the delivery of relatively

fine sediment to the stream channel. This material is carried mostly in suspension (wash load). Limited quantities of wash load normally do not pose serious problems for the stability of the arroyo channels. However, if the quantity of wash load being carried by the flows is significant (greater than approximately 20,000 ppm by weight), the bed material transport capacity of the flows in the arroyo can increase, resulting in increased erosion in the arroyo channel and deposition in flood detention structures.

Gullying results from the concentration of the overland flows into small headward channels and can result in delivery of relatively large quantities of coarser particles to the arroyo. The coarser sand and gravel is carried as bed material load and can have significant implications regarding the vertical and lateral stability of the arroyo and sediment deposition in flood detention structures.

The primary source of sand and coarser sediment delivered to in-channel detention structures is from bed and bank erosion within the arroyo upstream of the structures. The transport rate, and thus sediment yield, from arroyos varies considerably depending upon the stage of adjustment of the arroyo (Figures 1.2 and 1.3), with the highest rates occurring by incision and widening during the arroyo development process (Schumm et al., 1987; Begin, 1979). Sediment delivery to in-channel structures is related to the hydraulic conditions in the arroyo. In designing the storage capacity of detention and sedimentation basins, the estimated sediment yield should include both the amount of fine sediment delivered from the watershed and the amount of bed material based on the transport capacity in the arroyo. Procedures for performing the bed material computations are discussed in Chapter 3.

2.3.3 Methods for Estimating Sediment Yield. Accurate quantification of the sediment yield, either on an annual basis or in response to individual storms is, at best, a difficult problem. Evaluation of the watershed sediment yield first requires a qualitative evaluation of the sediment sources in the watershed and the types of erosion that are prevalent. Soil Conservation Service (SCS) soil surveys are a valuable source of data for quantifying watershed sediment yields (e.g., SCS, 1977 for the Albuquerque area). Other sources include maps, drilling logs, reservoir records, climate records and, of course, field observations.

Available methods for estimating sediment yield include a watershed rating procedure developed by the Pacific Southwest Interagency Committee (PSIAC, 1968), the Universal Soil Loss Equation (Wischmeier and Smith, 1965; 1978), and the Modified Universal Loss Equation (Williams and Berndt, 1972). These methods have been tested under a variety of conditions with mixed success.

The PSIAC method provides a general guide to estimating total sediment yields based on the climatic and physical characteristics of the watershed. This method is intended for broad planning purposes only. As shown in **Table 2.1**, the method predicts a range of annual sediment yields that may be expected based on a watershed rating

system. Shown (1970) and Renard (1980) tested the PSIAC method against sediment yields measured in ponds and dams with contributing watersheds of less than approximately 20 square miles located in the Southwestern U.S. They showed a strong correlation between estimates of the annual sediment yield using the PSIAC method and measured annual yield. The details of the rating system are presented in Appendix A of this Design Guide.

Table 2.1. Summary of PSIAC Classifications.

| Classification | Rating | Sediment yield (Annual) | |
|---|---|---|---|
| | | (ac-ft/sq.mi.) | (tons/ac.)* |
| 1 | >100 | 3.0 | 10.2 |
| 2 | 75-100 | 1.0-3.0 | 3.4-10.2 |
| 3 | 50-75 | 0.5-1.0 | 1.7-3.4 |
| 4 | 25-50 | 0.2-0.5 | 0.7-1.7 |
| 5 | 0-25 | <0.2 | <0.7 |

* Assuming bulked unit weight of sediment = 100 pcf (1 ac-ft/mi$^2$ = 3.4 t/ac)

The Universal Soil Loss Equation (USLE) is a widely used empirical relationship based on runoff and soil loss data from agricultural land. The USLE relates annual soil loss due to sheet-and-rill erosion to the product of six factors describing rainfall energy, soil erodibility, cropping and management, supplemental erosion control practices such as contouring and terracing, and a topographic factor involving the steepness and length of the overland slope. Applicability of the USLE to the Albuquerque area is limited since the original data upon which it is based are largely from the Central and Eastern U.S. where the precipitation patterns and land characteristics are significantly different. In the arid southwest, runoff-producing precipitation usually occurs in the form of high-intensity, short-duration thunderstorms that cannot be completely incorporated into the equation. In addition, the weathering process caused by the wind and sun between storms is much more severe in arid areas, which can increase the supply of easily erodible material. An additional drawback of the USLE is the need to define the sediment delivery ratio to estimate the amount of sediment eroded from the watershed that actually reaches a given point in the channel.

The Modified Universal Loss Equation (MUSLE) was developed to estimate sediment yields from watersheds based on single storms. The equation, as presented by Williams and Berndt (1972), differs from the USLE by inclusion of a runoff factor in

place of the rainfall energy factor. Since it directly considers the runoff associated with individual storms, it is more applicable to the ephemeral streams found in the arid southwest where runoff and sediment delivery to the channel system is primarily the result of high-intensity thunderstorms. The MUSLE relationship is given by:

$$Y_s = \alpha\ (Vq_p)^{\beta}\ KLSCP \qquad (2.1)$$

where $Y_s$ is the sediment yield for the storm in tons, K is the soil erodibility factor, LS is the topographic factor representing the combination of slope length and slope gradient, C is the cover and management factor, P is the erosion control practice factor, V is the runoff volume for the storm in acre-feet, and $q_p$ is the peak discharge of the storm in cfs. Values for $\alpha$ and $\beta$ can be derived through calibration when sufficient data are available. Once calibrated, the MUSLE can be used to evaluate the effect of watershed modifications on the sediment yield associated with a given storm event. The most commonly used values for $\alpha$ and $\beta$ are 95 and 0.56, respectively. These values were derived using data from experimental watersheds in Texas and Nebraska. Insufficient data are available to re-derive these coefficients for the Albuquerque area, although the results obtained using the above values appear to be low in comparison with observed sediment yields.

The MUSLE equation was originally developed to represent the total watershed sediment yield. For conditions in arroyos in the Albuquerque area, it should be used to estimate only the fine sediment (wash load) yield and should **not** be used to estimate the total sediment yield. The bed material component of the sediment yield should be estimated from hydraulic and sediment transport computations, as discussed in Chapter 3. The total sediment yield is then the sum of the wash load yield estimated from MUSLE and the bed material load based on the sediment transport computations.

From analyses of several watersheds in the area, it appears that the fine sediment yield is about three times higher than predicted using the standard values. For local use in the Albuquerque area, limited testing has shown that $\alpha$ should be increased by a factor of about three with no change in $\beta$; thus, the MUSLE equation for wash load is given by:

$$Y_s = 285\ (Vq_p)^{0.56}\ KLSCP \qquad (2.2)$$

If additional site-specific data become available in the future, it is recommended that the values of both $\alpha$ and $\beta$ be re-evaluated and adjusted accordingly. The wash load yield should be reduced by the percentage of impervious (noncontributing) area within the watershed.

The MUSLE can be used to estimate the long-term average annual sediment yield by computing the sediment yield associated with each return period storm event and applying Equation 1.1.

A detailed description of MUSLE is presented in Appendix B.

2.3.4 Available Sediment Yield Data. Several sources of data are available with which to verify the above relationships. These include publications by various government agencies, consultant reports, and AMAFCA records of sediment removal from detention ponds and channels.

As discussed in Section 2.3.3, sediment yield is related to drainage density (Schumm, 1977). Evaluation of the drainage densities in the four quadrants discussed in Section 2.3.3 indicates that they are highest in the southwest quadrant and lowest in the northeast and northwest quadrants.

**Table 2.2** contains a summary of the available sediment yield data for the Southwestern U.S from reports by government agencies. A more detailed discussion of this data is presented in "Unser Bridge/Calabacillas Arroyo Detention Basin" prepared for AMAFCA by RCI in 1989. The data from SCS (1936) and USGS (1952) are for relatively small watersheds similar in size to the individual drainages in the AMAFCA area of concern (less than 5-10 square miles). The majority of the remaining data are for larger systems with drainage areas of several hundred square miles. Due to the high variability in sediment yield data and the effect of local conditions, the values contained in Table 2.2 should only be used as a guide.

Table 2.2. Summary of Regional Sediment Yield Data.

| Source | Location | Sediment Yield Range (tons/ac/yr) |
|---|---|---|
| ARS, 1964 | Central New Mexico | 1.4-7.3* |
| Bondurant, 1951 | Conchas Reservoir | 0.1-4.3 |
| Curtis, 1976 | New Mexico | 0.2-31.0 |
| Norman, 1968 | Rio Grande, Rio Chama Rivers | 0.3-1.0 |
| SCS, 1936 | Rio Grande, Pecos, Zuni Rivers | 0.3-4.1 |
| USGS, 1952 | Navajo Indian Reservation | 0.03-4.1 |
| USGS, 1982 | San Juan River | 1.0-1.2 |

* Does not include two outliers which are clearly unrepresentative.

Using a combination of bed material transport calculations and wash-load estimates, RCI estimated the annual sediment yields for Calabacillas Arroyo to be about 2 tons/acre for undeveloped conditions and about 1.5 tons/acre for fully developed conditions.

AMAFCA silt-haul records were used by Bohannan-Huston (1990; 1991) to supplement other available information to estimate sediment yields for Black and Ladera Arroyos. These records indicate that about 3.4 tons/acre/year were removed from Black Arroyo between 1981 to 1989 and about 1 ton/acre/year was removed from the Ladera system between 1977 and 1989. Based on the AMAFCA records and the above data, Bohannan-Huston estimated the total annual sediment yields for the Ladera system to be about 1.7 tons/acre/year.

**Table 2.3** is a summary of AMAFCA silt haul records for the North Diversion Channel (NDC) system between 1980 and 1992 taken from RCE (1993b). These data are derived from records maintained by the maintenance supervisor based on the number of truck loads of material hauled from the various locations by either AMAFCA crews or contractors. The information was originally provided to RCE as total tons of material removed from the sites on a yearly basis. RCE compiled the data and converted it to a unit sediment yield basis as shown in the table. According to AMAFCA (John Kelley, personal communication, 1993), the material removed from the NDC expansion at the outfall is sand with silt (SM); therefore, it contains a significant amount of wash load-sized material. Material removed from other locations is nearly all sand with varying amounts of fine and medium gravel.

Limitations in using these data to estimate average annual sediment yields from the arroyos include uncertainty in the accuracy of the original records regarding the number of truck loads of material hauled from the sites, the possibility of material removed from the sites, but not recorded, and uncertainty as to the trap efficiency of the NDC system. Discussions with AMAFCA personnel indicate that the first problem is not considered to be significant; they feel that the records from monitored silt haul activity are reasonably accurate. The magnitude of the second problem is unknown, except to the extent that some excavation beyond the monitored activity is known to have occurred. The third problem is probably not significant with respect to the sand and coarser material since the silt basins and flow expansion at the NDC outfall trap essentially all of the sand that is delivered from upstream.

Since all of the sites are not necessarily excavated on a yearly basis and records of the runoff that delivered the sediment are not available, the data were combined to develop an estimate of the sediment deposited in the system on an average annual basis, and evaluate the relative amount of sediment delivered from each of the arroyos. The data show that approximately 0.7 tons per acre of sediment was removed from the NDC during the 13-year period, of which 0.1 to 0.2 tons per acre were finer than sand-sized material. If the trap efficiency of the overall system is assumed to be greater than 90

**Table 2.3. Unit Silt Haul (tons/acre*) Based on AMAFCA Silt Haul Records.**

| Year | NDC Outfall | NDC | Embudo | Camino Inlet | LaCueva Inlet | Baca Inlet | N. Pino Inlet | S. Pino Inlet | Bear Inlet | Vineyard Inlet | Hahn | Total NDC |
|---|---|---|---|---|---|---|---|---|---|---|---|---|
| Drainage Area ($mi^2$) | 101.01 | 39.38 | 20.68 | 5.8 | 8 | 11.55 | 2.82 | 9.33 | 15.5 | 0.98 | 5.8 | 101.01 |
| 1980 | 0.52 | | 0.16 | | | 0.16 | 0.22 | 2.49 | 1.58 | 2.58 | | 1.07 |
| 1981 | 0.30 | 0.33 | | | 1.37 | 10.14 | | 1.92 | 1.62 | | | 2.12 |
| 1982 | 1.37 | 0.17 | 1.02 | | 0.13 | 2.90 | | 0.09 | 0.72 | | 0.55 | 2.14 |
| 1983 | 0.15 | 0.25 | 0.73 | | | 1.28 | 1.27 | 0.29 | 1.25 | 0.86 | | 0.80 |
| 1984 | | 0.27 | 0.15 | | | | 0.07 | | 0.11 | 0.65 | | 0.16 |
| 1985 | 0.38 | 0.13 | 0.04 | | | | 3.07 | 0.25 | | | | 0.55 |
| 1986 | 0.23 | | | | 0.66 | | 0.30 | 0.50 | | 2.58 | | 0.37 |
| 1987 | 0.15 | 0.01 | | | | 0.51 | 1.68 | | | 3.65 | | 0.29 |
| 1988 | 0.75 | 0.10 | | | | | | | | | | 0.79 |
| 1989 | | 0.01 | 0.85 | | | | 1.63 | | | | 0.07 | 0.23 |
| 1990 | 0.12 | | | | | | | | | | | 0.12 |
| 1991 | 0.03 | 0.01 | | | | | 0.10 | | | 2.17 | | 0.05 |
| 1992 | 0.36 | 0.03 | | | | 0.09 | 1.32 | | | | | 0.41 |
| Annual (t/ac) | 0.33 | 0.10 | 0.23 | | 0.17 | 1.16 | 0.74 | 0.43 | 0.41 | 0.96 | 0.05 | 0.70 |
| Annual ($a\text{-}ft/mi^2$) | 0.10 | 0.03 | 0.07 | | 0.05 | 0.34 | 0.22 | 0.13 | 0.12 | 0.28 | 0.01 | 0.21 |

*Assumes $\gamma_s$ = 100 pcf

percent, which is believed to be reasonable, the average annual yield of sand and coarser material was about 0.6 to 0.7 tons per acre over the approximately 101 square-mile watershed during this period. **Figure 2.2** shows a plot of the quantity of sediment removed by year. From this plot it appears that a significant reduction in sediment delivery to the NDC system has occurred since 1982. Considering only the data after 1983, the average amount of sediment removed from the system is only about 0.4 tons per acre. Using the percentages discussed above, this indicates an average annual coarse sediment yield of about 0.4 tons per acre over the past decade.

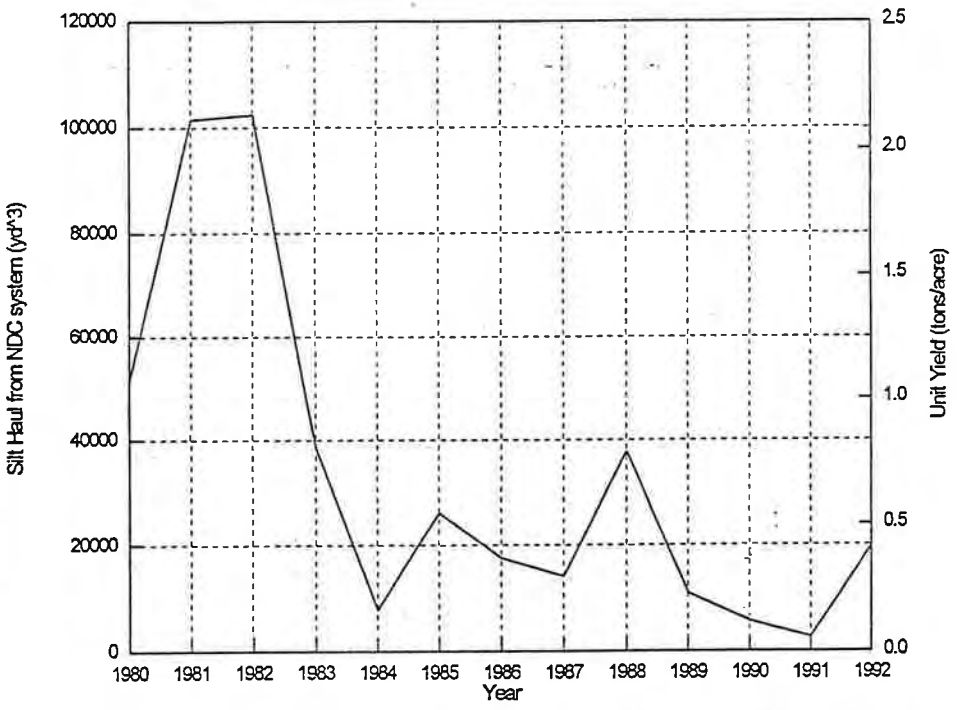


Figure 2.2. Quanitity of sediment removed from the system by year.

Considering the sites individually, the Domingo Baca and Vineyard inlets had the largest quantity of sediment removed on a per-unit area basis (1.2 and 1.0 tons per acre, respectively). At the present time (1993), Domingo Baca Arroyo is still unlined for approximately 1 mile upstream of the inlet to the NDC and thus has potential for transport and delivery of significant quantities of sediment to the silt basin leading to the NDC. Vineyard arroyo is lined over most of its length and drains a watershed that is nearly entirely urbanized; it will probably not continue to be a significant sediment producer to the NDC system.

Other significant sediment producers during the period include North and South Pino Arroyos and Bear Arroyo (0.7, 0.4, and 0.4 tons/acre/year, respectively). According

to AMAFCA, much of the sediment from North Pino was derived from an unlined reach between I-25 and San Pedro Boulevard; this reach was lined in 1991. North Pino Arroyo is currently lined from the silt basin at the NDC inlet to Holbrook Street, approximately 4 miles upstream. In the future, bed material sediment entering the North Pino system will be mostly derived from unlined reaches upstream of Holbrook Street. At the present time, the entrance to the arroyo is blocked with fill material, preventing normal runoff from entering from upstream. During a large storm event, however, it is likely that this blockage would breach, delivering a large quantity of sediment to the system. Until that occurs, it can be expected that sediment delivery from North Pino will be relatively small and derived from flushing of material already in the system.

South Pino is presently lined from the silt basin at the NDC inlet to Wyoming Boulevard. A sediment detention basin was constructed in 1991 on the grounds of the Albuquerque Academy just upstream of Wyoming Boulevard. According to surveys provided by Bohannan-Huston, Inc., approximately 3,360 tons of sediment accumulated in the basin between the time of its completion in July 1991 and March 1992 and an additional 2,140 tons accumulated between March 1992 and March 1993. This equates to an average of approximately 0.6 tons/acre/year of sediment. According to AMAFCA personnel (Cliff Anderson, personal communication, 1993), this watershed experienced large storms during both periods.

**Table 2.4** summarizes estimated average annual sediment yields for tributaries to the NDC system from the RCE (1993b) study. These estimates were made using the procedures presented in this Design Guide. While this information may be useful in evaluating the sediment yield from specific arroyos, **it is important to recognize that the bed material transport capacity estimates are based on site-specific conditions as they existed in 1993 at the entrance to the lined portion of the NDC. The results may not be applicable to other locations along the arroyo.** The reader should refer to the RCE (1993b) report for a more complete description of the assumptions and methodology used to make the estimates.

It is important to note that the above sediment yield estimates apply only to well-developed arroyos (e.g., Calabacillas, Embudo, Black, Ladera, and Bear). As discussed in Section 3.1, arroyo evolution follows a predictable pattern from unincised swales through an incision and widening process to a more stable, near equilibrium condition. Thus, this information applies primarily to those arroyos that have progressed to the latter, more stable stage of development. During the incision phase, sediment yields can be extremely high due to the unstable condition of the arroyo. Watson et al. (1986) found that approximately 75 percent of the sediment yield from incising channels in the Southeastern U.S. was derived from the channel bed and banks. The increased sediment load results from nickpoint migration and bank sloughing within the main arroyo and rejuvenated sediment supplies due to base-level lowering and resulting upstream migration of nickpoints in tributaries. A nickpoint is an abrupt oversteepening of the channel profile (**Figure 2.3**). The nickpoint migrates upstream through erosion of the

| Table 2.4. Summary of Average Annual Total Sediment Yield for the Study Area. | | | | | | |
|---|---|---|---|---|---|---|
| Location | Site Number | Reach | Drainage Area ($mi^2$) | Unit Sediment Yield | | |
| | | | | Bed Material (tons/acre) | Wash Load (tons/acre) | Total (tons/acre) |
| North La Cueva upstream Coronado Airport | 2a | | 5.91 | 1.62 | 0.08 | 1.70 |
| South La Cueva upstream Coronado Airport* | 2b | | 0.53 | 0.61 | 0.11 | 0.72 |
| Domingo Baca @ NDC | 3a | upstream arroyo | 11.55 | 0.67 | 0.17 | 0.84 |
| Domingo Baca @ NDC | 3a | silt basin output | 11.55 | 0.03 | 0.17 | 0.20 |
| South Domingo Baca @ Holbrook Street | 3b | upstream arroyo | 5.49 | 2.05 | 0.10 | 2.15 |
| South Domingo Baca @ Holbrook Street | 3b | silt basin output | 5.49 | 0.73 | 0.10 | 0.83 |
| North Pino @ NDC | 4a | silt basin output | 2.82 | 0.01 | 0.44 | 0.45 |
| North Pino @ Holbrook Street | 4b | | 0.80 | 2.14 | 0.71 | 2.85 |
| South Pino @ Wyoming | 5a | upstream arroyo | 5.98 | 0.34 | 0.04 | 0.41 |
| South Pino @ Wyoming | 5a | silt basin output | 5.98 | 0.00 | 0.06 | 0.06 |
| South Pino @ NDC | 5b | silt basin output | 9.33 | 0.00 | 0.09 | 0.09 |
| Bear @ NDC | 6 | upstream arroyo | 15.51 | 0.25 | 0.08 | 0.33 |
| Bear @ NDC | 6 | silt basin output | 15.51 | 0.00 | 0.08 | 0.09 |
| Embudito | 9e | | 0.82 | 4.52 | 0.07 | 4.59 |
| North Glenwood Hills | 9a | | 0.90 | 3.07 | 0.07 | 3.13 |
| South Glenwood Hills Tributary | 9c | | 0.19 | 2.43 | 0.28 | 2.71 |
| Piedra Lisa | 9d | | 0.63 | 0.21 | 0.01 | 0.22 |
| Embudo | 9f (right) | | 3.72 | 2.98 | 0.03 | 3.00 |
| Embudo | 9f (left) | | 3.72 | 1.36 | 0.03 | 1.39 |

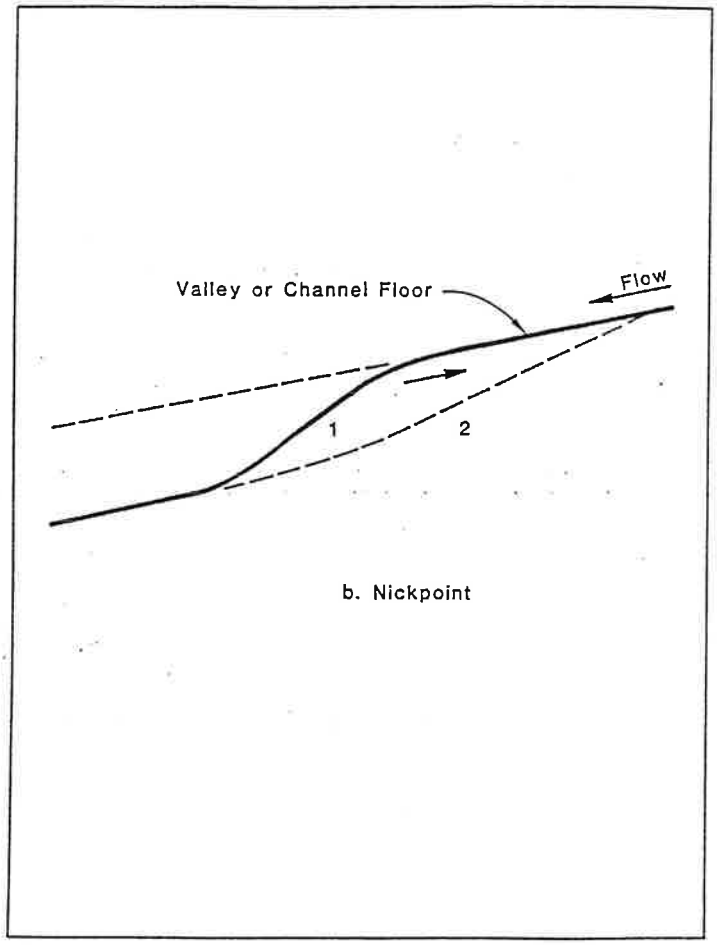


Figure 2.3. Schematic diagram of a nickpoint.

oversteepened area, lowering the channel bed. The associated deepening of the channel bed may induce bank instability and erosion. A similar increase in sediment load can occur through incision caused by release of essentially clear water from a detention basin or culvert crossing with upstream backwater. In either case, the local sediment yield may be many times greater than the regional average until the incising reach adjusts to a more stable form.

## 3.0 CHANNEL DYNAMICS

This chapter presents background and recommended techniques for analyzing geomorphic, hydraulic and sediment transport conditions in arroyos and drainageways in the Albuquerque area. The specific techniques presented in this chapter form the basis for the integrated Prudent Line analysis procedures in Chapter 4.

### 3.1 Arroyo Geomorphology

The arroyo is one type of incised channel that ranges in size from rills that are a few inches deep to major entrenched streams that may be up to 50 feet in depth. Incised channels have characteristically lowered their beds, thereby setting in motion a period of considerable channel instability. This instability has the potential for serious erosion, dewatering of riparian zones, downstream delivery of sediment to reservoirs, destruction of aquatic habitat, damage to infrastructures such as bridges and utility crossings, and damage to urban development. The causes of incision are highly variable, but the response of incised channels, regardless of scale or location, follows a very similar pattern (Schumm et al., 1984). Geomorphic models of channel evolution following incision have been used to develop cost-effective engineering solutions that incorporate an understanding of the system dynamics (Schumm et al., 1984; Harvey and Watson, 1986; Watson et al., 1988a; 1988b).

It should be understood that, while arroyos and drainage channels typically incise in response to urbanization, localized areas of deposition will also occur. This is particularly true in areas of reduced energy such as channel expansions, bends and reaches with flatter slopes in comparison to the upstream channel. It may also occur in reaches where land disturbance results in the delivery of large quantities of sediment to the arroyo in excess of its transporting capacity. As discussed in Chapter 2, the zone west (or downstream) of Tramway Boulevard in the northeast quadrant is largely depositional under existing conditions, as evidenced by the relatively shallow, branching drainage channels in the undeveloped portions of this zone. An increase in the tendency for channel incision will occur as the area continues to develop. Significant deposition during large storm events has also occurred in the otherwise incising zone upstream of Tramway Boulevard in the same area.

3.1.1 Channel Incision. The incised channel's characteristic morphology is the result of the force exerted by concentrated flowing water that exceeds the resistance of the material in which it is flowing. The development of an incised channel at a given location may depend on controls acting at that site, or the up- or downstream changes that affect the site. In addition, the response can be the result of extrinsic (external) controls which are imposed on the system, such as climatic fluctuations (Knox, 1972), change of base level (Schumm and Parker, 1973), change of land use (Graf, 1979), or channel modification (Schumm et al., 1984). Incision may also be the result of intrinsic (internal) controls that are inherent in the system, such as the steepening of valley floors

by deposition of sediment which, if it is of sufficient magnitude, can initiate channel incision (Schumm and Hadley, 1957; Patton and Schumm, 1975; Begin and Schumm, 1984). Regardless of whether the incision is caused by external or internal controls, the presence of the incision indicates that a threshold of stability has been exceeded (Schumm, 1977).

Once the threshold of stability is exceeded, bed degradation and channel incision will follow. Degradation is the morphologic expression of a sediment transport imbalance, since sediment transport capacity exceeds the supply (Pickup, 1977). The bed and banks of the channel then become sources of sediment. This degradation sets in motion a complex series of interacting events through which the system ultimately adjusts to a new state of dynamic equilibrium. Attainment of a new state of dynamic equilibrium involves interdependent adjustments between channel slope and cross-sectional area in response to the imposed discharge and sediment load (Leopold et al., 1964). The time required to attain the new state of dynamic equilibrium in incised channels varies with climatic region. In the humid Southeastern U.S., dynamic equilibrium is reattained within a period of about 30 years (Schumm et al., 1984); whereas, in the arid and semiarid Southwestern U.S., the time required is approximately 80 to 100 years (Gellis et al., 1991).

The concept of dynamic equilibrium is expressed very simply by the Lane (1974) relation:

$$QS \sim Q_s\ D_{50} \qquad (3.1)$$

where
- $Q$ = water discharge
- $S$ = energy slope
- $Q_s$ = sediment discharge
- $D_{50}$ = median sediment size

This relation means that alluvial channels tend toward a state of equilibrium in which the dominant discharge and slope are in balance with the sediment transport capacity and bed material size. If, for example, the sediment supply to a reach that was previously in equilibrium is reduced, with no change in dominant discharge or particle size, the channel will flatten (or degrade) to achieve a new state of equilibrium between the sediment transport capacity and supply. Conversely, if the sediment supply is increased, all other factors being the same, the channel will attempt to steepen (or aggrade) to achieve a new state of equilibrium. Equation 3.1 is a useful relation to **qualitatively** evaluate the response of an alluvial channel to changed conditions associated with natural or man-induced changes in the watershed or upstream reaches (see Richardson et al., 1990 for applications).

3.1.2 Channel Widening. As a result of mass failure of the banks once a critical bank height has been exceeded, bed degradation usually precedes and predisposes channel widening (Little et al., 1982; Harvey and Watson, 1986; Watson et al., 1988a).

In most incised channels, fluvial detachment of individual particles does not play a major role in bank retreat. However, fluvial removal of previously failed bank material is the key to continued bank erosion (Thorne, 1982). The critical bank height is dependent on the geotechnical properties of the bank materials. Identification of the critical bank height can be done with a formal geotechnical stability analysis (Osman and Thorne, 1988, Section 3.4.4) or it can be based on observations of bank heights and angles at failed bank sites where the failure has taken place in similar materials (Biedenharn et al., 1991).

Channel widening as a result of bed degradation will continue until such time as the failed bank materials are no longer removed by fluvial action. Localized erosion at bendways will continue to occur, but system-wide bank failure will eventually cease. The ultimate channel width can be related to the degree of incision, and the redevelopment of an equilibrium width-depth ratio that is dependent on the size of the drainage basin (Harvey and Watson, 1986) which is a surrogate for discharge (Leopold et al., 1964).

Channel widening may also occur in depositional zones due to the increase in stress on the channel banks as the material deposits in the bed. Under these conditions, avulsion and abrupt realignment of the channel is possible.

3.1.3 Arroyo Evolution. Numerous geomorphological studies have taken data from different locations and in some way used it to suggest landform development through time. This technique is referred to as location-for-time substitution. Application of the technique has permitted development of a five-stage geomorphic model of incised channel evolution (ICEM) that describes and quantifies evolution of the channel from a state of disequilibrium to a new state of dynamic equilibrium (**Figure 1.2**) for the channelized streams of the Southeastern U.S. (Schumm et al., 1984) and the arroyos of the Southwestern U.S. (Schumm and Gellis, 1989; Gellis et al., 1991)

The ICEM identifies, quantifies and integrates four important facets of the evolution process: (1) bank stability, (2) magnitude and frequency of the range of dominant discharges, (3) hydraulic energy of those discharges, and (4) the morphological adjustments of the channel. These factors in the evolution of the incised channel can be further reduced to two dimensionless stability numbers, $\mathbf{N_g}$, the geotechnical stability number, and $\mathbf{N_h}$, the hydraulic stability number (Watson et al., 1988a; 1988b).

The geotechnical stability number $\mathbf{N_g}$ is defined as the ratio of the actual bank height (h) at a given bank angle to the critical bank height ($h_c$) (defined computationally or observationally):

$$N_g = \frac{h}{h_c} \tag{3.2}$$

When $N_g$ is less than 1, the bank is geotechnically stable; when $N_g$ is greater than 1, the bank is unstable and bank failure and channel widening are likely.

The hydraulic stability factor ($N_h$) is defined as the ratio of the expected sediment supply to the sediment transport capacity. $N_h$ can be interpreted as a ratio of energy parameters. An example would be the ratio of shear stress or shear intensity at the effective or dominant discharge to the same parameter at conditions of equilibrium between sediment transport capacity and sediment supply. It is important to note that $N_h$ includes sediment transport and supply. This is in contrast to most channel design procedures, which are generally based on fixed boundary approximations. $N_h$ provides a rational basis for determining the equilibrium sediment transport - sediment supply relationship that will be required to achieve a state of dynamic equilibrium. Hydraulic stability in the channel is attained when $N_h=1$. If $N_h>1$, the channel will degrade, and if $N_h<1$, the channel will aggrade.

When $N_g$ and $N_h$ are combined, they provide a set of design criteria that define both geotechnical and hydraulic stability in the channel. Channel stability is attained when $N_g<1$ and $N_h = 1$. Since sediment supply to a channel fluctuates through time, it is prudent to aim for a hydraulic condition that is marginally aggradational; therefore, a more conservative approach is to allow for $N_h<1$.

The relationship between the ICEM and the stability numbers can be seen in **Figure 3.1**. The points labelled A through F can be viewed as individual locations along an incised arroyo, or as a sequence of locations that are linked spatially or temporally, with point A being upstream and point F being downstream, or moving from point A counter-clockwise to point F through time at a given location. These points generally correspond with the stages illustrated in **Figure 1.2**. For example, if the geotechnical and hydraulic calculations place a reach of channel at point A on the diagram, the strategy should be to prevent the channel depth from increasing to the point where the critical bank height is exceeded. In contrast, if the reach is located at point E, there will be no need to treat the channel because it is in a condition of quasiequilibrium. If no action is taken when a reach is in a condition represented by point A, the sequence of channel incision and widening will move from point A to point F through time as the channel evolves.

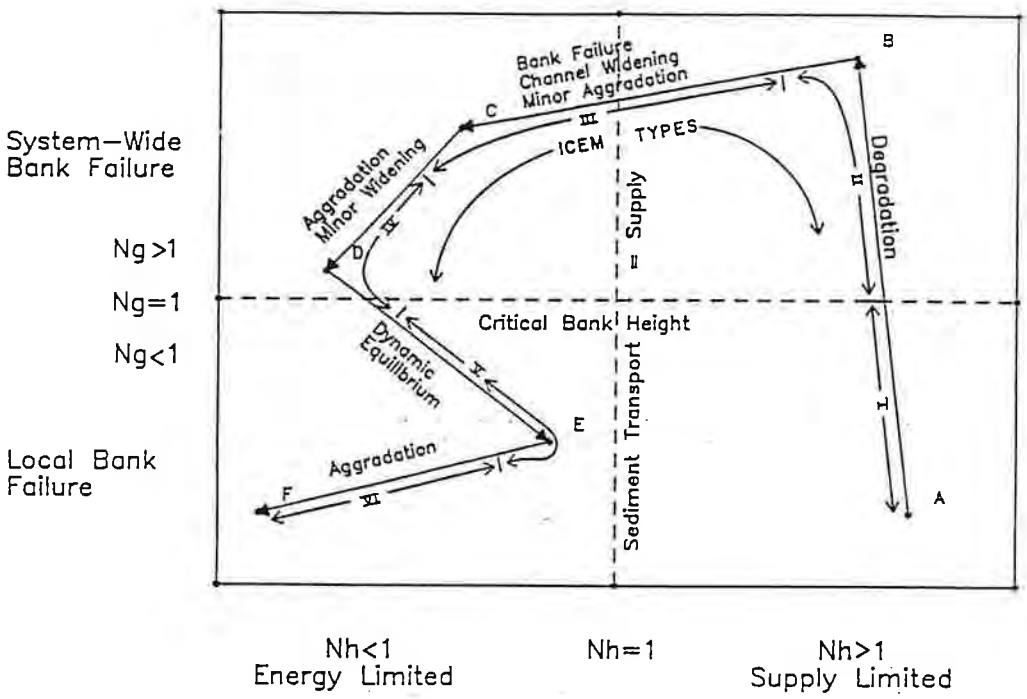


Figure 3.1. Stability number ($N_g/N_h$) diagram showing the thresholds of bank stability and hydraulic stability for an incised channel. Also shown are the ICEM stages. Note that the ICEM reach types form a continuum and the Type boundaries are gradational.

As the channel evolves from a state of disequilibrium (A) to a state of dynamic equilibrium (E), the reach types move from the lower right to the lower left quadrant via the upper right and upper left quadrants. Management of the channel should be aimed at keeping the channel in the lower right quadrant, or forcing it to move directly to the lower left quadrant, thereby eliminating the evolution cycle that is an inevitable consequence of bed degradation exceeding the critical bank height. Forcing the channel to move directly into the lower left quadrant generally requires the use of grade-control structures and bank protection. As noted in Chapter 1, the effects of urban development will, for practical purposes, prevent maintenance of a given arroyo in the lower right quadrant under most conditions.

Utilization of ICEM and the dimensionless stability numbers $N_g$ and $N_h$ enables not only equilibrium reaches to be identified (i.e., $N_g<1$: $N_h<1$), but it also permits reaches that are at risk to be identified, and provides a process-based rationale for selecting appropriate treatments. Further, this approach enables the effects of changed land use (runoff and sediment supply) to be evaluated in the context of channel stability.

## 3.2 Hydraulic Factors and Principles

3.2.1 Introduction. Knowledge of the hydraulic conditions that will occur during a given storm event is an essential element of a channel stability and Prudent Line analysis. The maximum depth of flow during the peak of the 100-year flood determines the location of the regulatory flood boundaries. The erosive power of the flow and thus, the potential for channel erosion or deposition is directly related to the flow velocities and depths for the range of flows in the hydrograph.

Typically, flood analyses consider the channel to have a rigid boundary with no deformation of the bed or banks during the passage of a flood. In erodible channels typical of many arroyos and drainageways in the Albuquerque area, interaction between the flow and boundary can have a significant influence on both the hydraulic characteristics of the flow and the form of the channel. This interaction is an important consideration when evaluating the potential response of the channel to storm flows.

In most applications, the hydraulic analyses are performed using standard computer programs which employ one-dimensional, step-backwater calculations [e.g., the Corps of Engineers' HEC-2 (USCOE, 1982) or the Federal Highway Administration's WSPRO (Shearman, 1990)]. These programs contain routines to estimate energy losses through expansions and contractions, bridge openings, and culverts as well as a variety of other options for evaluating energy losses along the channel.

Depending on the required level of accuracy for a specific study, in cases where the channel is uniform in slope and cross section, it may be acceptable to estimate the hydraulic conditions directly by assuming uniform flow and applying an empirical velocity equation such as the Manning or Chezy equation.

This Design Guide assumes that the user has a working knowledge of open-channel hydraulics. Numerous references are available to those needing to review open-channel flow concepts (e.g., Chow, 1959; Henderson, 1966). The purpose of this chapter is to discuss the techniques appropriate for analysis of hydraulic conditions in the steep, highly erodible channels characteristic of the Albuquerque area.

3.2.2 Uniform Flow Relationships. For uniform and gradually varied flow, channel velocity and depth are normally estimated using either the Manning or Chezy equations. These equations are empirical in nature and are given by:

Manning:

$$V = \frac{1.486}{n} R^{2/3} S_f^{1/2} \qquad (3.3)$$

where V = average channel velocity, in feet/second
R = hydraulic radius, in feet
$S_f$ = friction slope
n = Manning's roughness coefficient

and Chezy:

$$V = CR^{1/2} S_f^{1/2} \tag{3.4}$$

where C = Chezy's discharge coefficient (Chezy's C).

By equating the relationships, it can be seen that Manning's n and Chezy's C coefficients are related by the following equation:

$$C = \frac{1.486}{n} R^{1/6} \tag{3.5}$$

Another common method of representing the resistance to flow caused by grain roughness on the channel boundary in both open channels and closed conduits is the Darcy-Weisbach friction factor (f). The Darcy-Weisbach formula is given by:

$$h_l = \frac{fL}{D} \frac{V^2}{2g} \tag{3.6}$$

where $h_l$ = head loss
L = channel length
D = diameter of the conduit

By noting that $h_l/L$ is equivalent to the energy slope (S), the hydraulic radius (R) is related to D by:

$$R = \frac{A}{P} = \frac{\pi D^2/4}{\pi D} = \frac{D}{4} \tag{3.7}$$

The bed shear stress ($\tau_0$) is given by:

$$\tau_0 = \gamma RS \tag{3.8}$$

It can be shown that the bed shear stress, in terms of the Darcy-Weisbach friction factor, is:

$$\tau_0 = \frac{f\rho V^2}{8} \qquad (3.9)$$

In the above relations, $\gamma$ and $\rho$ are the unit weight and density of water (62.4 lb/ft$^3$ and 1.94 slugs/ft$^3$, respectively). By manipulating the above equations, it can be shown that Manning's roughness coefficient (n), Chezy's discharge coefficient (C) and the Darcy-Weisbach friction factor (f) are related by:

$$C = \sqrt{\frac{8g}{f}} = \frac{1.486}{n} R^{1/6} \qquad (3.10)$$

The accuracy of the result from any of the above relationships is dependent on the resistance coefficient selected for use in the computation. The following sections discuss factors to be considered in this regard.

### 3.2.3 Hydraulics in Steep, Alluvial Channels.

#### Bedforms and Flow Regime

Natural arroyos in the Albuquerque area are typically steep and highly erodible. Interaction between the flowing water-sediment mixture and the bed during runoff events creates different bed configurations that change the resistance to flow, velocity, water surface elevation, and sediment transport rates. Consequently, an understanding of the different types of bedforms that may occur under differing flow conditions and a knowledge of the resistance to flow and sediment transport associated with each is important in selecting appropriate boundary roughness values.

Flow in alluvial channels is divided into two regimes separated by a transition zone (Richardson et al., 1990). Forms of bed roughness in sand channels are shown in **Figure 3.2a. Figure 3.2b** shows the relationships between water surface and bed configuration. The flow regimes are:

Lower regime, where resistance to flow is large and sediment transport is small. The bedform is either ripples or dunes or some combination of the two. Water surface undulations are out of phase with the bed surface, and there is a relatively large separation zone downstream from the crest of each ripple or dune. The velocity of the downstream movement of the ripples or dunes depends on their height and the velocity of the grains moving up their backs.

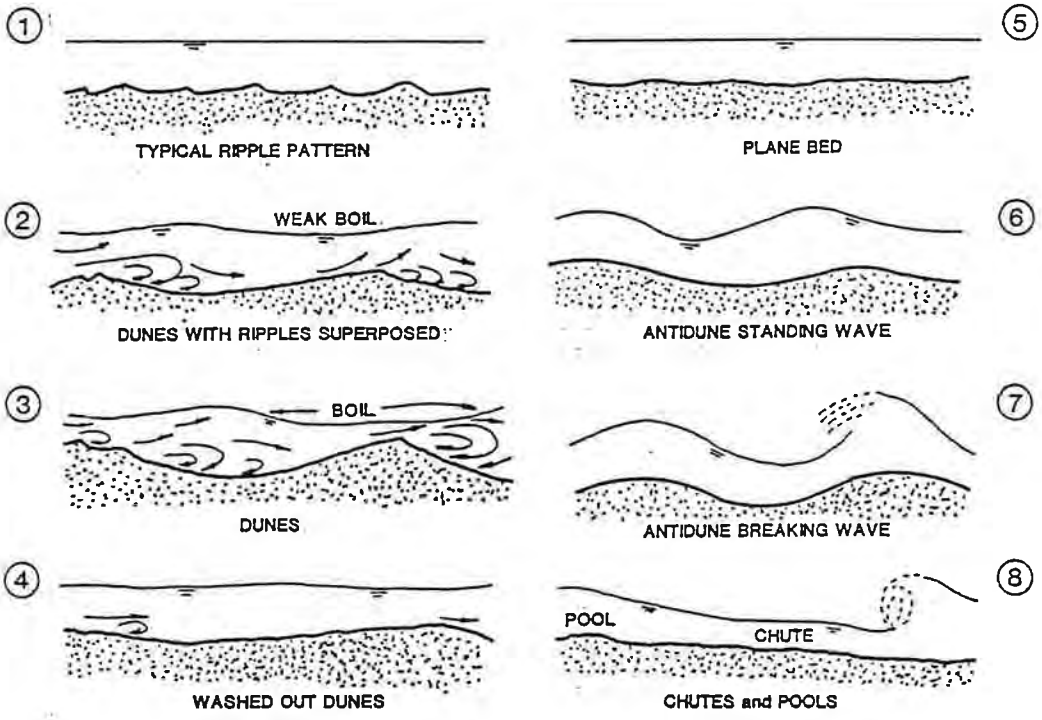


Figure 3.2a. Forms of bed roughness in sand channels.

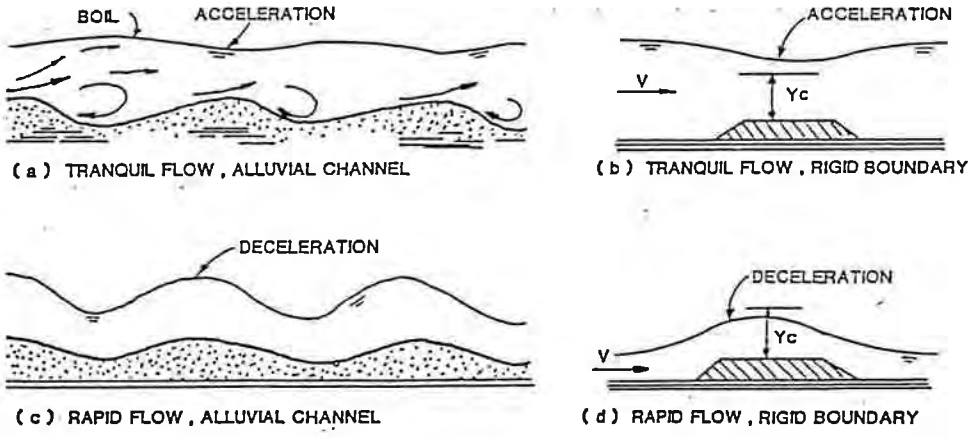


Figure 3.2b. Relation between water surface and bed configuration.

The transition zone, where the bed configuration may range from that typical of the lower flow regime to that typical of the upper flow regime, depending mainly on antecedent conditions. If the antecedent bed configuration is dunes, the depth or slope can be increased to values more consistent with those of the upper flow regime without changing the bedform; or, conversely, if the antecedent bed is plane, depth and slope can be decreased to values more consistent with those of the lower flow regime without changing the bedform. Resistance to flow and sediment transport also have the same variability as the bed configuration in the transition. This phenomenon can be explained by the changes in resistance to flow and, consequently, the changes in depth and slope as the bedform changes.

Upper regime, where resistance to flow is small and sediment transport is large. The usual bedforms are plane bed or antidunes. The water surface is in phase with the bed surface except when an antidune breaks, and normally the fluid does not separate from the boundary.

Due to the steepness and erodibility of most arroyos, it can generally be assumed that upper regime flow will occur during significant storm events.

Resistance to Flow - General

The general approach for estimating resistance to flow in a stream channel is to select a base value for materials in the channel boundaries assuming a straight, uniform channel, and then to make corrections to the base value to account for channel irregularities, sinuosity, and other factors which affect the resistance to flow (Richardson et al., 1990; Arcement and Schneider, 1984). The following equation is used to compute the equivalent total Manning's roughness coefficient (n) for a channel using this approach:

$$n = (n_b+n_1+n_2+n_3+n_4)m \qquad (3.11)$$

where
- $n_b$ = the base value for a straight, uniform channel
- $n_1$ = value for surface irregularities in the cross section
- $n_2$ = value for variations in shape and size of the channel
- $n_3$ = value for obstructions
- $n_4$ = value for vegetation and flow conditions
- m = correction factor for sinuosity of the channel

Arroyos and overbanks in the Albuquerque area frequently contain varying amounts of Chamiso. For relatively small flows and in locations where it is not expected to be taken out by the flows, the Chamiso can be treated as a minor obstruction(s) and $n_3$ used to adjust the base n-value to obtain total roughness. It should be noted that under high flow conditions, the Chamiso may be bent over in the flow, reducing the effective roughness. Other vegetation has similar properties. The reader is referred to Simons, Li & Associates, Inc. (1982a) for further discussion of this process.

**Table 3.1** provides base n values for stable and sand channels, while **Table 3.2** provides adjustment factors for use in Equation 3.11. Richardson et al. (1990) and Arcement and Schneider (1984) provide more detailed descriptions of conditions that affect the selection of appropriate values.

Resistance to flow in sand-bed channels.

The value of n varies significantly in sand-bed channels because of the varying bedforms that occur with different flow regimes. **Figure 3.3** shows the relative resistance to flow in channels in lower regime, transition, and upper regime flow and the associated bedforms. It is apparent from this figure that flow resistance increases with increasing stream power to a maximum value at the upper end of the lower flow regime, decreases rapidly in the transition zone between lower and upper regime and again increases with increasing stream power in the upper flow regime.

Brownlie (1983) developed relationships for the flow depth in terms of the hydraulic conditions and bed material characteristics for a large set of flume and river data. The U.S. Army Engineer Waterways Experiment Station (WES) rearranged Brownlie's relationships to directly solve for the Manning's n value (USCOE, 1991).

LOWER REGIME

$$n = [1.6940 \{\frac{R}{D_{50}}\}^{0.1374} S^{0.1112} G^{0.1605}] \, 0.034 \, D_{50}^{0.167} \qquad (3.12)$$

UPPER REGIME

$$n = [1.0213 \{\frac{R}{D_{50}}\}^{0.0662} S^{0.0395} G^{0.1282}] 0.034 \, D_{50}^{0.167} \qquad (3.13)$$

where R = hydraulic radius, in feet
S = channel slope, in foot per foot
$D_{50}$ = median particle size of bed material, in feet
G = gradation coefficient of the bed material given by:

$$G = \frac{1}{2}\left(\frac{D_{84}}{D_{50}} + \frac{D_{50}}{D_{16}}\right) \qquad (3.14)$$

and $D_{16}$, $D_{50}$, and $D_{84}$ are the particle sizes for which 16 percent, 50 percent, and 84 percent of the material is smaller. For slopes greater than about 0.6 percent, the flow will always be in upper regime, thus Equation 3.13 should be used and this value substituted for $n_b$ in Equation 3.11. For flatter slopes, the n-value for the transition between lower and upper flow regime is estimated based on the grain Froude Number and a transition relationship given by:

| Table 3.1. Base Values of Manning's n ($n_b$). | | | | |
|---|---|---|---|---|
| | Median size, bed material | | Base n value | |
| Channel or floodplain type | Millimeters | Inches | Benson and Dalrymple | Chow |
| Sand channels | | | | |
| (Only for upper regime flow where grain roughness is predominant) | 0.2 | ---- | 0.012 | ---- |
| | 0.3 | ---- | 0.017 | ---- |
| | 0.4 | ---- | 0.020 | ---- |
| | 0.5 | ---- | 0.022 | ---- |
| | 0.6 | ---- | 0.023 | ---- |
| | 0.8 | ---- | 0.025 | ---- |
| | 1.0 | ---- | 0.026 | ---- |
| Stable channels and flood plains | | | | |
| Concrete | ---- | ---- | 0.012 - 0.018 | 0.011 |
| Rock cut | ---- | ---- | ---- | 0.025 |
| Firm soil | ---- | ---- | 0.025 - 0.032 | 0.020 |
| Coarse sand | 1 - 2 | ---- | 0.026 - 0.035 | ---- |
| Fine gravel | ---- | ---- | ---- | 0.024 |
| Gravel | 2 - 64 | 0.08 - 2.5 | 0.028 - 0.035 | ---- |
| Coarse gravel | ---- | ---- | ---- | 0.026 |
| Cobble | 64 - 256 | 2.5 - 10.1 | 0.030 - 0.050 | ---- |
| Boulder | < 256 | < 10.1 | 0.040 - 0.070 | ---- |

| Table 3.2. Adjustment Factors for the Determination of n Values for Channels. | | |
|---|---|---|
| Conditions | n Value | Remarks |
| $n_1$ - Cross Section Irregularity | | |
| Smooth | 0 | Smoothest Channel |
| Minor | 0.001-0.005 | Slightly Eroded Side Slopes |
| Moderate | 0.006-0.010 | Moderately Rough Bed and Banks |
| Severe | 0.011-0.020 | Badly Sloughed and Scalloped Banks |
| $n_2$ - Variation in Cross-Sectional Shape and Size | | |
| Gradual | 0 | Gradual Changes |
| Alternating Occasionally | 0.001-0.015 | Occasional Shifts From Large to Small Sections |
| Alternating Frequently | 0.010-0.015 | Frequent Changes in Cross-Sectional Shape |
| $n_3$ - Obstructions | | |
| Negligible | 0-0.004 | Obstructions < 5% of Cross Section Area |
| Minor | 0.005-0.015 | Obstructions < 15% of Cross Section Area |
| Appreciable | 0.020-0.030 | Obstructions 15-50% of Cross Section Area |
| Severe | 0.040-0.060 | Obstructions > 50% of Cross Section Area |
| $n_4$ - Vegetation | | |
| Small | 0.002-0.010 | Flow Depth > 2x Vegetation Height |
| Medium | 0.010-0.025 | Flow Depth > Vegetation Height |
| Large | 0.025-0.050 | Flow Depth < Vegetation Height |
| Very Large | 0.050-0.100 | Flow Depth < 0.5 Vegetation Height |
| M - Sinuosity * | | |
| Minor | 1.0 | Sinuosity < 1.2 |
| Appreciable | 1.15 | 1.2 Sinuosity < 1.5 |
| Severe | 1.30 | Sinuosity > 1.5 |

*Sinuosity is the ratio of channel length to down-valley length.

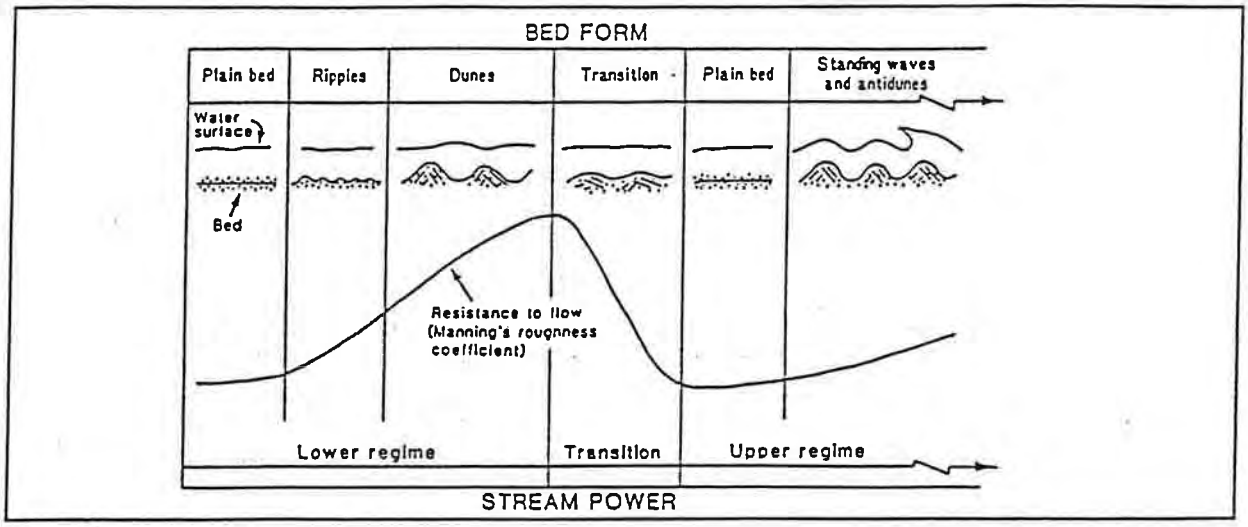


Figure 3.3. Relative resistance in sand-bed channels (after Arcement & Schneider, 1984).

$$F_g = \frac{V}{\sqrt{(S_g - 1) g D_{50}}} \tag{3.15}$$

and

$$F_g' = \frac{1.74}{S^{1/3}} \tag{3.16}$$

where v = channel velocity, in feet per second
$S_g$ = specific gravity of the sediment
g = acceleration of gravity = 32.2 feet / sec$^2$

When $F_g \leq F'_g$, use the lower regime equation (Equation 3.12) and when $F_g > F'_g$, use the upper regime equation (Equation 3.13). **For arroyos in the Albuquerque area, upper regime flow can be expected under most conditions.**

Burkham and Dawdy (1976) showed that the Limerinos equation could be used in sand-bed streams provided the regime was plane bed. In that analysis, they extended

the range of relative roughness parameter to $R/D_{84} > 600$. For a 2-foot deep channel, this results in a range of $D_{84}$ up to 1 mm; a condition commonly met in Albuquerque area arroyos. The Limerinos equation is discussed in the following section on coarse-bed channels.

Resistance to flow in coarse-bed channels. In gravel and cobble-bed channels, including riprap lined channels where the depth of flow is more than 2 to 3 times the size of the larger particles in the bed, resistance to flow can be estimated from either the Strickler relation given by (Anderson et al., 1970):

$$n = 0.04\ D_{50}^{1/6} \tag{3.17}$$

where $D_{50}$ = median size of the bed material, in feet,

or from the Limerinos (1970) equation given by:

$$n = \frac{0.0926 R^{1/6}}{1.16 + 2.0 \log\left(\frac{R}{D_{84}}\right)} \tag{3.18}$$

where $D_{84}$ = bed material size for percent of the particles, by weight, are smaller.

When only the $D_{50}$ of the bed material is available, the following formulation of the Limerinos equation, as presented in the roadside channels section of the HYDRAIN computer program (FHWA, 1992), can be used.

$$n = \frac{0.0926\ R^{1/6}}{0.796 + 1.85 \log\ (R/D_{50})} \tag{3.18a}$$

In Equations 3.18 and 3.18a, all dimensions are in feet. Flow depth, $Y_0$, may be substituted for the hydraulic radius, (R), in wide channels (i.e., width-depth ratio > 10).

For purposes of this Design Guide, it is recommended that the Limerinos equation (3.18 and 3.18a) be used in preference to Strickler's relation (3.17).

As an alternative, the n-value can be selected from Table 3.1. Since the roughness can vary significantly with flow depth in coarse-bed channels, it is advisable to verify the selected value by use of one of the above equations if flow depth or velocities will significantly affect the design. Other relations for the coarse bed case can be found in Richardson et al. (1990).

Resistance to flow on floodplains. Arcement and Schneider (1984) modified Equation 3.11 for use in estimating n-values for floodplains. The correction factor for sinuosity, m, becomes 1.0 for this case and the correction for variations in channel size and shape ($n_2$) is assumed to be zero. Equation 3.11, adapted for use on floodplains, becomes:

$$n = n_b + n_1 + n_3 + n_4 \tag{3.19}$$

where $n_b$ = base value of n for a bare soil surface

Selection of the base value for floodplains is the same as for channels. It is recommended that the user of this Design Guide refer to Arcement and Schneider (1984) for a detailed discussion of factors that affect flow resistance in floodplains.

Resistance to flow in concrete-lined channels. For concrete-lined channels carrying little or no sediment, the boundary roughness values can be selected from Table 3.1, or other appropriate references for concrete roughness (e.g., USCOE, 1991). When the channel carries a significant sediment load, the bed roughness may increase to values consistent with an alluvial channel. If the sediment transport capacity is significantly greater than the supply, most of the sediment particles are expected to be suspended above the bed and no adjustment to the roughness is required. As the sediment supply approaches the transport capacity, a layer of sediment will deposit and move along the bed which will impact channel roughness similar to an alluvial channel. If the sediment supply is greater than the transport capacity, aggradation will occur and the channel capacity and water surface must be adjusted accordingly. For this case, a composite n-value can be estimated using either the conveyance weighting or equal velocity methods. The conveyance weighting method is described by:

$$n_c = \frac{A_t R_t^{2/3}}{\sum \frac{A_i R_i^{2/3}}{n_i}} \tag{3.20}$$

where the subscripts i and t refer to individual subsections across the cross section and the total cross section (see **Figure 3.4**), respectively and $n_c$ is the composite n-value. The conveyance weighting method given by Equation 3.20 is recommended for purposes of this Design Guide when the Manning's equation is used for the hydraulic computations. Other compositing methods are also available; details can be found in USCOE (1991). Of these, the Equal Velocity Method, proposed by Horton and independently by Einstein (Chow, 1959) provides a good approximation for trapezoidal channels, although the method may not be as accurate as Equation 3.20. The Horton or Einstein method is given by:

$$n_c = \left[ \frac{\sum_{i=1}^{N} P_i \, n_i^{1.5}}{P} \right]^{\frac{2}{3}} \qquad (3.20a)$$

where P = total wetted perimeter
$P_i$ = wetted perimeter in section i
$n_i$ = n-value in section i

Normal Depth Calculations

As discussed above, when the flow is uniform along the channel, hydraulic conditions can be computed using Manning's or Chezy's equation (Equations 3.3 and 3.4). For these conditions, it is often reasonable to describe the variation in channel geometry (i.e., area, wetted perimeter, hydraulic radius, and topwidth) as single-valued functions of the total flow depth which can simplify the hydraulic and sediment transport

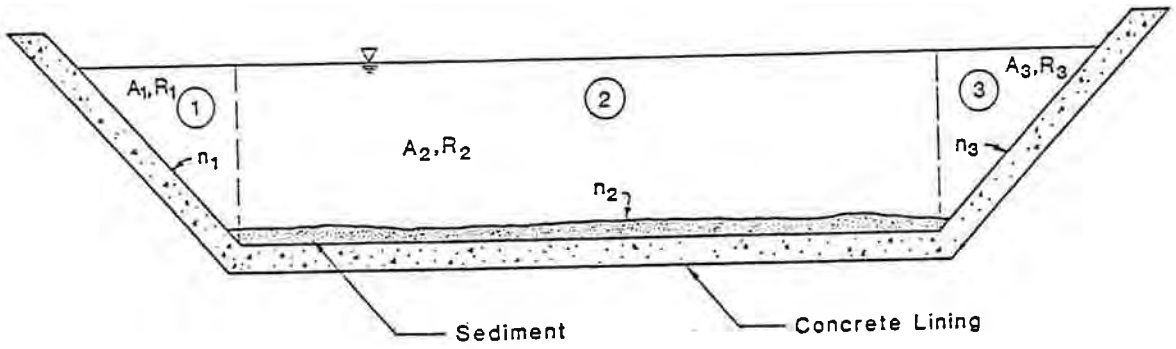


Figure 3.4. Schematic of a concrete-lined channel with significant sediment load.

computations. For prismatic cross sections (e.g., trapezoidal channels), relationships between the depth of flow and wetted perimeter can be substituted into Manning's equation and solved for the depth. For natural channel cross sections, two options are available for describing the cross-sectional geometry. The first is to develop relationships between the flow depth and the cross-sectional area, wetted perimeter and topwidth using least squares regression techniques. Power function relationships of the following form usually provide a sufficiently accurate definition of the cross-sectional geometry for most applications where normal depth calculations are appropriate:

$$X = aY^b \qquad (3.21)$$

where X = cross-sectional area, wetted perimeter, or topwidth
Y = depth of flow at the thalweg (maximum depth in the cross section)
a,b = constants

Of course, other forms of the equation can also be used. The power function form given by Equation 3.21 provides for easy solution of the normal depth equation.

Another alternative for natural channels is to compute the conveyance within each channel segment across the cross section incrementally and sum to obtain the total flow in the section. This method assumes constant energy grade line across the channel and requires significantly more computational effort than other methods. For highly irregular cross sections, it may however, provide more accurate results.

Appendix C shows the derivation of the normal depth relationships for the case of a trapezoidal channel and natural channel using the power function relationship given by Equation 3.21.

**As discussed in Chapter 2, incised arroyo channels tend to have relatively flat bottoms and shallow flow depths. For this case, the wide rectangular channel assumption is usually appropriate, eliminating the need for more detailed analysis of the cross-sectional shape for the hydraulic calculations.**

Water Surface Profiles

The water surface profile in a channel is a combination of gradually varied flow over long distances, and rapidly varied flow over short distances. Due to various obstructions in the flow (i.e., bridges, drop structures, well established vegetation such as Chamiso), the actual flow depth over longer reaches is either larger or smaller than the normal depth defined by Manning's uniform flow equation. In the immediate vicinity of the obstruction, the flow can be rapidly varied.

Gradually varied flow. In gradually varied flow, changes in depth and velocity take place slowly over a large distance, resistance to flow dominates and acceleration forces are neglected. The calculation of a gradually varied flow profile is well defined by analytical procedures, most commonly implemented with computer programs such as the Corps of Engineers' HEC-2 program (USCOE, 1982) or the FHWA's WSPRO program (Shearman, 1990).

Rapidly varied flow. In rapidly varied flow, changes in depth and velocity take place over short distances, acceleration forces dominate and resistance to flow may be neglected. The calculation of certain types of rapidly varied flow are well defined by analytical procedures, such as the analysis of hydraulic jumps, but analysis of other types of rapidly varied flow, such as flow through bridge openings are a combination of

analytical and empirical relationships. The FHWA document "Hydraulics of Bridge Waterways" (Bradley, 1978), provides a procedure for manual calculation of the backwater created by certain types of flow conditions at bridge openings. Gradually varied flow computer programs, such as HEC-2 and WSPRO, include analysis of bridge backwater, but do not calculate undular jump conditions or flow through the bridge when flow accelerations are large (i.e., large changes in velocity either in magnitude or direction).

Superelevation of Water Surface at Bends

Because of the change in flow direction which results in centrifugal forces, the water surface in bends tends to superelevate causing the water surface to be higher along the outside of this bend than along the inside (**Figure 3.5**). The resulting transverse slope can be evaluated quantitatively. The following relationship can be used to estimate superelevation for both subcritical (tranquil) and supercritical (rapid) flow (USCOE, 1970a).

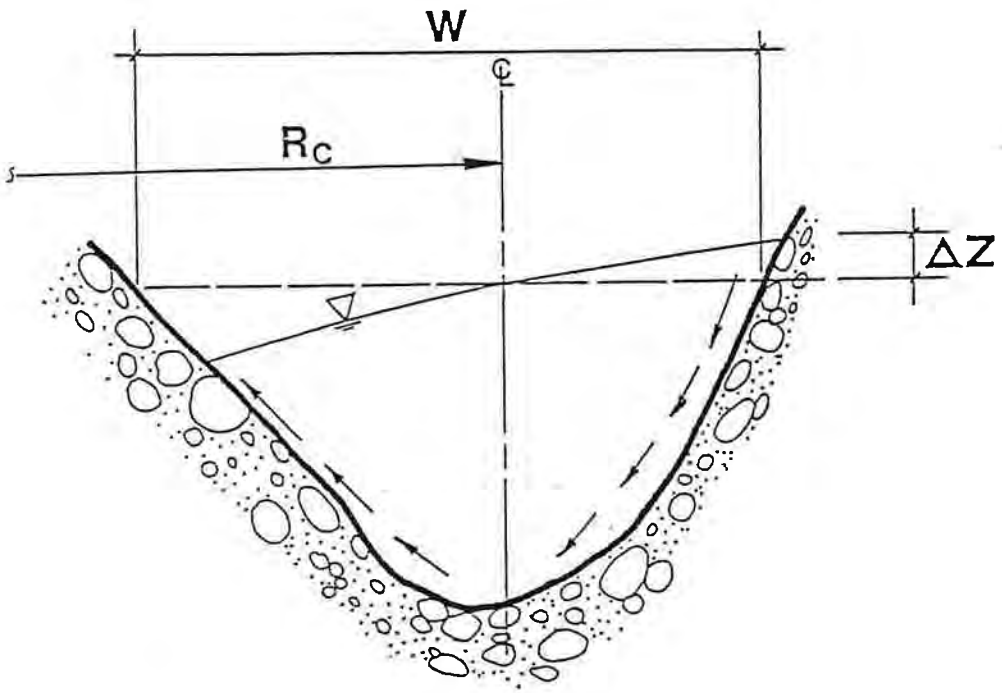


Figure 3.5. Superelevation of water surface in a bend.

$$\Delta Z = C \frac{V^2 W}{g R_c} \qquad (3.22)$$

where $g$ = acceleration of gravity in feet/second$^2$
$W$ = width of channel at centerline water surface elevation in feet
$R_c$ = radius of curvature of the centerline of the stream in feet
$\Delta Z$ = the difference in water surface elevation between the level water surface elevation at the channel centerline and the bank of the outside of the bend in feet
$V$ = average velocity in feet/second
$C$ = Coefficient (see **Table 3.3**)

Supercritical Flow in Natural Channels

Rigid boundary hydraulic analysis in arroyos often indicates supercritical flow. Due to the interaction of the water, sediment, and other boundary roughness elements, there is considerable doubt that supercritical flow conditions can be sustained, except over very short distances and very short timeframes. (Trieste, 1992) The energy loss associated with antidunes (or chutes and pools) and natural obstructions in the channel can create localized hydraulic jumps. For this reason, the sequent depth (depth to which the water surface will rise through a hydraulic jump) is recommended for determining flood elevations and floodplain limits. The following equation can be used to compute the water surface elevation associated with the sequent depth ($CWSEL_{seq}$) based on the computed supercritical water surface elevation from a rigid boundary analysis (CWSEL):

$$CWSEL_{seq} = CWSEL + 0.5(A/W)\left(\sqrt{1 + 8F_r^2} - 3\right) \qquad (3.23)$$

where $A$ = cross sectional area of the channel
$W$ = channel width
$F_r$ = Froude Number given by

$$F_r = \frac{V}{\sqrt{gY}} = \frac{Q}{A\sqrt{Ag/W}} \qquad (3.24)$$

where $V$ = average channel velocity
$Y$ = hydraulic depth
$g$ = acceleration of gravity

## 3.3 Sediment Transport in Steep, Erodible Channels

3.3.1 Introduction. The rate and magnitude of lateral and vertical adjustment of arroyo channels are dependent on the ability of the flowing water to erode and transport the material making up the channel boundary. In channels where the bed and banks are composed primarily of sand-sized material, the bed is adjustable in response to virtually the entire range of flows to which it is subjected. Channel size, shape, and gradient are therefore dependent on the magnitude and duration of the flow and the supply of

sediment from upstream sources. In channels where a significant percentage of the bed or bank material is made up of coarse gravel and cobble particles, adjustability may be limited.

Table 3.3. Superelevation Formula Coefficients (USCOE, 1970a).

| Flow Type | Channel Cross Section | Type of Curve | Value of C |
|---|---|---|---|
| Tranquil | Rectangular | Simple circular | 0.5 |
| Tranquil | Trapezoidal | Simple circular | 0.5 |
| Rapid | Rectangular | Simple circular | 1.0 |
| Rapid | Trapezoidal | Simple circular | 1.0 |
| Rapid | Rectangular | Spiral transitions | 0.5 |
| Rapid | Trapezoidal | Spiral transitions | 1.0 |
| Rapid | Rectangular | Spiral banked | 0.5 |

Other equations for superelevation are given in Richardson et al. (1990).

Incipient motion analysis provides a means for determining the ability of the flows to move the larger particles. In cases where there is a sufficient amount of coarse material in the bed or banks, an armor layer may develop that will act as a partial or complete control on the adjustability of the channel bed. The rate at which adjustment will occur depends on both the capability of the flows to transport the material and the quantity of material brought in from upstream sources. In addition to its utility in evaluating the tendency for channels to armor, the incipient motion concept is an integral part of many bed material transport relationships.

An understanding of the modes of sediment transport that occur in natural channels is important in selecting appropriate analysis techniques and interpreting the results of the analyses. **Figure 3.6** shows schematically the various modes of sediment transport. As illustrated in the figure, sediment transport can be separated into two general categories: wash load and bed material load. Wash load is that part of the total sediment load that is made up of particle sizes finer than those found in significant quantities in the bed and carried in suspension. The quantity of wash load carried by a stream is determined by the availability of material from banks and upstream areas of the watershed. Since it is controlled by the availability of material, wash load is generally not carried at the capacity of the stream. Based on the energy of the flow, the stream would

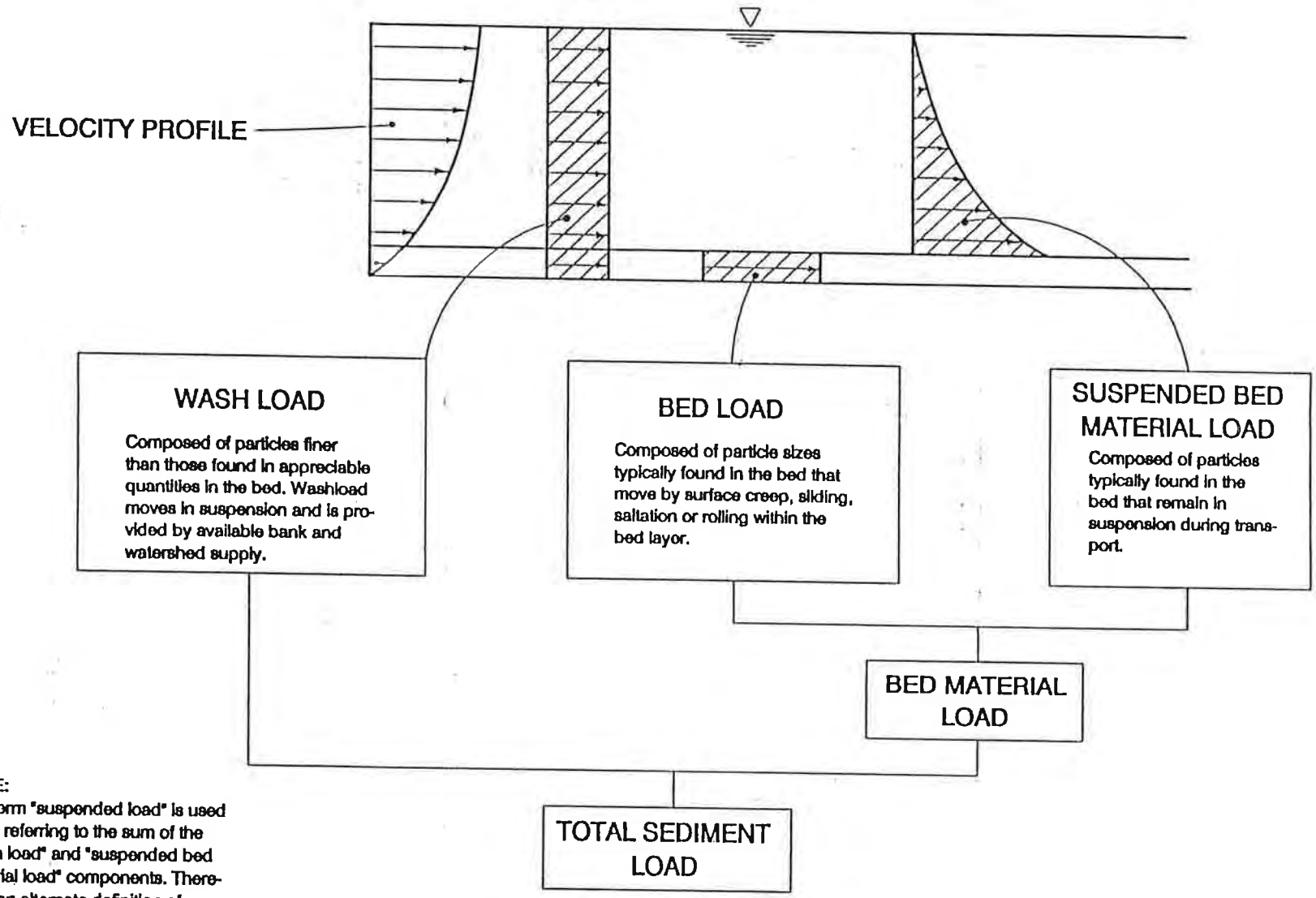


Figure 3.6. Definition of sediment load components.

usually be capable of carrying more wash load-sized sediment if it were available to the flow.

Bed material load is that part of the total sediment load that is made up of sediment sizes represented in the bed and carried both in suspension and as bed load. As shown in Figure 3.6, bed load moves in contact with the bed by various means including rolling, sliding, saltation (brief periods of suspension followed by longer periods of rest) and surface creep (gradual movement of groups of particles by a combination of gravity and fluid forces).

Since it is controlled by the availability of material from the watershed, the wash load is not directly related to the hydraulic conditions in the stream at any given time. The bed material load, on the other hand, is directly related to both the character of the bed material and the hydraulic conditions. As a rule of thumb, it is often assumed that wash load consists of silt and finer material (i.e., less than 0.0625 mm). The maximum size of sediment that can be considered as wash load can, however, vary depending on the characteristics of the stream being analyzed. In coarse-bed streams, the wash load may consist of material as large as coarse sand. Alternatively, it can be reasonably assumed that sediment finer than about the $D_{10}$ of the bed material (size for which 10 percent of the material, by weight, is finer) makes up the wash load (Richardson et al., 1990, Einstein, 1950). The quantity of wash load that a stream may be expected to carry can be estimated from the watershed sediment yield as discussed in Chapter 2. Methods of estimating bed material load are discussed in a later section of this chapter.

3.3.2 Analysis of Bed and Bank Material. Bed material is the sediment mixture of which the streambed is composed. Bed material can range in size from large boulders to fine clay particles. Knowledge of the bed material size gradation is necessary for most sediment transport analyses, including incipient motion, armoring potential, sediment transport capacity, and scour.

Bank material usually consists of particles the same size as, or smaller than, the bed particles. As a result, banks are often more easily eroded than the bed, unless protected by vegetation, cohesion, or channel lining.

Of the various sediment properties, size has the greatest significance to the hydraulic engineer since it is the most readily measured and related to other properties that affect the ability of the water to erode and transport the sediment particles. The size of individual particles is less important to the analysis of the channel stability than the distribution of sizes making up the bed and banks.

Particle size gradations consisting of significant quantities of clay material, are cohesive in nature. The strength of the cohesive bond will affect the resistance of that material to erosion. Particle size gradations having significant amounts of coarse gravel and cobbles may inhibit the ability of the channel to erode through the armoring process.

The characteristics of the bed and bank material are generally determined by collecting and analyzing representative samples. Important factors to consider in determining where and how many bed and bank material samples to collect include:

1. Size and complexity of the study area
2. Number, lengths, and drainage areas of tributaries
3. Evidence of or potential for armoring
4. Structural features that can impact or be significantly impacted by sediment transport
5. Bank failure areas
6. High bank areas
7. Areas exhibiting significant sediment movement or deposition (i.e., bars in channel)

Tributary sediment characteristics can be very important to channel stability, since a single major tributary or tributary source area could be the predominant supplier of sediment to a system.

The depth of bed material sampling depends on the homogeneity of surface and subsurface materials. Where possible, it is desirable to include material to some depth in establishing bed material characteristics. For example, in sand/gravel-bed systems the potential existence of a surface layer of coarser sediments on top of relatively undisturbed subsurface material must be considered. Samples containing material from both layers would contain materials from two populations in unknown proportions, and thus it is typically more appropriate to sample each layer separately. If the purpose of the sampling is to evaluate hydraulic friction or initiation of bed movement, then the surface sample will be of most interest. Conversely, if bed material transport during a flood large enough to disturb the surface layer is important, then the underlying layer may be more significant. It should be noted that the material found in bars is a good indication of the sizes of material being transported by the flow as bed material load.

Methods of sampling depend on the characteristics of the material being sampled and the intended use of the resulting gradation. The most common sampling method consists of collecting a quantity of material from the appropriate location (grab sample) and using standard laboratory analysis to determine the gradation of the material. **Table 3.4** provides guidelines for the minimum weight of samples to insure that the sample is large enough to be representative of the material being tested.

When the material is so coarse that a representative grab sample would be prohibitively large, the surface gradation can be estimated using the photographic grid technique. This method can be accomplished by laying a 2-foot by 2-foot grid sub-divided into 0.2-foot grids on a representative location, photographing the grid, and analyzing the distribution of sizes falling under the intersection of the grid points. Details of this method are discussed in Kellerhals and Bray (1971).

| Table 3.4. Minimum Recommended Sample Weights for Sieve Analysis (USCOE, 1970b). | | |
|---|---|---|
| Maximum Particle Size | Minimum Weight of Sample | |
| | h (grams) | lb |
| 3-inch | 6,000 | 13 |
| 2-inch | 4,000 | 9 |
| 1-inch | 2,000 | 14 |
| 1/2-inch | 1,000 | 2 |
| Finer than No. 4 sieve | 200 | 0.5 |
| Finer than No. 10 sieve | 100 | 0.25 |

When the material is too large to be sampled by the grid method, the sample area is under water or a sample over a larger area is desirable, the pebble count technique can be used. This method involves pacing back and forth across the area to be sampled in a grid pattern, picking up and measuring the intermediate axis of the stone at the toe of the boot at each pace, and analyzing the size distribution of those stones. This method is described in Wolman (1954) and Kellerhals and Bray (1971). In analyzing the size gradation of the samples obtained using the pebble count technique, it has been demonstrated (Kellerhals and Bray, 1971) that the percent-by-count method is the most directly equivalent to the percent-by-weight that would be obtained by laboratory sieving.

### 3.3.3 Incipient Motion and Armoring

Estimation of the Incipient Particle Size. Incipient motion refers to the condition where the hydrodynamic forces acting on a grain of sediment are of sufficient magnitude that, if increased even slightly, the grain will move. Under critical conditions, or at the point of incipient motion, the hydrodynamic forces acting on the grain are just balanced by the resisting forces of the particle. In cases where there is a significant amount of coarse material (gravel and cobbles) in the bed, the relative susceptibility of the channel bed to degradation can be evaluated by analyzing the magnitude of flows required to produce incipient motion conditions.

Incipient motion conditions are analyzed using the Shields relation which is given by:

$$D_c = \frac{\tau_o}{F_*(\gamma_s - \gamma)} \tag{3.25}$$

where $D_c$ = diameter of the sediment particle at incipient motion conditions
$\tau_o$ = bed shear stress
$\gamma_s$ & $\gamma$ = specific weights of sediment and water, respectively
$F_*$ = dimensionless shear stress often referred to as the Shields parameter (Typical values for $F_*$ range from .03 to .06; a value of 0.047 is used in the Meyer-Peter, Muller Equation)

For gradually varied flow, the boundary shear stress is given by Equation 3.8 which represents the total shear stress acting on the channel and is derived from a simple force balance between the flowing water and the channel boundary. For sediment transport purposes, only the shear acting on the individual particles in the bed (referred to as grain shear) should be considered (Meyer-Peter and Muller, 1948; Taylor and Brooks, 1962; Bajorunas, 1952). When significant bed forms are present in the flow, the channel boundary contains large immobile particles, or there are irregularities in the channel, Equation 3.8 may overestimate the shear stress acting on the individual grains. For these cases, an equation based on the vertical velocity profile is recommended. This equation is given by:

$$\tau_0 = \frac{\rho V^2}{\left[5.75 \log (12.27 \frac{y_0}{k_s})\right]^2} \tag{3.26}$$

where $V$ = average velocity in the channel
$k_s$ = characteristic grain size (usually taken as 3.5 $D_{84}$ of the bed material)
$y_o$ = flow depth

Note that Equation 3.26 is identical to Equation 3.9, where:

$$f = 8 \,/\, [5.75 \log (12.27 \frac{y_o}{k_s})]^2 \tag{3.27}$$

Evaluation of the incipient size for various discharges provides information on the magnitude of flood that might disrupt channel stability. The results of such an analysis are generally most useful when applied to gravel- or cobble-bed systems. When applied to sand-bed channels, incipient motion results usually show that all particles in the bed material are capable of being moved by even very small discharges.

Evaluation of Armoring Potential. Armoring occurs when material finer than the incipient size is winnowed (or removed) from the channel bed leaving a layer of coarser, relatively immobile material on the surface. This process occurs because the finer particles in the bed are inherently more transportable than the coarser particles. As sediment movement continues, an increasing percentage of coarse particles accumulate in the surface layer. In a degradational stream, if sufficient coarse particles are present in the bed material, a layer of particles larger than the incipient size can accumulate to shield, or "armor" the entire bed surface, arresting further degradation.

An armor layer sufficient to protect the bed against moderate discharges can be disrupted during high flow, but may be restored as flows diminish. Therefore, as in any hydraulic design, the analysis must be based on a certain magnitude event. If the armor layer is stable for that event, it is reasonable to conclude that no degradation will occur under design conditions. However, flows exceeding the design event may disrupt the armor layer, resulting in degradation.

Potential for development of an armor layer can be assessed using incipient motion analysis and a bed material gradation typical of the material within the depth of anticipated degradation. For given hydraulic conditions, the incipient particle size can be computed using the Shields relation (Equation 3.25). If no sediment of the computed size or larger is present in significant quantities in the bed, armoring will not occur. Within practical limits of planning and design, the $D_{95}$ size is considered to be about the maximum size for pavement formation (Gessler, 1970a). Therefore, armoring is probable when the computed incipient size is equal to or smaller than the $D_{95}$ size of the bed material.

By observing the percentage of the bed material equal to or larger than the incipient particle size ($D_c$), the depth of scour necessary to establish an armor layer can be calculated using the following relation (USBR, 1984):

$$Y_s = y_a\left(\frac{1}{P_c} - 1\right) \qquad (3.28)$$

where $y_a$ is the thickness of the armor layer and $P_c$ is the decimal fraction of material coarser than the armoring size. The thickness of the armor layer ($y_a$) is normally assumed to be in the range from 2 to 3 times the critical particle size ($D_c$). Equation 3.28 is conceptually illustrated in **Figure 3.7.** Field observations suggest that an armor layer thickness of approximately twice the diameter of the incipient particle size is usually necessary for stability, thus the minimum recommended value for $y_a$ in Equation 3.28 is $2D_c$. To increase the factor of safety of a design based on the armor depth indicated by Equation 3.25, values of 2 to 4 times $D_c$ may be used.

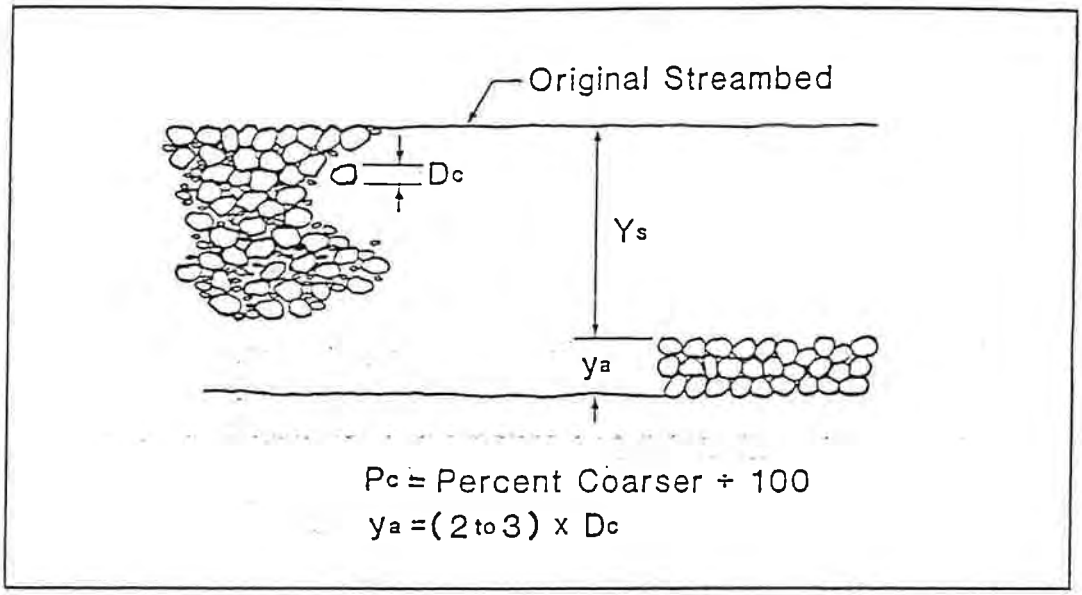


Figure 3.7. Conceptual illustration of armor layer development.

3.3.4 Methods for Computing Bed Material Transport Capacity. Quantitative analysis of the aggradation/degradation and lateral migration tendency of a stream requires knowledge of both the sediment transport capacity of the stream and the sediment supply. (see Section 3.4.1 for a discussion of the sediment continuity concept). Numerous equations are available for estimating the bed material transport capacity. (See for example, Vanoni, 1977; Simons, Li & Associates, Inc., 1982a; Chang, 1988.) These equations consider the hydraulic conditions (i.e., velocity, depth, width, shear stress, stream power, etc.) in various combinations and the size characteristics of the bed material. **It is important to note that the bed material transport rate computed from these equations does not include the wash-load component of the total sediment load (see Figure 3.6).**

Most available bed material transport equations are essentially empirical in nature, with the independent variables, and to a lesser extent, their form, selected from either dimensional analysis or theoretical considerations. Since the specific parameters in the equations are mostly derived from empirical data, the equations should be applied to field conditions that are similar to those for which they were developed. For example, some formulas were developed from data collected in sand-bed streams where most of the sediment is transported as suspended load. Other equations pertain to streams where bed-load transport is dominant. If sufficient information is available, it is sometimes possible to calibrate the parameters to improve the accuracy of the results.

The conditions for which most of the available bed material transport relations were developed are significantly different from those encountered in most arroyos in the Albuquerque area, due to the combination of steep gradients and relatively small sediment sizes found in the typical arroyos. In spite of this shortcoming, various transport equations have been applied to specific projects in the area. Several of these relations are discussed in the following sections to provide a basis for understanding previous studies. These include the Meyer-Peter, Muller-Einstein (MPM-Einstein) method, the Colby method, Yang's equation, and an empirical power function relation developed by Zeller and Fullerton (1983).

In addition to the above, a power function relation developed by Resource Consultants & Engineers, Inc. (Mussetter, 1993, in-press) specifically for steep, sand-bed channels with high suspended sediment concentrations is presented. As discussed below, this relation overcomes many of the shortcomings of the other relations when applied to steep, sand-bed channels such as those found in the Albuquerque area and thus may provide more realistic results over the range of conditions encountered in these channels. **It is recommended that this power function relation (Equation 3.41) be used in the Albuquerque area, unless further analysis and calibration demonstrates that other methods are more representative of actual conditions.**

Meyer-Peter, Muller-Einstein Method

This method gives good results when both the bed-load and suspended load compose a significant portion of the total bed material load. The Meyer-Peter, Muller (MPM) formula, because of its formulation as an excess shear stress equation, is well suited to modeling the transport of sand as well as gravel- and cobble-sized material. The formula, rearranged by USBR (1960), is given by:

$$q_b = \frac{12.85}{\sqrt{\rho}\gamma_s}(\tau_0 - \tau_c)^{1.5} \qquad (3.29)$$

where $q_b$ = bed load transport capacity per unit width of channel (cfs/ft) for particle size i
$\rho$ = density of water (1.94 slugs/cu ft)
$\gamma_s$ = unit of weight of the sediment (pounds/cu ft)
$\tau_0$ = bed shear stress in (lb/sq ft)
$\tau_c$ = critical shear stress (lb/sq ft)

The value of $\tau_c$ is computed from the Shields relation (Equation 3.25) with Shields dimensionless shear stress equal to 0.047. (Note that at critical conditions the bed shear and critical shear are equal, thus $\tau_c$ is obtained by substituting $\tau_c$ for $\tau_o$ in Equation 3.25 and rearranging.) To apply Equation 3.29 by size fraction, divide the particle size distribution into discrete size ranges (usually 5 to 10 ranges is sufficient), compute the

geometric mean of each size range and compute the unit bed load, transport capacity is the sum of each transport capacity times the percentage of material in each size range given by:

$$q_{Btotal} = \Sigma\, q_{Bi}\, \Delta\%_i \qquad (3.30)$$

where $q_{Btotal}$ = transport capacity
$q_{Bi}$ = transport capacity of the i-th size range
$\Delta\%_i$ = incremented percentage of material in the i-th size range

The suspended sediment-transport capacity is estimated using a solution developed by Einstein (1950). This method relies upon integration of the sediment concentration profile over the depth of flow assuming equilibrium conditions such that the rate at which sediment is transported upward due to turbulence is exactly equal to the rate at which the sediment is settling downward due to gravity. This equilibrium condition is described by the diffusion equation. The equations used in this method are quite complex and are beyond the scope of this Design Guide. They are discussed in detail in Vanoni (1977) and Simons, Li & Associates, Inc. (1982a). Additional discussion of the applicability of the method and computer code to solve the equations is presented in USGS (1989).

Yang's Bed Material Equation

Yang (1972) developed a relationship for the concentration of bed material discharge as a function of the rate of energy dissipation in the flow using dimensional analysis and the unit stream power concept. The basic form of Yang's equation is

$$\log C_s = M + N \log \frac{VS}{\omega} \qquad (3.31)$$

where $C_s$ = bed material concentration in ppm by weight
V = flow velocity
S = slope
$\omega$ = fall velocity of the sediment
M and N = dimensionless parameters related to the flow

The values of M and N were determined by regression analysis of laboratory data.

For sand-bed conditions, Yang's equation is given by:

$$\log C_s = 5.435 - 0.286\log\frac{\omega D_{50}}{\nu} - 0.457\log\frac{V_*}{\omega} + \left(1.799 - 0.409\log\frac{\omega D_{50}}{\nu} - 0.314\log\frac{V_*}{\omega}\right)\log\left(\frac{VS}{\omega} - \frac{V_*S}{\omega}\right) \quad (3.32)$$

where $\nu$ = kinematic viscosity
$V_*$ = shear velocity given by:

$$V_* = \sqrt{(gRS)} \quad (3.33)$$

For gravel-bed conditions, Yang's equation is given by:

$$\log C_s = 6.681 - 0.633\log\frac{\omega D_{50}}{\nu} - 4.816\log\frac{V_*}{\omega} + \left(2.784 - 0.305\log\frac{\omega D_{50}}{\nu} - 0.282\log\frac{V_*}{\omega}\right)\log\left(\frac{VS}{\omega} - \frac{V_*S}{\omega}\right) \quad (3.34)$$

In the above equations, the dimensionless critical velocity ($V_{cr}$) is given by:

$$\frac{V_{cr}}{\omega} = \frac{2.5}{\log\frac{V_* D_{50}}{\nu} - 0.06} + 0.66 \quad for \quad 1.2 < \frac{V_* D_{50}}{\nu} < 70 \quad (3.35)$$

and

$$\frac{V_{cr}}{\omega} = 2.05 \quad for \quad \frac{V_* D_{50}}{\nu} \geq 70 \quad (3.36)$$

The sand equation is applicable for sizes up to 2 mm and the gravel equation is applicable for sizes between 2 and 10 mm. The equations can be applied by size fractions using the following relation:

$$C_s = \sum p_i C_{si} \quad (3.37)$$

where $p_i$ = percentage of sediment in the i-th size range
$C_{si}$ = concentration from Equations 3.32 or 3.34 for the geometric mean size of the i-th size range

Colby's Method

Colby (1964) developed the graphical procedure shown in **Figures 3.8 and 3.9** for determining bed material discharge (tons/day of dry sediment) in sand-bed channels. In developing his computational curves, Colby was guided by Einstein's bed-load function (Einstein, 1950) and an immense amount of data from streams and flumes (Simons and Richardson, 1966). However, it should be understood that all curves for the 100-foot depth, most curves of the 10-foot depth, and some of the curves of 1.0-foot and 0.1-foot depths (Figure 3.8) are not based entirely on data, but are developed from limited data and theory.

In utilizing Figures 3.8 and 3.9 to compute the bed material discharge, the following procedure is used:

1. Estimate the mean velocity (V), depth (Y), median-size bed material ($D_{50}$), water temperature, and fine-sediment concentration ($C_f$):

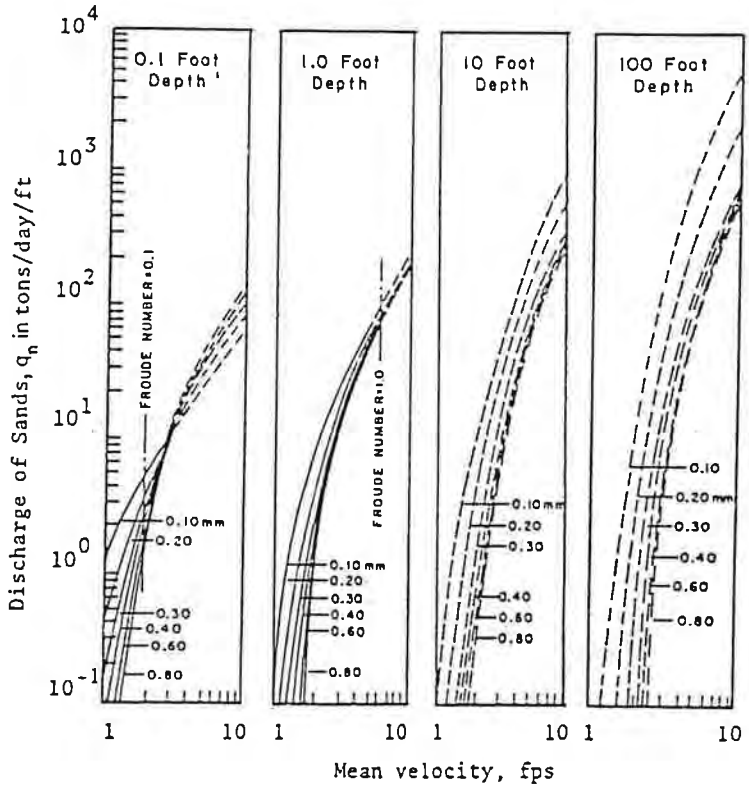


Figure 3.8. Colby's curves for discharge of source vs. mean velocity for various increments of flow depth (Colby, 1964).

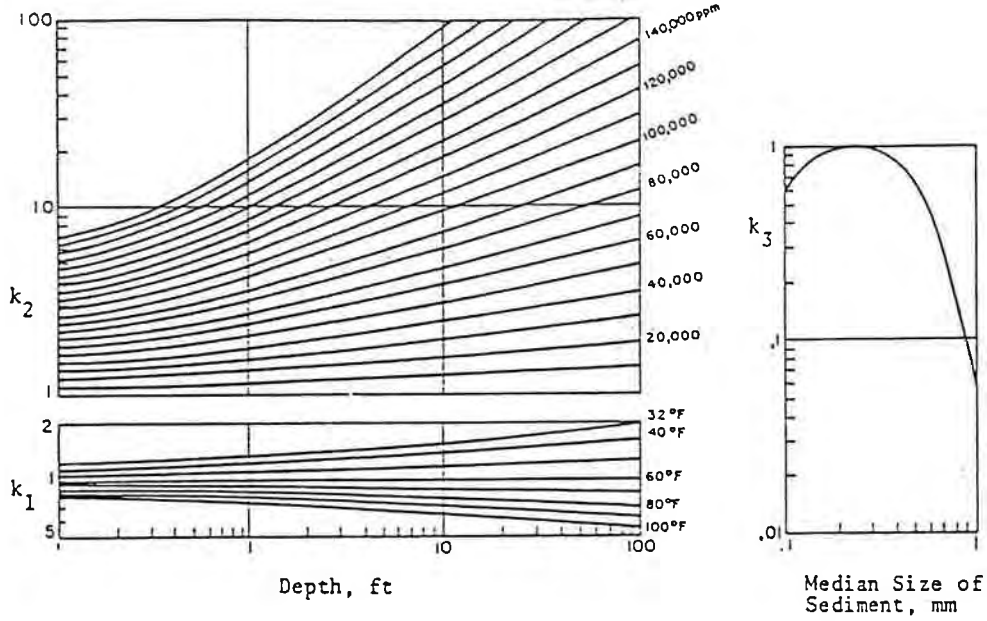


Figure 3.9. Colby's corrections factors (Colby, 1964).

2. Estimate the uncorrected bed material discharge for V and $D_{50}$ from Figure 3.8 for the two depths that bracket Y. Use logarithmic interpolation between the two depths to determine the uncorrected unit bed material discharge ($q_{si}$) for the given conditions.

3. Estimate the correction factors for water temperature ($k_1$), fine sediment concentration ($k_2$), and sediment size ($k_3$) from Figures 3.9a and 3.9b. Compute the corrected unit bed material discharge using the following relation:

$$Q_s = [1 + (K_1K_2 - 1)k_3]\ q_{si} \qquad (3.38)$$

The fine sediment concentration refers to the concentration by weight of silt and clay-sized sediment (wash load) in the water/sediment mixture and can be derived from the watershed sediment yield analysis. As shown in Figure 3.9a, $k_1 = 1$ when the temperature is 60° F, $k_2 = 1$ when the concentration of fine sediment is negligible, and $k_3 = 1$ when $D_{50}$ lies between 0.2 and 0.3 mm.

Power Function Relations

To simplify calculations associated with the channel stability analyses, the bed material transport capacity for a range of flow and bed material conditions can be computed using one of the previous methods and power function relations of the following form developed using multiple regression:

$$q_s = aY^bV^c \tag{3.39}$$

where $q_s$ = unit width bed material transport capacity
$Y$ = hydraulic depth
$V$ = average velocity

Zeller and Fullerton Relation. One such relationship was developed by Zeller and Fullerton (1983) for low fine sediment loads. This relationship is given by:

$$q_s = 0.0064 \frac{n^{1.77} V^{4.32} G^{0.45}}{Y^{0.30} D_{50}^{0.61}} \tag{3.40}$$

where $G$ = gradation coefficient of the bed material, given by Equation 3.14.

*(Note that $D_{50}$ in Equation 3.40 is in millimeters; all other variables are in the foot-pound-second system. Also note that Equation 3.40 is identical to Equation 3.39 for a given channel resistance (n) and bed material gradation ($D_{50}$, G).)* ***Table 3.5*** *summarizes the range of conditions for which Equation 3.40 was developed.*

Effect of Fine Sediment Concentration on Bed Material Transport Capacity

Leopold and Miller (1956) observed suspended sediment concentrations in arroyos in north central New Mexico approaching 200,000 ppm by weight (9 percent by volume). Nordin (1963) reported concentrations in the Rio Puerco, Paria, and Little Colorado Rivers as high as 650,000 ppm by weight (41 percent by volume), with sand concentrations up to nearly 450,000 ppm by weight (24 percent by volume). Others (Beverage and Culbertson, 1964; Lane, 1974) have reported similar observations. Based on the watershed sediment yield discussions in Chapter 2, similar concentrations may occur in the arroyos in the Albuquerque area during large storm events.

| Table 3.5. Range of Conditions for Which Equation 3.40 is Applicable. | |
|---|---|
| Parameter | Range |
| Velocity | 3-30 (ft/sec) |
| Manning's n | 0.018-0.035 |
| Bed Slope | 0.001-0.040 |
| Unit Discharge | 10-200 (cfs/ft) |
| Particle Size | $0.05 \text{ mm} \leq D_{50} \leq 10 \text{ mm}$ |
| Depth | 1-20 ft |
| Gradation Coefficient | 2-5 |

The presence of high concentrations of fine suspended sediment enhances the capacity of the stream to transport coarser sediments (Vanoni, 1977). As a result, the bed material loads computed from the relationships discussed in the previous section should be adjusted accordingly. The following procedure is recommended:

1. Compute the bed material load ($q_{si}$) using one of the previous relationships,

2. Estimate the fine sediment concentration based on the watershed sediment yield relationships discussed in Chapter 2, or from field data, and

3. Use **Figure 3.9** and Equation 3.38 from Colby's procedure to correct the clear water estimate of bed material load for the presence of high suspended sediment concentrations.

Transport Equation for High Suspended Sediment Concentrations

The above relations were developed primarily for channels carrying relatively low concentrations of suspended sediment. Under intense flow conditions in steep, sand bed streams, the suspended sand concentration can be very large. The presence of silt and clay in the mixture can result in further significant increases in the suspended sand concentration. The Einstein suspended sediment method (see MPM-Einstein method above) is based on Rouse's (1937) equation for the suspended sediment concentration profile, which was derived from the diffusion equation.

For suspended sediment concentrations less than about 4 percent by weight, the original derivation provides reasonable results for most conditions. Einstein and Chien (1955) however, found that the vertical distribution of sands in the water column deviates significantly from that predicted by the original Einstein method for suspended sediment concentrations above approximately 4 percent, The concentration profile becomes progressively more uniform with depth with increasing concentration. Based on their experimental results, they suggested a correction for the exponent on the concentration profile equation to partially compensate for the differences. Subsequent investigators (Chien and Wan, 1965; Ordonez, 1970; Lavelle and Thacker, 1978, van Rijn, 1984; Woo, 1985 and Woo et al., 1988) considered the effects of fall velocity reduction, fluid viscosity, and fluid density on the suspended sand concentration profile. The work of Woo (1985) and Woo et al. (1988) resulted in a complex differential equation that appears to account for the significant changes in fluid characteristics with increasing sediment concentration, and converges to essentially the same solution as obtained from Rouse's (1937) equation at low concentrations. Results obtained from the application of this relationship match the available measured data well.

Mussetter (1993, in-press) linked Woo's (1985) relationship for computing the suspended sediment concentration with the MPM bed-load equation to obtain a method for computing bed material load in streams carrying high concentrations of suspended sediment. Results obtained from this method were compared with the results from other available relations and, to the extent possible, measured sediment yield data. This comparison indicates that the new method may provide more realistic results over the range of flow and sediment transport conditions encountered in arroyos in the Albuquerque area.

The MPM-Woo method was used to estimate bed material transport capacities for a broad range of hydraulic and bed material conditions (see **Table 3.6**) typical of the Albuquerque area. The results of these computations were then used to develop the following power function relation using multiple regression:

$$q_s = a' V^b Y^c (1 - C_f/10^6)^d \qquad (3.41)$$

Table 3.6. Range of Conditions for which Equation 3.41 was Developed.

| q (cfs/ft) | V (vps) | Y (ft) | $S_o$ | $C_f$ (ppm) | $D_{50}$ (mm) |
|---|---|---|---|---|---|
| 1 | 1.9 | 0.3 | 0.005 | 0 | 0.2 |
| 80* | 20.8* | 7.2* | 0.04* | 60,000* | 4.0* |

* Larger values may be used with expected loss of accuracy; the amount of inaccuracy is unknown, but would depend on the specific conditions being analyzed.

where $q_s$ = unit width **bed material** load in cfs/ft
$V$ = average velocity in fps
$Y$ = hydraulic depth in feet
$C_f$ = fine sediment (silt and clay) concentration by weight.
$S_o$ = channel slope

Values for the coefficient (a) and exponents (b, c, and d) are shown in **Figure 3.10** as a function of the median bed material size. **In applying Equation 3.41, the predicted bed material concentration ($C_s$) should not exceed the maximum concentration given by the equation:**

$$C_{s_{max}} = 510{,}000 - 65{,}000\ D_{50} \tag{3.42}$$

where $D_{50}$ = medium bed material size in mm
$C_s$ = bed material concentration by weight computed from the relation:

$$C_s = \frac{2.65\ x\ 10^6 Q_s}{(Q + 2.65 Q_s)} \tag{3.43}$$

and

$$Q_s = q_s W \tag{3.44}$$

When $C_{smax}$, as given by Equation 3.42 is exceeded, non-Newtonian flow conditions are indicated and the assumptions upon which Equation 3.41 (and the other bed material transport equations presented in this Design Guide) is based are no longer valid. For these conditions, procedures applicable for non-Newtonian fluids (e.g., mudflows) should be considered.

Note that Equation 3.41 predicts bed material load only; the total sediment load is computed by adding the bed material and fine sediment loads, where the fine sediment load is computed from:

$$Q_{s_f} = \frac{C_f\ Q}{2.65\ x\ 10^6} \tag{3.45}$$

and the total sediment load is given by:

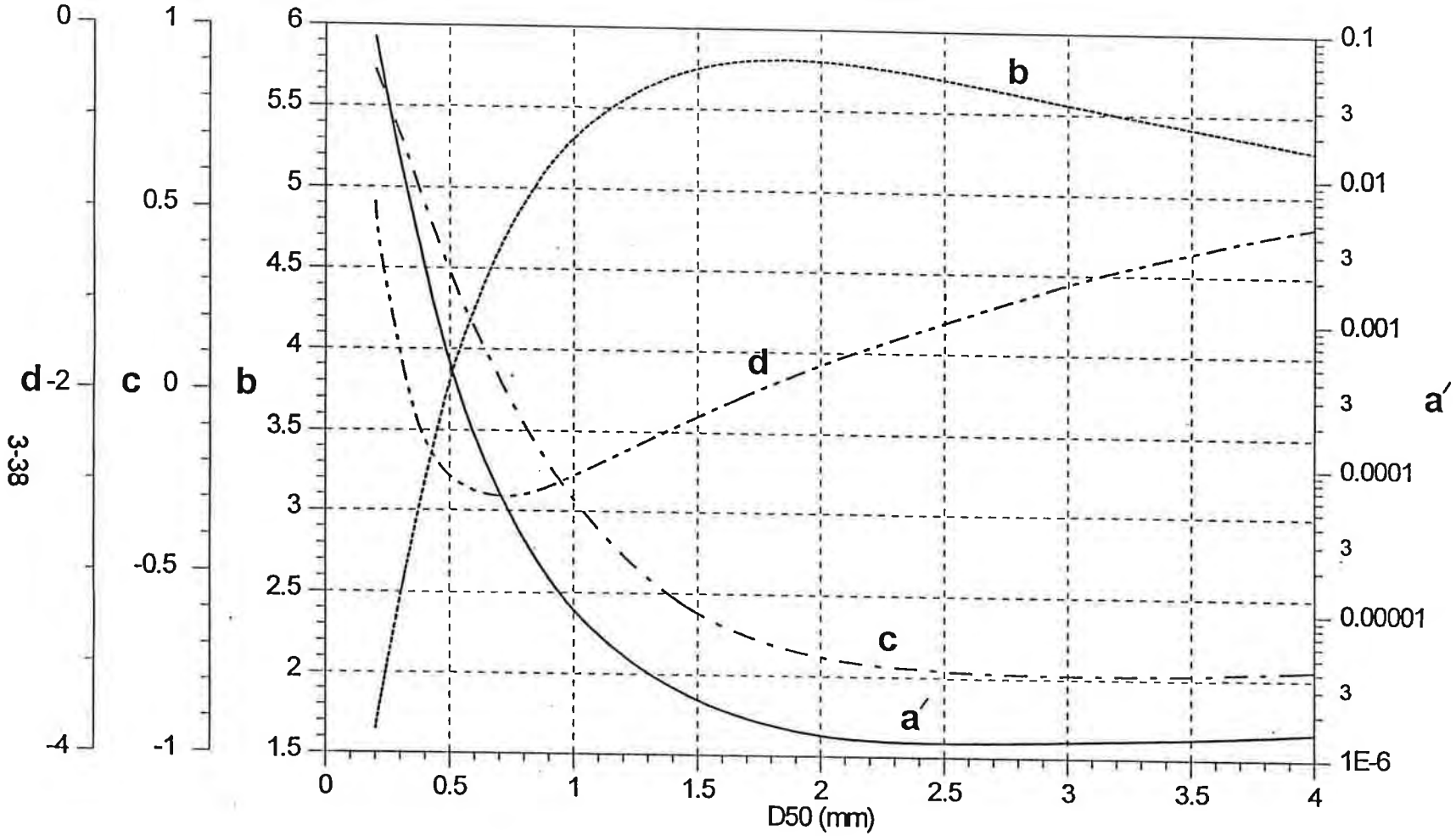


Figure 3.10. Coefficient and exponents for Equation 3.41, developed using MPM-Woo method.

$$Q_{s_{total}} = Q_s + Q_{s_f} \tag{3.46}$$

Derivation of Equation 3.41 and Figure 3.10 involved the following assumptions:

1. The bed load was computed by size fraction using the MPM bed-load equation.

2. The suspended sediment load is computed for the median size only due to the mathematical formulation of the differential equation used in the computation.

3. The bed layer thickness used to estimate the reference concentration for the suspended sediment computations was assumed to vary as a function of the ratio of the shear velocity ($V_*$) to the critical shear velocity ($V_{*_{cr}}$) for the median particle size, following Karim and Kennedy (1983), limited to values between $2D_{50}$ and $2D_{84}$. The reference bed layer concentration was limited to values not exceeding 650,000 ppm by weight.

4. The viscosity of the fine sediment/water mixture was estimated using the following empirical relationship suggested by O'Brien and Julien (1989), and Julien and Lan (1991):

$$\mu = \alpha e^{\beta C_v} \tag{3.47}$$

where $\mu$ = dynamic viscosity in lb-s/ft$^2$

The values of $\alpha$ and $\beta$ of $2.38 \times 10^{-5}$ and 9.21, respectively, were developed from Figure 2 in Julien and Lan (1991) for the data sets excluding O'Brien and Julien (1989). These data were excluded because they were based on highly bentonitic clays in suspension which, as indicated by the figure have a significant effect on the viscosity of the fluid which would not be expected to occur for materials in the Albuquerque area (Julien, 1992, personal communication). The kinematic viscosity used in the suspended load computation was computed from:

$$\nu = \frac{\mu}{\rho_f} \tag{3.48}$$

where $\rho_f$ = bulk density of the water sediment mixture computed from:

$$\rho_f = \rho\ [1-(1-S)\ C_v/10^6] \qquad (3.49)$$

where $C_v$ = sediment concentration by volume

$C_v$ is related to the fine sediment concentration by weight ($C_f$) by the relation:

$$C_v = \frac{C_f/10^6}{SG-(C_F/10^6)\ (SG-1)} \qquad (3.50)$$

5. The fall velocity of the sediment was computed using Ruby's equation (Simons and Senturk, 1976) for clear water adjusted for the presence of fine sediment using the relation suggested by Maude and Whitmore (1958) given by:

$$\omega_s = \omega\ (1-C_v/10^6)^{3.5} \qquad (3.51)$$

where $\omega$ = fall velocity in clear water
$\omega_s$ = fall velocity in the water/sediment mixture;

To prevent unrealistically high bed material concentrations, the reference bed layer concentration is limited to values less than 650,000 ppm by weight. As discussed in the previous section, this is the approximate upper limit for mud flooding. Above this value, the water/sediment mixture is no longer a Newtonian fluid and the basic hydraulic and sediment transport assumptions no longer apply. Mud and debris flows occur at higher concentrations. Based on field evidence in the Albuquerque area, mud and debris flows have occurred in the past in steeper areas at the base of the Sandia front, but are of very limited extent and probably are of limited time during the passage of any given hydrograph. The 650,000 ppm limitation is, therefore considered to be reasonable for conditions where the analysis procedures in this Design Guide are applicable.

### 3.3.5 Effect of Sediment Load on Fluid Characteristics

The bed material sediment yield associated with individual storms in incising arroyos is limited by the capability of the water to carry the available sediment. Sediment transport relationships can be used to estimate the capacity of a given channel to carry sediment under approximately steady conditions. In steep channels with very erodible material, extremely high concentrations of sediment can occur. Additionally, due to the unsteady nature of the flow during major storm events, sediment concentrations can significantly exceed those predicted by the equations.

Previous studies of high concentration water and sediment flows have established limits on the amount of sediment that can physically be carried by the flow. **Table 3.7** is a summary of sediment concentration limits associated with various types of high concentration flows. For concentrations exceeding approximately 65 percent by weight, the water/sediment mixture is no longer a Newtonian fluid and the basic hydraulic and sediment transport assumptions no longer apply. Mud and debris flows occur at higher concentrations.

Mud and debris flows are rare in the Albuquerque area because the amount of cohesive material in the watershed soils is relatively small and, with the possible exception of the slopes below the Sandia Crest, overland slopes are generally too flat to sustain mud-flow conditions. There is, however, field evidence of historic mud and debris flows along the base of the Sandia Mountains in the Northeast Heights area of Albuquerque, although these appear to be of limited extent. **For purposes of this Design Guide, it is reasonable to assume that the maximum sediment concentration that can be expected in the arroyos will not exceed the upper limit of mud flooding, a concentration of approximately 65 percent by weight.**

For water flood conditions with sediment concentration less than approximately 10 percent (100,000 ppm) by weight, the effect of the entrained sediment on the total volume of the water/sediment mixture is relatively small. For high concentration flows associated with mud flooding and mud flows, the total volume of the mixture is considerably larger than the water volume alone. If the sediment concentration is known, the total volume of the mixture can be estimated using the following relationship:

$$V_m = B_f V_w \tag{3.52}$$

where $V_m$ is the total volume of the mixture, $V_w$ is the clear-water volume, and $B_f$ is the bulking factor. The bulking factor ($B_f$) can be computed by:

Table 3.7. Fluid Matrix Characteristics (O'Brien, 1986).

| Type of Flow | Solids Concentration by Volume $C_v$ (%) | Solids Concentration by Weight $C_w$ (%) | Flow Characteristics |
|---|---|---|---|
| Landslide | >64% | >88% | Will not flow; failure by block sliding or tumbling. Unsaturated soil conditions. |
| Landslide | 50%-64% | 73%-88% | Will not flow; block sliding failure with some internal deformation, slow creep prior to failure; saturated. |
| Mudflow | 45%-50% | 69%-73% | Flow initiates; plastic deformation with slow sustained creep. Begins spreading; moves subject to repeated vibration. |
| Mudflow | 40%-45% | 65%-69% | Mixes easily; shows some fluid properties. Surface may be inclined at rest. Waves dissipate rapidly. |
| Mud flood | 35%-40% | 59%-65% | Spreads on horizontal surface; marked particle settling, liquid horizontal surface, two-phase separation in quiescent condition;' waves travel easily. |
| Mud flood | 30%-35% | 54%-59% | Sand and gravel settle; distinct wave action. |
| Mud flood | 20%-30% | 41%-54% | Particles rest on bottom in wave motion. |
| Water flood | <20% | <41% | Water flood with bed and suspended load. |

$$B_f = \frac{1}{1 - \frac{C_s/10^6}{S-(C_s/10^6)\ (S-1)}} = \frac{Q + Q_{s_{total}}}{Q} \qquad (3.53)$$

where $C_s$ is the **total** sediment concentration by weight and S is the specific gravity of the sediment. **Figure 3.11** shows the relationship between the bulking factor and concentration for sediment with a specific gravity of 2.65. As shown in the figure, the upper limit of mud flooding with a concentration by weight of about 65 percent (650,000 ppm) corresponds to a bulking factor of about 1.7 (i.e., the total volume of the water/sediment mixture is about 1.7 times the clear-water volume).

## 3.4 Evaluation of Channel Adjustments

3.4.1 Sediment Continuity. Vertical adjustment of stream channels results from removal of sediment from the channel bed (degradation or scour) or deposition of sediment on the channel bed (aggradation). Within a given reach, the magnitude of vertical adjustment is a function of the difference between the amount of sediment that is carried into the reach by the flow (supply) and the amount that is carried out of the reach (capacity). This concept is a simple statement of the law of conservation of mass. It is commonly referred to as the continuity concept and forms the basis for estimating the magnitude of adjustments to the channel cross section that may occur in response to a given sequence of flows. The sediment continuity concept, illustrated in **Figure 3.12**, can be expressed by the following equation:

$$\Delta V = V_{s\ (inflow)} - V_{s\ (outflow)} \qquad (3.54)$$

where $\Delta V$ = volume of sediment stored (+) or lost (-) in the reach
$V_{s(inflow)}$ = volumetric sediment transport rate into the reach from upstream and material sources
$V_{s(outflow)}$ = volumetric sediment transport rate out of the reach

For aggradation and degradation calculations, the sediment transport and sediment volume in Equation 3.54 relate only to the bed material load. For most conditions, wash load is assumed to pass through the reach since it is carried in suspension and has little interaction with the bed of the channel. The sediment transport rate out of the reach ($Q_{s(outflow)}$) is, therefore, assumed to be the bed material transport capacity, which can be estimated using the procedures described in the previous section. The sediment inflow rate is the sum of the bed material transport capacity (or supply) of the upstream channel and any input of bed material-sized sediment from lateral sources, including tributaries, sheet flow, or bank erosion within the reach.

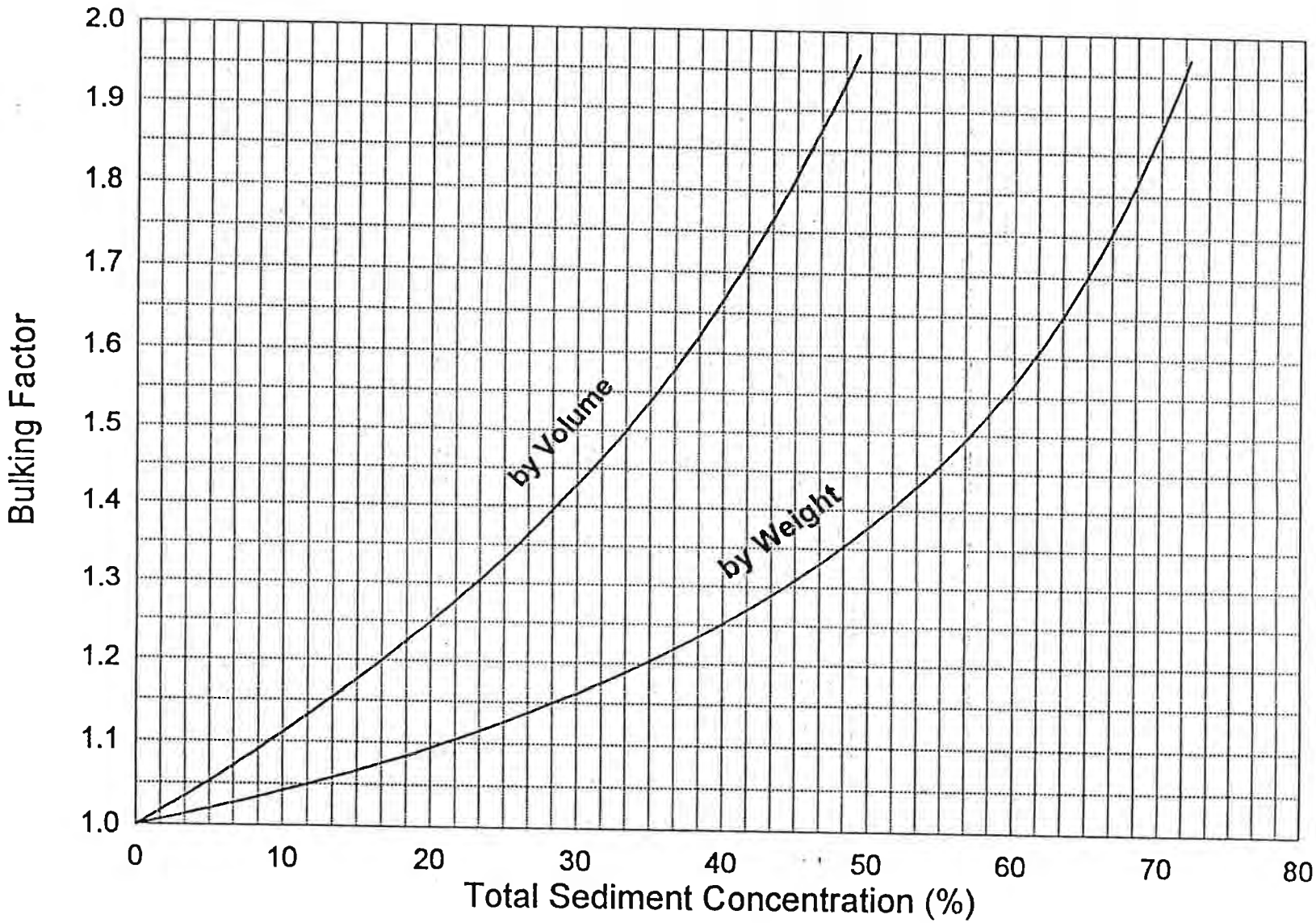


Figure 3.11. Relationship between total sediment concentration and bulking factor.

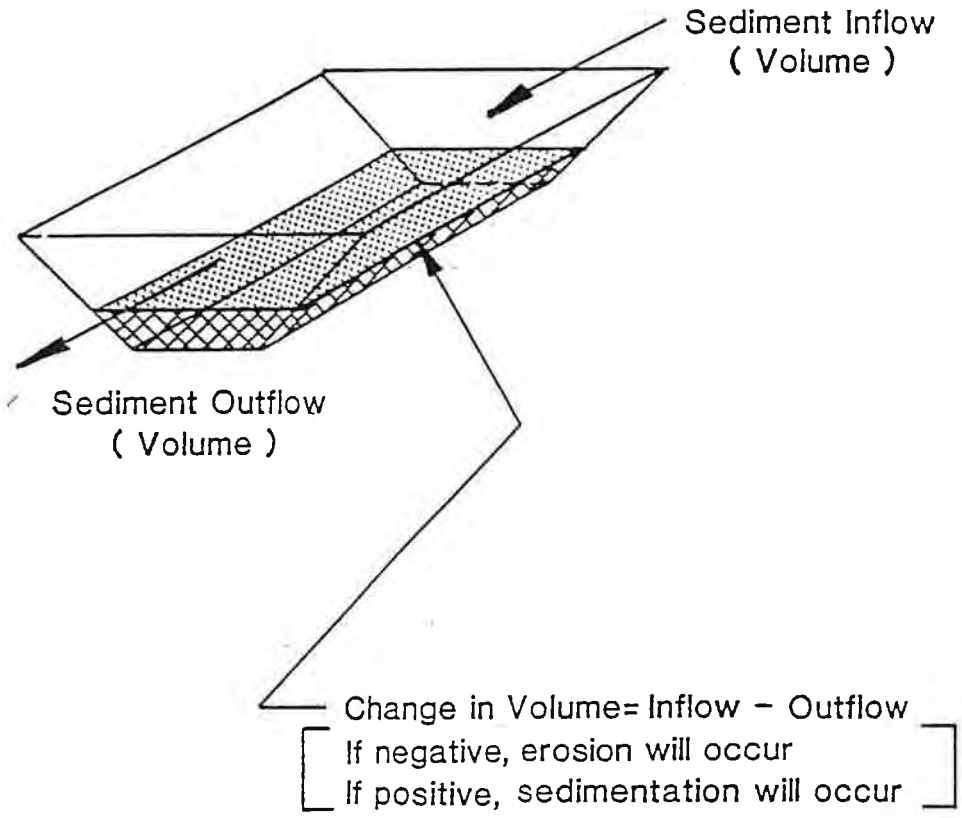


Figure 3.12. Illustration of sediment continuity concept.

3.4.2 The Equilibrium Concept. Stream channels tend to adjust toward a state of dynamic equilibrium such that the ability of the channel to carry water and sediment is in balance with the amount of water and sediment delivered from upstream and lateral sources. The condition of dynamic equilibrium with respect to sediment can be expressed by Equation 3.54 with the loss or storage term ($\Delta V$) equal to zero (i.e., the amount of sediment entering the reach is equal to the amount of sediment leaving the reach).

Adjustments to the channel can occur in several ways, including changes in the cross-sectional shape (primarily width), changes in the gradation of the material on the bed, and changes in the slope. In natural channels, adjustments can occur in all of these ways. The relative importance of each depends on the specific characteristics of the channel being analyzed. As described in Section 3.3, if a degrading stream has sufficient coarse material in the bed, winnowing of the fines during degradation will coarsen the bed

material, potentially reducing the availability of transportable material. The channel will reach a state of static equilibrium when the bed coarsens sufficiently to balance the inflowing and outflowing sediment loads. If the bed is made up of finer material that is transportable over the entire range of flows and the stream is capable of carrying more material than is being delivered from upstream, the dimensions will adjust and the slope will continue to reduce until the transport capacity is equal to the supply. The concept of dynamic equilibrium applies to the condition to which the channel tends over a long period of time and is the accumulated result of all of the flows to which the channel is subjected.

3.4.3 Evaluation of Vertical Stability. If the channel width remains unchanged, the average change in bed elevation that will result from the change in volume computed from Equation 3.51 can be estimated using the following relation:

$$\Delta z = \frac{\Delta V}{WL(1-\eta)} \tag{3.55}$$

where $\Delta z$ = average change in bed elevation in the reach
$W$ = average width of the channel bed
$L$ = length of the reach
$\eta$ = porosity of the bed material

For the type of bed material in arroyos in the Albuquerque area, the porosity ($\eta$) is usually about 0.4.

Equilibrium Slope. As indicated by the Lane relation (Equation 3.1), when the sediment delivered to a reach is reduced (or is less than the capacity of the reach), the channel will tend to flatten its slope to attain an equilibrium condition so that the capacity is in balance with the supply. Conversely, when the sediment delivered to the reach is increased (or is greater than the capacity of the reach), the channel will tend to steepen. The ultimate slope to which the channel will tend for this condition is referred to as the equilibrium slope.

Using hydraulic and sediment transport relationships and assumptions regarding the channel geometry, it is possible to estimate the equilibrium slope for specific discharge and sediment inflow conditions. Since the analysis is used to evaluate the long-term conditions toward which the channel is adjusting, the appropriate discharge for calculation purposes is the discharge that is predominantly responsible for the channel characteristics (the dominant discharge). For adjustable, perennial streams, this is often assumed to be the bankfull discharge which is further commonly assumed to be equal, in magnitude, to the mean annual flood peak. For ephemeral streams, the frequency of occurrence of the channel-forming discharge is less, due to the absence of sustained flows and the flashy nature of the storm hydrographs. For design purposes, the

dominant discharge to be used in equilibrium slope calculations in arroyos in the Albuquerque area can reasonably be assumed to be the 5- to 10-year peak discharge. Equation 1.1 may provide a better estimate of the dominant discharge. The dominant discharge can be estimated as the peak of the storm event that will produce a bed material sediment yield equal to the mean annual bed material sediment yield. In most cases, the equilibrium slope is relatively insensitive to the actual discharge used to compute it, within the range of frequencies discussed above.

A critical step in an equilibrium slope analysis is determination of the sediment supply from the upstream reach for the dominant discharge. In the absence of actual sediment supply data, the sediment supply is estimated as the transport capacity of the reach immediately upstream of the reach of concern. For natural, undisturbed channels and/or watersheds, this is a reasonable assumption that can often be verified through examination of historical data (e.g., profile analysis or aerial photographs). For developed conditions, the impact of the changed land use and upstream channel configuration must be considered in the analysis. In general, urbanization will increase the peak discharges and reduce the sediment supply. For unconfined arroyos such as those typical of the Northeast quadrant, future urbanization may concentrate the flow into fewer channels, further increasing the peak discharge and volume associated with a given flood event at any point in the channel. If the existing channel has not adjusted to the developed conditions, the transport capacity of the existing supply reach may not accurately reflect the reduced sediment supply that can be expected in the future as the upstream channel adjusts. For this case, it may be necessary to reduce the sediment supply appropriately to reflect future conditions. In general, considerable engineering judgment is required to ensure that the assumptions on which the sediment supply estimates are based accurately reflect conditions controlling the amount of sediment delivered to the reach of concern.

After establishing the upstream sediment supply, the transport capacity of the study reach is evaluated. If the transport capacity and supply for the dominant discharge or individual storm being considered are not equal, the slope and geometry of the channel are adjusted and the transport capacity re-evaluated (assuming that armoring is not a consideration). An iterative procedure can be used to obtain a transport capacity that matches the supply. For the equilibrium slope condition, the sediment supply to all reaches being analyzed is the estimated upstream supply to the overall study reach.

Selection of the proper channel geometry is important in equilibrium slope analysis. Sediment transport is proportional to approximately the third to fifth power of velocity and is directly proportional to the channel width. The equilibrium slope is, therefore, very sensitive to these values.

Arroyo channels tend to have a rectangular shape with flat bottom and steep banks. The width-depth ratio of the flow is quite large (normally on the order of at least 20 to 40. For such channels (width-depth ratios exceeding about 10), a wide rectangular

channel assumption is reasonable for hydraulic calculations (Chow, 1959). When the wide rectangular channel assumption is valid and significant changes in channel width are not anticipated during the degradation process, the equilibrium slope can be estimated as a function of the unit discharge using the following relation:

$$S_{eq} = \left(\frac{a}{q_s}\right)^{\frac{10}{3(c-b)}} q^{\frac{2(2b+3c)}{3(c-b)}} \left(\frac{n}{1.49}\right)^2 \qquad (3.56)$$

where $S_{eq}$ = equilibrium slope
$q_s$ = bed material supply per unit width of channel
$q$ = water discharge per unit width of channel
$n$ = Manning's roughness coefficient
$a, b, c$ = exponent and coefficients of the power function relationship given in Equation 3.39
(Note: If Equation 3.41 is used to compute $Q_s$, $a = a'(1-(C_f/10^6))^d$ )

For a derivation of this equation, see Simons, Li & Associates, Inc. (1982a).

For cases where the equilibrium slope of a series of reaches having similar roughness, discharge, and channel geometry is of interest, Equation 3.56 can be expressed as a function of the existing channel slope, as follows:

$$S_{eg} = S_{ex}\left(\frac{Q_{s(supply)}}{Q_{s(existing)}}\right)^{\left(\frac{2}{b-x}\right)} \qquad (3.57)$$

where

$$x = (3/5)\ (2b/3 + c) \qquad (3.58)$$

and $S_{ex}$ is the existing channel slope.

Results of the equilibrium slope calculations are used to predict long-term changes to the channel bed profile. Two important factors that must be considered in evaluating the results of these calculations are the presence of vertical controls, both natural and man-made, and the height of the banks that would develop as the channel flattens in a degradational reach. Vertical controls can be assumed to act as a pivot point where the existing bed will remain fixed. The equilibrium slope will develop upstream of that point until another control is encountered. Natural controls include bedrock outcrops, sections of channel with an accumulation of large immovable material, or clay outcrops. The characteristics of the clay outcrop material should be carefully evaluated since it is

probably erodible over time and may act only as a temporary control. Man-made controls include grade control structures, detention ponds, roadways, dip crossings, culverts, etc. that will prevent further lowering of the channel.

When the equilibrium slope calculations indicate significant lowering of the channel bed, the bank heights may become too high to remain stable. When this occurs, bank failure may result, rejuvenating the sediment supply, at least temporarily, slowing or arresting the degradation and resulting in widening and/or lateral migration of the channel. Concepts and methods of analyzing this situation are discussed in a later section.

An Alternative Approximation of the Equilibrium Slope. From Equations 3.56 and 3.57, it is apparent that the equilibrium slope depends on the magnitude of the upstream bed material supply. In many cases, an accurate estimate of the supply is very difficult to obtain. Factors that contribute to this uncertainty include the timing and magnitude of delivery of bed material-sized sediment from overland and tributary areas, inability to define the long-term condition of the upstream channel (particularly if it has not adjusted to a state of equilibrium), imprecision of available bed material transport relationships, and uncertainty in the timing and effect of point inputs of bed material due to upstream bank failure.

In such cases, where there is unacceptable uncertainty in the estimated bed material supply, an alternative method of estimating the channel slope for equilibrium conditions may be appropriate. This method is based on the observation that stable alluvial channels rarely, if ever, sustain supercritical flow for extended periods of time. Chang (1988), for example, states that "*stable alluvial channels must stay in lower flow regime*" and Trieste (1992) states that *while* [the] *assumption* [of supercritical flow] *may be valid for man-made channels of smooth, nonerosive materials, and some smooth, uniform, bedrock natural channel, it is questionable for most natural channels ...* Recalling that the sediment transport rate is proportional to the velocity to the third to fifth power, it is apparent that high velocities associated with supercritical flow in sand-bed streams will result in extreme rates of bed material transport. The stream will react to this high transport capacity by eroding its bed and banks to a condition that will sustain transport rates consistent with the upstream supply. Average Froude ($F_r$) Numbers in stable sand-bed streams rarely exceed 0.7 to 1.0 (Richardson, personal communication) at high discharges. In fact, the current FEMA procedures for evaluating hydraulic conditions on alluvial fans is based on the assumption of critical flow ($F_r = 1$).

Using this argument, the maximum stable slope for a channel of given geometry and dominant discharge can be computed by combining the relationship for the Froude Number with a uniform flow formula. Noting from previous discussions that the wide rectangular channel assumption is valid for most arroyo channels, the following relationship can be derived based on Manning's formula:

$$S_s = CQ^{-0.133} \quad (3.59)$$

where

$$C = 18.28n^2F^{0.133}F_r^{2.133} \quad (3.60)$$

The width of the channel resulting from these assumptions can be computed from the relation:

$$W = 0.5F^{0.6}F_r^{-0.4}Q^{0.4} \quad (3.61)$$

In the above equations,

$S_s$ = maximum stable slope
W = width of the channel
n = Manning's roughness coefficient
$F_r$ = maximum Froude Number (0.7 to 1.0)
Q = dominant discharge
F = width-depth ratio of the flowing water in the arroyo

Data from existing arroyos indicate that a width-depth ratio of the flowing water of about 40 is reasonable. (Leopold and Miller, 1956; Harvey et al., 1985).

The results of this computation can be used to obtain an initial approximation of the stable slope for use in locating grade control structures and bank protection measures.

Contraction Scour. Contraction scour occurs when the flow area of a stream at flood stage is locally decreased, either by a natural constriction or by a structure such as a bridge. With the decrease in flow area, there is an increase in average velocity and bed shear stress resulting in an increase in the amount of bed material transported and, possibly, degradation of the contracted reach. As the bed elevation is lowered, the flow area increases and the velocity and shear stress decrease until a state of relative equilibrium is reached. Contraction scour can also be caused by constriction of the floodplain at flood flows. When floodplain constriction occurs, the overbank flows are forced back into the channel, increasing the main channel discharge. In addition, the overbank flows typically carry very little bed material-sized sediment, increasing the tendency for scour.

Contraction scour can also be caused by flow around a bend where the concentration of flow on the outside of the bend increases the velocity and shear stress causing erosion of the bed, as well as the banks. Other factors that can cause contraction scour include:

1. Change in downstream water surface elevation or drop in base level

2. A natural stream constriction or bend

3. Street or highway crossings where the crossing narrows the channel

4. Deposition of lateral and point bars along the channel

5. Debris blockage

6. Growth of vegetation within the channel or floodplain

Contraction scour is typically cyclic. That is, the bed scours during the rising stage of a runoff event, and fills on the falling stage. The maximum contraction scour depth may occur at or slightly after the peak of the runoff event. The elevation of the channel bed after the event has passed may, therefore, not be a good indication of the depth of scour during the event.

Contraction Scour Equations

Contraction scour equations are based on the sediment continuity principle. This simply means that the fully developed scour in the bridge cross section reaches equilibrium when sediment transported into the contracted section equals sediment transported out, or the shear stress in the contracted section has been decreased by scour increasing the flow area so that it is equal to the critical shear stress of the sediment at the bottom of the contracted cross section (Richardson et al., 1991).

There are two forms of contraction scour depending upon the ability of the uncontracted approach flow to transport bed material into the contraction. Live-bed scour occurs when there is sediment being transported into the contracted reach. Clear-water scour is the case when bed material transport in the uncontracted approach flow is insignificant. In this case, the scour reaches equilibrium when the average bed shear stress is the critical stress required for incipient motion of the bed material. Incipient motion concepts (see Section 3.3.3) assist in determining whether conditions are conducive to live-bed or clear-water scour.

Typical clear-water scour situations include (1) coarse-bed material streams, (2) flat gradient streams during low flow, (3) local deposits of larger bed materials that are larger than the biggest fraction being transported by the flow (rock riprap is a special case of this situation), (4) armored streambeds where the only locations that tractive forces are

adequate to penetrate the armor layer are at piers and/or abutments, and (5) vegetated channels or floodplain/overbank areas.

During a flood event, contracted sections in regions of local scour such as streams with coarse-bed material are often subjected to clear-water scour at low discharges, live-bed scour at the higher discharges and then clear-water scour on the falling stages. Clear-water scour reaches its maximum over a longer period of time than live-bed scour. This is because clear-water scour occurs mainly in coarse-bed material streams. In fact, clear-water scour may not reach a maximum until after several floods. Maximum clear-water scour is about 10 percent greater than the maximum live-bed scour.

Richardson et al. (1991) presented a modified form of Laursen's (1960) live-bed contraction scour equation which was based on Laursen's simplified transport function and several other simplifying assumptions:

$$\frac{y_2}{y_1} = \left(\frac{Q_2}{Q_1}\right)^{\frac{6}{7}} \left(\frac{W_1}{W_2}\right)^{K_1} \qquad (3.62)$$

where $y_s$ = $y_2 - y_1$ (average scour depth)
$y_1$ = average depth in the upstream main channel, ft
$y_2$ = average depth in the contracted section, ft
$W_1$ = bottom width of the upstream main channel
$W_2$ = bottom width of the main channel in the contracted section, ft
$Q_1$ = flow in the upstream channel that is transporting sediment
$Q_2$ = flow in the contracted channel. This is often $Q_{total}$ (but not always)
$K_1$ = exponent determined by **Table 3.8**

Table 3.8. Values for Exponents in Equation 3.62.

| $V_{*c}/w$ | $K_1$ | Mode of Bed Material Transport |
|---|---|---|
| <0.50 | 0.59 | mostly contact bed material discharge |
| 0.50 to 2.0 | 0.64 | some suspended bed material discharge |
| >2.0 | 0.69 | mostly suspended bed material discharge |

where $V_{*c}$ = $(gy_1S_1)^{0.5}$, shear velocity
$w$ = fall velocity of $D_{50}$ of bed material (see **Figure 3.13**).
$g$ = gravity constant
$S_1$ = slope, energy grade line of main channel

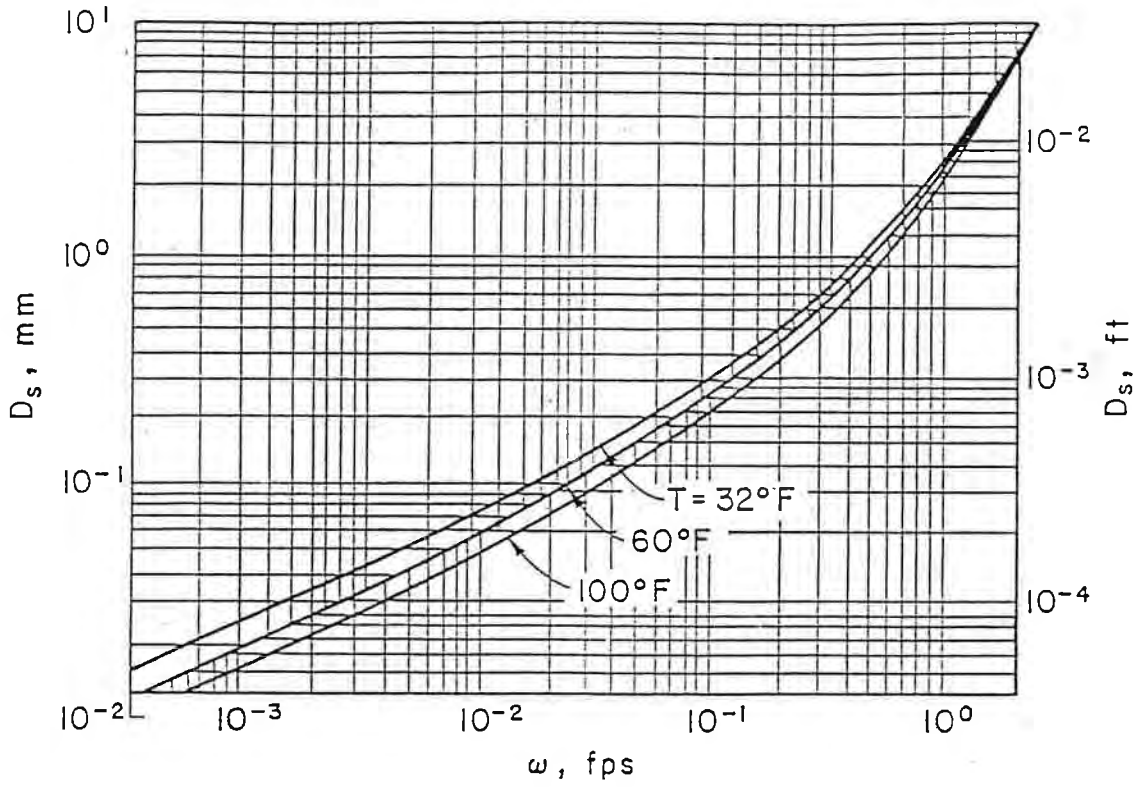


Figure 3.13. Fall velocity of sand-sized particles.

The parameters used in Laursen's equation are illustrated in **Figure 3.14.** As shown, the equation can be applied to various contraction configurations. A significant issue in the application is whether overbank flow on the floodplain is forced through the contracted section, for example, by bridge approach embankments extending across the floodplain. Figure 3.14a shows conditions at an upstream cross section approaching the contraction. Figure 3.14b shows contraction of the channel by bridge abutments with overbank flow being forced into the channel by the bridge approach embankments. For this situation:

$$Q_1 < Q_2 \tag{3.63}$$

where $Q_2$ = total flow going through the channel at the bridge (on contracted section)

$$W_1 > W_2 \tag{3.64}$$

where $W_2$ = bottom width of the channel at the bridge (less the width of any bridge piers).

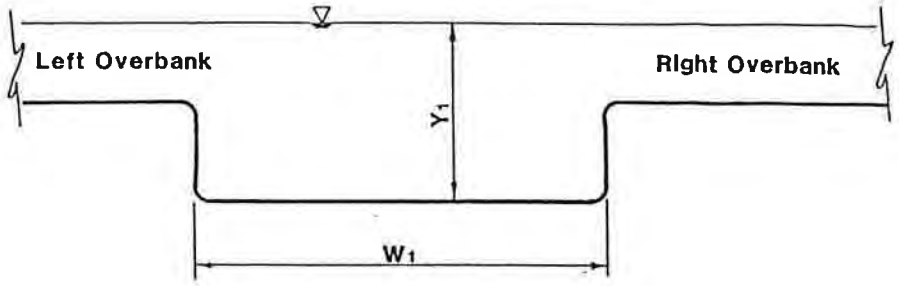


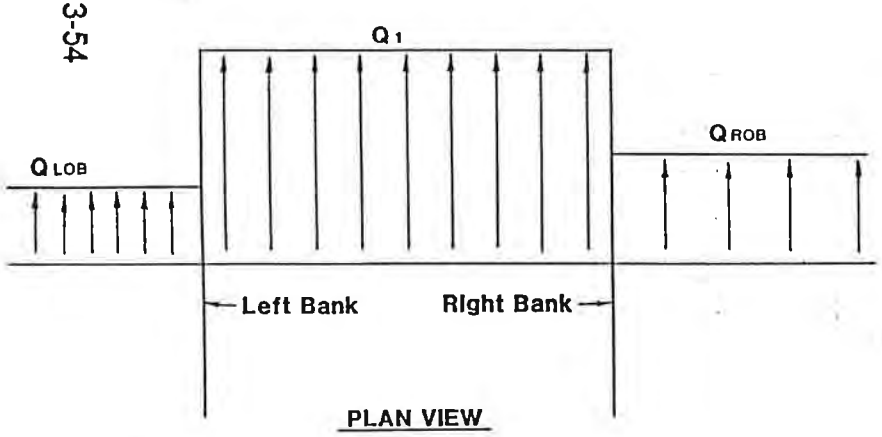


Figure 3.14a. Unconstricted reach upstream of bridge.

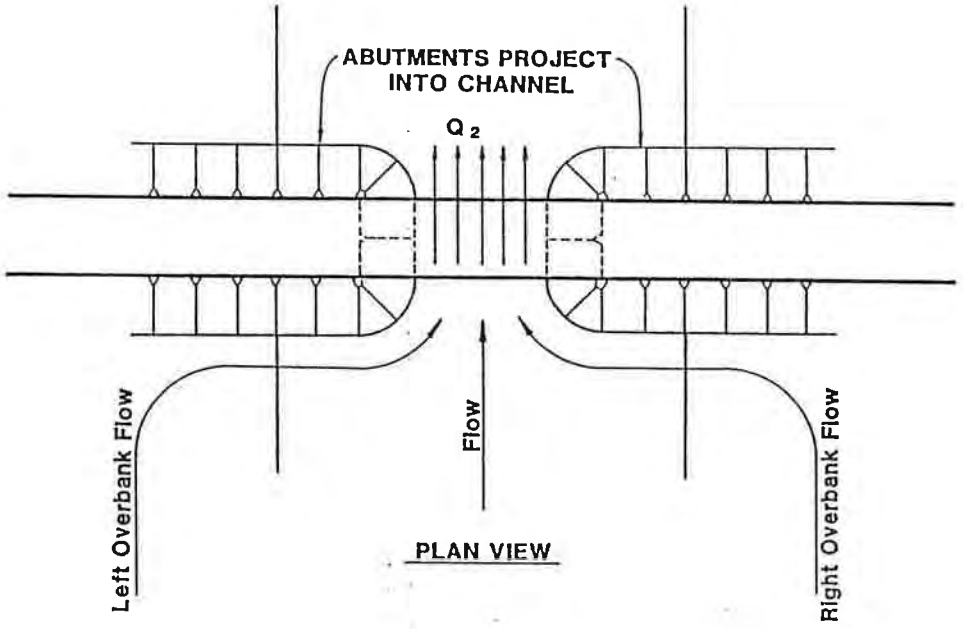


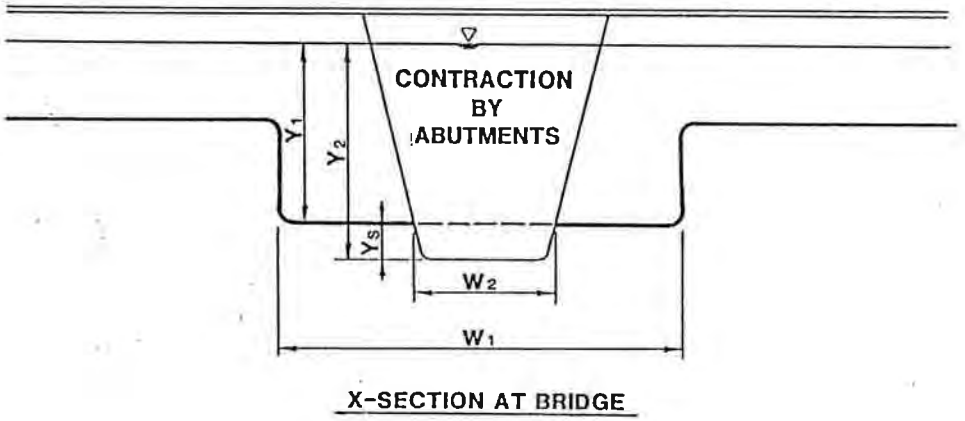


Figure 3.14b. Overbank flow with abutments set into channel.

Another common situation could be no encroachment or contraction of the main channel flow, but overbank flow is forced into the main channel by a structure. Here conditions are as discussed above except:

$$W_1 = W_2 \tag{3.65}$$

It is also possible to have no overbank flow, but a constriction of the main channel caused by a structure or a natural narrowing of the main channel. For this situation:

$$Q_1 = Q_2$$
$$W_1 > W_2 \tag{3.66}$$

To compute clear-water contraction scour, Laursen's (1960) equation is suggested. The most common application of this equation is for coarser (or armored) channels or to compute contraction scour on vegetated floodplains or overbank areas, with no bed material in transport.

$$\frac{Y_s}{Y_1} = 0.13 \left[ \frac{Q}{D_m^{\frac{1}{3}} \, y_1^{\frac{7}{6}} \, W} \right]^{\frac{6}{7}} - 1 \tag{3.67}$$

$Y_s$ = depth of scour
$Y_1$ = depth of flow in the channel or on the floodplain prior to scour, ft
$Q$ = discharge through the contracted section or on the overbank at the contracted section, ft
$D_m$ = effective mean diameter (ft) of the bed material (1.25 $D_{50}$) in the contracted section
$D_{50}$ = median diameter (ft) of bed material in the contracted section. Use a weighted average of the material in the scour zone
$W$ = bottom width of the contracted section, the bridge less pier widths, or overbank width (set back distance), ft

It is also possible to have a contraction configuration in the field that does not fit the situations described above. Reference to the definition of parameters in Equations 3.62 and 3.67 and consideration of the sediment continuity principle that is the basis for the Laursen equation should support adapting the equations to virtually any field situation. Additional applications of the concept to complex bridge and overbank configurations are discussed in Richardson et al. (1991).

Antidune Scour. In steep, sand-bed channels typical of arroyos in the Albuquerque area, antidunes will form on the channel bed during high flows. Passage of the antidunes past a point in the channel can increase the magnitude of scour at that location. The potential scour depth associated with the antidunes must be accounted for in evaluating the total scour near structures for stability analysis. Scour associated with antidunes is illustrated in **Figure 3.15**, taken from Simons, Li & Associates, Inc. (1985). The height of the antidunes can be estimated from the following relation (Kennedy, 1963):

$$h_a = 0.14 \frac{2\pi V^2}{g} = 0.28 \pi y F_r^2 \qquad (3.68)$$

where
- $h_a$ = antidune height
- $V$ = flow velocity
- $g$ = acceleration of gravity
- $y$ = hydraulic depth of flow
- $F_r$ = Froude Number

**Scour associated with the antidunes is estimated as one-half the antidune height.**

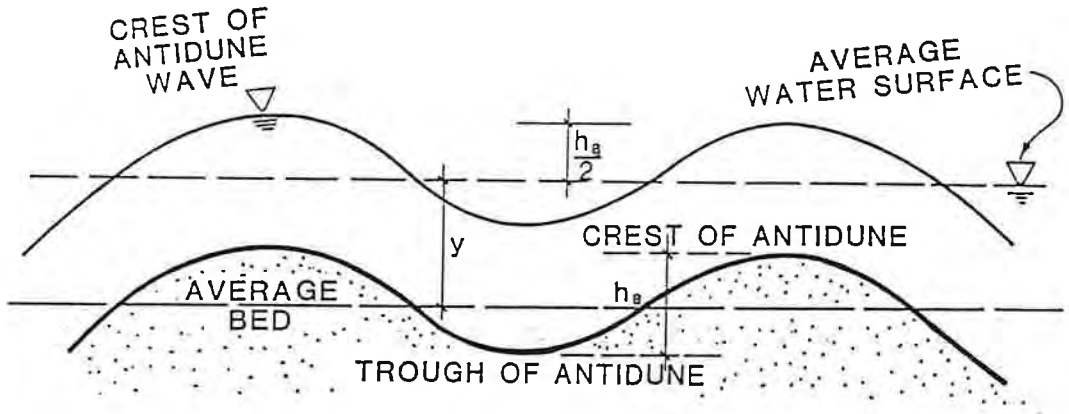


Figure 3.15. Definition sketch for antidune height (SLA, 1985).

3.4.4. Sediment Transport and Channel Stability at Culverts. Culverts can have significant effects on the stability and dynamics of arroyos. If backwater or flow expansion occurs upstream of the culvert, sediment will deposit, reducing the flood-carrying capacity of the upstream arroyo and trapping sediment that would otherwise be carried to downstream reaches. Severe deposition can cause total plugging and failure of culverts; even minor deposition over a period of time can reduce culvert capacity. Trapping of sediment upstream (or within) the culvert can cause degradation of the

downstream channel and the attendant effects on channel stability. The high velocity jet that normally occurs at the outlet of the culvert can cause local scour which may further aggravate channel instability and may endanger the stability of the crossing, itself. Numerous examples of these effects can be seen throughout the Albuquerque area. Evaluation of this problem requires consideration of four basic factors:

1. The potential for sediment deposition in the channel upstream of the culvert resulting from backwater due to energy losses at the culvert entrance and/or expansion of the upstream channel,

2. The sediment transport capacity of the culvert and resulting potential for excessive head loss and/or plugging,

3. Reduction of bed material sediment supply and resulting bed degradation in the downstream channel, and

4. Local scour at the culvert outlet.

A qualitative discussion of the first three processes is presented below. A method for computing the size of the local scour hole for noncohesive bed material is presented in Section 3.5.5.

Sediment Deposition Upstream of Culverts

The potential for sediment deposition in the channel upstream of a culvert is related to the configuration of the channel and amount of energy loss that occurs as the flow enters the culvert. Backwater caused by the energy loss reduces the flow velocity and thus, sediment transport capacity, of the upstream channel. The magnitude of the backwater and its effect on the channel velocity can be evaluated using standard computations that consider the hydraulics of the culvert entrance and upstream channel [e.g., "Hydraulic Design of Highway Culverts" (FHWA, 1985) and HEC-2 (USCOE, 1982)]. An expansion of the channel upstream of the culvert will also cause deposition. This has occurred, for example, at crossings where the arroyo banks leading to the culvert are not continuous across the roadside drainage ditch. In most such cases, degradation of the channel downstream of the crossing will occur.

The magnitude of the deposition upstream of the culvert must be evaluated on a case-by-case basis using the sediment continuity concepts presented in previous sections. If the backwater creates a significant ponding effect (i.e., reduce the average channel velocities to less than 1 to 2 fps in the backwater zone), trap efficiency calculations may be necessary to determine the amount of the inflowing sediment load that will be carried into the culvert. If the backwater effect is less significant, sediment routing may be required to evaluate the dynamic effects of backwater and channel bed changes through the storm hydrograph. In certain instances, backwater during the peak flows may cause deposition upstream of the culvert which will steepen the energy gradient into the culvert at lower flows during the recession limb of the hydrograph. This,

in turn, will re-entrain all or part of the deposited sediment and return the channel bed toward its original elevation.

The above process appears to have occurred upstream of the Tramway Road crossing of a tributary to La Cueva Arroyo just north of Modesto Avenue. Hydraulic calculations indicate significant backwater at higher flows, yet the existing channel upstream of the crossing shows little or no evidence of aggradation, in spite of a large storm flow that occurred in 1991 (estimated to be about a 10-year event). Detailed analyses of the reach showed analytically that deposition probably occurred during the peak flows, but were subsequently eroded during the recession (RCE, 1994). A sediment routing study by Anderson (1992) using the Corps of Engineers HEC-6 model (USCOE, 1991) indicated that significant deposition may occur during the 100-year event that may not be removed during the recessional flows. Significant features of this particular crossing that may reduce the tendency for upstream deposition and increase the likelihood that the deposits will be removed during recessional flows include the relatively large size of the culverts (2 - 6 foot x 6 foot box culverts) and the relatively continuous channel geometry through the backwater region.

Other similar locations exist in this same area where significant deposition has occurred and persists upstream of the culvert entrance. These locations are generally characterized by smaller culvert size which increases the extent of the backwater and, in some cases, flow expansion because the arroyo banks are not continuous through the roadside ditch. In any case, the potential for blockage of the culvert entrance by debris during the flood must be considered. Such blockage would have potentially serious consequences in terms of overbank flooding, instability of both the up- and downstream arroyo, and the crossing itself.

Sediment Transport in Culverts

The ability of the culvert to carry the sediment passing through the culvert entrance is basically a sediment transport capacity problem. A comprehensive treatment of sediment transport in closed conduits is beyond the scope of this Design Guide. General information is provided here to give the reader a general introduction to the subject and to provide guidance regarding the need to employ more sophisticated methods. More detailed treatment of the problem can be found in several references, including ASCE Manual No. 54 (Vanoni, 1977) and Graf (1984).

**Figure 3.16** is a conceptual plot taken from ASCE Manual No. 54 (Vanoni, 1977) illustrating the various modes of sediment transport through a closed conduit. This figure shows that the transport mode depends on the particle size and flow velocity in the pipe. Information by Graf (1984) indicates that it is also a function of pipe size. In general, the transport mode can range from an essentially homogeneous mixture the sediment being uniformly distributed throughout the fluid for high velocities and small particle sizes to an armored bottom with the no-sediment motion on the bottom of the conduit.

For sand-sized sediment in culverts, it is reasonable to assume that the transport mode will normally be in the range of heterogenous flow (i.e., solids in suspension or flow with moving bed). For practical purposes, if the velocities are sufficiently high to put all of the sediment into suspension, it can be assumed that the transport capacity is sufficiently high to pass any sediment that enters the culvert and, in the absence of obstructions, the potential for internal culvert blockage is minimal. Data presented in both of the above publications indicate that the transport potential through closed conduits is similar to that in open channels for similar hydraulic and sediment characteristics. Based on this observation, the transport capacity within the culvert can be estimated using one of the previously presented bed material transport capacity equations.

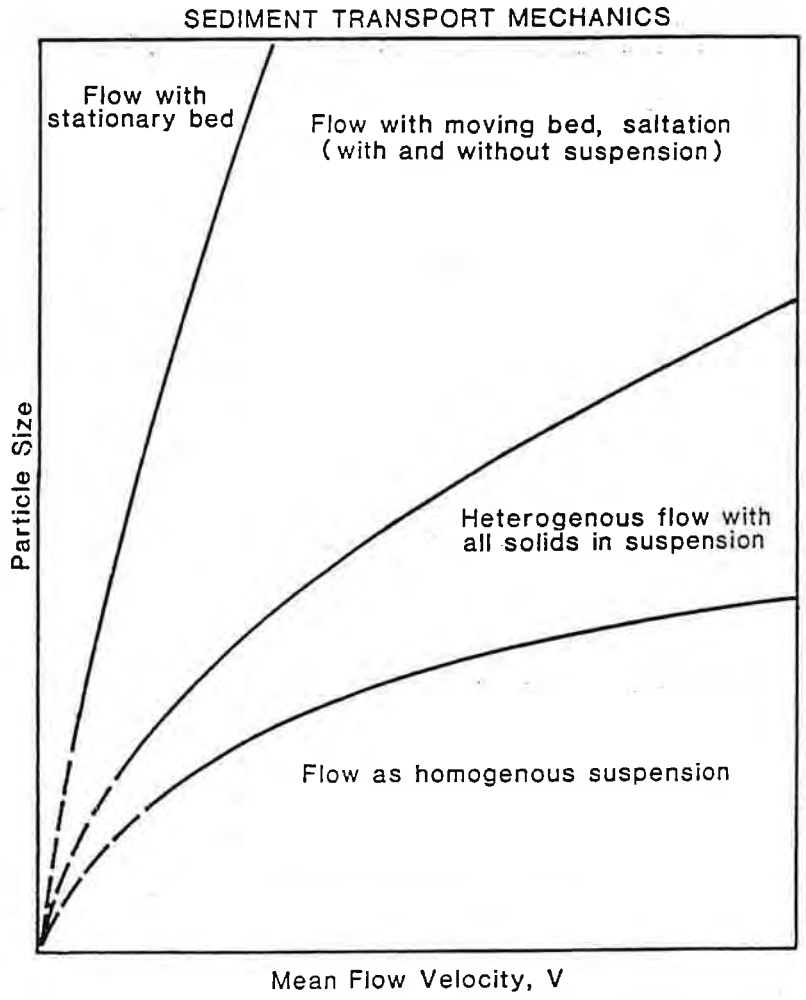


Figure 3.16. Conceptual illustration of modes of sediment transport in closed conduits.

Degradation of the Downstream Channel

The potential for general degradation of the channel downstream of the culvert can be evaluated using the continuity and equilibrium slope concepts presented in previous sections of this Design Guide. The culvert will act as a control point in the channel, and the dynamics of the downstream arroyo will be a function of the sediment delivery into and through the culvert in relation to the transport capacity of the reach.

### 3.4.5 Evaluation of Lateral Stability

Bank Erosion Processes. Lateral migration and widening of natural channels occurs through bank retreat resulting from two primary mechanisms: grain-by-grain erosion and mass failure. Commonly, mass-wasting and grain-by-grain erosion act in concert; fluvial erosion scours the toe of the bank, and mass failure follows. (Simon et al., 1991) Removal of the failed bank material from the bed of the channel occurs through fluvial erosion and the process is repeated.

The bank erosion process can result from channel incision (degradation), flow around bends, flow deflection due to local deposition or obstructions, aggradation, or a combination of the above. For the case of an incising channel, exceedence of the maximum stable bank height will lead to mass failure and bankline retreat. Flow around a bend can cause erosion at the toe of the bank and subsequent bank failure due to increased shear stress on the outside of the bend. Both local deposition and aggradation over a longer reach create mid-channel bars that can deflect flow into the bank with essentially the same result as flow on the outside of a bend.

The specific failure mechanisms at a given location are related to the characteristics of the bank material. Typical bank failure surfaces for various bank material types are shown in **Figure 3.17**. In general, bank material can be broadly classified as cohesive, noncohesive, and composite. Although the bank material in most arroyos in the Albuquerque area are composed primarily of noncohesive sands and fine gravels, they generally contain sufficient amounts of cohesive material to influence the bank erosion characteristics. The following discussion relates to the bank failure conditions indicated in the figure:

1. Noncohesive bank material tends to be removed grain by grain from the bank. The rate of particle removal and hence the rate of bank erosion, is affected by factors such as particle size, bank slope, the direction and magnitude of the velocity adjacent to the bank, turbulent velocity fluctuations, the magnitude and fluctuations in the shear stress exerted on the banks, seepage forces, piping, and wave forces. Figure 3.17a illustrates failure of noncohesive banks from flow slides resulting from a loss of shear strength because of saturation, and failure from sloughing resulting from the removal of material in the lower portion of the bank.

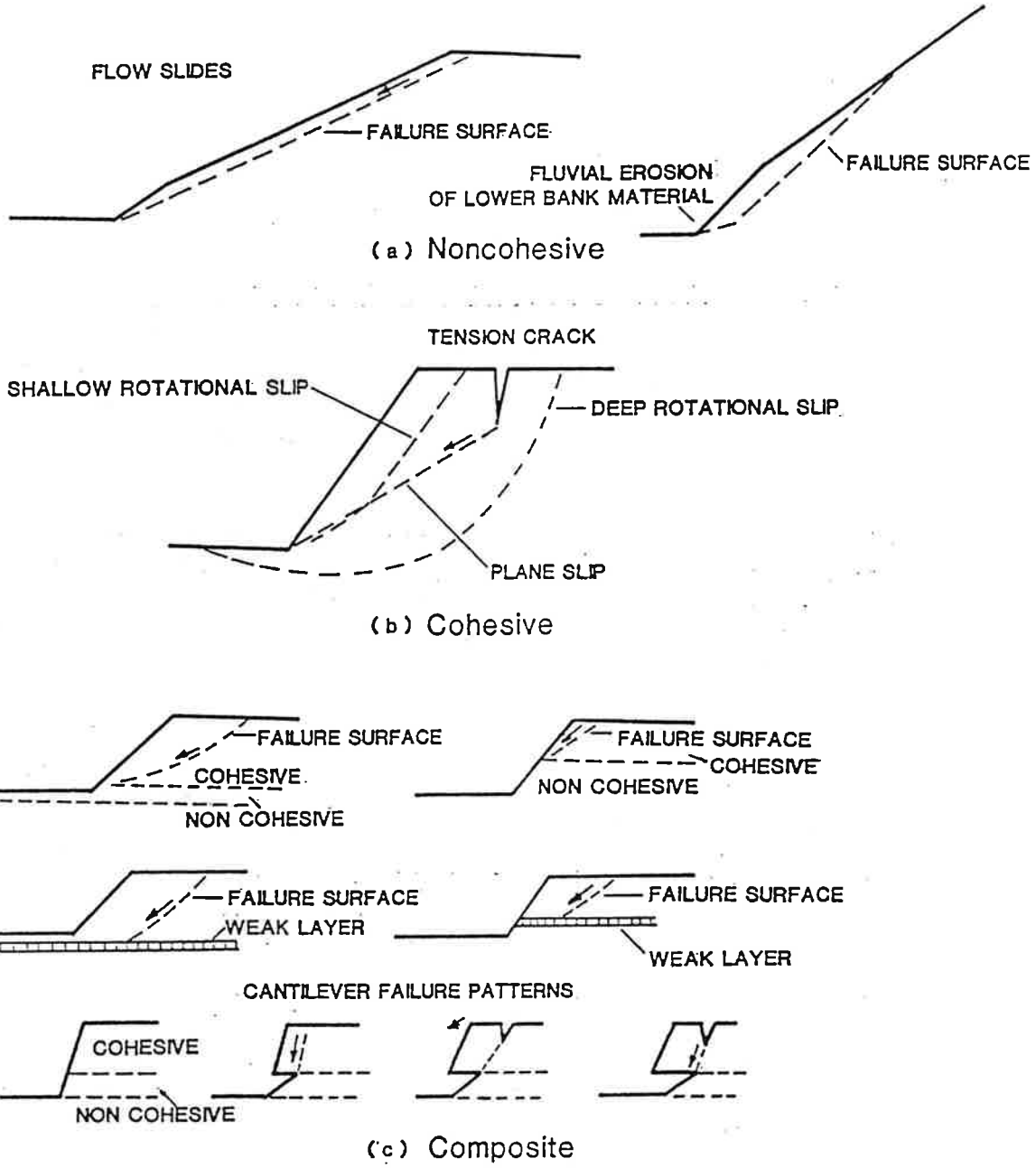


Figure 3.17. Typical bank failure surfaces: (a) noncohesive, (b) cohesive, (c) composite (after Brown, 1985b).

2. Cohesive material is more resistant to surface erosion and has low permeability, which reduces the effects of seepage, piping, frost heaving, and subsurface flow on the stability of the banks. However, when undercut and/or saturated, such banks are more likely to fail due to mass wasting processes. Failure mechanisms for cohesive banks are illustrated in Figure 3.17b.

3. Composite or stratified banks consist of layers of materials of varying size, permeability, and cohesion. The layers of noncohesive material are subject to surface erosion, but may be partly protected by adjacent layers of cohesive material. This type of bank is vulnerable to erosion and sliding as a consequence of subsurface flows and piping. Typical failure modes are illustrated in Figure 3.17c.

Grain-by-grain erosion can be a significant process in areas of concentrated flow and high shear stress (e.g., on the outside of bends). However, studies of bank erosion processes in both perennial streams and arroyos indicate that mass failure and subsequent fluvial transport of the failed material is the primary mechanism by which the lateral adjustments occur. For example, Leopold and Miller (1956) in a study of arroyos in the Santa Fe area, observed that

> *Flash floods in arroyos ... appear to do but insignificant amounts of bank cutting as a direct result of impingement of flow on the banks. Wetting of the banks, however, results in subsequent collapse of arcuate slabs of alluvium which tumble into the channel to become important additions to the load of later floods.*

Lohnes and Handy (1968) identified two major failure mechanisms for gully banks that were formed in loess: (1) shear failure along a planar slip surface through the toe of the bank, and (2) slab failure of vertical banks by tension cracking and planar slip. Their analysis investigated the relationship between the height, slope angle, and strength properties of the banks to predict maximum stable bank heights. In their analysis, pore water pressures were neglected; their approach should, therefore, only be used for highly permeable soils with a low degree of saturation.

Bradford and Piest (1980) identified three major mechanisms of gully-wall failure: (1) deep-seated circular arc toe failure, (2) slab failure, and (3) "pop out" failure with shear failure of the remaining cantilevered bank section. Their study indicated that slab failures were associated with vertical banks whereas circular arc failures were associated with lower angle banks. A significant conclusion of their study was that fluvial erosion of *intact* bank material (grain-by-grain erosion) appears to contribute very little to bank retreat. Similar observations have been made by Little et al. (1982) and Schumm et al. (1981) and reinforce the idea that most incised channel gully bank failures are due to gravitational forces which are primarily controlled by the degree of channel incision. It is important to note, however, that fluvial erosion of *previously failed* bank material does play a significant role in determining the rates of bank retreat. As observed by Thorne (1981), fluvial activity controls the state of *basal endpoint control*; removal of the failed material results in the formation of steeper banks and may induce toe erosion by removing the material along

the toe that tends to buttress the bank slope. These factors rejuvenate the process of bank erosion by mass failure. Without basal erosion, mass failure of the bank material would lead to bank slope reduction and stabilization within a relatively short period of time (Lohnes and Handy, 1968; Thorne, 1981).

Bank Stability Analysis Techniques. In view of the above discussion, it is apparent that analysis of the potential for lateral migration and widening of the arroyo channels must include bank stability considerations and the resulting potential for mass failure. The geotechnical stability number ($N_g$), which is the ratio of the actual bank height to the critical bank height, as discussed in Chapter 3, is the basic parameter with which to evaluate the stability of the channel banks. Due to the relatively large number of factors and complexity of the processes, a relationship between bank angle and bank height using field data **on a site-specific basis** would provide the most accurate means of evaluating bank stability in arroyos in the Albuquerque area. Such a relationship could also provide a means of calibrating the parameters in available analytical relationships for evaluating bank stability. Since little or no site-specific data are available with which to develop such a relationship, the analytical relationships must be used with parameters estimated from the geotechnical properties of the bank soils. The appropriate method for determining the critical bank height depends on the assumed shape of the failure surface and the composition and stratigraphy of the banks (Simon et al., 1991).

Ponce (1978) presented a method for analyzing an initially stable bank subject to undermining resulting from base-level lowering. He assumed a circular failure arc with the failure surface passing through the toe of the bank and used the simplified Bishop method to develop stability curves relating the stable bank height to the soil properties (angle of repose, cohesion, and unit weight) and the bank angle. He neglected the effect of pore water pressure in his analysis. For arroyos and drainageways in the Albuquerque area, the later assumption may be reasonable since the water table is usually well below the level of the channel bed and the soils are typically well drained. Ponce's approach was adopted for the Prudent Line analysis developed originally for Calabacillas Arroyo (Lagasse et al., 1985).

Osman and Thorne (1988) developed a model for wedge-type failures for steep (bank angle $>60°$) cohesive banks with failure through the toe which is more representative of the bank failure process discussed in the last section. Osman and Thorne's study included a detailed treatment of the combined effects of fluvial erosion and bank stability for analyzing bank retreat. The geometry of the banks assumed in their analysis is illustrated in **Figures 3.18 and 3.19**. Figures 3.18a and 3.18b show the assumed initial condition of the bank and its configuration after the first failure, respectively. Figures 3.19a and 3.19b illustrate the initial and failure condition for subsequent failures of the bank during parallel retreat. This method provides relationships to determine the magnitude of degradation ($\Delta Z$) and toe erosion ($\Delta w$) required to produce a condition of incipient failure.

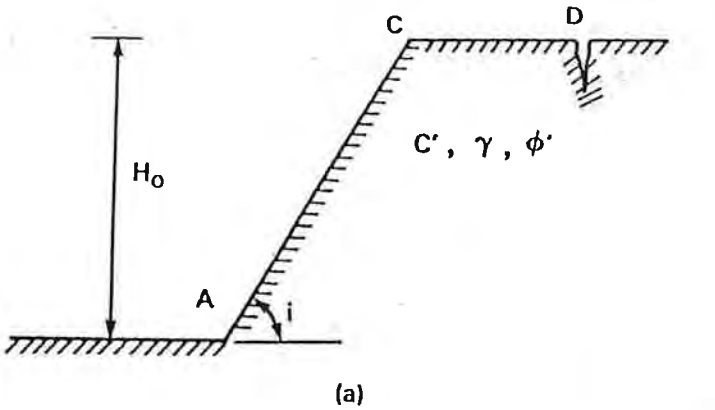


(a)

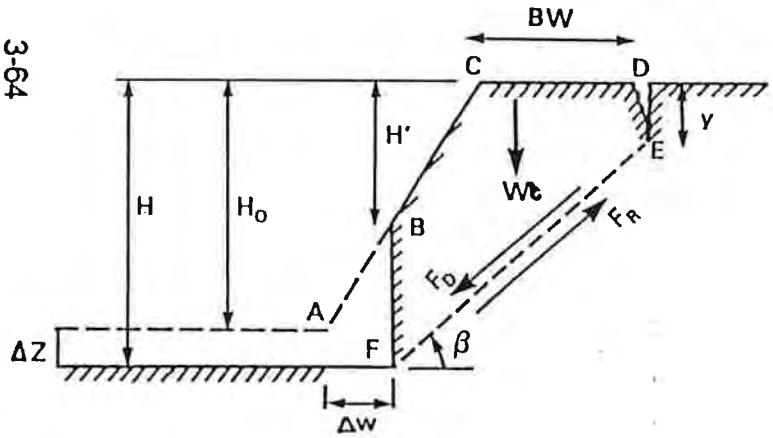


(b)

Figure 3.18. (a) Right arroyo bank before erosion (b) right arroyo bank after erosion to point of failure (Osman and Thorne, 1988).

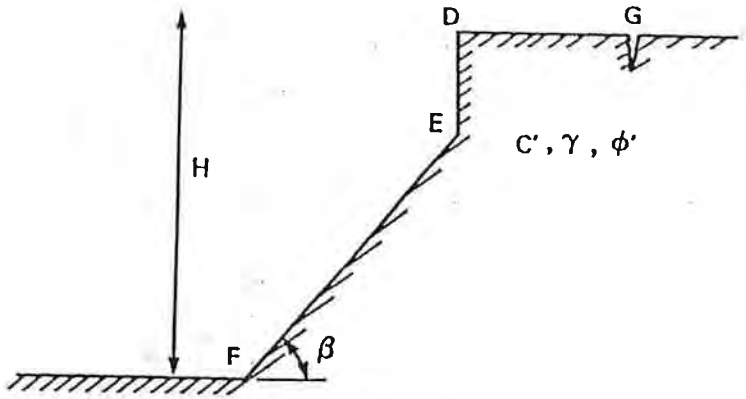


(a)

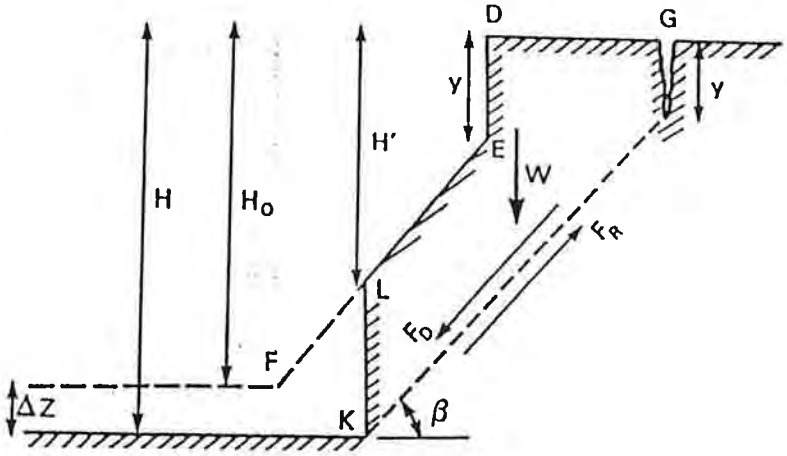


(b)

Figure 3.19. Parallel bank retreat: (a) arroyo bank after initial failure; (b) arroyo bank after erosion to point of failure.

**It is important to note that the soil properties to be used in the analysis are for in-situ conditions, where the cohesion and unit weight may be substantially less than customary values used in geotechnical engineering design for compacted soil conditions.** The internal friction angle ($\phi$) for most soils along arroyos in the Albuquerque area vary from about 28° to 32°. The cohesion (c) varies from about 200 psf to 400 psf and the in-situ unit weight ($\gamma_s$) is about 100 pcf. These values are for average conditions and are very approximate. They should, therefore, be used for planning purposes only. It is strongly recommended that the bank material be tested on a site-specific basis prior to performing a detailed stability analysis using this method.

Little et al. (1982) discuss methods for determining the in-situ properties of the bank material. Thorne (1993, personal communication) has found in subsequent work that the effective tensile strength (tensile strength is a function of cohesion (c) and internal friction angle ($\phi$) under conditions conducive to bank failure tends to be significantly lower than would be indicated by even the in-situ tests. He believes this is due to a combination of soil moisture effects that occur at failure, but may not be present at the time or exact location of the testing and other local weaknesses in the soil matrix that may not be indicated by the in-situ test. In general, the strength of the bank at a given location will be controlled by the weakest zone in the bank. For this reason, the low end of the range of reasonable c and $\Phi$ values should be used for conservative design purposes.

Since the processes described by Osman and Thorne (1988) are similar to those that have been observed in incising arroyos in the Albuquerque area, this is the recommended method for estimating the maximum height at which the banks will remain stable and the amount of bank retreat associated with channel incision that may be expected to occur. The maximum stable bank height predicted by this method for a range of internal friction angles ($\phi$) and cohesion (c) typical of soils in the Albuquerque area is shown in **Figure 3.20**. These curves were developed assuming an in-situ unit weight of 100 pcf, bank angle of 70° and tension crack depth of half the bank height. The assumed bank angle and tension crack depths are consistent with observations of Little et al. (1982) for incised channels in other areas and corroborated by data collected on several incising arroyos in the Albuquerque area by RCE.

The method was also used to develop relationships for the amount of bank retreat (BW in Figure 3.18) and the associated volume of material resulting from block failures from the bank as a function of the degradation depth. The relationships are presented in **Figures 3.21a and 3.21b** and are based on conservative values for cohesion (c) and internal friction angle ($\phi$) of 200 psf and 28°, respectively. The bank retreat distance indicated by Figure 3.21a represents the minimum horizontal distance from the existing bankline that would be unstable as a result of block failures from the bank during degradation. This figure should be used in conjunction with the lateral erosion distances predicted in the following sections to establish the erosion setback required to prevent damage to structures or property along the arroyo.

Estimation of Lateral Migration. The recommended technique for estimating the rate and magnitude of lateral migration depends on the sediment balance in the reach being analyzed. If the continuity analysis indicates that the reach is degradational (i.e., bed material transport capacity exceeds supply) either on an average annual basis or in response to the 100-year storm, lateral migration will be primarily the result of failure due to undercutting at the toe of the bank or exceedance of the critical bank height.

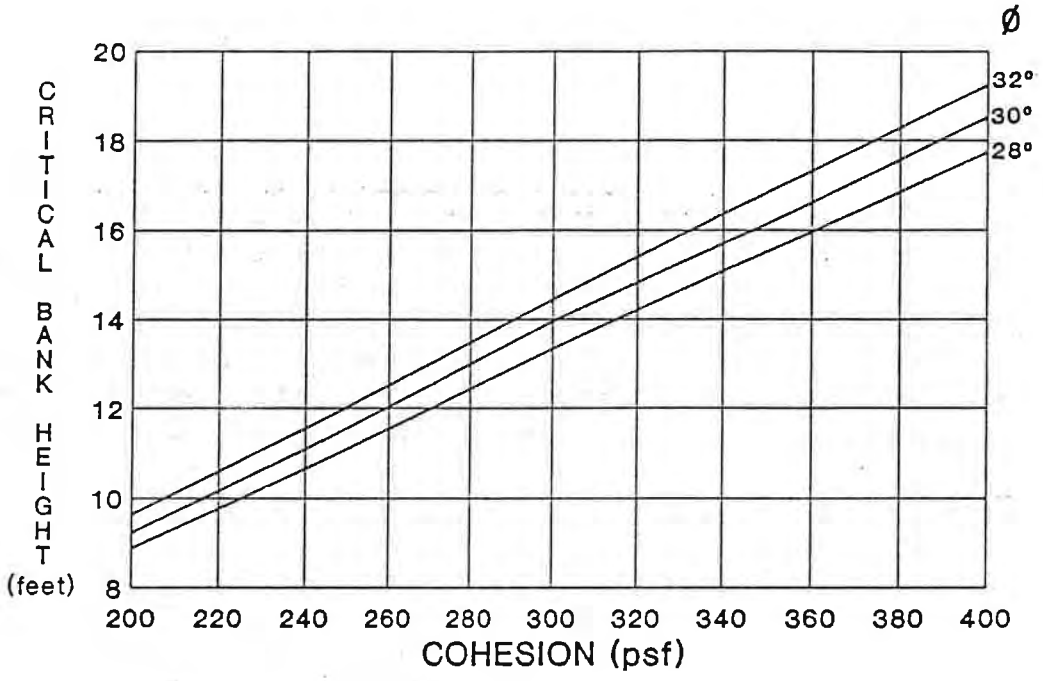


Figure 3.20. Critical bank height predicted by Osman and Thorne (1988) model for varying internal friction angle ($\phi$) and cohesion (c). (Assumes in-situ unit weight of bank material = 100 pcf).

When the bed material transport capacity and the supply are approximately equal, no net erosion or deposition of sediment is expected within the reach. For this case, lateral migration is the result of localized fluvial entrainment of the bank material as the stream adjusts toward an equilibrium planform. The preferred method for estimating the rate and magnitude of migration involves the use of empirical data or historical migration rates. When such data are not available or future conditions are significantly different than historical conditions, lateral migration can be estimated by approximating the volume of material fluvially entrained from failed bank material resulting from undercutting of the toe within a given bend as a proportion of the transport capacity of the stream based on the sharpness of the bend. The assumptions and computational procedure for making this estimate are discussed in a later section. The maximum lateral migration distance that can be expected over the long term can also be estimated based on the optimal bend shape.

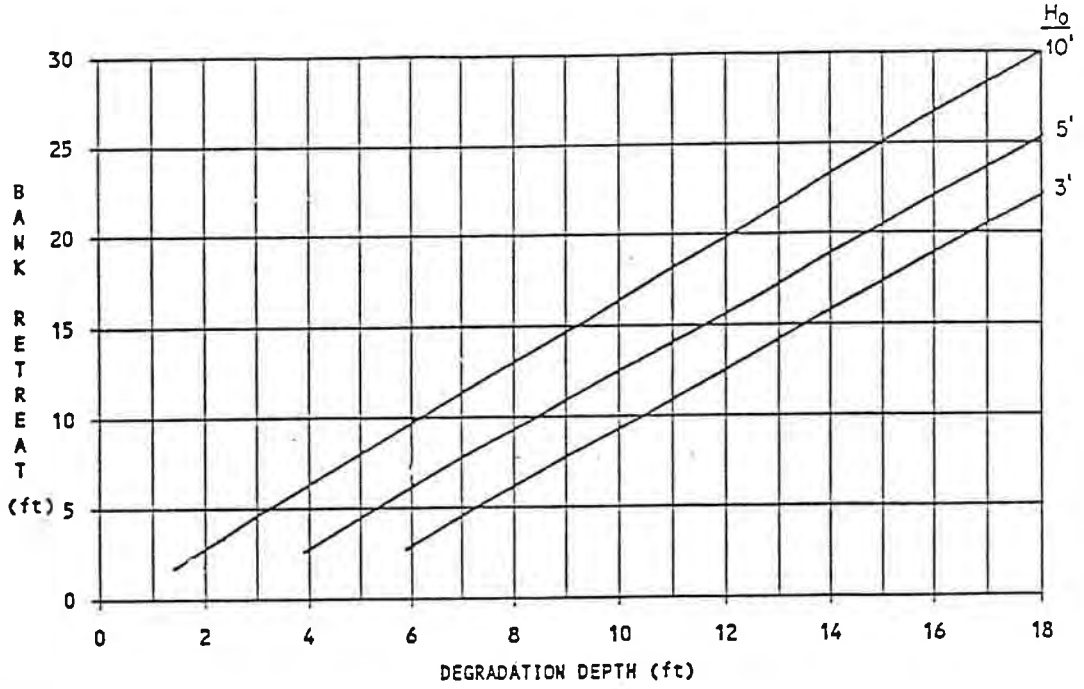


Figure 3.21a. Bank retreat versus degradation depth.

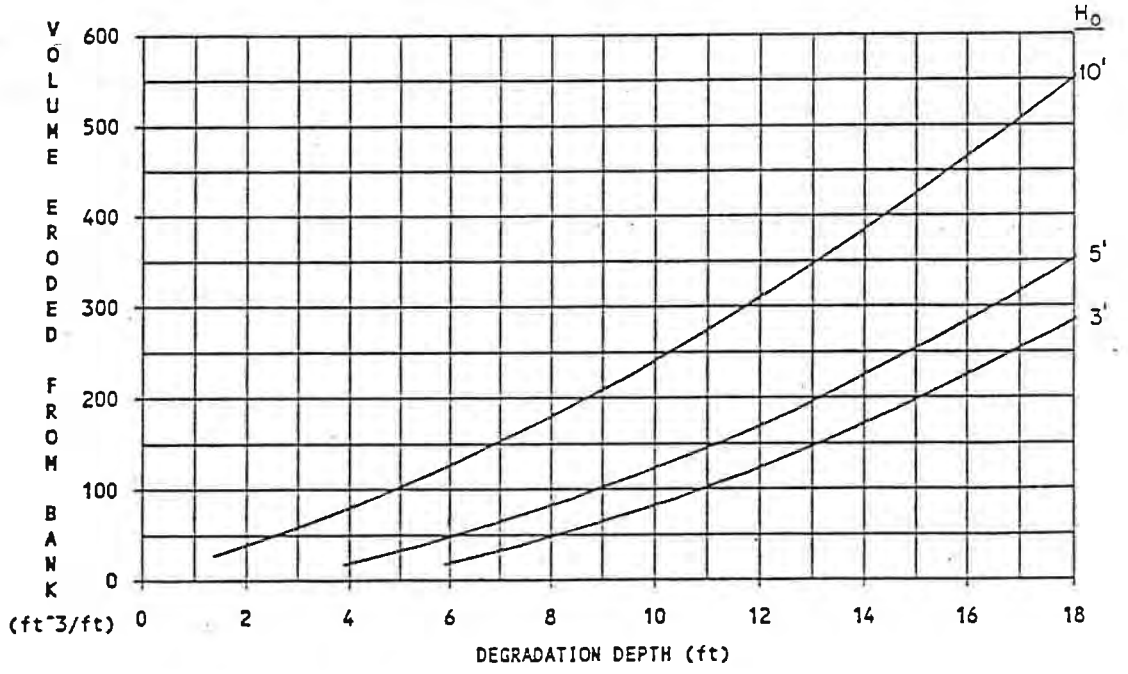


Figure 3.21b. Volume of material eroded from bank versus degradation depth.

For degradational reaches (i.e., bed material supply-transport capacity), bank failure occurs due to a combination of undercutting of the toe and/or exceedence of the critical bank height. The process leading to lateral migration of the bank are, therefore, similar to the quasiequilibium state. The primary difference relates to changes in bank height (and this volume of material) that must be removed to create a given migration distance.

When the reach is strongly aggradational and the overbank area is relatively flat, the channel alignment and extent of flooding is essentially a random phenomenon (e.g., alluvial fan flooding) and prediction of the erosion boundaries by analytical means is not possible. For this case, however, the flood limits are usually wider than the erosion limits. This problem is therefore unlikely to be a limitation in establishing the prudent limits, as discussed in the next chapter.

The following sections describe the background and procedure for estimating the maximum erosion limits that can be expected to occur over a long period of time and a procedure for estimating the rate of migration as the arroyo adjusts toward the maximum condition. **For the reasons discussed in the previous paragraph, unless otherwise specified, the information in the following sections applies only to an arroyo that is degrading or vertically stable. It does not apply to an arroyo that is aggrading.**

Approximate Maximum Erosion Distance based on Optimal Bend Shape

This section presents supporting concepts leading to a simplified method for estimating the maximum limits of a lateral erosion envelope along an arroyo. Due to the loss of energy associated with flow through a bend, a maximum bend sharpness exists beyond which further significant lateral erosion is unlikely to occur. It has been shown that the maximum lateral erosion rate for a meander bend occurs when the ratio of radius of curvature ($R_c$) to channel width (W) is in the range of about 2 to 4 (Hickin, 1975; Nanson and Hickin, 1983; Begin, 1981; Odgaard, 1987). For values less than about 2, the erosion rate reduces sharply due to energy loss in the bend (Bagnold, 1960; Nanson and Hickin, 1983) (**Figure 3.22**). In fact, Carey (1969) and Page and Nanson (1982) showed that in very tight bends (i.e., $R_c/W < 2$), deposition actually occurred on the outside of the bend. For this condition, the rate of lateral migration significantly reduces or migration stops and the bend either cuts off or avulses.

Leopold and Wolman (1960) and Bagnold (1960) observed that river meanders tend to a constant $R_c/W$ of between 2 and 3. This range of bend sharpness seems to result in a minimum value of resistance to flow, with flow resistance increasing rapidly as $R_c/W$ decreases below 2. Langbein and Leopold (1966) showed that meanders develop to minimize the variance of shear and friction through the bend. They also showed that the planform for such a meander follows the approximate shape of a sine-generated curve described by the relation:

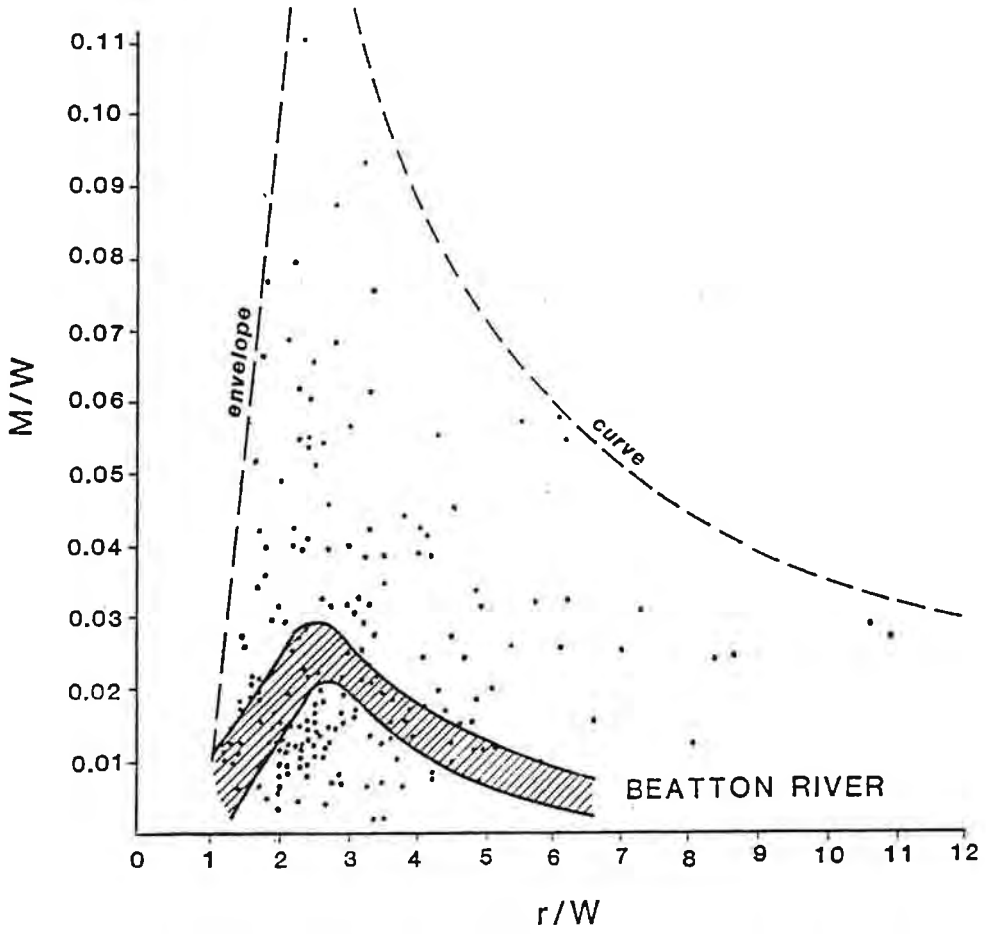


Figure 3.22. The relation between relative migration rate (expressed in channel widths per year) and bend curvature ratio (r/W) for all field sites (from Nanson and Hickin, 1983).

$$\tilde{\phi} = \omega \sin \left(2\pi \frac{s}{M} + \frac{\pi}{2}\right) \qquad (3.69)$$

where $\phi$ = angle of the channel alignment with the down-valley direction at location s

$\omega$ = maximum angle of the meander relative to the general direction of the channel

M = total channel length along the meander (**Figure 3.23**)

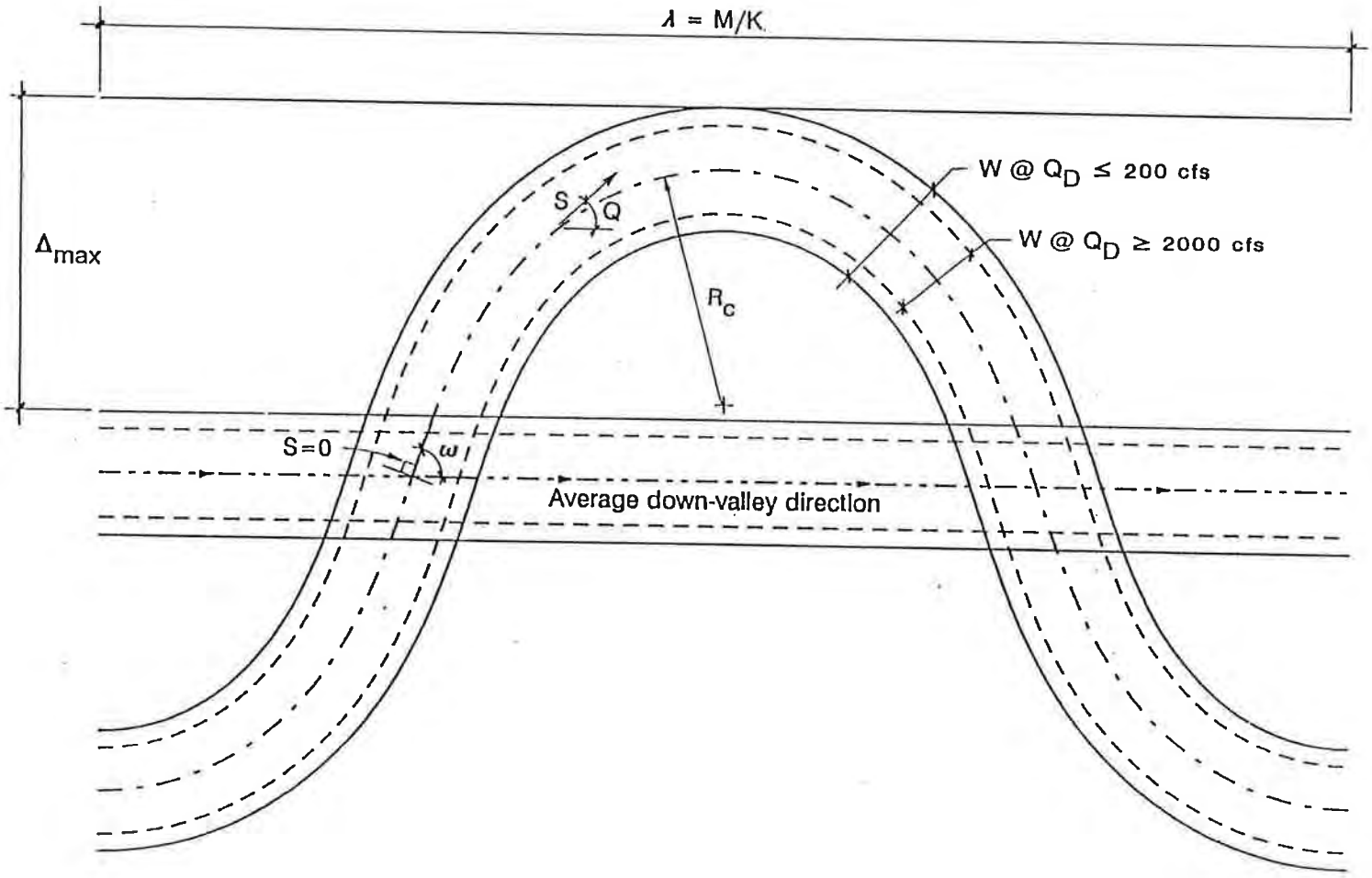


Figure 3.23. Schematic of an idealized meander bend illustrating the variables in Equations 3.66 through 3.71.

The maximum angle ($\omega$) is related to the sinuosity (k) by the approximate relationship:

$$\omega = 2.2\sqrt{\frac{k-1}{k}} \tag{3.70}$$

The meander wavelength ($\lambda$) is related to the sinuosity by the relation:

$$\lambda = kM \tag{3.71}$$

and the radius of curvature of the bend ($R_c$) in approximately 75 percent of the bend length between the inflection points is given by the approximate relationship:

$$R_c = \frac{\lambda}{13}\frac{k^{3/2}}{\sqrt{k-1}} \tag{3.72}$$

The exact radius of the curve at any point in the bend can be computed from

$$R_c = [\frac{2\pi\omega}{M} \sin (\frac{2\pi s}{M})]^{-1} \tag{3.73}$$

From Equation 3.73, the minimum radius of curvature ($R_c$) occurs at S = M/4 or $R_{cmin} = M/2\pi\omega$. Using Equation 3.72, it can be shown that the minimum value of $R_c/W$ (i.e., maximum sharpness)for a sine generated curve occurs at a sinuosity of 1.5.

It has been shown that the length of a typical meander is approximately 10 to 14 channel widths (Leopold et al., 1964). Although the original data for this relation was derived primarily from perennial streams, the relationship was also verified for arroyos (Leopold et al., 1966). Drury (1964) suggested that the ratio of meander wavelength to channel width tends to increase with increasing mean annual discharge. To facilitate development of reasonable relationships between the maximum erosion envelope and channel size, it is therefore assumed that $\lambda/W$ will vary according to the following relationships:

$\lambda/W_D = 10$ for $Q_D \leq 200$ cfs (3.74a)

$\lambda/W_D = 0.8 + 4\log(Q_D)$ for 200 cfs $< Q_D <$ 2000 cfs (3.74b)

$\lambda/W_D = 14$ for $Q_D \geq$ 2000 cfs (3.74c)

where $Q_D$ = dominant discharge.

Considering the above information, it can be concluded that the maximum deviation of a channel from a straight line ($\Delta_{max}$) will occur when the ratio $R_c/W$ is at its minimum (i.e., sinuosity of 1.5). The average value of $R_c/W$ in the portion of the

bend where Equation 3.72 is applicable varies from 2.0 for $\lambda/W = 10$ to 2.8 for $\lambda/W = 14$. For these conditions, the maximum offset of the channel from a straight line for a sine-generated curve with minimum radius of curvature is approximately one-fourth the meander wavelength, or one-half the distance between the endpoints (crossings) for a given channel bend, thus:

$$\Delta_{max} = 2.5W_D \quad \text{for } Q_D \leq 200 \text{ cfs} \tag{3.75a}$$

$$\Delta_{max} = [0.2 + \log(Q_D)]W_D \quad \text{for } 200 \text{ cfs} < Q_D < 2000 \text{ cfs} \tag{3.75b}$$

$$\Delta_{max} = 3.5\, W_D \quad \text{for } Q_D \geq 2000 \text{ cfs} \tag{3.75c}$$

where $W_D$ = channel width associated with the dominant discharge.

For fully adjustable, perennial streams, it is normally assumed that the dominant (or channel forming) discharge is approximately equivalent to the mean annual flood peak, varying from about the 1.5-year return period peak discharge to the 10-year peak discharge. It has been argued that arroyos are inherently a nonequilibrium channel form (i.e., they are a product of the last major flow) (Thornes, 1976). Their size is, however, related to the magnitude and frequency of the flows that pass through them. Since arroyos normally flow only in response to intense storm events, the frequency of flows capable of causing significant adjustment of the channel is reduced. For this reason, the dominant discharge for arroyos corresponds to a less frequent event, on the order of the 10-year flood peak.

The dominant discharge in perennial arroyos can be estimated as the peak discharge of the storm event that would deliver the average annual sediment load. This is accomplished using Equation 1.1:

$$Y_{s_m} = 0.015Y_{s_{100}} + 0.015Y_{s_{50}} + 0.04Y_{s_{25}} + 0.08Y_{s_{10}} + 0.2Y_{s_5} + 0.4Y_{s_2} \tag{1.1}$$

where the values of $Y_i$ are the sediment yields associated with each storm event. The value of the dominant discharge ($Q_D$) is then determined by logarithmic interpolation between the peak discharges for the appropriate storms, or:

$$\log(Q_d) = \log(Q_{R-1}) + [\log(Q_R) - \log(Q_{R-1})]\left[\frac{\log(Y_m) - \log(Y_{i-1})}{\log(Y_i) - \log(Y_{i-1})}\right] \tag{3.76}$$

If only the 100-year peak discharge is available, the dominant discharge for arroyos in the Albuquerque area can be estimated by

$$Q_d = 0.2Q_{100} \tag{3.77}$$

which is a reasonable approximation of the 5- to 10-year peak discharge. (C.A. Anderson, 1993, personal communication)

In Section 3.4.3.2, it was shown that the channel width for a given width-depth ratio (F = W/D), Froude Number ($F_r = V/\sqrt{gd}$), and discharge (Q) can be computed from the relation:

$$W = 0.5F^{0.6}F_r^{-0.4}Q^{0.4} \tag{3.61}$$

Data from existing arroyos indicate that the width-depth ratio of the flowing water of about 40 is typical (Leopold and Miller, 1956; Harvey et al., 1985). Using this value for F, a Froude number ($F_r$) of 1 (See discussion in Section 3.4.3.2), and the dominant discharge ($Q_D$), the channel width can be estimated from the relation:

$$W_D = 4.6Q_D^{0.4} \tag{3.78}$$

where $Q_D$ = dominant discharge

For subcritical flow (i.e., $F_r < 1$) and a Manning's n of 0.035, the width can be estimated by:

$$W_D = 2.46\ Q_D^{0.375}\ S^{-0.188} \tag{3.79}$$

Based on the discussion in Section 3.4.3.2, Equation 3.78 should be used to approximate the width for slopes greater than or equal to than the critical slope ($S_c$) which can be estimated from the following relation, based on the above assumptions (wide rectangular channel, uniform flow, n = 0.35, F = 40):

$$S_c = 0.037\ Q_D^{-0.133} \tag{3.80}$$

Combining the above relationships, the maximum lateral erosion distance can be estimated, in terms of the dominant discharge ($Q_D$), from the following relationships, when $S \geq S_c$:

$\Delta_{max} = 11.5Q_D^{0.4}$ for $Q_D \leq 200$ cfs (3.81a)

$\Delta_{max} = [0.92+4.6\log(Q_D)]Q_D^{0.4}$ for 200 cfs$< Q_D <$2000 cfs (3.81b)

$\Delta_{max} = 16.1Q_D^{0.4}$ for $Q_D \geq$ 2000 cfs (3.81c)

or, when $S < S_c$:

$$\Delta_{max} = 6.2Q_D^{0.375}S^{-0.188} \quad \text{for } Q_D \leq 200 \text{ cfs} \quad (3.82a)$$

$$\Delta_{max} = [0.45+2.5\log(Q_D)]Q_D^{0.375}S^{-0.188} \quad \text{for } 200 \text{ cfs} < Q_D < 2000 \text{ cfs} \quad (3.82b)$$

$$\Delta_{max} = 8.6Q_D^{0.375}S^{-0.188} \quad \text{for } Q_D \geq 2000 \text{ cfs} \quad (3.82c)$$

As discussed above, when only the 100-year storm peak is available, Equation 3.74 can be substituted into the above relations to provide an estimate of the maximum lateral erosion distance in terms of the 100-year peak.

In the ideal case, where the channel is assumed to be constant width ($W_D$) and is aligned along the average downvalley direction, the limits of the erosion envelope are defined by measuring a distance from the approximate **bankline** of the channel prior to the start of meandering. This distance is termed the bankline setback (BSB). In those cases where the bankline is difficult to define, the limits of the erosion envelope can be determined by measuring a distance $\Delta_{max}+W_D/2$ from the approximate centerline of the channel. This distance is termed the centerline setback (CSB). When both distances can be clearly defined, the most conservative (largest) distance defines the erosion setback.

Equations 3.81 and 3.82 define the expected maximum lateral erosion distance from the downvalley direction based on an idealized bend geometry. These relations are believed to provide reasonable, but somewhat conservative, estimates for most cases, particularly where the arroyo is relatively unincised or where the overbanks are relatively flat lateral to the channel. When the arroyo is deeply incised, the overbanks slope upward lateral to the channel, or controls are present, the lateral erosion potential may be reduced at any given location along the arroyo. In addition, for small arroyos (i.e., $Q_{100}$ <~100 cfs), the relative effects of local cementation of the overbank soils (i.e., caliche), boulders, and manmade structures become more significant. For this reason, engineering judgment, on a site-specific basis, may indicate that a more limited erosion envelope may be acceptable, particularly where the hazard associated with the relatively small discharges in smaller arroyos would be limited even if the erosion envelope were exceeded. The decision to accept a more limited erosion envelope should be made carefully, in consultation with the reviewing agencies.

The following steps summarize the procedure for estimating the maximum lateral erosion distance:

I. Estimate the magnitude of the dominant discharge ($Q_D$). As noted above, if only the 100-year peak discharge is available, the dominant discharge for arroyos in the Albuquerque area can be estimated as $0.2Q_{100}$ (Equation 3.77).

II. Estimate the channel width associated with $Q_D$ using Equation 3.79 if $S<S_c$ (i.e., subcritical flow), where $S_c$ is the critical slope and S is the equilibrium channel slope or from Equation 3.78 if $S \geq S_c$.

III. Estimate the downvalley length of arroyo ($L_v$) over which the lateral erosion can occur for unconstrained conditions using Equations 3.74 where $L_v = \lambda/2$.

IV. If controls that will prevent lateral erosion of the arroyo (e.g. rock outcrop, bridges, culverts, grade control structures, spurs, etc.) are present and the controls are less than $L_v$ apart, use the distance between the controls for $L_v$.

V. Compute the maximum lateral erosion distance ($\Delta_{max}$) as 1/2 $L_v$ if no lateral controls are present or if the spacing between the controls is greater than $L_v$. By constructing lateral controls at spacings less than $L_v$, the maximum lateral erosion distance is reduced. **Figure 3.24** shows the relationship between the maximum lateral erosion distance and the downvalley spacing of lateral controls.

VI. Determine the required erosion setback as $\Delta_{max}$ from the existing channel bank (BSB), when the bankline is clearly defined or ($\Delta_{max} + 0.5W_D$) when the bankline is not well defined (CSB). When both can be readily defined, use the largest of the two distances.

VII. If the channel is expected to degrade such that the critical bank height will be exceeded (see Section 3.4.5.2), an additional distance corresponding to the bank retreat associated with block failure of the banks should be added to the erosion setback. The required distance can be found from Figure 3.21.

VII. Compare the location of the erosion setback line with the location of the edge of the 100-year flood zone. The largest of the two distances is the required setback. When the hydraulic analysis indicates supercritical flow for the conditions being analyzed, the 100-year flood zone should be defined based on the water surface elevation associated with the sequent depth (depth to which the water would rise through a hydraulic jump (see Section 3.2.3, Equation 3.23).

Procedure for Estimating Migration Rate for Vertically Stable or Degrading Reaches. Lateral and vertical adjustment of stream channels is basically a sediment transport phenomenon; adjustments occur through erosion, transport and re-deposition of the sediment making up the channel boundary. As previously discussed, the preferred method of estimating the rate of lateral migration is based on historical data, avoiding the necessity for simplifying assumptions and the inherent variation between channel changes predicted by analytical means and field-measured changes. This approach is, of course, only applicable when adequate data are available and future conditions are expected to be similar to historic conditions during the time period over which the data were collected. In most problems, these conditions are not met, necessitating the use of analytical techniques.

This section presents a procedure for estimating the rate and magnitude of lateral migration using the sediment continuity, bank stability, and ideal bend geometry concepts discussed in previous sections of this Design Guide.

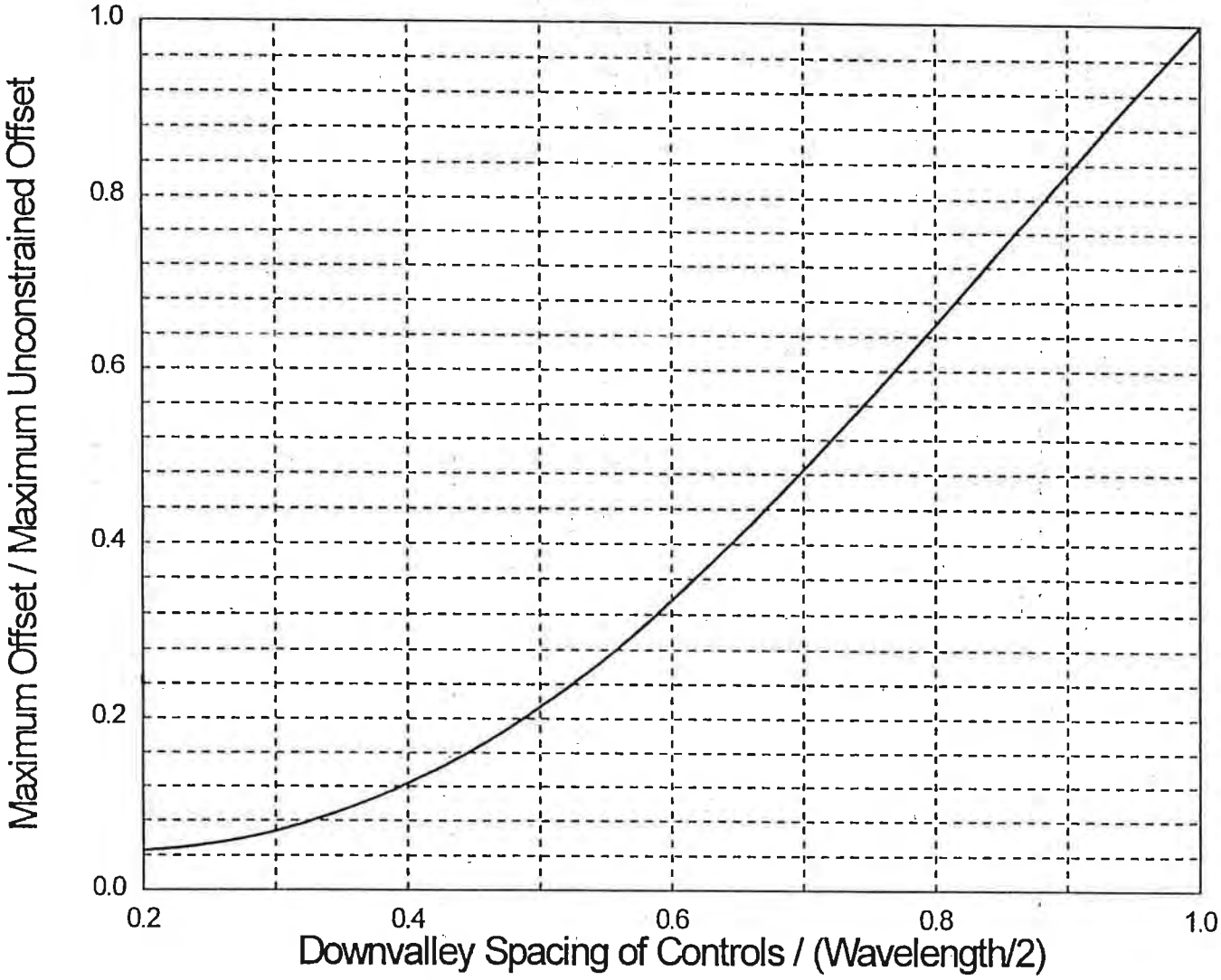


Figure 3.24. Maximum lateral erosion distance for control spaced at less than half the assumed unconstrained meander length.

Lateral migration of the top of the bank will occur as a result of bank failure and fluvial entrainment as the flow attacks the bank on the outside of the bend. For channels that are in an approximate state of equilibrium (i.e., the sediment supply is approximately the same as the transport capacity), no net erosion will occur within the reach. However, lateral migration of the channel can still occur through erosion on the outside of the bend and deposition of the eroded material on the inside of the next downstream bend. In a rapidly migrating bend, field evidence has shown that the amount of sediment eroded from one bend and deposited on the next point bar downstream will be approximately equivalent to the bed material transport capacity of the channel (i.e., there will be an approximate complete exchange of the particles being transported through one bend sequence). Since the erosion rate is related to the shear on the outside of the bend, it can be assumed that the percentage of the transport capacity exchanged between the erosion and re-deposition within a bend sequence will also vary as a function of the bend sharpness, reaching its maximum of 100 percent when $R_c/W \approx 2$. The variation in the percentage of particles exchanged can be estimated by noting that the erosion rate is proportional to the shear stress.

**Figure 3.25** shows the relationship between the ratio of shear on the outside of the bend to the mean channel shear stress ($\tau_b/\tau_0$) and $R_c/W$ which is an index of the bend sharpness, as previously defined. The relationship in Figure 3.25 was originally presented by the Lane (1955) based on empirical data. Begin (1981) derived an analytical relationship for the force per unit area on the bank that follows the general shape of the migration rate curve in Figure 3.21. The key dimensionless coefficient in the relationship is given by:

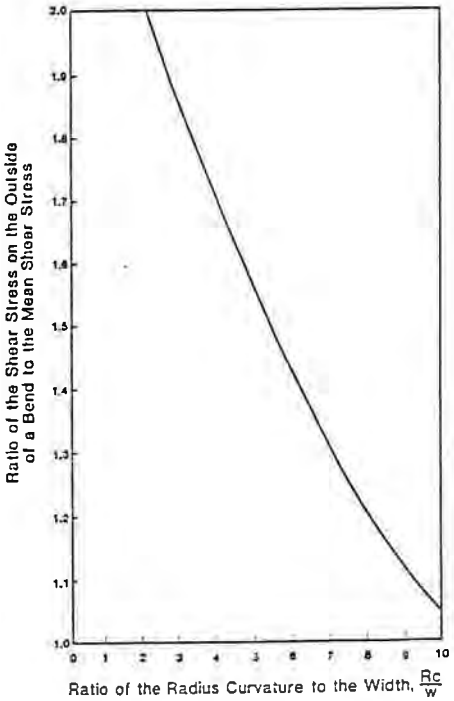


Figure 3.25. Increase in shear stress at outside of a bend.

$$C_\alpha = \frac{(1+ \frac{1}{2R_c/W})^{-4.07}}{(R_c/W + 1/2)} \qquad (3.83)$$

The coefficient ($C_\alpha$) in Equation 3.83 is directly proportional to the bend shear, thus, it describes the variation in shear with bend sharpness. From Equation 3.41, the sediment transport rate ($q_s$) is proportional to $V^b$ and from Equation 3.9, $V\alpha\sqrt{\tau}$. It is therefore assumed that the erosion rate is porportional to $C\alpha^{b/2}$ and the percentage of the transport capacity exchanged within the bend sequence ($P_B$) can be approximated:

$$P_B = (C_\alpha/C_{max})^{1.5} \qquad (3.84)$$

where $C_{max}$ = value of $\alpha$ at minimum $R_c/W$ (2 for $\lambda/W$ = 10 to 2.8 for $\lambda/W$ = 14)

Based on the above discussion, the procedure for computing the rate and magnitude of lateral migration consists of the following steps:

1. Perform a sediment continuity analysis for the events to be considered in the analysis. This may involve one or more specific storm events and/or sediment continuity on a mean annual basis.

   a. If the reach is **aggradational**, these procedures **do not** apply; refer to the next section for guidance.

   b. If the reach is approximately in equilibrium or is degradational, proceed with the steps listed below.

2. Determine if lateral and vertical controls exist within the reach and their location. Vertical controls may consist of grade control structures, road crossings, rock outcrops, or other features that will prevent or inhibit vertical adjustment of the channel bed. These features may also act as lateral controls. Other lateral controls may include bank protection, spurs, or training walls.

3. Compute the maximum lateral erosion distance for the reach using the procedures in the previous section.

4. From the continuity analysis, determine the bed material sediment supply and transport capacity of the reach for each of the events to be considered in the analysis.

5. Measure the channel length and average downvalley length between controls.

6. Determine the channel width by measurement or by estimating the width to which the channel will adjust for the 10-year peak discharge which is an approximation of the dominant discharge using Equations 3.78 or 3.79.

7. From field measurements, estimate the existing average bank height within the reach.

8. From **Figure 3.20**, determine the maximum stable (or critical) bank height.

9. Determine the existing average slope of the channel through the reach.

10. If the channel is degradational, estimate the volume of material degraded from the reach and the approximate length of the degradation wedge. **Figure 3.26** illustrates the assumed longitudinal geometry to be used in estimating the length of the degradational wedge. This geometry assumes that the degradation will occur from up- to downstream starting at the upstream control point, with the final bed slope within the degradation zone equal to the equilibrium slope. To provide a conservative estimate of the potential lateral migration distance and rate, assume that the maximum bank height will not exceed the critical height determined in step 8. Thus, degradation at any point in the reach is assumed to stop when the critical bank height is reached and any deficit of sediment is removed from the bank.

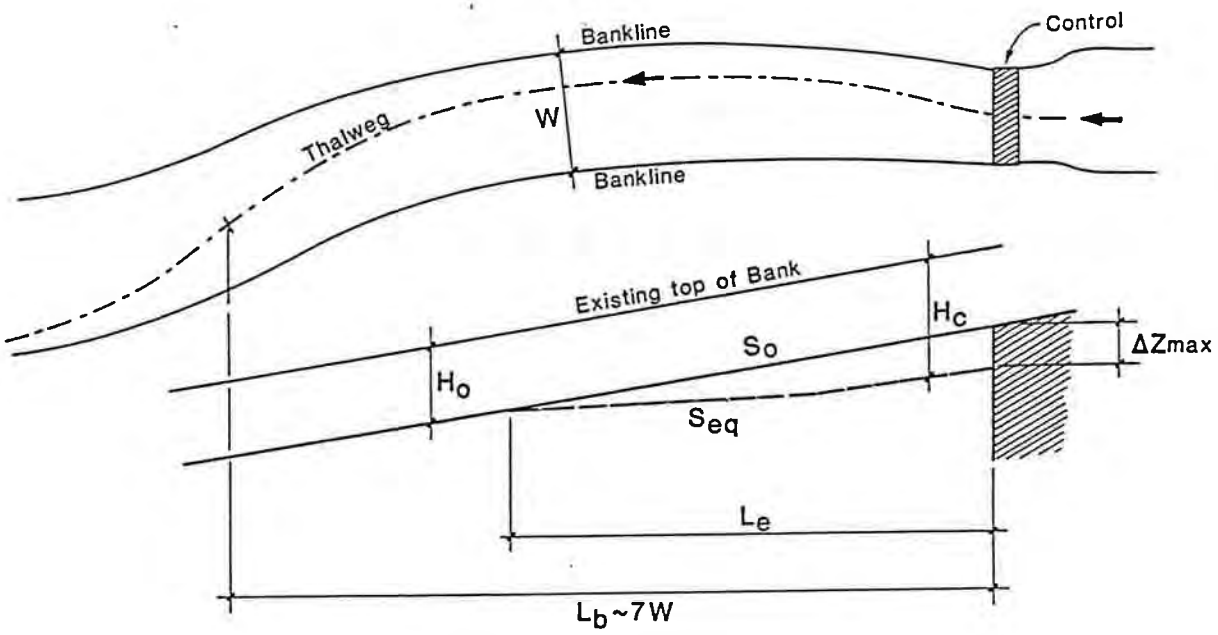


Figure 3.26. Schematic diagram illustrating geometry of the degradational channel reach.

11. Compute the percentage of the bed material transport capacity that will be removed from the bend using Equation 3.83 and the volume of sediment represented by that percentage. If the degradation is limited by the critical bank height, as discussed in step 10, add the portion of the degraded volume of sediment not accounted for by lowering of the channel to the volume removed from the bank due to the bend geometry. If this adjustment is made, check to ensure that the total volume of sediment removed from the bank does not exceed the transport capacity of the reach.

12. Compute the sine-generated curve that will result from removal of the sediment volume estimated in step 11. This can be accomplished in an iterative manner using the following steps:

    a. Assume a curve geometry (maximum angle ($\omega$) in Equation 3.69),

    b. Compute the coordinates of the curve and the average lateral offset from the straight line downvalley direction,

    c. Compute the area in the horizontal plane between the initial curve and assumed curve and volume of sediment represented by that area based on the average bank height through the bend,

    d. Compare the sediment volume with the volume removed from the bank, as estimated in step 11,

    e. Adjust the curve geometry, as appropriate, and repeat steps b. through d. until satisfactory agreement between the volume represented by the change in curve geometry and the eroded volume is obtained, and

    f. Compute the lateral erosion distance as the difference between the maximum lateral offset of the final and initial curves.

13. Repeat steps 2 through 12 for each storm event or time increment considered in the analysis, checking to ensure that the computed lateral migration distance does not exceed the maximum computed in step 3. If the maximum distance is reached, the computations can be stopped and the erosion buffer estimated based on the maximum erosion envelope.

A computer program has been developed to perform the above computations. This program is available from AMAFCA. A description of the program with input and output file formats are presented in Appendix D.

Guidelines for Aggradational Channels. As previously discussed, localized aggradational reaches can be expected to occur along arroyos in the Albuquerque area. These locations include the zone in the Northeast quadrant downstream of Tramway

Road and other locations where rapid incision, caused for example by urbanization, significantly increases the sediment load to the downstream reach above that which occurred prior to urbanization. When significant deposition occurs, channel capacity will be reduced, deposition may cause localized bank erosion and/or channel avulsion, and overbank flooding may increase. In many cases, a multibranched channel will result. The dynamics of the arroyo under aggradational conditions become very uncertain, making analytical estimates of lateral erosion distance impractical or meaningless. The lateral migration potential of the channel is more a function of possible flow paths that may be taken by the overbank flows than that of bank erosion. For this case, the boundary along the arroyo within which it is not considered prudent to develop, is most likely controlled by the limits of flooding rather than migration of the arroyo. The flood limits may be substantially larger than indicated by fixed-bed models without consideration of aggradation.

## 3.5 Local Scour

Local scour occurs where the flow is accelerated due to obstructions in the flow and involves removal of bed and bank material from around piers, abutments, spurs, embankments, and downstream of grade control structures or channel drops. The principal erosion mechanism is the creation of vortices by the obstruction and resultant acceleration of the flow. Like contraction scour, local scour is cyclic in nature, scouring during the rising limb with subsequent refilling during the recession of a hydrograph.

3.5.1 Pier Scour at Bridge Crossings. For piers placed in the flow, vortices form around the base of the pier. The formation of these vortices results from a pileup of water on the upstream face of the pier and subsequent acceleration of flow around the pier. The action of the base vortex (otherwise known as the horseshoe vortex - see **Figure 3.27**) removes sediment from the bed of the channel near the pier base resulting in a scour hole. Vertical wake vortices form downstream of the pier which can also remove sediment from around the base of the pier.

The following factors influence the size and formation of scour holes around piers:

1. Pier width has a direct influence on depth of local scour. As pier width increases, there is an increase in scour depth.

2. Pier length has no appreciable effect on local scour depth as long as the pier is aligned with the flow. When the pier is skewed to the flow, the length has a significant effect.

3. Flow depth has an effect on the depth of local scour. An increase in flow depth can cause increase scour depth by a factor of 2 or greater for piers.

4. The greater the approach velocity, the deeper the scour.

5. Angle of attack of the flow to the pier has a significant effect on local scour.

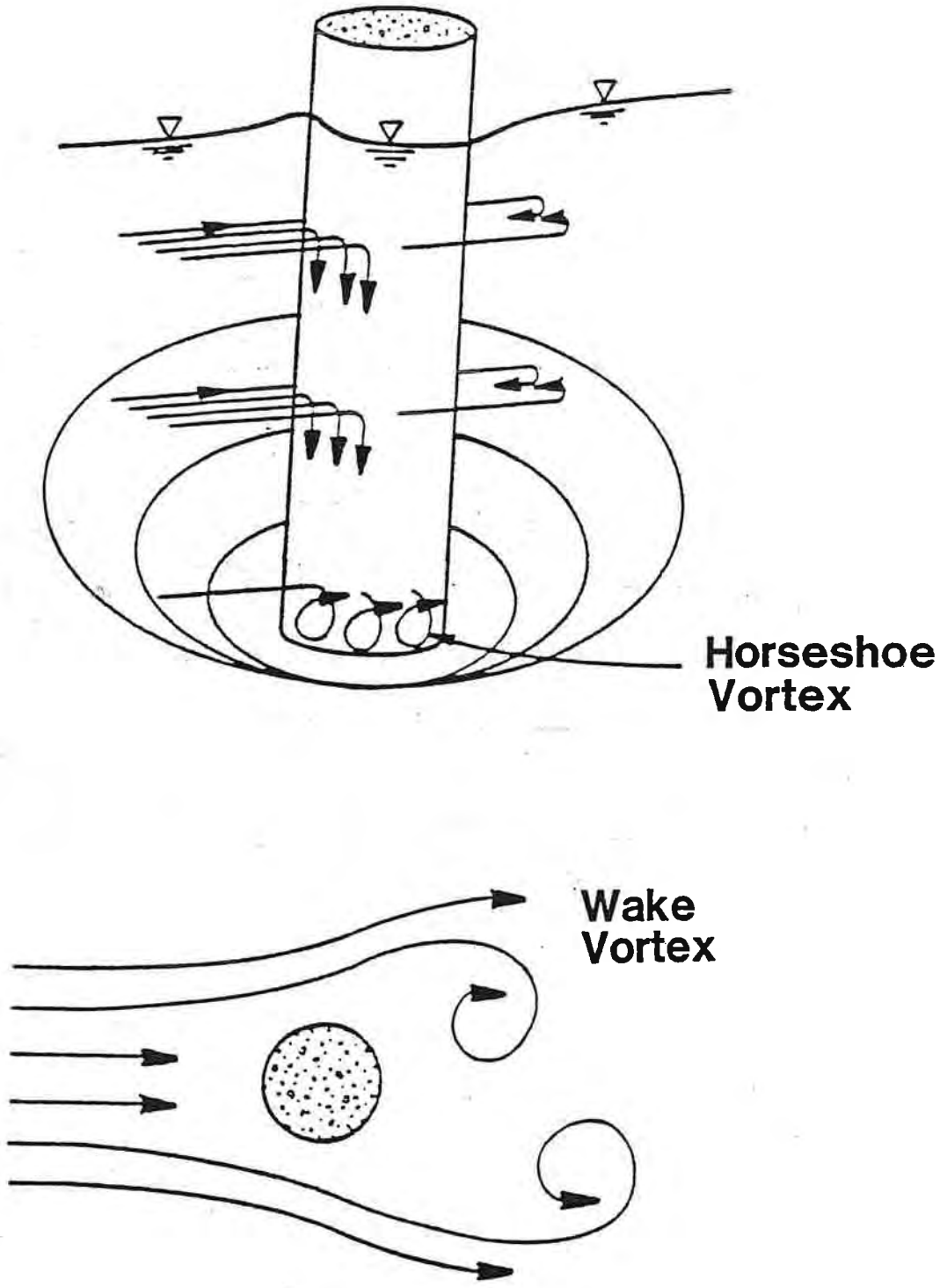


Figure 3.27. Schematic representation of scour at a cylindrical pier.

6. Shape of the nose of a pier or an abutment has a significant effect on scour. Streamlining the front end of a pier reduces the strength of the horseshoe vortex, thereby reducing scour depth. Streamlining the downstream end of piers reduces the strength of the wake vortices. A square-nose pier will have maximum scour depths about 20 percent greater than a sharp-nose pier and 10 percent greater than either a cylindrical or round-nose pier.

7. Debris can potentially increase the width of the piers, change the shape of piers and abutments, and cause the flow to plunge downward against the bed. This can increase both the local and contraction scour. The magnitude of the increase is still largely undetermined. Debris can be taken into account in the scour equations by estimating how much the debris will increase the width of a pier.

8. Bed material characteristics such as size, gradation, and cohesion can affect local scour. Bed material in the sand size range has no effect on local scour depth. Larger size bed material that can be moved by the flow or by the vortices and turbulence created by the pier will not affect the maximum scour, but only the time it takes to attain it. Very large particles in the bed material, such as cobbles or boulders, may armor the scour hole. However, the extent to which large particles will minimize scour is not clearly understood.

Fine bed material (silts and clays) will have scour depths as deep as sand-bed streams. This is true even if the fine material is bonded together by cohesion. The effect of cohesion is to influence the time it takes to reach the maximum scour. With sand-bed material, the time to reach maximum depth of scour is measured in hours and can result from a single flood event. With cohesive bed materials, it may take days, months, or even years to reach the maximum scour depth, the result of many flood events.

For computing pier scour, the Colorado State University equation is currently recommended by the Federal Highway Administration (Richardson et al., 1991) and is as follows:

$$\frac{y_s}{y_1} = 2.0\ K_1\ K_2\ \left(\frac{a}{y_1}\right)^{0.65}\ F_{r_1}^{0.43} \qquad (3.85)$$

where
- $y_s$ = equilibrium scour depth, ft
- $y_1$ = flow depth just upstream of the pier, ft
- $K_1$ = correction for pier nose shape from **Figure 3.28** and **Table 3.9**
- $K_2$ = correction for angle of attack of flow from **Table 3.10**
- $a$ = pier width
- $F_{r1}$ = Froude Number = $V_1/\sqrt{(gy_1)}$ exponent based on conditions just upstream of the pier

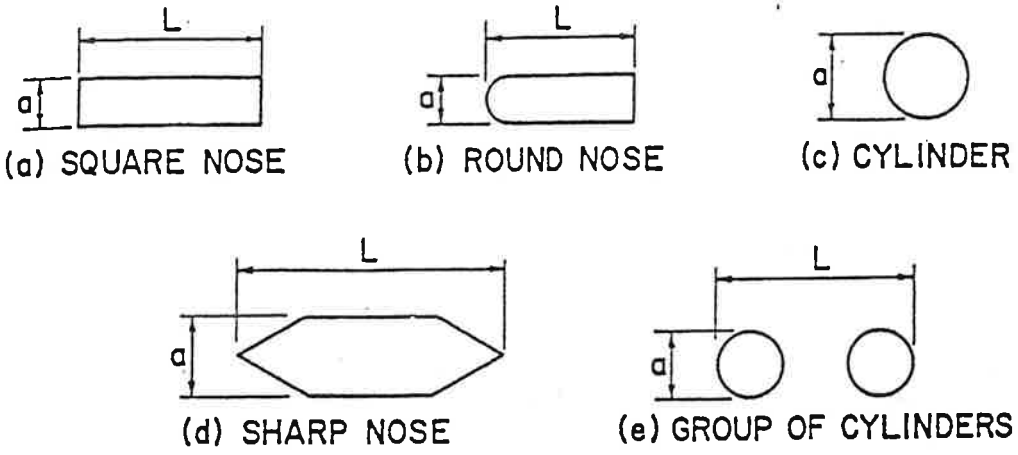


Figure 3.28. Common pier shapes.

| Table 3.9. Correction Factor $K_1$ for Pier Nose Shape. | | |
|---|---|---|
| | Shape of Pier Nose | $K_1$ |
| a. | Square nose | 1.1 |
| b. | Round nose | 1.0 |
| c. | Circular cylinder | 1.0 |
| d. | Sharp nose | 0.9 |
| e. | Group of cylinders | 1.0 |

| Table 3.10. Correction Factor $K_2$ for Angle of Attack of the Flow. | | | |
|---|---|---|---|
| Angle | L/a=4 | L/a=8 | L/a=12 |
| 0 | 1.0 | 1.0 | 1.0 |
| 15 | 1.5 | 2.0 | 2.5 |
| 30 | 2.0 | 2.5 | 3.5 |
| 45 | 2.3 | 3.3 | 4.3 |
| 90 | 2.5 | 3.9 | 5.0 |

Note 1: The correction factor $K_1$ for pier nose shape should be determined using Table 3.9 for flow angle of attack up to 5 degrees. For greater angles, pier nose shape loses its effect and $K_1$ should be considered as 1.0.

Note 2: For dune bed configuration (in large rivers) increase computed local scour by 30 percent. For plane bed and antidunes (common in arroyos), increase computed depth of scour by 10 percent or compute antidune height using Equation 3.68.

Live-bed scour (see Section 3.4.3) in sand-bed streams with a dune-bed configuration fluctuates about the equilibrium scour depth. The reason for this is the variability of the bed material sediment transport in the approach flow when the bed configuration of the stream is dunes. In this case (dune bed configuration in the channel upstream of the bridge), maximum depth of scour is about 30 percent larger than equilibrium depth of scour for large rivers. Normally, arroyos under flood-flow conditions will be in upper regime with either plane bed or antidunes. For these conditions, the maximum depth of scour is about 10 percent larger than the equilibrium depth of scour computed with Equation 3.85.

The maximum depth of scour is the same as the equilibrium depth of scour for live-bed scour with a plane bed configuration (see Section 3.2.3). With antidunes occurring upstream and in the bridge crossing, the maximum depth of scour is about 10 percent greater than the equilibrium depth of scour. In most cases, arroyos in the Albuquerque area will contain antidunes during flood flows.

3.5.2 Scour at Grade Control Structures. Accelerating flow over the crest of grade control and drop structures induces local scour immediately downstream of these structures. Additionally, turbulent flow downstream of these structures can also cause lateral instability of banks and subsequent widening and possible outflanking of the grade control structures.

Grade control and drop structures are discussed in "Design Guide for Riprap-Lined Flood Control Channels" (AMAFCA, 1983) which provides references to evaluation and control of scour at drop structures. An alternative approach to estimating scour at channel drop and grade control structures is the use of the Veronese equation, Equation 3.85 (Pemberton and Lara, 1984) as discussed below.

The most conservative estimate of scour downstream of channel drop structures is for vertical drops with unsubmerged flow conditions. For purposes of design, the maximum expected scour can be assumed to be equal to the scour for a vertical, unsubmerged drop, regardless of whether the drop is actually sloped or submerged.

A typical vertical drop structure is diagrammed in **Figure 3.29.** The Veronese equation is:

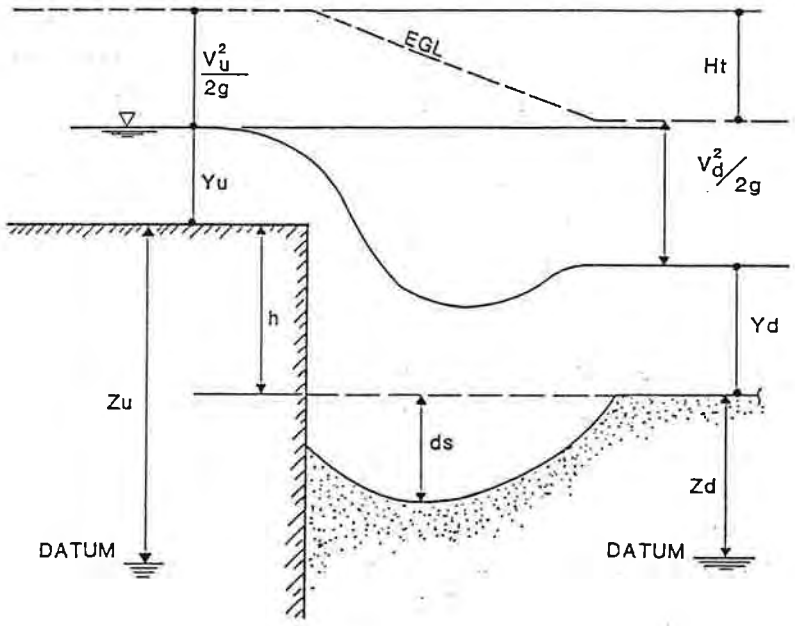


Figure 3.29. Schematic of a vertical drop caused by a check dam.

$$d_s = K H_t^{0.225} q^{0.54} - d_m \qquad (3.86)$$

where $d_s$ = local scour depth for a free overfall, measured from the streambed downstream of the drop, ft
$q$ = discharge per unit width, cfs per foot of width
$H_t$ = total drop in head, measured from the upstream to the downstream energy grade line, ft
$d_m$ = tailwater depth, ft
$K$ = 1.32

It should be noted that $H_t$ is the difference in the total head from upstream to downstream. This can be computed using the energy equation for steady uniform flow:

$$H_t = \{ Y_u + \frac{V_u^2}{2g} + Z_u \} - \{ Y_d + \frac{V_d^2}{2g} + Z_d \} \quad (3.87)$$

where Y = depth, ft
V = velocity, ft/sec
Z = bed elevation referenced to common datum, ft
g = acceleration due to gravity 32.2 $(ft/sec)^2$

The subscripts u and d refer to upstream and downstream of the channel drop, respectively.

The depth of scour as estimated by the above equation is independent of the grain size of the bed material. This concept acknowledges that the bed will scour regardless of the type of material composing the bed, but the rate of scour depends on the composition of the bed.

The drop structure must be designed structurally to withstand the forces of water and soil assuming that the scour hole is as deep as estimated using the equation above. Therefore, the designer should consult soils and structural engineers so that the drop structure will be stable under the full scour condition. In some cases, a series of drops may be employed to minimize drop height and construction costs of foundations, or riprap or energy dissipation could be provided to limit depth of scour.

3.5.3 Scour at Revetments, Spurs and Abutments. Local scour must be considered at other obstructions to flow such as revetments, flood walls, spurs, guide banks, or at abutments of bridges. Local scour occurs at the nose of spurs, at the base and ends of revetments, and at abutments of bridges when either the bridge encroaches into the channel or when there is overbank flow which must return to the main channel at the bridge opening. Richardson et al. (1991) provides guidance for estimating local scour at these types of hydraulic structures.

Field data for scour at abutments and similar structures such as a flood wall for various size streams are scarce, but data collected at rock dikes on the Mississippi River indicate the equilibrium scour depth for large $a/Y_1$ values can be estimated by the following equation:

$$\frac{Y_s}{Y_1} = 4\ F_{r_1}^{0.33} \qquad (3.88)$$

where $Y_s$ = equilibrium depth of scour (measured from the mean bed level to the bottom of the scour hole)
$Y_1$ = average upstream flow depth in the main channel
a = abutment and embankment or wall length projecting into main channel
$F_{r1}$ = upstream Froude Number

3.5.4. Scour Along a Flood Wall

Flow Parallel to the Wall. The probable mechanism causing scour along a flood wall when the flow is parallel to the wall is an increased boundary shear stress produced by locally increased velocity gradients that result from the reduced roughness of the flood wall, as compared to the natural channel. It is reasonable to conclude that this scour will continue until the local flow area has increased enough to reduce the local velocity, and hence the local boundary shear stress, to values typical of the rest of the channel cross section.

The distribution of boundary shear stress around the perimeter of a channel is not constant. In channels of uniform roughness, this distribution has been quantified both analytically (Olson and Florey, 1952; and Replogle and Chow, 1966) and experimentally (Ippen and Drinker, 1962; Davidian and Cahal, 1963; Rajaratnam and Muralidhar, 1969, Kartha and Leutheusser, 1970; and Schall, 1979). These results indicate that the boundary shear stress has a maximum value near the channel centerline, and a secondary peak about one-third of the way up the sideslope. On average, the maximum on the bottom is about 0.97 times the average boundary shear stress (e.g., as defined by $\gamma RS$) for the cross section and the maximum on the side is about 0.76 times the average boundary shear stress. However, experimental data indicated a range of values, with maximum shear stresses as much as 1.6 times the average. In general, the boundary shear stress distribution is more uniform as the width to depth ratio increases.

Similar information is not available for channel cross sections of nonuniform roughness; however, reasonable conclusions can be drawn from intuitive arguments. For a straight channel with a flood wall with smoother roughness than the rest of the channel along one side, the boundary shear stress distribution would be skewed towards the flood wall side of the channel. The sideslope peak value would be larger and could possibly be greater than the peak along the channel bed, which would also be shifted off the centerline location. These effects would be more pronounced in narrow channels and/or channels with steep sideslopes. As the channel gets wider, or the sideslope flattens, these effects would be diminished.

Insight on the magnitude of these effects can be obtained by consideration of local velocity conditions as determined by conveyance weighting concepts. The analysis assumes that the boundary roughness within the channel can be divided into two distinct regions: one region defining the roughness of the channel and the other defining the roughness of the channel bottom (note that this division of roughness, while logical, is not always analytically useful as it can create numerical problems leading to errors in the computation of conveyance for the entire cross section).

For purposes of illustration, assume a wide, shallow natural channel has uniform roughness with an n value of 0.03, but with a concrete flood wall the n value of the bank region is reduced by a factor of two, to 0.015. Evaluation of the distribution of discharge by conveyance weighting shows that this reduction of n nearly doubles the conveyance, discharge and velocity adjacent to bank (i.e., next to the flood wall). Now, recognizing that boundary shear stress is proportional to velocity squared, this increase in velocity increases the boundary shear stress by a factor of 4.

Based on the results for a uniform roughness channel, where the maximum boundary shear on the channel sideslope is about 0.76 times the average boundary shear stress, these results suggest that the maximum boundary shear stress along the flood wall could be as much as 3 times the average boundary shear stress. However, this is not totally accurate given the simplistic assumptions made and the likely changes in the distribution pattern that would result under flood wall conditions. In any event, this simplified analysis suggests that significant increases in the boundary shear stress are possible adjacent to the flood wall.

For purposes of the Design Guide, it is appropriate to define a shear stress multiplier that can be applied to the average boundary shear stress to define the locally increased boundary shear stress adjacent to a flood wall. Based on the above argument, a shear stress factor of 3 will be utilized. Recognizing that boundary shear stress is proportional to velocity squared, the reduction in velocity necessary to lower the shear stress to an acceptable value is defined by the inverse of the square root of the shear stress multiplier (0.577) for a shear stress factor of 3. For the reduction in velocity to occur, the flow area must then be increased by the inverse of this factor (1/0.577 = 1.73). For a vertical flood wall, this calculation simplifies to a unit width basis and the scour depth is a multiplier of the flow depth ($0.73Y_1$).

It is important to understand that this provides a first approximation of the potential scour along a flood wall due to flow parallel to the wall. Using this relation, the total scour along the wall due to parallel flow can be approximated as the sum of the above relation which results from a differential in shear stress plus scour associated with the passage of antidunes (see Equation 3.68). This results in the following relationship:

$$\frac{Y_s}{Y_1} = 0.73 + 0.14\pi F_r^2 \qquad (3.89)$$

This equation is applicable only where parallel flow can be assured (e.g., flood walls along both arroyo banks).

Flow Impinging on the Wall at an Angle

As discussed in the previous section, when an obstruction such as an abutment projects into the flow, the depth of scour at the nose of the obstruction can be estimated from Equation 3.88. Considering the physical configuration of the channels for which the data on which this relation is based, this can reasonably be assumed to be the upper limit of the scour that could be expected for flow along a flood wall when the flow impinges on the wall at an approximately 90° angle. The total scour along a flood wall, thus, will vary as a proportion of that given by Equations 3.88 and 3.89. If it is assumed that the relative significance of the two scour mechanisms is related to the change in momentum associated with the change in flow direction from some angle to the wall to a direction parallel to the wall (see **Figure 3.30**), the two relations can be combined using a weighting factor based on the sine or cosine of the angle, respectively. The resulting relationship is given by:

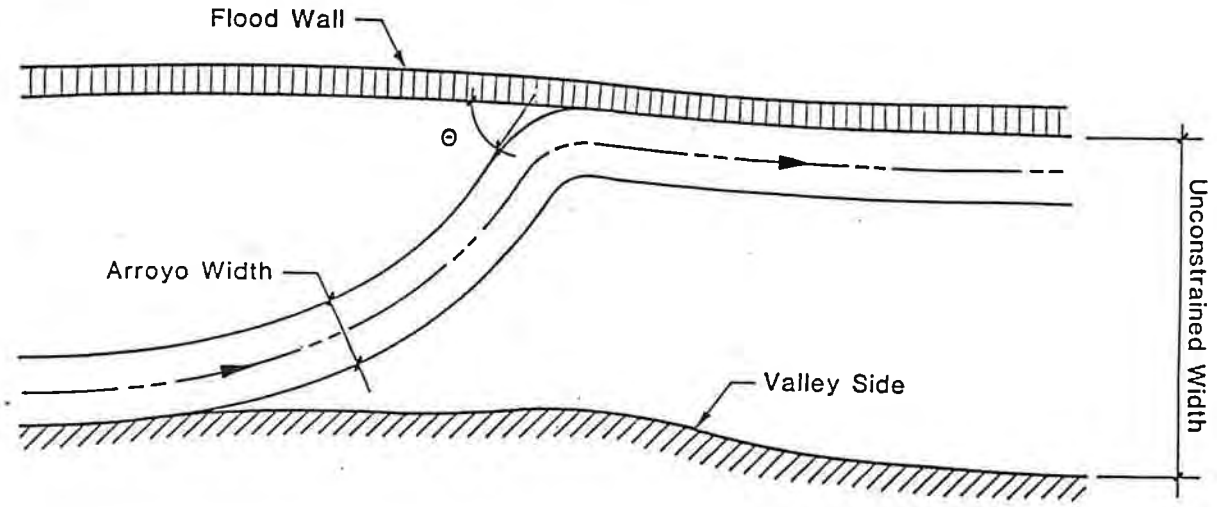


Figure 3.30. Schematic of channel alignment associated with a flood wall.

$$\frac{Y_s}{Y_1} = (0.73 + 0.14\pi F_r^2)\cos\theta + 4F_r^{0.33}\sin\theta \qquad (3.90)$$

where $\theta$ = angle between the flow direction and the flood wall

Scour Along a Flood Wall in Relation to Unconstrained Valley Width

The potential scour that could occur along a flood wall due to changes in planform as the arroyo evolves can be estimated by combining Equation 3.90 with the relationships for ideal meander geometry discussed in Section 3.4. Using these relationships, it can be shown that the maximum angle will vary from zero when the width of the valley is constrained to the width of the arroyo to approximately 71° when the unconstrained valley width is approximately 3.5 times the width of the arroyo. (These values are based on the assumption that the meander wavelength is 14 times the channel width). It is of course possible for the channel to impinge perpendicularly to the wall due to local flow deflection or other local factors. For this case, the angle of impingement is no longer related to the valley width and the maximum scour depth can best be estimated based strictly on Equation 3.88. The resulting dimensionless scour depth as a function of the unconstrained valley width is plotted in **Figure 3.31** for a range of Froude Numbers ($F_r$).

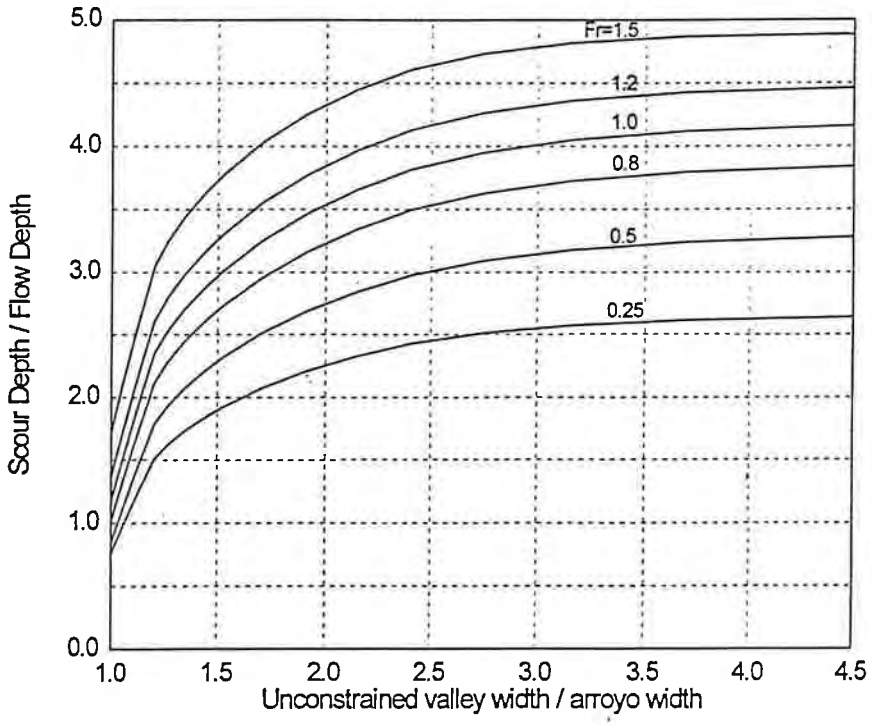


Figure 3.31. Scour along a flood wall as a function of unconstrained valley width.

In using **Figure 3.31**, it is important to recognize that the relationships are based on an assumed ideal meander geometry and scour relationships that, while they are the best available, are very approximate. Considering the extreme local variability that can occur in a given arroyo and the approximate nature of the relationships upon which these results are based, engineering judgment is critical in evaluating the reasonableness of the results for a specific problem. In particular, the potential for flow deflection and its effect on the angle of impingement on the wall should be considered and a conservatively large angle applied in Equation 3.90. If there is any reasonable possibility of flow perpendicular to the wall, an angle of 90° (thus, Equation 3.88) is recommended. Further, as will be discussed in Chapter 4, when the results of this analysis are used to design the burial depth for a flood wall, a safety factor of at least 1 foot should be added to the predicted scour depth.

Equation 3.90 and **Figure 3.31** are commonly used in arroyo applications where lateral migration and bank erosion must occur before channel flows impinge on a flood wall. Lateral erosion can occur rapidly, including the early portion of major storm events, and the geometry of the arroyo sections may change as a result of lateral erosion. For the condition where arroyo geometry must change for flow to reach the flood wall, it is reasonable to use the arroyo hydraulic depth (area / top width) as the flow depth in Equation 3.90 and **Figure 3.31**. An estimate of hydraulic depth may be obtained by using the dominant arroyo width ($W_D$, see Section 3.4.5) and Manning's equation. Depth of scour is measured from the minimum bed elevation (thalweg elevation) of the existing arroyo, or from the minimum bed elevation (future degraded thalweg) for the case of degrading arroyo reaches. **Figure 3.32** shows the final wall scour depth for a typical arroyo section.

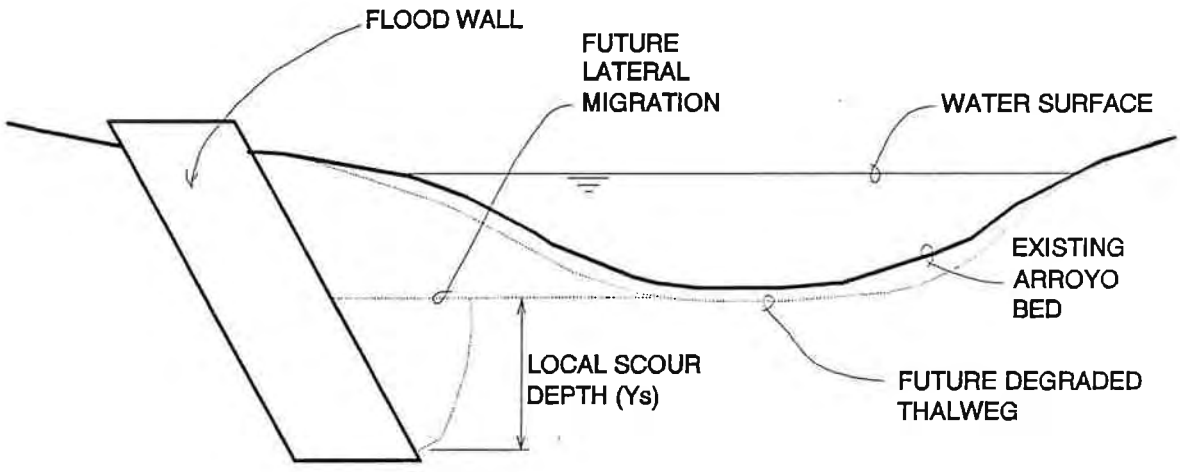


Figure 3.32 Schematic of flood wall scour at arroyo section

### 3.5.5. Local Scour at Culvert Outlets

High-velocity flow at the culvert outlet will create a local scour hole in locations where bed and bank protection are not present. In some instances, energy dissipation structures may be required to prevent excessive erosion in this location. The size and depth of the local scour hole can be computed using equation presented in "Hydraulic Design of Energy Dissipators for Culverts and Channels" (FHWA, 1983). Since most soils in the Albuquerque area are noncohesive, only the equation applicable to these conditions is presented here. The equation for scour hole geometry is given by:

$$A^* = \alpha\left(\frac{Q}{\sqrt{g}D^{5/2}}\right)^{\beta}\left(\frac{t}{t_0}\right)^{\Theta} \qquad (3.91)$$

where $A^*$ is the dimensionless scour geometry,($h_s/D$, $W_s/D$, $L_s/D$, or $V_s/D^3$) and ($h_s/y_e$, $W_s/y_e$, $L_s/y_e$, or $V_s/y_e^3$), $Q$ is the discharge, $g$ is the acceleration of gravity, $D$ is the culvert diameter, $t$ is the duration of the flow and $t_0$ = 316 minutes, the base time used in the experiments upon which the relations are based. For noncircular culverts or culverts flowing partially full, the diameter (D) is replaced by the equivalent depth ($y_e$) defined by:

$$y_e = \sqrt{\frac{A}{2}} \qquad (3.92)$$

where $A$ = cross-sectional area of the flow and the coefficient $\alpha$ is replaced by $\alpha_e$ given by the following relation:

$$\alpha_e = \alpha\ 0.63^{(2.5\,\beta\,-1)} \qquad (3.93)$$

for computing $h_s$, $W_s$, and $L_s$, and by the relation:

$$\alpha_e = \alpha\ 0.63^{(2.5\,\beta\,-3)} \qquad (3.94)$$

for computing $V_s$. The coefficient ($\alpha$) and exponents ($\beta$ and $\theta$) are summarized in **Table 3.11**. This formulation for scour depth assumes that the elevation of the culvert outlet is at the elevation of the downstream channel. If the culvert outlet is above the channel or if the downstream channel is lowered by degradation, additional scour depth will result and the vertical drop structure procedures, using Equations 3.85 and 3.86 should be used to estimate the scour depth.

Gradation. The cohensionless bed materials presented in **Table 3.11** are categorized as either uniform (U) or graded (G). The standard deviation of the grain size distribution ($\sigma$) is used to determine the category. The standard deviation ($\sigma$) is computed as:

$$\sigma = (d_{84} / d_{16})^{1/2}$$

If $\sigma \leq 1.5$, the material is considered to be uniform; if $\sigma \geq 1.5$, the material is classified as graded.

Time of Scour. The time of scour is based on a knowledge of peak flow duration. Lacking this knowledge, it is recommended that a time of 30 minutes be used in Equation 3.91. Tests indicate that approximately 2/3 to 3/4 of the maximum scour occurs in the first 30 minutes of the flow duration.

Headwalls. Installation of headwalls flush with the culvert outlet moves the scour hole downstream. However, the magnitude of the scour geometries remain essentially the same as for the case without the headwall. If the culvert is installed with a headwall, the headwall should extend to a depth equal to the maximum depth of scour.

| Table 3.11. Experimental Coefficients for Culvert Outlet Scour. | | | | | | | | | | | | | | | | | |
|---|---|---|---|---|---|---|---|---|---|---|---|---|---|---|---|---|---|
| Material | Nominal Grain Size $d_{50}$ (mm) | Scour Equation | Depth $h_s$ | | | | Width $W_s$ | | | | Length $L_s$ | | | | Volume $V_s$ | | | |
| | | | $\alpha$ | ß | $\Theta$ | $\alpha_e$ | $\alpha$ | ß | $\Theta$ | $\alpha_e$ | $\alpha$ | ß | $\Theta$ | $\alpha_e$ | $\alpha$ | ß | $\Theta$ | $\alpha_e$ |
| Uniform Sand | 0.20 | V-1 or V-2 | 2.72 | .375 | 0.10 | 2.79 | 11.73 | 0.92 | .15 | 6.44 | 16.82 | 0.71 | 0.125 | 11.75 | 203.36 | 2.0 | 0.375 | 80.71 |
| Uniform Sand | 2.0 | V-1 or V-2 | 1.86 | 0.45 | 0.09 | 1.76 | 8.44 | 0.57 | 0.06 | 6.94 | 18.28 | 0.51 | 0.17 | 16.10 | 101.48 | 1.41 | 0.34 | 79.62 |
| Graded Sand | 2.0 | V-1 or V-2 | 1.22 | 0.85 | 0.07 | .75 | 7.25 | 0.76 | 0.06 | 4.78 | 12.77 | 0.41 | 0.04 | 12.62 | 36.17 | 2.09 | 0.19 | 12.94 |
| Uniform Gravel | 8.0 | V-1 or V-2 | 1.78 | 0.45 | 0.04 | 1.68 | 9.13 | 0.62 | 0.08 | 7.08 | 14.36 | 0.95 | 0.12 | 7.61 | 65.91 | 1.86 | 0.19 | 12.15 |
| Graded Gravel | 8.0 | V-1 or V-2 | 1.49 | 0.50 | 0.03 | 1.33 | 8.76 | 0.89 | 0.10 | 4.97 | 13.09 | 0.62 | 0.07 | 10.15 | 42.31 | 2.28 | 0.17 | 32.82 |



V-1. FOR CIRCULAR CULVERTS. Cohesionless material or the 0.15 mm cohesive sandy clay.

$$\left[\frac{h_s}{D}, \frac{W_s}{D}, \frac{L_s}{D}, \text{ or } \frac{V_s}{D^3}\right] = \alpha\left(\frac{Q}{\sqrt{g}\,D^{5/2}}\right)^{\beta}\left(\frac{t}{t_o}\right)^{\theta} \qquad \text{where } t_o = 316 \text{ min.} \qquad (3.91)$$

V-2. FOR OTHER CULVERT SHAPES. Same material as above.

$$\left[\frac{h_s}{y_e}, \frac{W_s}{y_e}, \frac{L_s}{y_e}, \text{ or } \frac{V_s}{y_e^3}\right] = \alpha_e\left(\frac{Q}{\sqrt{g}\,y_e^{5/2}}\right)^{\beta}\left(\frac{t}{t_o}\right)^{\theta} \qquad \text{where } t_o = 316 \text{ min.} \qquad (3.91a)$$

# 4.0 ANALYSIS PROCEDURES

## 4.1 General Solution Procedure

This chapter describes the general solution procedure recommended for conducting a Prudent Line analysis. The recommended procedure progresses from a qualitative analysis of existing and future conditions (Level 1) to a more detailed quantitative analysis using basic engineering calculation techniques (Level 2). In more complex situations where the consequences of failure are particularly significant, mathematical and/or physical modeling may be required (Level 3). (A Level 3 analysis requires highly specialized knowledge and/or equipment and is beyond the scope of this Design Guide.) The concepts discussed in Chapter 3 provide the detailed techniques for conducting individual components of the Level 1 and Level 2 analyses. The following discussion provides an organized framework with which to tie the individual components of the analysis together to establish an appropriate erosion buffer zone, and thus the Prudent Line, within which it is not considered prudent to develop. The solution procedure incorporates analytical and computational techniques presented in Chapters 2 and 3. Some discussion is also included to assist the user in determining when a more detailed Level 3 analysis may be appropriate.

The analysis of any complex problem should begin with an overview or general evaluation, including a qualitative assessment of the problem and its solution. This fundamental initial step should be directed towards providing insight and understanding of significant physical processes, without being too concerned with the specifics of any given component of the problem. The understanding generated from such analyses ensures that subsequent detailed analyses are properly designed.

The progression to more detailed analyses should begin with application of basic principles, followed as required, with more complex solution techniques. This solution approach, beginning with qualitative analysis, proceeding through basic quantitative principles and then utilizing, as required, more complex or state-of-the-art solution procedures ensures that accurate and reasonable results are obtained while minimizing the expenditure of time and effort.

The inherent complexities of arroyo and drainageway stability in the Southwest requires such a solution procedure. The evaluation of flooding and erosion risk, determination of Prudent Line offset distances, and design of erosion barriers should begin with a qualitative assessment of stream stability. This involves application of geomorphic concepts to identify potential problems and alternative solutions. This analysis should be followed with quantitative analyses using basic hydrologic, hydraulic and sediment transport engineering concepts. Such analyses could include evaluation of flood history, channel hydraulic conditions (up to and including, for example, water surface profile analysis) and basic sediment transport analyses such as evaluation of watershed sediment yield, computation of transport rates, incipient motion analysis, and

scour calculations. This analysis can be considered adequate for many locations if the problems are resolved and the relationships between different factors affecting stability are adequately explained. If not, a more complex quantitative analysis based on detailed mathematical modeling and/or physical hydraulic models should be considered.

In summary, the general solution procedure for analyzing arroyo and drainageway stability could involve the following three levels of analysis:

Level 1: Application of Geomorphic Concepts and Other Qualitative Analyses

Level 2: Application of Basic Hydrologic, Hydraulic and Sediment Transport Engineering Concepts

Level 3: Application of Mathematical or Physical Modeling Studies

## 4.2 Data Requirements

The types and detail of data required to analyze a sediment area or channel stability problem are highly dependent on the relative instability of the stream and the depth of study required to obtain adequate resolution of potential problems. More detailed data are needed where quantitative analyses are necessary, and data from an extensive reach of stream may be required to resolve problems in complex and high risk situations.

4.2.1 Level 1: Geomorphic and Other Qualitative Analyses. The data required for preliminary stability analyses include maps, aerial photographs, notes, and photographs from field inspections, historic channel profile data, information on man's activities, and changes in stream hydrology and hydraulics over time.

Area, vicinity, site, geologic, soils, and land use maps each provide essential information. Unstable channel reaches up- or downstream of the study site can cause instability at the site. Area maps are needed to locate unstable reaches relative to the site. Vicinity maps help to identify more localized problems. They should include a sufficient reach of channel to permit identification of geomorphic characteristics of the arroyo or drainageway, and to locate bars, braids, and channel controls. Site maps are needed to determine factors that influence local stability and flow alignment, such as bars and tributaries. Geologic maps provide information on deposits and rock formations and outcrops that control stream stability. Soils and land use maps provide information on soil types, vegetative cover, and land use which affect the character and availability of sediment supply.

Aerial photographs record much more ground detail than maps and are frequently available at 5- to 10-year intervals. This permits measurement of the rate of progress of

bend migration, bankline failure, and other channel changes that cannot be measured from maps made less frequently.

Notes and photographs from field inspections are important to gaining an understanding of channel stability problems, particularly local stability. Field inspections should be made during high- and low-flow periods to record the location of bank cutting or slumping and deposition in the channel. Flow directions should be sketched, signs of aggradation or degradation noted, properties of bed and bank materials estimated or measured, and the locations and implications of impacting activities recorded.

If historic channel profile data are available, they will provide information on channel stability. Stage trends at gaging stations and comparisons of bed elevations with elevations before construction at structures will provide information on changes in channel profile. As-built bridge data and cross sections are frequently useful. Structure-induced scour should be taken into consideration where such comparisons are made.

Man's activities in a watershed are frequently the cause of channel instability. Information on urbanization, land clearing, clearing in arroyo channels, channelization, bend cutoffs, streambed sand and gravel mining, dam construction, reservoir operations, and other activities, either existing or planned, are necessary to evaluate the impact on channel stability.

Data on changes in morphology are important because change in a channel is rarely at a constant rate. Instability can often be associated with an event, such as an extreme flood or a particular activity in the watershed or channel. If association is possible, the rate of change can be more accurately assessed.

Similarly, information on changes in hydrology or hydraulics can sometimes be associated with activities that caused the change. Where changes in channel hydraulics are associated with an activity, changes in channel morphology are also likely to have occurred.

4.2.2 Level 2: Basic Engineering Analyses. Data requirements for basic hydrologic, hydraulic, and sediment transport engineering analysis are dependent on the types of analysis that must be completed. Hydrologic data needs include flood-flow frequency curves, flood hydrographs, dominant discharge (or bankfull flow) and flow-duration curves. Hydrologic methods are reviewed in Chapter 2. Hydraulic data needs include cross sections, channel and bank roughness estimates, channel alignment, and other data for computing channel hydraulics, up to and including water surface profiles calculations. Analysis of basic sediment transport conditions requires information on land use, soils, and geologic conditions, sediment sizes in the watershed and channel, and available measured sediment transport rates (e.g., from U.S. Geological Survey gaging stations).

More detailed quantitative analyses require data on the properties of bed and bank materials and, at times, field data on bed load and suspended load transport rates. Properties of bed and bank materials that are important to a study of sediment transport include size, shape, fall velocity, cohesion, density, and angle of repose.

4.2.3 Level 3: Mathematical and Physical Model Studies. Application of mathematical and physical model studies requires the same basic data as a Level 2 analysis, but typically in much greater detail. For example, water and sediment routing by mathematical models [e.g., the Corps of Engineers' HEC-6 (USCOE, 1991) or the National Cooperative Highway Research Program (NCHRP) BRI-STARS (Molinas, 1993)] and construction of a physical model, would both require detailed channel cross-sectional data. The more extensive data requirements for either mathematical or physical model studies, combined with the additional level of effort needed to complete such studies, results in a relatively large scope of work.

4.2.4 Data Sources. Preliminary stability data may be available from government agencies such as the U.S. Army Corps of Engineers, U.S. Geological Survey, Soil Conservation Service, local Commissions and Authorities, and local watershed districts. These agencies may have information on historic streambed profiles, stage-discharge relationships, and sediment load characteristics. They may also have information on past and planned activities that affect stream stability. **Table 4.1** provides a list of sources for the various data needed to assess stream stability at a site.

## 4.3 Level 1: Geomorphic Concepts and Other Quantitative Analysis

A flow chart of the typical steps in qualitative and other geomorphic analyses is provided in **Figure 4.1**. The six identified steps are generally applicable to most arroyo or drainageway stability problems. These steps are discussed in more detail in the following paragraphs. As shown on Figure 4.1, the qualitative evaluation leads to a conclusion regarding the need for more detailed (Level 2) analysis or a decision to proceed directly to establishing a flooding and erosion risk line (Prudent Line) and/or design of countermeasures (erosion barriers) based only on the qualitative and other geomorphic analyses. Guidelines and criteria for selection and design of countermeasures are discussed in Chapter 5.

4.3.1 Step 1. Define Channel Characteristics. The first step in stability analysis is to identify arroyo or drainageway characteristics according to the factors discussed in Chapter 3., Section 3.1, Arroyo Geomorphology. Defining the various geomorphic characteristics of the channel can provide insight into channel behavior and response, and information on impacting activities in the watershed.

4.3.2 Step 2. Evaluate Watershed Conditions. Water and sediment yield from a watershed is a function of watershed conditions and past or proposed land-use practices. Thus, knowledge of the land-use and historical changes in land use is essential to understanding conditions of channel stability and potential channel response to natural and man-induced changes.

Table 4.1. List of Data Sources (after Richardson et al., 1990).

Topographic Maps:

(1) 1" = 500' scale floodplain mapping of the Albuquerque area, available from City of Albuquerque, Public Works Department.

(2) Quadrangle maps - U.S. Department of the Interior, U.S. Geological Survey, Topographic Division; and U.S. Department of the Army, Army Map Service.

(3) River plans and profiles - U.S. Department of the Interior, U.S. Geological Survey, Conservation Division.

(4) National parks and monuments - U.S. Department of the Interior, National Park Service.

(5) Federal reclamation project maps - U.S. Department of the Interior, U.S. Bureau of Reclamation.

(6) Local areas - commercial aerial mapping firms.

(7) American Society of Photogrammetry.

Planimetric Maps:

(1) Plats of public land surveys - U.S. Department of the Interior, U.S. Bureau of Land Management

(2) National forest maps - U.S. Department of Agriculture, U.S. Forest Service.

(3) County maps - State Highway Agency.

(4) City plats - city or county recorder.

(5) Federal reclamation project maps - U.S. Department of the Interior, U.S. Bureau of Reclamation.

(6) American Society of Photogrammetry.

(7) ASCE Journal - Surveying and Mapping Division.

| Table 4.1. List of Data Sources (after Richardson et al., 1990). |
|---|
| Aerial Photographs:<br><br>(1) 1" = 200' scale aerial photographs of the Albuquerque area from the City of Albuquerque, Public Works Department.<br><br>(2) The following agencies have aerial photographs of portions of the United States: U.S. Department of the Interior, U.S. Geological Survey, Topographic Division; U.S. Department of Agriculture, Commodity Stabilization Service, Soil Conservation Service and U.S. Forest Service; U.S. Air Force; various state agencies; commercial aerial survey; National Oceanic and Atmospheric Administration; and mapping firms.<br><br>(3) Historic aerial photography, available from the University of New Mexico, Earth Data Analysis Department.<br><br>(4) American Society of Photogrammetry.<br><br>(5) Photogrammetric Engineering.<br><br>(6) Earth Resources Observation System (EROS) - Photographs from Gemini, Apollo, Earth Resources Technology Satellite (ERTS) and Skylab. |
| Transportation Maps:<br><br>(1) State highway agency. |
| Triangulation and Benchmarks:<br><br>(1) Control survey for the City of Albuquerque.<br><br>(2) State engineer.<br><br>(3) State highway agency. |
| Geologic Maps:<br><br>(1) U.S. Department of the Interior, U.S.Geological Survey, Geologic Division; and New Mexico Bureau of Mines and Mineral Resources at the New Mexico Institute of Mining and Technology. (Note - some regular quadrangle maps also show geological data). |

| Table 4.1. List of Data Sources (after Richardson et al., 1990). | |
|---|---|
| Soils Data: | |
| (1) | County soil survey reports - U.S. Department of Agriculture, Soil Conservation Service. |
| (2) | Land use capability surveys - U.S. Department of Agriculture, Soil Conservation Service. |
| (3) | Land classification reports - U.S. Department of the Interior, U.S. Bureau of Reclamation. |
| (4) | Hydraulic laboratory reports - U.S. Department of the Interior, U.S. Bureau of Reclamation. |
| Climatological Data: | |
| (1) | National Weather Service Data Center. |
| (2) | Hydrologic bulletin - U.S. Department of Commerce, National Oceanic and Atmospheric Administration. |
| (3) | Technical papers - U.S. Department of Commerce, National Oceanic and Atmospheric Administration. |
| (4) | Hydrometeorological reports - U.S. Department of Commerce, National Oceanic and Atmospheric Administration; and U.S. Department of the Army, Corps of Engineers. |
| (5) | Cooperative study reports - U.S. Department of Commerce, Oceanic and Atmospheric Administration; and U.S. Department of the Interior, U.S. Bureau of Reclamation. |

| Table 4.1. List of Data Sources (after Richardson et al., 1990). |
|---|
| Streamflow Data:<br><br>(1) Water supply papers - U.S. Department of the Interior; U.S. Geological Survey, Water Resources Division.<br><br>(2) Reports of state engineers.<br><br>(3) Annual reports - International Boundary and Water Commission, United States and Mexico.<br><br>(4) Annual reports - various interstate compact commissions.<br><br>(5) Hydraulic laboratory reports - U.S. Department of the Interior, Bureau of Reclamation.<br><br>(6) U.S. Bureau of Reclamation.<br><br>(7) Corps of Engineers, U.S. Army, flood control studies. |
| Sedimentation Data:<br><br>(1) Water supply papers - U.S. Department of the Interior, U.S. Geological Survey, Quality of Water Branch.<br><br>(2) Reports - U.S. Department of the Interior, U.S. Bureau of Reclamation; and U.S. Department of Agriculture, Soil Conservation Service.<br><br>(3) Geological Survey Circulars - U.S. Department of the Interior, U.S. Geological Survey. |

| Table 4.1. List of Data Sources (after Richardson et al., 1990). |
|---|
| Quality of Water Reports:<br><br>(1) Water supply papers - U.S. Department of the Interior, U.S. Geological Survey, Quality of Water Branch.<br><br>(2) Reports - U.S. Department of Health, Education, and Welfare, Public Health Service.<br><br>(3) Reports - state public health departments.<br><br>(4) Water resources publications - U.S. Department of the Interior, U.S. Bureau of Reclamation.<br><br>(5) Environmental Protection Agency, regional offices.<br><br>(6) State water quality agency. |
| Irrigation and Drainage Data:<br><br>(1) Agriculture census reports - U.S. Department of Commerce, Bureau of the Census.<br><br>(2) Agricultural statistics - U.S. Department of Agriculture, Agricultural Marketing Service.<br><br>(3) Federal reclamation projects - U.S. Department of the Interior, U.S. Bureau of Reclamation.<br><br>(4) Reports and progress reports - U.S. Department of the Interior, U.S. Bureau of Reclamation. |
| Power Data:<br><br>(1) Directory of Electric Utilities - McGraw Hill Publishing Company.<br><br>(2) Directory of Electric and Gas Utilities in the United States - Federal Power Commission.<br><br>(3) Reports - various power companies, public utilities, state power commissions, etc. |

| Table 4.1. List of Data Sources (after Richardson et al., 1990). |
| --- |
| Basin and Project Reports and Special Reports:<br><br>(1) U.S. Department of the Army, Corps of Engineers.<br><br>(2) U.S. Department of the Interior, Bureau of Land Management, Bureau of Mines, U.S. Bureau of Reclamation, U.S. Fish and Wildlife Service, and National Park Service. |

# LEVEL 1: QUALITATIVE ANALYSES

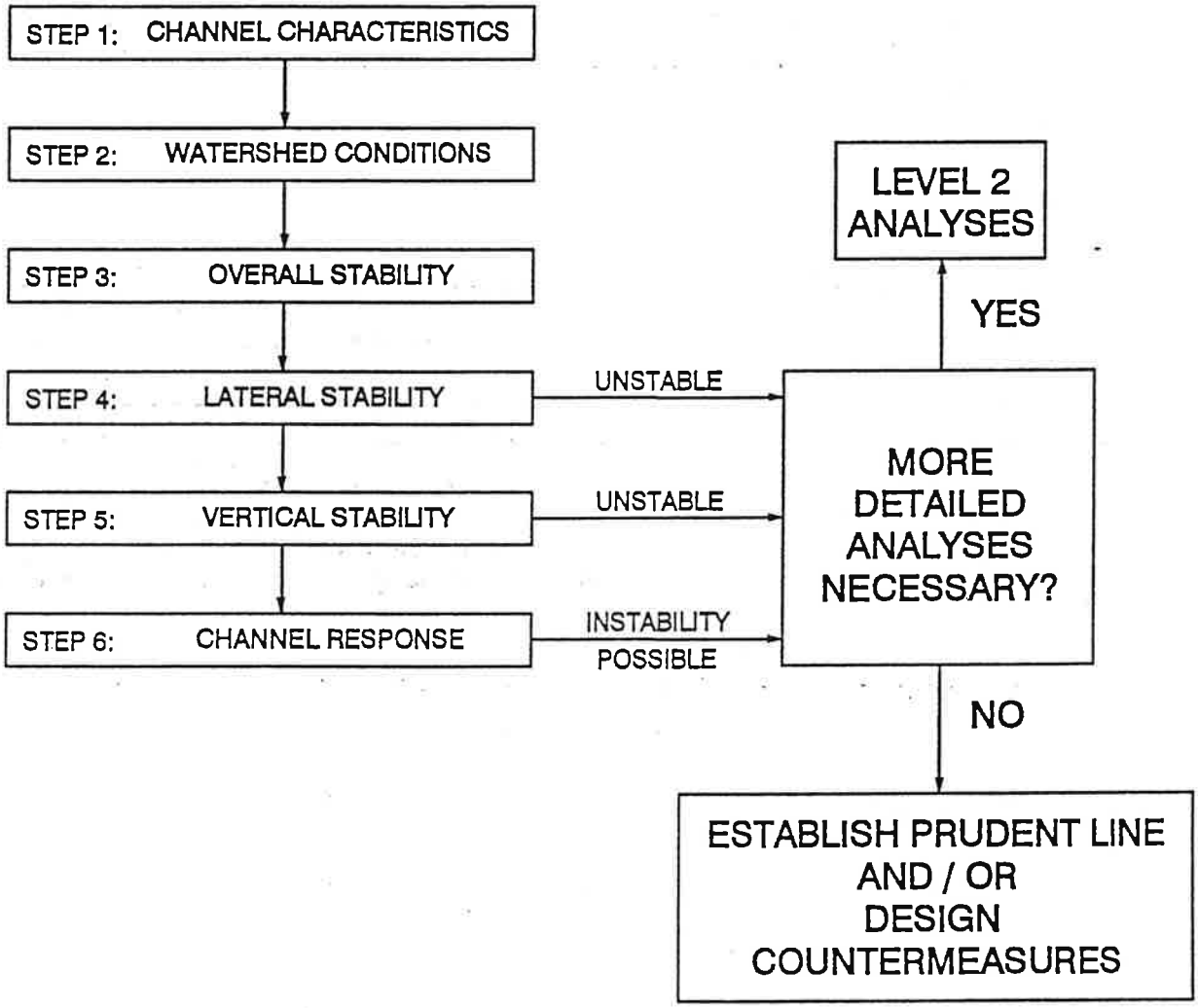


Figure 4.1. Flow chart for Level 1: Qualitative Analyses.

The presence or absence of vegetative growth can have a significant influence on the runoff and erosional response of a fluvial system. Large-scale changes in vegetation resulting from fire, logging, land conversion, and urbanization can either increase or decrease the total water and sediment yield from a watershed. For example, fire and logging tend to increase water and sediment yield, while urbanization promotes increased water yield and peak flows, but decreased sediment yield from the watershed. Under some conditions, urbanization may increase sediment yield from the channel.

Information on land-use history and trends can be found in federal, state, and local government documents and reports (i.e., census information, zoning maps, future development plans, etc.). Additionally, analysis of historical aerial photographs can provide significant insight on land-use changes. Land-use change due to urbanization can be classified based on estimated changes in pervious and impervious cover. Changes in vegetative cover can be classified simply as no change, vegetation increasing, vegetation damaged, and vegetation destroyed. The relationship or correlation between changes in channel stability and land-use changes can contribute to a qualitative understanding of system response mechanisms.

4.3.3 Step 3. Assess Overall Stream Stability. **Table 4.2** summarizes possible channel stability interpretations according to various channel characteristics. **Figure 4.2** is also useful in making a qualitative assessment of channel stability based on channel planform characteristics and the type of sediment load in the channel. It shows that straight channels are relatively stable only where flow velocities and sediment load are low. As velocity and sediment load increase, flow meanders in the channel causing the formation of alternate bars and the initiation of a meandering channel pattern. Similarly, meandering channels are progressively less stable with increasing velocity and bed load. At high values of these variables, the channel becomes braided. The presence and size of point and middle bars are indications of the relative lateral stability of a stream channel.

Bed material transport is directly related to stream power, and relative stability decreases as stream power increases as shown by Figure 4.2. Stream power is the product of shear stress at the bed and the average velocity in the channel section. Shear stress can be determined from the gross shear stress equation ($\gamma RS$) where $\gamma$ is the specific weight of water, $R$ is the hydraulic radius, and $S$ is the slope of the energy grade line (see Section 3.2.2).

Section 3.1 presents a more detailed discussion of the evolutionary process of arroyo development. The stability diagram in Figure 3.1 is a useful tool for evaluating the relative stability of a given reach of arroyo. In general, an arroyo must be in the lower left quadrant of Figure 3.1 to be considered stable. This implies that the slope has reduced and the width adjusted so that the reach is either in equilibrium or mildly aggradational (i.e., $N_h < 1$) over a period of time. It also implies that the banks do not exceed the critical height (i.e., $N_g < 1$). It is important to note that, even in this condition, local bank erosion can lead to channel migration in specific areas.

| Table 4.2. Interpretation of Observed Data (after Keefer et al., 1980). | | | | |
|---|---|---|---|---|
| | CHANNEL RESPONSE | | | |
| OBSERVED CONDITION | STABLE | UNSTABLE | DEGRADING | AGGRADING |
| Alluvial Fan[1]<br>Upstream<br>Downstream | | <br>X<br>X | <br><br>X | <br>X<br> |
| Dam and Reservoir[1]<br>Upstream<br>Downstream | | <br>X<br>X | <br><br>X | <br>X<br> |
| Bank Erosion | | X | Unknown | Unknown |
| Vegetated Banks | X | | Unknown | Unknown |
| Head Cuts | | X | X | |
| Diversion<br>Clear-water diversion<br>Overloaded w/sediment | | <br>X<br>X | <br><br>X | <br>X<br> |
| Channel Straightened | | X | X | |
| Clear Watershed | | X | | |
| Drought Period | X | | | X |
| Wet Period | | X | X | |
| Bed Material Size<br>Increase<br>Decrease | | <br>X<br>X | <br><br>Unknown | <br>X<br>X |

[1] The observed condition refers to location of the study reach on the alluvial fan, i.e., on the up- or downstream portion of the fan or up- or downstream of a dam.

4.3.4 Step 4. Evaluate Lateral Stability. A field inspection is a critical component of a qualitative assessment of lateral stability. A comparison of observed field conditions with the descriptions of stable and unstable channel banks presented in Section 3.4.5 helps to define bank stability. Similarly, field observations of bank material composition and existing failure modes can provide insight on bank stability, based on the descriptions of cohesive, noncohesive, and composite banks given in Section 3.4.5. The mechanical aspects of arroyo bank stability are also discussed in detail in Section 3.4.5.

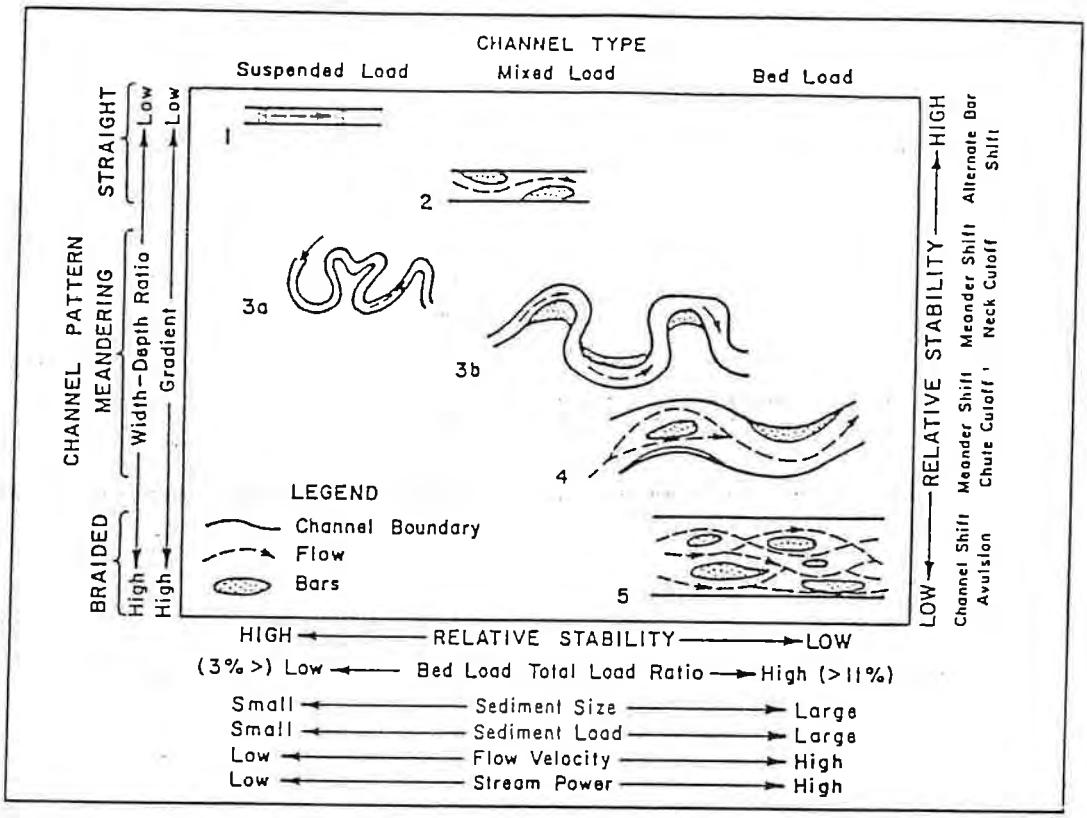


Figure 4.2. Channel classification and relative stability as hydraulic factors are varied (after Schumm, 1977).

A qualitative lateral stability assessment can also be completed from records of the position of a bend or bankline at two or more different times; aerial photographs or maps are usually the only records available. Surveyed cross sections are extremely useful although rarely available for meander migration. Some progress is being made on the numerical prediction of loop deformation and bend migration (Level 3 analysis). At present, however, the best available estimates are based on past rates of lateral migration at a particular reach. In using the estimates, it should be recognized that erosion rates may fluctuate substantially from one period of years to the next.

Measurements of bank erosion on two time-sequential aerial photographs (or maps) require the identification of reference points which are common to both. Useful reference points include roads, buildings, irrigation canals, bridges, and fence corners. The analysis of lateral stability is greatly facilitated by a drawing of changes in bankline position with time. To prepare such a drawing, aerial photographs are matched in scale and superimposed holding the reference points fixed.

A site of potential avulsion (channel shifting to new flow path) in a study reach should be identified during this step so that measures can be taken to mitigate the effects of avulsion when it occurs. A careful study of aerial photographs will show where overbank flooding has been taking place consistently and where a channel exists that can capture the flow in the existing channel. In addition, topographic maps and special surveys may show that the channel is indeed perched above the surrounding alluvial surface, with the inevitability of avulsion. Generally, avulsion, as the term is used here, will only be a hazard on alluvial fans, alluvial plains, deltas, and wide alluvial valleys. In a progressively aggrading situation, as on an alluvial fan, the stream will build itself out of its channel and be very susceptible to avulsion. In other words, in a cross profile on an alluvial fan or plain, it may be found that the river is flowing between natural levees at a level somewhat higher than the surrounding area. In this case, avulsion is inevitable.

4.3.5 Step 5. Evaluate Vertical Stability. Problems most commonly associated with degrading channels include bank failure and the undermining of hydraulic structures such as cutoff walls, flow-control structures, and bank protection. Bank sloughing because of degradation often greatly increases the amount of debris carried by the channel and decreases the available conveyance in the channel. The hazard of local scour becomes greater in a degrading stream because of the lower streambed elevation.

Aggradation in a stream channel increases the frequency of backwater that can cause flood-related damage. Lateral erosion as a result of increased flood stages can threaten to "outflank" hydraulic structures and bank protection and can also increase the debris load in a channel.

Data records for at least several years are usually needed to detect gradation (bed elevation) changes. In ephemeral channels, gradation changes develop over long periods of time even though rapid change can occur during an extreme flood event. The data needed to assess gradation changes include historic streambed profiles and long-term trends in stage-discharge relationships. Occasionally, information on bed elevation changes can be gained from a series of maps prepared at different times. Bed elevations at railroad, highway, and pipeline crossings monitored over time may also be useful. A qualitative assessment of potential vertical stability problems can be based on the Lane relationship (Section 3.1), the sediment continuity principle (Section 3.4.1), or equilibrium concepts (Section 3.4.2).

4.3.6 Step 6. Evaluate Channel Response to Change. The knowledge and insight developed from evaluation of present and historical channel and watershed conditions, as developed above on Steps 1 through 5, provides an understanding of potential channel response to previous impacts and/or proposed changes in the channel or watershed. Additionally, the application of simple, predictive geomorphic relationships, such as the Lane Relationship (see Section 3.1) can assist in evaluating overall channel response mechanisms.

## 4.4 Level 2: Basic Engineering Analyses

A flow chart of the typical steps in basic engineering analyses is provided in **Figure 4.3**. The flow chart illustrates the typical steps to be followed if a Level 1 qualitative analysis (Figure 4.1) resulted in a decision that Level 2 analyses were required. The eight basic engineering steps are generally applicable to most arroyo and drainageway stability problems and are discussed in more detail in the following paragraphs. The basic engineering analysis steps lead to a conclusion regarding the need for more detailed (Level 3) analysis or a decision to proceed to establishing a Prudent Line and/or design of countermeasures without more complex studies. Guidelines and criteria for selection and design of countermeasures are discussed in Chapter 5.

4.4.1 Step 1. Evaluate Historical and Potential Flooding. Hydrologic analysis techniques recommended for the Albuquerque area are discussed in Section 2.2. Several additional hydrologic concepts of particular significance to evaluation of arroyo stability are summarized below.

Consideration of flood history is an integral step in attempting to characterize watershed response and morphologic evolution. Analysis of flood history is of particular importance to understanding arid region stream characteristics. Many dryland streams flow only during the spring and immediately after major storms. For example, Leopold et al. (1966) found that arroyos near Santa Fe, New Mexico, flow only about three times a year. As a consequence, arid region channel response can be considered to be more hydrologically dependent than streams located in a humid environment. Whereas the simple passage of time may be sufficient to cause change in a stream located in a humid environment, time alone, at least in the short term, may not necessarily cause change in an arid system due to the infrequency of hydrologically significant events. Thus, the absence of significant morphological changes in an arid region channel, even over a period of years, should not necessarily be construed as being indicative of system stability.

# LEVEL 2: BASIC ENGINEERING ANALYSES

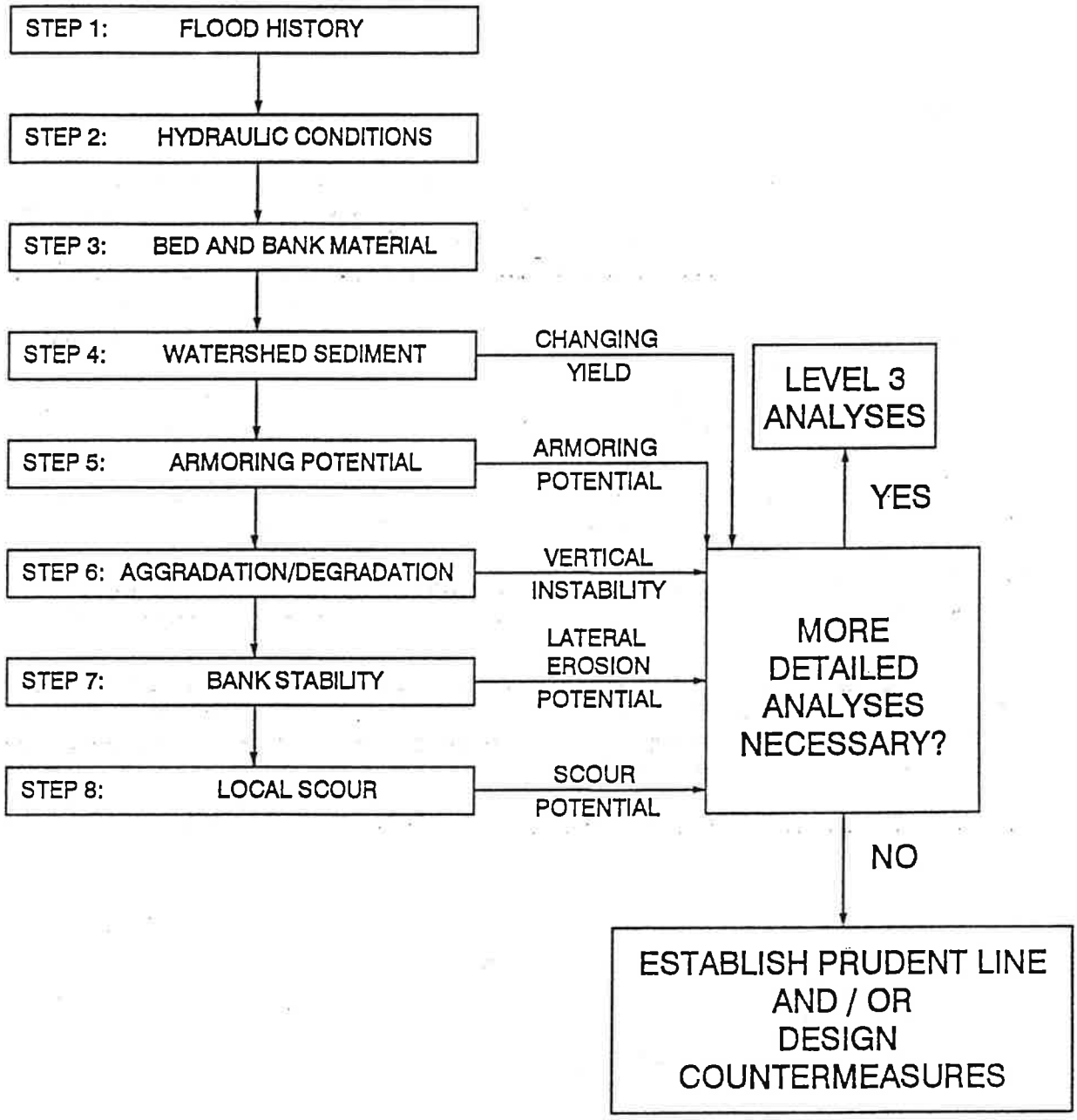


Figure 4.3. Level 2: Basic Engineering Analyses.

Although the occurrence of single large storms can often be directly related to system change in any region of the country, this is not always the case. In particular, the succession of morphologic changes may be linked to the concept of geomorphic thresholds as proposed by Schumm (1977). Under this concept, although a single major storm may trigger an erosional event in a system, the occurrence of such an event may be the result of a cumulative process leading to an unstable geomorphic condition.

Where available, the study of flood records and corresponding system responses, as indicated by time-sequenced aerial photography or other physical information, may help determine the relationship between morphological change and flood magnitude and frequency. Evaluation of wet-dry cycles can also be beneficial to an understanding of historical system response. Observable historical change may be found to be better correlated with the occurrence of a sequence of events during a period of above-average rainfall and runoff than with the single large event. The study of historical wet-dry trends may explain certain aspects of system response. For example, a large storm preceded by a period of above-average precipitation may result in less erosion, due to better vegetative cover, than a comparable storm occurring under dry antecedent conditions; however, runoff volumes might be greater due to saturated soil conditions.

A good method to evaluate wet-dry cycles is to plot annual rainfall amounts, runoff volumes and maximum annual mean daily discharge for the period of record. A comparison of these graphs will provide insight to wet-dry cycles and flood occurrences. Additionally, a plot of the ratio of rainfall to runoff is a good indicator of watershed characteristics and historical changes in watershed conditions (see **Figure 4.4**).

4.4.2 Step 2. Evaluate Hydraulic Conditions. Knowledge of basic hydraulic conditions, such as velocity, flow depth, top width, etc., for given flood events is essential for completion of Level 2 stream stability analysis. Incipient motion analysis, scour analysis, assessment of sediment transport capacity, etc. all require basic hydraulic information. Hydraulic information is sometimes required for both the main channel and overbank areas.

Evaluation of hydraulic conditions is based on the factors and principles reviewed in Section 3.2. For many larger river systems (e.g., the Rio Grande), particularly near urban areas, hydraulic information may be readily available from previous studies, such as flood insurance studies, channel improvement projects, etc., and complete re-analysis may not be necessary. However, in other areas, hydraulic analysis based on appropriate analytical techniques will be required prior to completing other quantitative analyses in a Level 2 stream stability assessment. Normal depth calculations (Section 3.2.2) or use of standard water surface profile models will usually be required. The most common computer models for analysis of water surface profiles and hydraulic conditions are the Corps of Engineers HEC-2 (USCOE, 1982) and Federal Highway Administration WSPRO (Shearman, 1990). The Corps' HEC-2 model is generally used for floodplain and flood risk analyses (e.g., FEMA Flood Insurance Studies). The computational procedure in WSPRO for evaluating bridge loss is superior to that utilized in other models, and the input structure of the model has been specifically developed to facilitate bridge design.

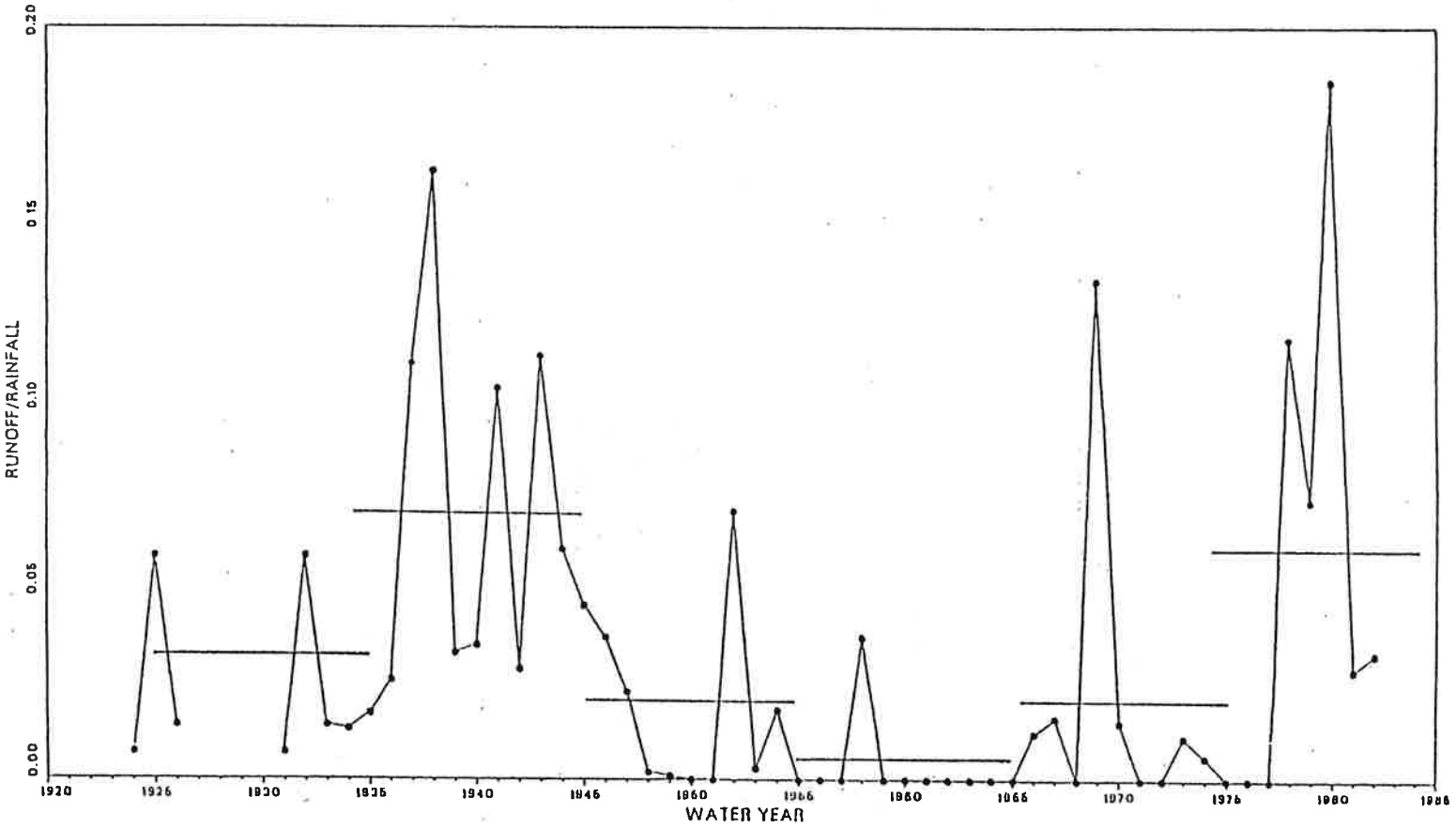


Figure 4.4. Annual runoff rainfall relationship - Santa Margarita River, California.

4.4.3 Step 3. Analyze Bed and Bank Material Characteristics. As discussed in Section 3.3.2, quantification of the characteristics of the bed and bank material in the arroyo is essential to performing channel stability analyses. Of the various sediment properties, size has the greatest significance to the hydraulic engineer, not only because size is the most readily measured property, but also because other properties, such as shape and fall velocity, tend to vary with particle size. A comprehensive discussion of sediment characteristics, including sediment size and its measurement, is provided in Vanoni (1977) or Richardson et al. (1990). A discussion of sediment sampling techniques is presented in Section 3.3.2.

4.4.4 Step 4. Evaluate Watershed Sediment Yield. Evaluation of watershed sediment yield, and in particular, the relative change in yield resulting from changes in the watershed (e.g., construction, urbanization, fire, etc.) can be an important factor in channel stability assessment. Sediment eroded from the land surface can cause silting problems in channels, reservoirs, and detention ponds, resulting in increased flood stage and damage. Conversely, a reduction in sediment supply can also cause adverse impacts to river systems by reducing the supply of incoming sediment, thus promoting channel degradation and headcutting. A radical change in sediment yield as a result of some disturbance, such as a recent fire or long-term land-use changes, would suggest that channel instability conditions either already exist, or might readily develop.

Quantification of sediment yield is at best an imprecise science. The most useful information is typically obtained not from analysis of absolute magnitude of sediment yield, but rather the relative changes in yield as a result of a given disturbance or change in the watershed. Section 2.3 describes sediment yield processes in the Albuquerque area and recommends several methods for estimating sediment yield. For example, both the Pacific Southwest Interagency Committee (PSIAC, 1968) and Modified Universal Soil Loss Equation (MUSLE) are introduced and their applications to the Albuquerque area discussed (see also Appendices A and B). Section 2.3.4 summarizes available sediment yield data for the Albuquerque area.

4.4.5 Step 5. Analyze Potential for Bed Armoring. An evaluation of relative channel stability can be made by performing an incipient motion analysis. The definition of incipient motion is based on the critical or threshold conditions where hydrodynamic forces acting on one grain of sediment have reached a value that, if increased even slightly, will move the grain. Under critical conditions, or at the point of incipient motion, the hydrodynamic forces acting on the grain are just balanced by the resisting forces of the particle. A computational technique for incipient motion is presented in Section 3.3.3.

Evaluation of the incipient motion size for various discharge conditions provides insight into the magnitude of flow that might disrupt channel stability in gravel- or cobble-bed systems. When applied to a sand-bed channel, incipient motion results usually indicate that all particles in the bed material are capable of being moved for even very small discharges, a physically realistic result for most channels in the Albuquerque area.

As discussed in Section 3.3.3, the armoring process results from differential transport of the fine and coarse material in the bed. The fine material is easily transported by the flow, leaving behind a lag deposit of coarser particles that are not moved or are moved at a much slower rate. As the process continues, fine bed material is leached up through this coarse surface layer to augment the material in transport. As sediment movement continues and degradation progresses, an increasing number of nonmoving particles accumulate in the surface layer. Eventually, enough coarse particles can accumulate to shield, or "armor" the entire bed surface.

An armor layer sufficient to protect the bed against moderate discharges can be disrupted during high flow, but may be restored as flows diminish. Therefore, as in any hydraulic design, the analysis must be based on a certain design event. If the armor layer is stable for that design event, it is reasonable to conclude that no degradation will occur under design conditions. However, flows exceeding the design event may disrupt the armor layer, resulting in degradation. A simple technique for estimating the degradation depth necessary to armor the channel bed is given by Equation 3.28 and illustrated in Figure 3.7.

4.4.6 Step 6. Evaluate Degradation/Aggradation Potential. While evaluation of incipient motion parameters (Step 5) provides a quick check of local channel stability, evaluation of long-term degradation or aggradation potential requires a more comprehensive sediment transport analysis. The sediment continuity concept (Section 3.4.1) as given by Equation 3.54 and illustrated in Figure 3.12 is the basis for estimating degradation or aggradation tendencies in relation to vertical channel dynamics. As shown in Figure 3.12, if the inflow (supply) of sediment to a given reach of channel is known or can be estimated and the transport capacity (outflow) of sediment from the reach can be calculated, then the storage (aggradation or degradation) in the reach can be estimated for selected discharge levels of a flood hydrograph or cumulatively over the entire hydrograph. A simple sediment continuity analysis assumes rigid boundary hydraulic conditions and that the sediment volume (aggradation or degradation) is distributed uniformly in the reach. Obviously, a more accurate analysis would update channel cross sections at each time step or discharge level of the flood hydrograph. However, to extend the analysis to quasidynamic or dynamic routing of water and sediment would involve a Level 3 analysis as discussed in Section 4.5, using mathematical models such as the Corps of Engineers' HEC-6 model (USCOE, 1991) or the NCHRP's BRI-STARS program (Molinas, 1993). This level of complexity is not usually required for **(and may not be applicable to)** most small arroyo and drainageway problems (see Section 4.5).

The first requirement for a Level 2 sediment continuity analysis is delineation of the study reach into a number of subreaches. Delineation of subreaches is generally based on:

1. Physical characteristics of the channel, such as top width, slope, and sinuosity

2. Hydraulic parameters, such as depth and, particularly, velocity
3. Bed-material sediment characteristics
4. Areas of particular interest to study objectives, such as bridges or locations of proposed channel improvements
5. The desire to maintain reach lengths as uniform as possible throughout the system

Items 1, 2, and 3 are generally selected to provide consistency within the subreach, so that representative average conditions may be determined (Simons, Li & Associates, Inc., 1985).

After subreach delineation, characteristic geometric and hydraulic information must be developed for each subreach for the discharge(s) under consideration. This information may be computed manually through uniform flow or gradually varied flow calculations, or through computer programs such as HEC-2 (see Section 3.2). For example, the velocity, depth and top width at cross sections within the subreaches from the HEC-2 output can be averaged to define values representative of conditions in that reach for the given discharge.

After establishing representative hydraulic characteristics in each subreach for the given discharge(s), the sediment transport capacity of each subreach is calculated using an appropriate method (see Section 3.3.4). The sediment continuity principle is then applied by comparing transport capacity on a reach-by-reach basis, under the assumption that the sediment supply to any given subreach is equal to the transport capacity of the adjacent upstream reach. For long-term conditions, the upstream supply to the study reach is used as the supply to all subreaches under the assumption that the channel must eventually adjust to a state of equilibrium between the sediment supply and capacity. The comparison begins at the upstream end of the study reach by designating the first subreach as a supply reach, which initiates the calculation to the next subreach downstream.

To expedite the calculation procedure when evaluating a single storm or several hydrographs, the following analysis procedure is suggested. First, identify five to ten discharges adequate to span the discharge range of the hydrograph(s). After computing the average hydraulic characteristics in each subreach for each discharge, compute the corresponding sediment transport capacities. Then, for each subreach, develop a relationship of the form $Q_s = a\,Q^b$ where $Q_s$ is the sediment transport capacity in cfs, Q is the water discharge in cfs and a and b are regression coefficients (see Section 3.3.4). The analysis of the discretized hydrographs then proceeds as outlined above, with the sediment transport capacity for each discharge in any given reach obtained by using the appropriate regression relationship. For more detail on this simplified sediment continuity procedure, refer to Simons, Li & Associates, Inc. (1985).

As indicated by the Lane relation (Equation 3.1), when the sediment delivered to a reach is reduced (or is less than the capacity of the reach), the channel will tend to flatten its slope to attain an equilibrium condition so that the capacity is in balance with the supply. Conversely, when the sediment delivered to the reach is increased (or is greater than the capacity of the reach), the channel will tend to steepen its slope. The ultimate slope for this condition is referred to as the equilibrium slope. The equilibrium slope concept provides an alternative means of estimating long-term degradation or aggradation trends. Equilibrium slope calculations are discussed in detail in Section 3.4.3.

The equilibrium slope analysis should be performed using the dominant discharge. A reasonable estimate of the dominant discharge can be obtained by estimating the return period of a flood that would produce the mean annual sediment yield given by Equation 1.1 and using the peak discharge associated with that flood.

Contraction scour occurs when the flow area of a stream at flood stage is locally decreased, either by a natural constriction or by a structure such as a bridge. With the decrease in flow area, there is an increase in average velocity and bed shear stress resulting in an increase in the amount of bed material transported and, possibly, degradation of the contracted reach. As the bed elevation is lowered, the flow area increases and the velocity and shear stress decrease until a state of relative equilibrium is reached. The contribution of contraction scour to lowering of bed elevations should be included in an estimate of long-term degradation potential.

To include contraction scour in an estimate of long-term degradation potential, the following sequence of computations is suggested:

1. Estimate the natural channel hydraulics for a fixed-bed condition based on existing conditions.
2. Assess the expected profile and planform changes (aggradation, degradation).
3. Adjust the fixed-bed hydraulics to reflect any expected long-term profile or planform changes.
4. Estimate contraction scour using the appropriate contraction scour formula and the adjusted fixed-bed hydraulics (see Section 3.4.3).

4.4.7 Step 7. Lateral Erosion Potential. Lateral erosion potential can be evaluated using a combination of qualitative (Level 1) and quantitative (Level 2) analysis techniques. As suggested in Level 1, Step 4, field inspection and time-sequenced comparison of aerial photography or mapping can be used to establish historic changes and trends in channel planform alignment, particularly meander wave length and meander belt width. These comparisons can establish historic rates of lateral migration in a given reach and provide a check on the results of more quantitative techniques for estimating lateral migration rates.

A detailed procedure for estimating bank stability and lateral migration rates is presented in Section 3.4.5. Bank stability is based on wedge-type bank failures for steep, cohesive banks with failure through the toe and is representative of many arroyo bankline instability problems. Lateral migration rates and limits are based on a combination of ideal bend geometry, bend shear stress, and the sediment continuity concept. The use of Level 1 and Level 2 analysis techniques to evaluate lateral instability and erosion potential is discussed further in the Prudent Line analysis section (Section 4.6).

4.4.8 Step 8. Evaluate Local Scour Conditions. For bridge piers and other objects/obstructions placed in the flow, vortices form around the base of the object. The formation of these vortices results from a pileup of water on the upstream face of the object and subsequent acceleration of flow around the object. The action of the base vortex (otherwise known as the horseshoe vortex, see Figure 3.26) removes sediment from the bed of the channel near the base of the object, resulting in a scour hole. Vertical wake vortices form downstream of the object which can also remove sediment from around the base of the object. **Figure 4.5** illustrates common scour-related problems at a bridge.

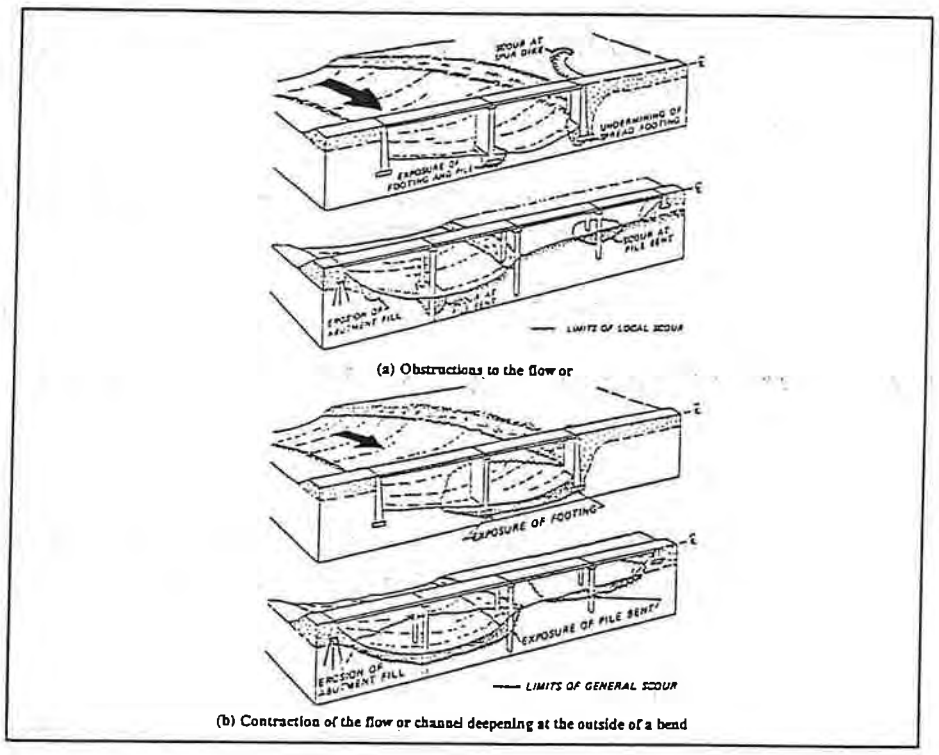


Figure 4.5. Local scour and contraction scour related hydraulic problems at bridges related to (a) obstructions to the flow or (b) contraction of the flow or channel deepening at the outside of a bend (Brice and Blodgett, 1978a, b).

Computational procedures for local scour at bridge piers and similar objects are presented in Section 3.5.1. Scour downstream from check dams and other grade control structures is discussed in Section 3.5.2 and scour at revetments, spurs, abutments, and similar structures is covered in Section 3.5.3. Scour along flood walls is discussed in Section 3.5.4 and scour at culvert outlets is discussed in Section 3.5.5.

Total scour is generally considered to be the additive result of the components contributing to channel bed lowering in a given reach. These include long-term aggradation/degradation and contraction scour as estimated in Step 6 (Section 4.4.6), scour associated with antidunes and local scour. As with contraction scour, the hydraulic parameters to calculate local scour should be determined after the fixed-bed channel hydraulics have been adjusted to reflect any expected long-term profile or planform changes. With significant amounts of contraction scour (e.g., 4-5 feet), one could use an iterative procedure to further adjust the fixed-bed channel hydraulics for contraction scour before estimating local scour. However, in most cases, this is not necessary and both local scour and contraction scour estimates can be added independently (and algebraically) to the aggradation/degradation potential to provide an estimate of total channel bed lowering.

Bridge piers and similar objects in the flow are susceptible to the accumulation of debris (trees, brush, trash, etc.) which can substantially increase local scour depths. One approach to simulating debris blockage and its effects on local scour depth is to increase the pier width parameter in the pier scour equation in Section 3.5.1 and recalculate local scour. Judgment must be used, since there is obviously a point beyond which this approach will not provide a realistic estimate of the local scour depth. As a rule of thumb, one should not assume increased pier widths beyond the point where the conveyance of the original channel section (without debris) is reduced by more than 40-50 percent.

## 4.5 Level 3: Mathematical and Physical Model Studies

Detailed evaluation and assessment of stream stability can be accomplished using either mathematical or physical model studies. A mathematical model is simply a quantitative expression of the relevant physical processes involved in stream channel stability. Various types of mathematical models are available for evaluation of sediment transport, depending on the application (watershed or channel analysis) and the level of analysis required [HEC-6 (USCOE, 1991); BRI-STARS (Molinas, 1993); see also Chang 1988)]. The use of such models can provide detailed information on erosion and sedimentation throughout a study reach, and allows evaluation of a variety of "what-if" questions.

In applying mathematical models such as HEC-6, however, the user must have a clear understanding of the limitations of the computational procedures being employed to ensure their applicability to the problem at hand. For example, as discussed in Chapters 2 and 3, arroyos adjust in response to individual storm events due to the

ephemeral nature of their flows. Most sediment routing models are designed to analyze long-term scour and deposition. Single event analyses using these models must, therefore, be performed with extreme caution. As noted in the HEC-6 Users Manual (USCOE, 1991),

> *HEC-6 assumes that equilibrium conditions are reached within each time step (with certain restrictions ...); however, the prototype is often influenced by unsteady, non-equilibrium conditions during flood events. Equilibrium is never achieved under these conditions because of the continuously changing hydraulic and sediment dynamics. If these situations predominate, single event analysis should be performed only on a qualitative basis.*

This limitation applies to most such sediment routing models. The conditions being described in the above statements are precisely those that occur in most arroyos during flood flows.

Similarly, physical model studies completed in a hydraulics laboratory can provide detailed information on flow conditions and to some extent, sediment transport conditions, in a complex study reach. The hydraulic laws and principles involved in scaling physical model studies are well defined and understood, allowing accurate extrapolation of model results to prototype conditions. Physical model studies can often provide better information on complex flow conditions than mathematical models, due to the complexity of the processes and the limitations of 2- and 3-dimensional mathematical models. Often the use of both physical and mathematical models can provide complementary information.

However, the need for detailed information and accuracy available from either mathematical or physical model studies must be balanced by the time and money available. As the analysis becomes more complicated, accounting for more factors, the level of effort necessary becomes proportionally larger. The decision to proceed with a Level 3 type analysis has historically been made only for high risk locations, extraordinarily complex problems, and for forensic analysis where losses and liability costs are high. However, the widespread use of personal computers and the continued development of more sophisticated software have greatly facilitated completion of Level 3 type investigations and have reduced the level of effort and cost required, and suggest that Level 3 type analysis techniques may be applied routinely in the future.

## 4.6 Prudent Line Analysis

4.6.1 Erosion and Flood Risk. In establishing a buffer zone for erosion and flooding potential within which development would not be considered prudent if the arroyo or drainageway is to remain in a "natural" state, the operational definition of the term "prudent" can be related to the concepts of hydrologic uncertainty (see Section 1.2.1). In the design of flood-control projects, it would obviously be desirable to provide

protection against the maximum probable flood, if this were feasible within acceptable limits of cost. However, it is seldom practical to provide absolute protection, and, as a rule, some degree of risk must be accepted. The problem, then, is one of relating the term "prudent" to an acceptable degree of risk in an urban setting. That risk is commonly based on the calculated return period (recurrence interval) of a hydrologic event.

The National Flood Insurance Program (USWRC, 1979) establishes as a precedent that, when considering hydrologic events, it is generally not sound to accept a degree of risk greater than that associated with the 100-year event (base flood). With reference to the calculated risk diagram (Figure 1.1), using the 100-year event as a basis for the definition of "prudent" implies that there is a 90 percent certainty that the event will not occur in a 10-year period and about a 74 percent certainty that it will not occur in a 30-year period. Conversely, this means acceptance of a calculated risk of 10 percent in a 10-year period and 26 percent in a 30-year period if boundaries of the buffer zone are based on the erosion and flooding potential of a 100-year flood. Asking a property owner to accept a greater risk than this would not appear to be prudent.

While damages due to flooding are generally associated with a single, short-term event, the impacts of erosion are often cumulative over the long term. Consequently, one must assess the erosion potential not only of a single event, such as a 100-year flood, but also the cumulative impact of a series of smaller flows. One approach to evaluating long-term erosion impacts is to develop a "representative" annual storm and then to extrapolate in time the effect of this storm. This concept is similar to the practice in hydrology of adopting the 2-year flood as being representative of the annual event; however, for purposes of long-term erosion analysis, particularly in ephemeral arroyos, the representative annual event should be more accurately defined by a probability weighting of the erosion resulting from several single storms. With this approach, the long-term analysis of erosion potential accounts for the probability of occurrence of various flood events during any one year.

After establishing the representative annual storm for evaluating long-term erosion potential, the duration in years defining the "long term" must be determined. Based on both the limitations of the probability weighting approach and the single-event probability of occurrence of a 100-year flood in a 30-year period (26 percent), a reasonable definition of the "long term" for an urban area is 30 years. Thus, the boundaries of an erosion and flooding buffer zone represent the envelope established by the reach-by-reach calculation of the erosion and flooding potential of both the 100-year flood (short term) and the cumulative erosion impact of a series of smaller events over a 30-year period (long term).

In this context, the operational definition of the term "prudent" is to avoid risk greater than that associated with the single-event erosion and flooding potential of a 100-year flood and the cumulative erosion potential of a series of smaller flows extending over a 30-year period. The selection of this definition is supported by the short- and long-term degree of risk associated with the 100-year return period event, the accuracy of the

methodology used for estimating long-term erosion impacts if extrapolated beyond a 30-year period, and the legal and policy precedents of the National Flood Insurance Program (USWRC, 1979). The short- and long-term processes are not necessarily mutually exclusive and the erosion rates are assumed to be additive to provide a reasonable, but conservative result.

It should be noted that this approach differs from the Prudent Line analysis as originally developed and applied to Calabacillas Arroyo (Simons, Li & Associates, Inc., 1983; Lagasse et al., 1985). There, the prudent limit was established as an envelope considering either the short-term (100 years) flooding and erosion risk or the long-term erosion impact of a series of smaller events. With the wider application of the Prudent Line concept, particularly to smaller arroyo and drainage systems, it is necessary to take a more conservative approach. Adding the effects of both short- and long-term processes envisions a fixed design life for the natural or naturalistic drainageway, similar to a lined channel, and considers the possibility that the drainageway could be subjected to a 100-year event at any time in that design life.

4.6.2 General Analysis Procedure. The analysis procedure emphasizes the use of available data and, where possible, well-established computational techniques. The general approach is an extension of Level 1 (field reconnaissance, data gathering, and qualitative assessment of the watershed and channel system) and Level 2 procedures (a quantitative analysis based on hydraulic data and sediment continuity concepts) as presented earlier in this chapter. The hydrologic and hydraulic data are generated with the methods outlined in Chapters 2 and 3. Again, the procedure as outlined in the following paragraphs assumes that the arroyo or drainageway is to remain in a "natural" state. Where a "naturalistic" design is acceptable (that is, one where some structural controls can be implemented), a reduced erosion buffer may be possible (see Section 4.7).

Specifically, there are four elements to the analysis approach:

1. Complete a Level 1 analysis as outlined in Section 4.3; that is, collect, review, and evaluate available hydrologic, hydraulic, cross-sectional, aerial photographic, structural, sediment, and soils data pertinent to the arroyo system and associated watershed. A field reconnaissance of the watershed and arroyo system is mandatory for several reasons, including development of the basic understanding and insight necessary for conducting analysis and interpreting analytical results, and to fill gaps in the existing database. The field work generally consists of cross section surveys of the arroyo channel, collection of sediment samples from the watershed area and bed, banks, and overbank areas of the channel and mapping and documentation of the bed and bank stratigraphy. The Level 1 analysis procedure is completed by performing a qualitative analysis using available data, historical information, aerial photographs, and geomorphic principles to identify key factors that govern vertical and lateral stability of the arroyo or drainage system.

2. (Level 2 analysis, Steps 1 and 2), use existing hydrologic data, or use standard techniques (Section 2.2) to develop the necessary hydrologic data to determine hydrographs for a range of flows (for example, the 2-, 5-, 10-, 25-, 50-, and 100-year return period events), and select a design event for long-term erosion analysis. **(Based on the arguments in the previous paragraph, AMAFCA has established 30 years as the recommended period for the long-term erosion analysis - see also Section 4.6.3)**. The hydraulic parameters for the discharge levels selected to characterize the design event can then be established using the methods outlined in Section 3.2.

3. The sediment transport characteristics of the watershed and arroyo must be determined. A laboratory analysis of the sediment samples obtained during field reconnaissance is generally required to establish the sediment properties and develop gradation curves (Level 2, Step 3). The gradation curves and hydraulic data are then used to develop sediment transport relationships for the arroyo system. Sediment continuity concepts are then applied to determine aggradation and degradation trends for selected flows for characteristic subreaches of the arroyo (Level 2, Steps 4, 5, and 6). With the results of the qualitative assessment and the analysis of aggradation and degradation trends, the lateral migration potential of the arroyo channel can be evaluated, considering both short-term (100-year flood) and long-term (30-year) response (Level 1, Steps 7 and 8). An equilibrium slope analysis can also be used to estimate the long-term degradation potential for degrading reaches, particularly where natural or man-made grade controls exist, fixing the bed elevation at specific locations.

4. Erosion boundaries are delineated along the arroyo or drainageway to establish a buffer zone within which development would not be considered prudent. If necessary, the boundaries can be described as offset tangents that relate to existing survey data, such as section corners, platting, or a local plane coordinate system. These offset tangents provide identifiable guidelines for future platting or permit comparison of the buffer zone with existing platting to aid in assessing impacts or risks.

4.6.3 Design Event for Erosion Risks Analysis. Selection of an appropriate design event for erosion risk analysis is not as straightforward as it is for other water resource projects. For example, the design of hydraulic structures is usually based on a requirement to withstand a single large flood. The selection of the appropriate design event is generally based on an acceptable level of risk. By comparison, the selection of the design event for erosion analysis depends largely on project objectives. For example, information on long-term, cumulative erosion rates resulting from numerous floods through an arroyo system over many years may be of interest. Conversely, the short-term erosion or scour occurring during a single event at a bridge crossing may be required. Therefore, temporal considerations established by project objectives will influence the selection of the design event.

For short-term analysis, the single event is often a frequency-based flood, such as the 100-year event. For long-term analysis, the objective is to evaluate the cumulative effects of a range of flow conditions. One approach that can be used is based on the concept of dominant discharge, where the dominant discharge is that flow value which is predominantly responsible for the geometric characteristics of the channel. Although it is difficult to establish precisely the dominant discharge, the value is typically between the 2- and 5-year event for perennial streams and between the 5- and 10-year event for intermittent and ephemeral channels. The aggradation or degradation occurring for this dominant discharge can then be assumed to represent an average annual value which can be extrapolated in time to evaluate long-term conditions.

A better approach to long-term analysis of erosion or sedimentation accounts for the probability of occurrence of various flood events during any one year (Chang, 1988). For example, if $Y_s$ is the sediment yield for a given flood and $P$ is the probability of occurrence of that flood in one year, the product $Y_s \cdot P$ represents the contribution of that one flood to the long-term mean annual yield. To account for the contribution of all possible flows the integration

$$\bar{Y}_s = \int_0^1 Y_s dP \qquad (4.1)$$

is required. For practical purposes, the integration can be accomplished by determining the area under the sediment yield, frequency curve. The frequency curve for sediment yield can be estimated by computing the sediment yield expected for each of several floods of known return periods. **Figure 4.6** illustrates a typical sediment yield frequency curve. The area under this curve then represents the mean annual sediment yield, and can be computed graphically or numerically. The numerical procedure involves summing the incremental trapezoidal areas established by calculation of $Y_s$ for discrete return periods. Assuming this calculation is completed for the 2-, 5-, 10-, 25-, 50-, and 100-year events, the mean annual sediment yield would be approximated by the following relation:

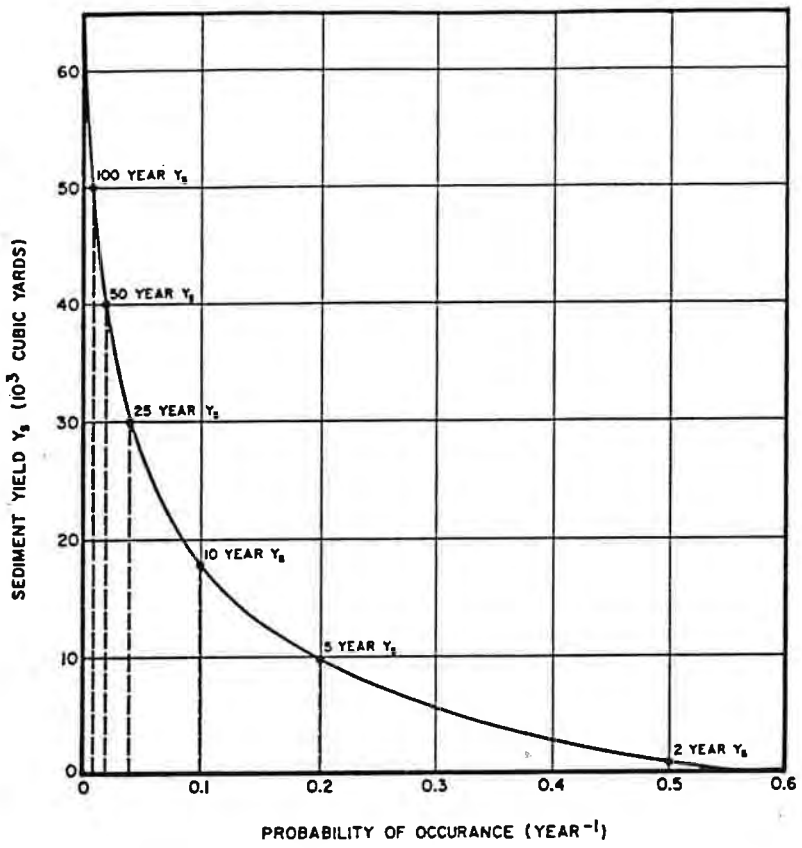


Figure 4.6. Integration of sediment yield frequency curve.

$$(Y_s)_m = 0.01(Y_s)_{100} + (.02-.01)\left[\frac{(Y_s)_{100} + (Y_s)_{50}}{2}\right] + (.04-.02)\left[\frac{(Y_s)_{50} + (Y_s)_{25}}{2}\right] + (.10-.04)\left[\frac{(Y_s)_{25} + (Y_s)_{10}}{2}\right] + (.20-.10)\left[\frac{(Y_s)_{10} + (Y_s)_5}{2}\right] + (.50-.20)\left[\frac{(Y_s)_5 + (Y_s)_2}{2}\right] + (1.0-.50)\left[\frac{(Y_s)_2 + (Y_s)_0}{2}\right] \quad (4.2)$$

By combining terms, Equation 4.2 reduces to Equation 1.1:

$$Y_{s_m} = 0.015Y_{s_{100}} + 0.015Y_{s_{50}} + 0.04Y_{s_{25}} + 0.08\ Y_{s_{10}} + 0.2\ Y_{s_5} + 0.4Y_{s_2} \quad (1.1)$$

A similar equation to Equation 1.1 can be developed from the 2-, 10-, and 100-year events using a formulation similar to Equation 4.2. This formulation is less accurate than using the six events of Equation 1.1, and should only be used when a less accurate estimate of sediment yield will provide acceptable results. The three event relation is:

$$Y_{sm} = 0.055\ Y_{s_{100}} + 0.245\ Y_{s_{10}} + 0.45\ Y_{s_2} \qquad (4.3)$$

Evaluation of the cumulative erosion or sedimentation occurring during a given event can be accomplished by discretizing the associated hydrograph, computing the sediment yield associated with each discrete interval, and summing over the hydrograph. The discretization process provides a series of constant discharges acting over short time intervals, as illustrated in **Figure 4.7**. The discharge levels are selected so that the total volume of the discretized hydrograph is approximately the same as the original hydrograph. AMAFCA's AHYMO computer program (Anderson, 1994) may be used to obtain sediment yield for a given event. The SEDIMENT TRANS function in AHYMO has been developed to use Equation 3.39 with a computed hydrograph to obtain sediment yield.

When this process is completed for the range of return period events, Equation 4.2 can be combined with the results of sediment transport analysis to estimate an annual sediment yield. A sediment continuity analysis is performed using the annual yields to estimate the annual sedimentation or erosion rate. This value is then extrapolated to provide a long-term estimate of sedimentation or erosion. For an urban area a 30-year period has been recommended as a reasonable limit on this extrapolation.

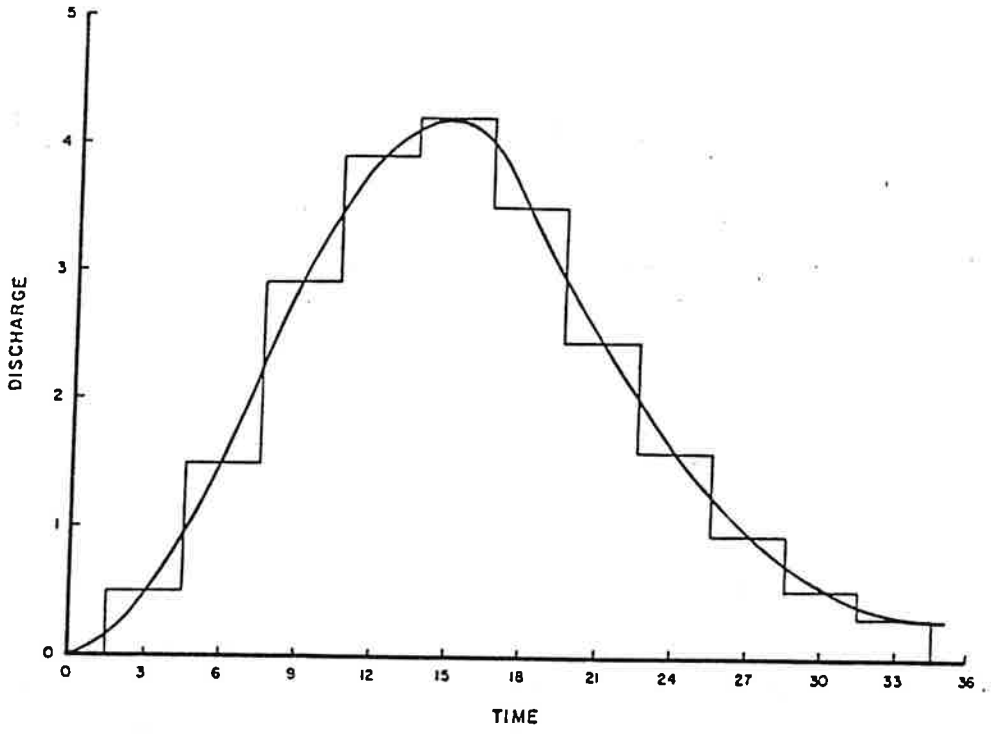


Figure 4.7. Definition sketch of hydrograph discretization process.

4.6.4 Erosion Risk Boundaries. Establishing erosion risk boundaries along an arroyo or drainage system requires combining the results of Level 1 and Level 2 analyses as discussed in Section 4.6.2 with specific hydrologic and sediment transport analysis techniques presented in Section 4.6.3. The synthesis of simple qualitative concepts with the aggradation or degradation trends calculated for each subreach of the arroyo system provides a basis for assessing short- and long-term lateral migration (erosion) potential in the system. Here lateral migration is defined as bankline shifting due to the processes of bank erosion (change in the horizontal direction).

The two basic mechanisms of lateral migration can be related to aggradation and degradation trends (change in the vertical direction) in the arroyo. The first mechanism, associated with aggrading channel reaches, occurs through bank instability, lateral migration and/or avulsion as a wide, potentially multichannel condition develops. The second mechanism, associated with vertically stable of degrading channel reaches results from increased bank instability and erosion by undercutting, oversteepening, and failure due to increased bank height and/or direct fluvial entrainment by flow along the banks.

There are several variations of the first mechanism involving a typically aggradational reach of channel. Deposition normally occurs as midchannel bars, increasing the local energy gradient and the local stress on the banks as the bar deposits deflect the flow towards the more erodible banklines. Consequently, severe localized bank failures or channel avulsions may occur.

Using results of the Level 1 and Level 2 analyses, lateral migration in vertically stable or degradational subreaches can be evaluated for both the short- and long-term. The potential lateral migration distance can be computed by applying the methods discussed in Section 3.4.5. A basic assumption of these methods is that all of the sediment eroded from the banks within a given reach is derived from only one bank. This assumption is realistic in curved reaches. In reaches that are initially approximately straight, the direction of lateral migration is not known with certainty. For this case, the required volume of sediment should be first assumed to come entirely from one bank, and then from the opposite bank, unless geologic or other controls inhibit movement in a given direction. For example, a rock outcrop along one arroyo bank would obviously inhibit lateral erosion of that bank and in a well established meander bend, erosion of the outside of the bend would be most likely, while erosion in the point bar area on the inside of the bend would be unlikely. This approach provides a conservative estimate of lateral migration potential. It is important to note that maximum meander locations will not necessarily remain at the same point on an arroyo or channel reach, but can migrate downstream over time.

The determination of a typical flooding and erosion buffer zone along an arroyo is shown schematically in Figure 4.8. **Figure 4.8a** shows a plan view of a typical reach of arroyo indicating the relative position of the short- and long-term erosion lines and the floodplain boundary that might be expected as the arroyo changes from nonincised to incised to aggrading conditions. The anticipated effect of the bend is also illustrated. **Figure 4.8b** shows typical cross sections with each zone. The use of a water surface

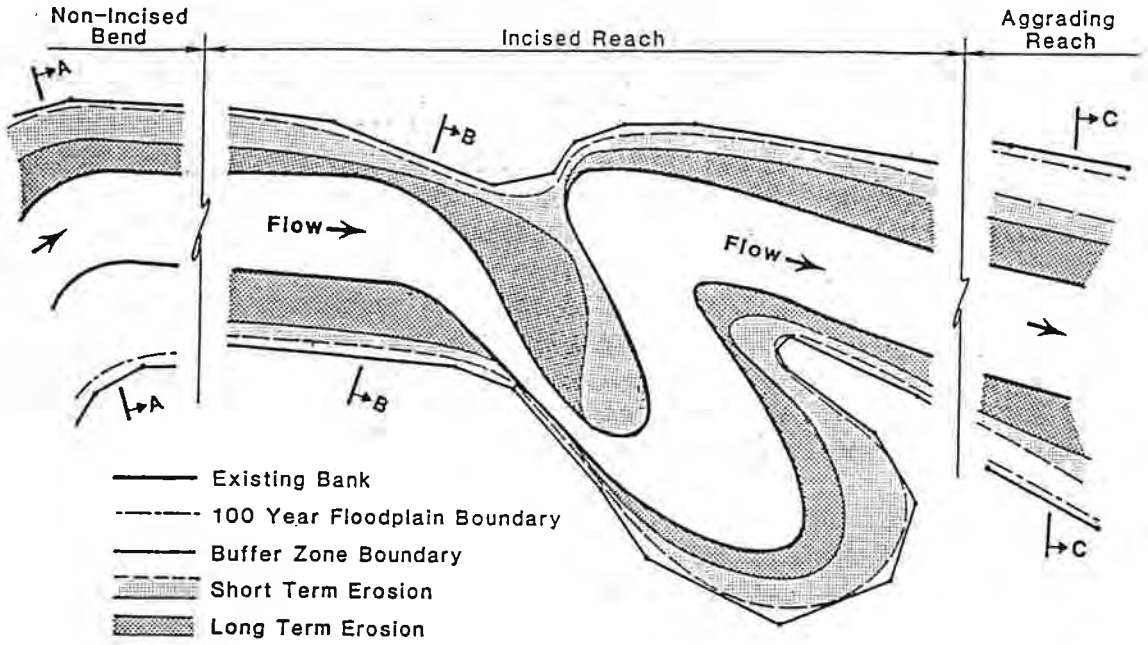


Figure 4.8a. Schematic illustration of flooding and erosion buffer zone.

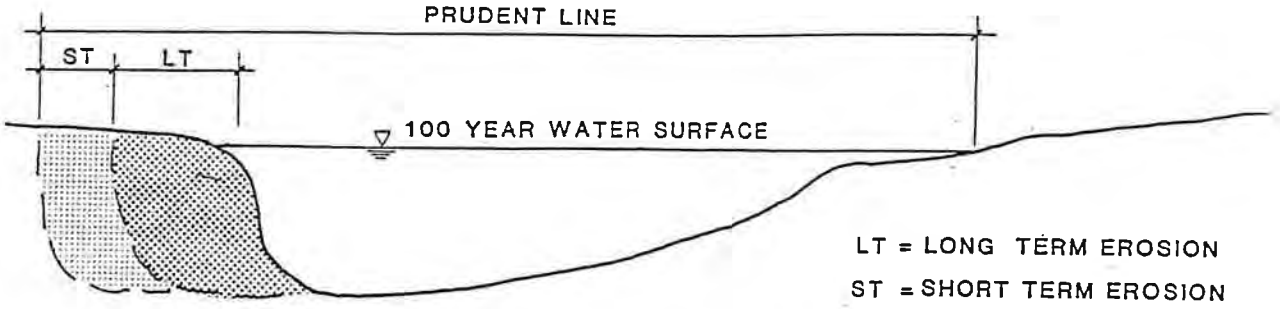


**SECTION A-A**
**NON-INCISED BEND**

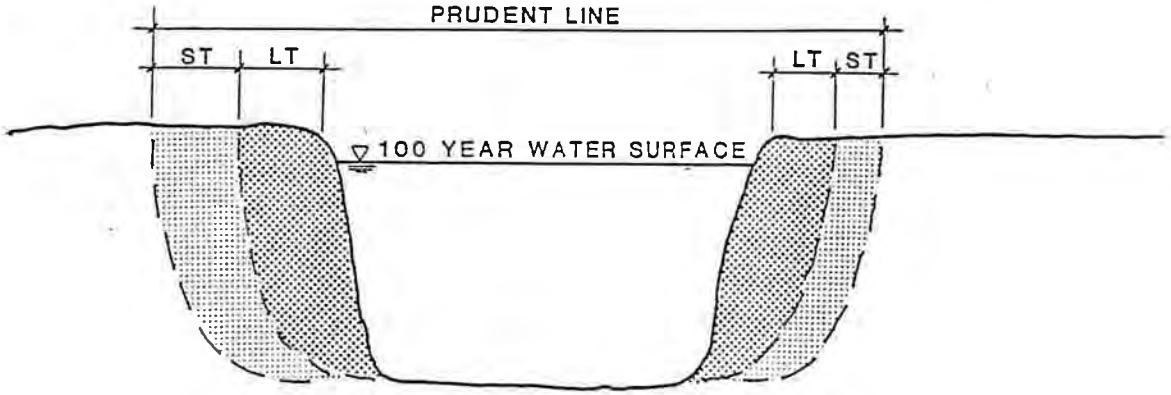


**SECTION B-B**
**INCISED REACH**

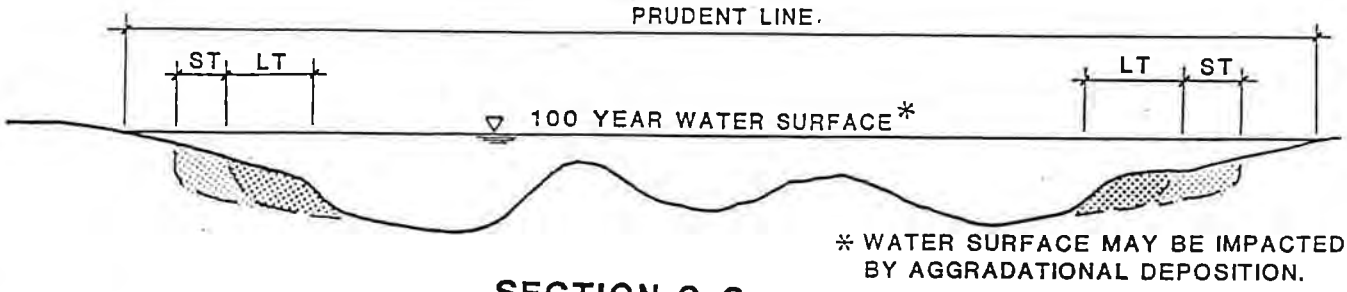


**SECTION C-C**
**AGGRADING REACH**

Figure 4.8b. Schematic cross sections nonincised reach, incised reach and aggrading reach showing flooding and erosion buffer zone.

profile model such as HEC-2 to calculate hydraulic conditions permits establishing a 100-year floodplain boundary along the arroyo in accordance with Federal Emergency Management Agency (FEMA) flood insurance study procedures (USCOE, 1982; USWRC, 1979). Assuming that there will be no structural improvements to the channel, the 100-year floodplain boundaries should be taken as the minimum extent of the flooding and erosion buffer zone along the arroyo.

The erosion buffer zone is then established by plotting, for each cross section used in the hydraulic analysis, the estimated extent of short- and long-term erosion. For aggradational reaches the historical extent of lateral migration can help determine the erosion buffer limits for both short- and long-term conditions. If local topography indicates potential for avulsion, the outer limits of potential flow paths must be plotted, and the flooding and erosion buffer zone established outside these limits. When the procedures of Section 3.4.4 are used for either aggradational, degradational, or quasi-equilibrium reaches the lateral migration potential is estimated independently for the short- and long-term. Bankline erosion volumes are applied from the existing bankline outward. Where the arroyo can migrate in either direction, the long-term erosion potential is plotted for both sides of the arroyo with respect to the existing bankline. Where controls prevent migration in one direction, professional judgment may indicate that the erosion buffer should apply only to the side of the arroyo where migration is likely to occur. The short-term (100-year flood) erosion potential is then added so that the erosion buffer zone is established as an envelope along the arroyo such that the limit of erosion will not exceed the "prudent line" in response to a single 100-year storm occurring at any time during the long-term (30-year) period. The boundary of the buffer zone can be drawn as a smooth curve, or, as shown in Figure 4.8, as a series of tangent lines (offset tangents) that can be easily referenced to existing survey data and readily compared with existing platting.

In certain reaches with a strong potential for lateral migration, it may be useful to establish a maintenance line within the Prudent Line boundary. One approach to establishing a maintenance line would be to use the long-term erosion boundary, as plotted above, to establish a limit beyond which erosion for a "natural" arroyo could not be accepted. When erosion reaches this point, the planning concept for the arroyo must change from one of a natural channel to a naturalistic channel with some erosion barrier provided at the threatened point. Thus, the planned design life of the natural/naturalistic arroyo could be assumed. Installation of such an erosion barrier must, of course, consider the potential effect on erosion rates in nearby unprotected areas along the arroyo.

The maximum lateral erosion distance from the average downvalley direction for an unconstrained arroyo can be estimated from the concepts presented in Section 3.4.5.

For those cases where the maximum lateral migration distance is large, the amount of lateral migration that will occur over a 30-year period plus a 100-year storm can be estimated using the computer program in Appendix D. Prior to using the results from the

program for design purposes, the user must clearly understand the assumptions inherent in the procedure to ensure their applicability to each specific problem. (Refer to Section 3.4.5 for discussion of the procedure and assumptions used in the computer program.) Depending upon the circumstances involved in specific problem being analyzed, the results may indicate that the maximum lateral migration distance is unlikely to be attained during the 30-year period plus a 100-year storm, thus reducing the extent of the erosion buffer zone. To apply the program, a complete continuity and bank stability analysis is required. This may involve a level of effort that is not warranted by the potential gains in reducing the size of the erosion buffer zone. As an alternative, as indicated in Figure 3.24, lateral controls, properly designed to withstand local scour, flanking, undercutting or other damage, spaced at distances less than 7 channel widths can significantly reduce the potential with of the erosion buffer zone.

4.6.5 Application to the Albuquerque Area. The procedure for establishing flooding and erosion boundaries along an arroyo in an urban area has been applied to Calabacillas Arroyo in the West Mesa region of Bernallilo County, northwest of Albuquerque (Simons, Li & Associates, Inc., 1983; Lagasse et al., 1985). The arroyo drains an area of approximately 100 square miles to the Rio Grande. The length of the study reach was 5 miles and the slope of the arroyo bed ranges from 1.0 to 1.5 percent. Platting for residential development had been completed north and south of the arroyo prior to the completion of a flood insurance study, but construction had not started on lots adjacent to the arroyo.

It should also be noted that this early application of the Prudent Line concept assumed a 25-year period as a basis for hydrologic risk, and this Design Guide recommends a 30-year long-term period. In addition, the Calabacillas Prudent Line used an envelope based on the largest of either the short- or long-term erosion, where this Design Guide now recommends a worst-case erosion buffer established by adding the short- and long-term erosion potential.

Hydrologic data were available from previous studies, but required updating and extension to include the range of flows desired for analysis. The 2-year flood event had a peak discharge of approximately 400 cfs, and the 100-year event was approximately 12,000 cfs. The HEC-2 analysis performed for a flood insurance study provided basic hydraulic data (Bohannan-Huston, Inc., 1982), but also required updating to reflect current conditions. High-quality aerial photography of the study reach was obtained for the years 1935, 1967, and 1980, and supported the qualitative analysis.

Based on the hydraulic data and sediment sampling, the analysis of sediment transport capacity in the study reach produced regression equations similar to those discussed in Section 3.3.4 using site-specific data. The arroyo was divided into 10 representative subreaches of about 3,000 feet in length for the sediment continuity analysis. For degradational subreaches, the average short-term lateral migration was 160 feet, while the average long-term lateral migration potential was 176 feet over the 25-year

period. For the slope, geometry and soil characteristics of the one deeply incised subreach, slope stability analysis indicated a maximum stable vertical bank height of 40 feet. Slip circle analysis for this subreach indicated, that in a failure mode, bank instability would progress laterally a distance of approximately 60 feet. The methods of Section 3.4.5 are considered a significant refinement of the slip circle failure model used in the 1982 analysis of Calabacillas Arroyo.

Plat plans along Calabacillas Arroyo were used to estimate impacts of the buffer zone on proposed residential development adjacent to the arroyo. This comparison indicated that erosion offset tangents impacted part or all of approximately 150 residential lots. However, 70 lots were located in the 100-year floodplain and, of these, 53 lots were located in the 100-year floodway. Since adoption of FEMA guidelines prohibits all development within the regulatory floodway, these 53 lots could not be developed regardless of the erosion risk.

## 4.7 Application of Analysis Procedures

The Level 1 and Level 2 analysis procedures presented in Figures 4.1 and 4.3 provide guidelines for qualitative and quantitative analyses of arroyo and drainageway stability problems applicable to the Albuquerque area. The six steps of the Level 1 procedure and eight steps of Level 2 are supported by detailed analysis techniques presented in Chapters 2 and 3. These steps can be integrated into a comprehensive analysis of arroyo and drainageway stability to establish erosion and flood risk boundaries for natural or naturalistic channels. The procedure recognizes that, in many cases, application of the Prudent Line for a completely natural arroyo will not be an economically feasible approach to development along Albuquerque's arroyos and drainageways. In these cases, erosion barriers or other techniques such as detention basins will need to be included in the design of a "naturalistic" arroyo or drainageway considering project economics. These techniques may include:

1. Grade control structures to prevent or minimize degradation which may undercut structures within or adjacent to the channel and/or cause unstable banks heights, which will accelerate lateral migration of the channel.

2. Bank protection to prevent or minimize lateral migration of the arroyo channel.

3. Installation of erosion barriers (e.g., cutoff walls set at or just inside the stabilized flood zone boundary) to prevent migration beyond the limits of the stabilized flood zone.

4. Flow training devices (e.g., guide banks, spurs, hardpoints) to improve the alignment of flow through bridge crossings, culverts or channel bends.

5. Detention ponds to control the magnitude and duration of flood discharges and reduce the delivery of sediment to downstream reaches.

The alternatives listed above will generally be used in combination to maximize the level of protection while achieving the goal of maintaining a naturalistic arroyo. For example, a series of grade controls can be installed with spacing such that the maximum bank height that would develop through channel degradation (e.g., based on an equilibrium slope analysis) will not exceed the critical height indicated by a bank stability analysis such as that discussed in Chapter 3. This concept is illustrated in **Figure 4.9.**

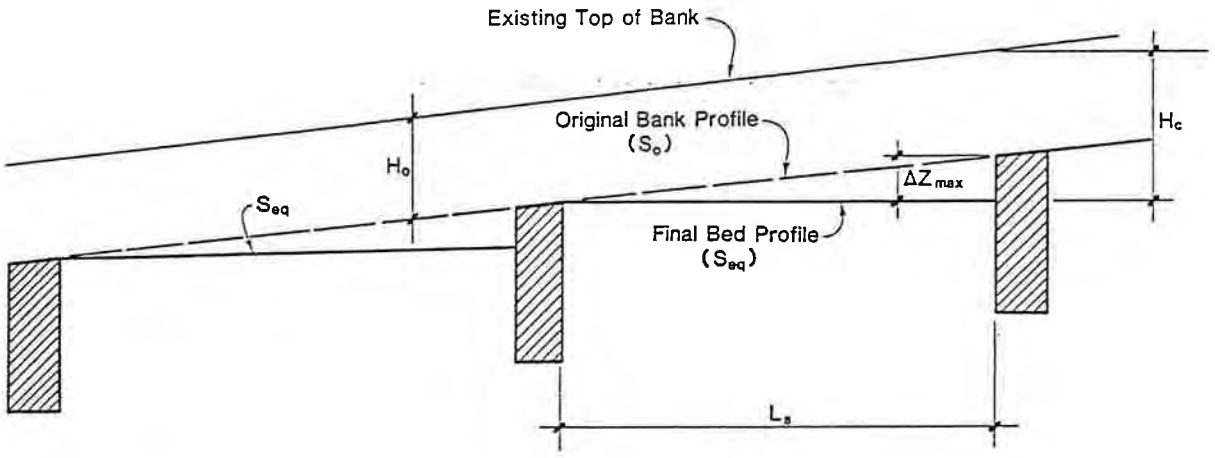


Figure 4.9. Illustration of method for determining the spacing of grade control structures based on equilibrium slope ($S_{eq}$) concept and maximum stable (critical) bank height ($H_c$).

The spacing is computed by noting that the maximum allowable degradation ($\Delta Z_{max}$) is the difference between the critical bank height ($H_c$) (see Figure 3.20) and the existing bank height ($H_o$), or:

$$\Delta Z_{max} = H_c - H_o \tag{4.4}$$

and the maximum spacing of the structures ($L_s$) is given by:

$$L_s = \frac{\Delta Z_{max}}{(S_o - S_{eq})} \tag{4.5}$$

where $S_o$ = the existing bed slope
$S_{eq}$ = the equilibrium slope computed using the procedures in Section 3.4.3.

It is critical to provide bank protection for an appropriate distance up- and downstream of each structure to prevent flanking. A good rule of thumb is to provide bank protection for two channel widths on either side of the structure. This, in effect, fixes the lateral location of the channel at the location of each structure, shortening the length of channel available for development of channel bends, and thus the potential magnitude of lateral migration. Additional bank protection on the outside of bends between the grade control structures can slow or check the rate of bend migration and further reduce the area within the flood and erosion zone. Figure 3.24 provides a method of quantifying the reduction in potential lateral migration distance for controls spaced in distances less than the typical, unconstrained bend length.

In areas where it is impractical or inadvisable to install bank protection directly along the existing arroyo, it may be feasible to install an erosion buffer at or just inside the desired boundary of the stabilized flood zone. This may consist of a cutoff wall or trench fill revetment that will stop further migration of the channel at the desired location. It is important that the design of such an erosion buffer be based on the anticipated conditions in the arroyo when the buffer is encountered, including the appropriate sizing of material and toedown to prevent undercutting, flanking or failure due to hydraulic forces. Toedown should be based on the potential scour depth along the wall as discussed in Section 3.5.4.

Training devices can be installed to improve the alignment of flow through bridges, culverts or channel bends to minimize the potential for local scour and prevent deposition of sediment and debris that may plug the channel opening. For example, guide banks at bridges are an effective method of aligning the flow through the bridge opening to minimize the potential for scour around the bridge piers and abutments. Guide banks are particularly effective in controlling abutment scour since they move the scour hole upstream of the bridge to the end of the guide bank, protecting the bridge abutments from direct attack by the flow. In some cases, installation of hard points or spurs at channel bends can slow or check lateral migration. By improving the flow alignment through the bridge or culvert opening, backwater can be minimized, reducing the tendency for deposition of sediment and debris buildup that may cause channel avulsion or increased upstream flooding. Design criteria for spurs and guide banks are presented in the next chapter (Section 5.9).

Detention structures can provide relief from flooding in downstream reaches by temporarily storing floodwaters and reducing the peak flows. Detention structures also trap significant quantities of sediment. In some cases, the reduced peak flows result in reduced erosive forces associated with the flood. It is important to recognize, however, that the total volume of water that must ultimately pass through the channel is usually not

significantly affected by the detention structure. A modest reduction in flood peak may significantly increase the duration of relatively high flows, actually increasing the overall potential for channel instability. Additionally, in degradational arroyos, trapping of sediment reduces sediment delivery to the downstream reach, increasing the degradational tendency of the arroyo. It is critical to consider both the magnitude and duration of the flows and the potential effect on the sediment balance in the arroyo before drawing conclusions regarding the ability of a given installation to protect downstream reaches of the channel.

**Figure 4.10** illustrates the procedure for combining of the Level 1 and 2 analysis approach with natural/naturalistic development concepts. As shown, the Level 1 and 2 analyses for existing and future conditions provide the basis for determining the flood and erosion risk setback limits of a natural arroyo or drainageway. If the project is viable with this Prudent Line, one could proceed directly with the planning and development process without consideration of countermeasures or erosion barriers. In many cases, however, a project will require consideration of techniques to stabilize the flood and erosion risk zone, as a minimum. As shown in Figure 4.10, some situations may require confining the flood and erosion risk zone by channelizing part or all of the channel or drainageway through the reach proposed for development by the selective use of erosion barriers and other techniques. Guidelines for these techniques are presented in Chapter 5. In all cases, potential impacts upstream and downstream of the study reach from flood/erosion zone stabilization or channelization by the use of erosion barriers or other countermeasures must be considered in evaluating the acceptability of proposed naturalistic channel techniques and before proceeding with the planning and development process.

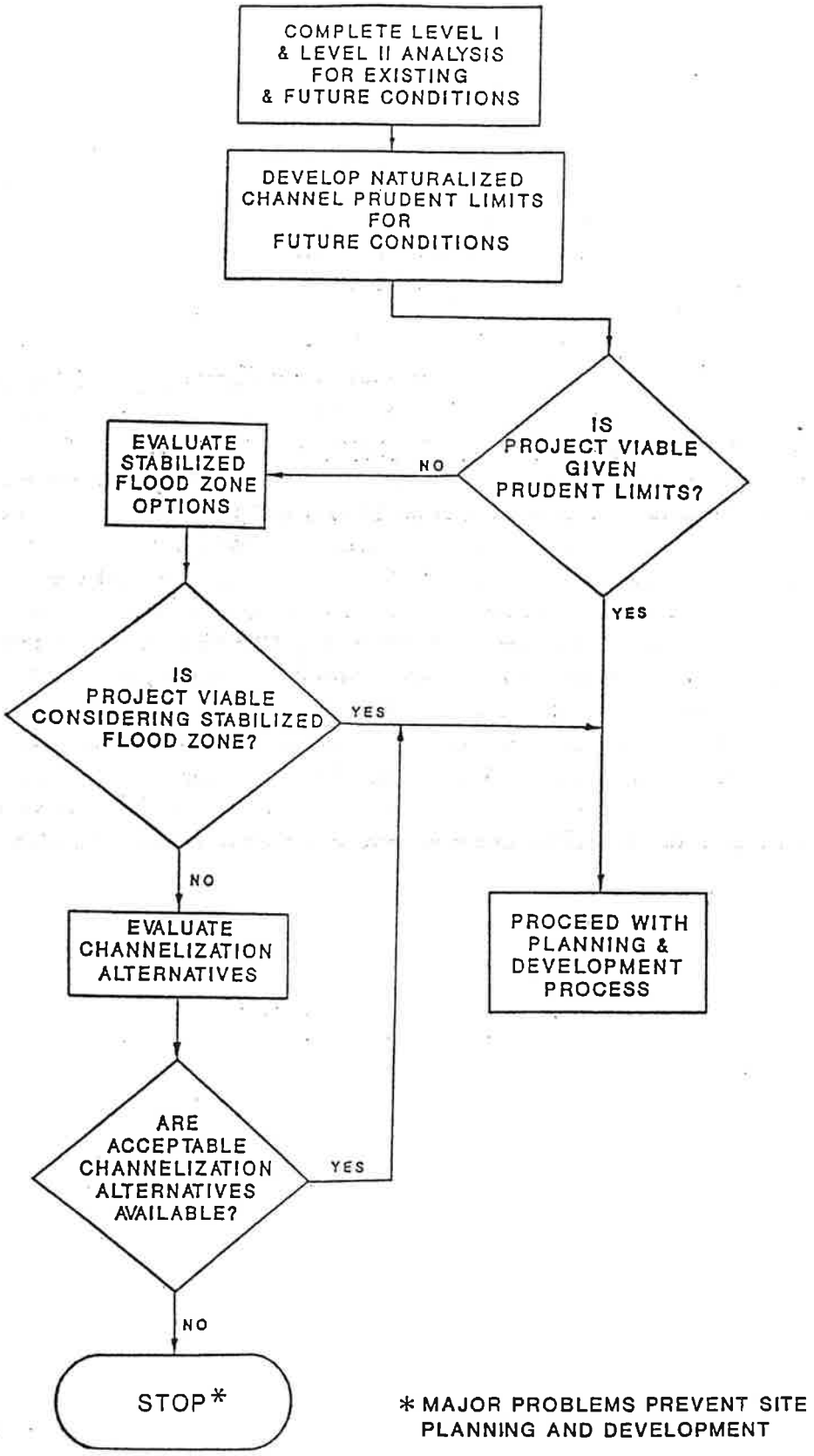


Figure 4.10. Flow chart of analysis procedures.

# 5.0 EROSION CONTROL AND COUNTERMEASURE CRITERIA

## 5.1 Introduction

A countermeasure is defined as a measure incorporated into the arroyo or drainageway to control, inhibit, change, delay, or minimize stream stability problems. Countermeasures may be installed at the time of initial development of the drainageway or retrofitted to resolve stability problems as they develop. Retrofitting can make good economic sense and can be good engineering practice in many locations because the magnitude, location, and nature of potential stability problems are not always discernible at the initial development stage, and indeed, may take a period of several years to develop. In selecting a countermeasure it is necessary to evaluate how the stream might respond, to the countermeasure.

This chapter provides some general criteria for the selection of countermeasures for channel instability. Then, selection and design criteria for countermeasures for specific channel instability problems are discussed. Case history data compiled by the Federal Highway Administration are summarized to provide information on the relative success of various countermeasures for stream stabilization.

## 5.2 Criteria for the Selection of Countermeasures

The selection of an appropriate countermeasure for a specific channel erosion problem is dependent on factors such as the erosion mechanism, stream characteristics, construction and maintenance requirements, potential for vandalism, and costs. Perhaps more important, however, is the effectiveness of the measure selected in performing the required function.

Protection of an existing bank line may be accomplished with revetments, spurs, retardance structures, longitudinal dikes, or barrier wells. Spurs, longitudinal dikes, and area retardance structures can be used to establish a new flow path and channel alignment, or constrict flow in a channel. Barrier walls may be used for any of these functions, but because of their high cost, are appropriate for use only where space is at a premium. Channel relocation may be used separately or in conjunction with other countermeasures to change the flow path and flow orientation.

5.2.1 Erosion Mechanism. Bank erosion mechanisms are surface erosion and/or mass wasting. Surface erosion is the removal of soil particles by the velocity and turbulence of the flowing water. Mass wasting is by slides, rotational slip, piping, and block failure. In general slides, rotational slip and block failure result from the bank being under cut by the flow. Also, seepage force of the pore water in the bank is another factor that can cause surface erosion or mass wasting. The type of mechanism is determined by the magnitude of the erosive forces of the water, type of bed and bank material, vegetation, and vertical stability of the stream.

5.2.2 Stream Characteristics. Stream characteristics that influence the selection of countermeasures include: channel width; bank height, configuration, and material; vegetative cover; channel bed sediment transport condition; bend radii; channel velocities and flow depth; and floodplains.

Channel Width

Channel width influences only the use of spur-type countermeasures. On smaller streams, flow constriction resulting from the use of spurs may cause erosion of the opposite bank. However, spurs can be used on small channels where the purpose is to shift the location of the channel.

Bank Height

Low banks (< 10 feet) may be protected by any of the countermeasures, including barrier walls. Medium height banks (from 10 to 20 feet) may be protected by revetment, retardance structures, spurs, and longitudinal dikes. High banks (> 20 feet) generally require revetments used alone or in conjunction with other measures.

Channel Configuration

Spurs and jack fields have been successfully used as a countermeasure to control the location of the channel in meandering and braided streams. Also, walls, revetments, and riprap have been used to control bank erosion resulting from stream migration. On multi-branched channels, revetments, riprap, and spurs have been used to control bank erosion and channel shifting. Channels that do not carry large flows can and have been closed off with these types of countermeasures.

Channel Material

Spurs, revetments, riprap, jack fields, or check dams can be used in any type of channel material if they are designed correctly. However, jack fields should only be placed on streams that carry appreciable debris and sediment since the jacks must cause deposition to function properly.

Bank Vegetation

Vegetation can enhance the performance of structural countermeasures and may, in some cases, reduce the level of structural protection needed. Meander migration and other bank erosion mechanisms are accelerated on many streams in reaches where vegetation has been cleared. In arid and semi-arid areas, rainfall may not provide enough moisture to sustain significant plant density and supplemental irrigation may be required to provide measurable benefit from vegetation.

Sediment Transport

In general, sediment transport conditions can be described as regime, threshold, or rigid. Regime channel beds are those which are in motion under most flow conditions, generally in sand or silt-size noncohesive materials. Threshold channel beds have no bed material transport at normal flows and become mobile at higher flows. They may be cut through cohesive or noncohesive materials, or an armor layer of coarse-grained material may have developed on the channel bed. Rigid channel beds are cut through rock or boulders and rarely or never become mobile. In general, permeable structures will cause deposition of bed material in transport and are better suited for use in regime and some threshold channels than in rigid channel conditions. Impermeable structures are more effective than permeable structures in channels with little or no bed load, but impermeable structures can also be very effective in mobile bed conditions. Revetments can be effectively used with mobile or immobile channel beds.

Bend Radii

Bend radii affect the design of countermeasures. Thus, the cost per foot of bank protection provided by a specific countermeasure may differ considerably on short-radius and longer radius bends.

Channel Velocities and Flow Depth

Channel hydraulics affect countermeasure selection because structural stability and induced (local) scour must be considered. Some of the permeable flow retardance measures may not be structurally stable and countermeasures which utilize piles may be susceptible to scour failure in high velocity environments.

Debris

Debris (trees, limbs, trash, etc.) can damage or destroy countermeasures and should always be considered during the selection process. On the other hand, the performance of some permeable spurs and area retardance structures is enhanced by debris where debris accumulation causes increased sediment deposition.

5.2.3 Construction and Maintenance Requirements. Standard requirements regarding construction or maintenance such as the availability of materials, construction equipment requirements, site accessibility, time of construction, contractor familiarity with construction methods, and a program of regular maintenance, inspection, and repair are applicable to the selection of appropriate countermeasures. Additional considerations are the extent of bank disturbance which may be necessary and the desirability of preserving stream bank vegetative cover to the extent practicable.

5.2.4 Vandalism. Vandalism is always a maintenance concern in an urban setting since effective countermeasures can be made ineffective by vandals. Documented vandalism includes dismantling of devices, burning, and cutting or chopping with knives, wire cutters, and axes. Countermeasure selection or material selection for construction may be affected by concern for vandalism. For example, rock-filled baskets (gabions) may not be appropriate in some urban environments simply because they become a source for landscaping rock.

5.2.5 Costs. Cost comparisons should be used to study alternative countermeasures. However, it should be understood when comparing costs of existing installations that the measures were probably installed under widely varying stream conditions, that the conservatism (or lack thereof) of the designer is generally not accounted for, that the relative effectiveness of the measures cannot be quantitatively evaluated, and that some measures included in the cost data may not have been fully tested by floods.

## 5.3. Countermeasure Applications

5.3.1 General. Various devices and structures have been developed to control channel stability problems and serve as barriers to erosion. Most have been developed through trial and error applications, aided in some instances by hydraulic model studies. Case studies which report successes and failures are often the best sources of countermeasure design criteria and can provide valuable guidance in selecting a countermeasure for a specific instability or erosion problem. The following sections discuss, in general, the applicability of common types of countermeasures to typical lateral and vertical instability problems in arroyos and arid region drainageways.

5.3.2 Countermeasures for Meander Migration. Stabilizing the outside of channel bends is a common approach to countering lateral migration problems; however, stabilizing channel banks in a reach of channel can cause a change in the channel cross section and an increase in stream sinuosity upstream of the stabilized banks. **Figure 5.1a** illustrates a natural channel section in a bend with the deeper section at the outside of the bend and a gentle slope toward the inside bank resulting from point bar deposition. **Figure 5.1b** also illustrates the scour which results from stabilizing the outside bank of the channel and the steeper slope of the point bar on the inside of the bend. This effect must be considered in the design of countermeasures. It should also be recognized that the thalweg location and flow direction can change as sinuosity upstream increases.

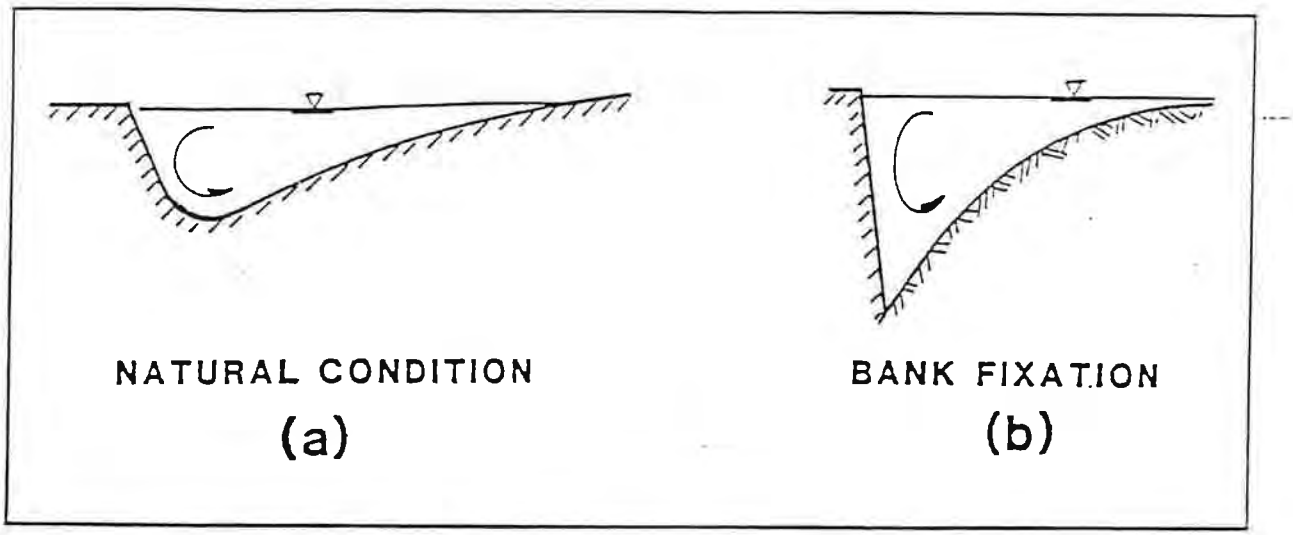


Figure 5.1. Comparison of channel bend cross sections (a) for natural conditions, and (b) for stabilized bend (after Brown, 1985a).

**Figure 5.2a** illustrates lateral migration in a natural stream and **Figure 5.2b**, the effects of bend stabilization on upstream sinuosity. As sinuosity increases, bend amplitude may increase, bend radii will become smaller, deposition may occur because of reduced slopes, and the channel width-depth ratio may increase as a result of bank erosion and deposition. Ultimately, cutoffs can occur. These changes can also result in changing hydraulic problems downstream of the stabilized bend.

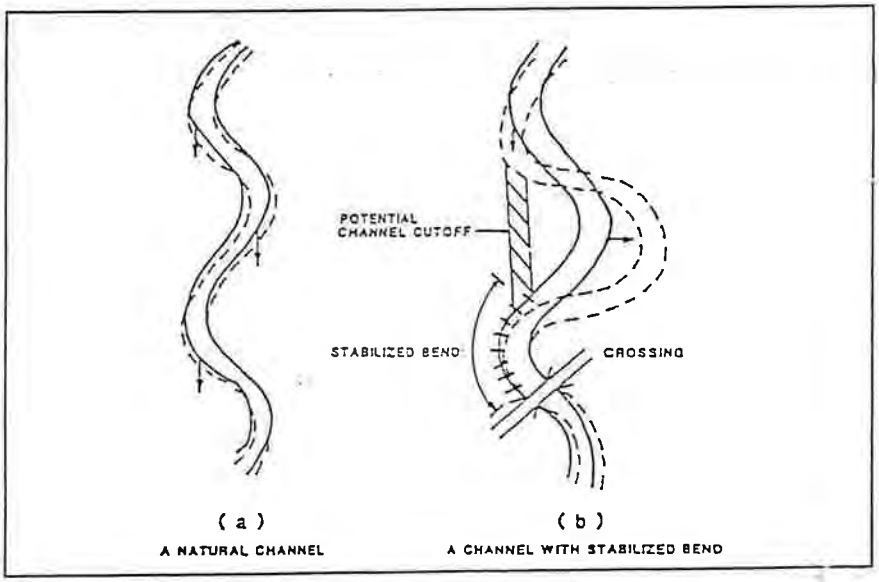


Figure 5.2. Bend migration in (a) a natural channel, and (b) a channel with stabilized bend (after Brown, 1985a).

Countermeasures for bend migration include those that:

1. Protect an existing bank line
2. Establish a new flow line or alignment
3. Control and constrict channel flow

The classes of countermeasures identified for bank stabilization and bend control are bank revetments, spurs, retardance structures, longitudinal dikes, barrier walls and channel relocations. These measures may be used individually or in combination to combat bend migration at a site. Some of these countermeasures are also applicable to bank erosion from causes other than bend migration.

5.3.3 Countermeasures for Channel Braiding and Multiple Channels. Channel braiding occurs in streams with an overload of sediment, causing deposition and aggradation. As aggradation occurs, the slope of the channel increases, velocities increase, and multiple, interlaced channels develop. The overall channel system becomes wider and multiple channels are formed as bars of sediment are deposited in the main channel. Braiding can also occur where banks are easily eroded and there is a large range in discharge. The channel becomes wider at high flows, and at low-flow forms multiple interlaced channels. Braided channels change alignment rapidly, and are very wide and shallow even at flood flow. In an island braided stream, flow is divided by islands rather than bars, and the branch channels are more permanent than braided channels and generally convey more flow.

Countermeasures used on braided and multi-branched streams are usually intended to confine the multiple channels to one channel. This tends to increase sediment transport capacity in the principal channel and encourage deposition in secondary channels. These measures usually consist of spur fields or dikes. At bridge crossings, guide banks (spur dikes) used in combination with revetment on highway fill slopes, riprap on highway fill slopes only, and spurs arranged in the stream channels to constrict flow to one channel, have also been used successfully.

5.3.4 Countermeasures for Degradation and Aggradation. Degradation problems are common on alluvial channels in the southwest. Degradation can cause bankline instability and can contribute to the loss of previously installed countermeasures. Aggradation can increase flooding potential and cause the loss of channel conveyance. Where channels become wider because of aggrading streambeds, existing countermeasures can be "outflanked." At its worst, aggradation may cause streams to abandon their original channels and establish new flow paths.

Countermeasures used to control degradation include check dams and channel linings. Check-dams and structures which perform functions similar to check-dams include drop structures and cutoff walls. A check-dam is a low dam or weir constructed across a channel to prevent degradation.

Linings of the channel banks with concrete riprap or other nonerosive material generally aggravates the tendency of degradation. To protect the lining, check-dams may be necessary to prevent undercutting.

Bank erosion is a common hydraulic hazard in degrading streams (see Section 3.4.4.). As the channel bed degrades, bank slopes become steeper and bank caving failures occur. The U.S. Army Corps of Engineers found that longitudinal stone dikes, or rock toe-dikes, provided the most effective toe protection of all bank stabilization measures studied for very dynamic and/or actively degrading channels (USCOE, 1981).

The following is a condensed list of recommendations and guidelines for the application of countermeasures in drainageways experiencing degradation:

1. Check-dams or drop structures are the most successful techniques for halting degradation on small to medium streams.

2. Channel lining alone with no bed protection is usually not appropriate to counter degradation problems.

3. Riprap or other nonerosive material on channel banks will fail if unanticipated channel degradation undercuts the toe of the riprap.

4. Rock-and-wire mattresses (gabions) are recommended for use only on small (<100 foot) channels experiencing lateral instability and little or no vertical instability. Even in these cases, the mattresses must have adequate burial depth to prevent undercutting by local scour.

5. Longitudinal stone dikes placed at the toe of channel banks are effective countermeasures for bank caving in degrading streams. Precautions to prevent outflanking, such as tiebacks to the banks, are usually necessary.

Currently, measures used in attempts to alleviate aggradation problems include channelization, debris (detention) basins, and/or continued maintenance, or combinations of these. Channelization may include excavating and clearing channels, constructing small dams to form debris basins, constructing cutoffs to increase the local slope, constructing flow control structures to reduce and control the local channel width, and constructing relief channels to improve flow capacity at the crossing. Except for debris basins and relief channels, these measures are intended to increase the sediment transport capacity of the channel, thus reducing or eliminating problems with aggradation. Cutoffs must be designed with considerable study as they increase local slope and can cause erosion upstream and deposition downstream. These studies would involve the use of sediment transport relations given in Chapter 3 or the use of sediment transport models.

A program of continuing maintenance has been successfully used to control problems at hydraulic structures on aggrading streams. In such a program, a monitoring system is set up to survey the affected reach at regular intervals. When some preestablished deposition depth is reached, the channel is dredged or cleared of the deposited material. In some cases, this requires opening a clearing after every major flood. This solution requires surveillance and dedication to the continued maintenance of adequate channel capacity in the aggrading reach. Otherwise, it is only a temporary solution. A debris basin or a deeper channel upstream of the bridge may be easier to maintain. Continuing maintenance is not recommended if analysis shows that other countermeasures are practicable.

Over the short-term, maintenance programs prove to be very cost effective when compared with the high cost of countermeasures such as channelization. When costs over the entire life of the structure are considered, however, maintenance programs may cost more than some of the initially more expensive measures. Also, the reliability of maintenance programs is generally low because the programs are often abandoned for budgetary or priority reasons. However, a program of regular maintenance could prove to be the most cost-efficient solution if analysis of the transport characteristics and sediment supply in a stream system reveals that the aggradation problem is only temporary (perhaps the excess sediment supply is coming from a construction site) or will have only minor effects over a relatively long period of time.

An alternative similar to a maintenance program which could be used on streams with persistent aggradation problems, such as those on alluvial fans, is the use of controlled sand and gravel mining from a debris basin constructed upstream of the aggrading reach. Use of this alternative would require careful analysis to ensure that the gravel mining did not upset the balance of sediment and water discharges downstream of the debris basin. Excessive mining could produce a degrading profile downstream, potentially impacting bankline stability or other countermeasures.

Following is a list of guidelines regarding aggradation countermeasures:

1. Extensive channelization projects have generally proven unsuccessful in alleviating general aggradation problems, although some successful cases have been documented. A sufficient increase in the sediment-carrying capacity of the channel is usually not achieved to significantly reduce or eliminate the problem. Channelization should be considered only if analysis shows that the desired results will be achieved.

2. Maintenance programs have proved unreliable, but they provide the most cost-effective solution where aggradation is from a temporary source or on small channels where the problem is limited in magnitude.

3. At aggrading sites on wide, shallow streams, spurs or dikes with flexible revetment have been successful in several cases in confining the flow to narrower, deeper sections.

4. A debris basin and controlled sand and gravel mining might be the best solution at alluvial fans and other crossings with severe problems.

## 5.4 General Design Criteria

Countermeasures can be incorporated into a naturalistic channel design to control, inhibit, delay or minimize stream stability problems. Countermeasures can be used to control vertical instability such as head cuts and channel degradation, as well as to control lateral instability and local scour. Countermeasures should be considered whenever excessive degradation or channel incision is anticipated, and when structures and utilities pertaining to or within the channel right-of-way may be endangered by either lateral migration, channel degradation, or local scour.

The selection of an appropriate countermeasure for a specific erosion problem depends on factors such as erosion mechanism, stream characteristics, construction and maintenance requirements, vandalism, esthetics and costs (see Section 5.2). However, effectiveness is probably the most important consideration in the selection of a specific countermeasure.

## 5.5 Detention Ponds

5.5.1 General Criteria. A detention pond can be an effective method of reducing flood peaks during storm events. Such structures temporarily detain flows from drains and collectors in urban areas, allowing for a slower, controlled release of flow over a longer time period. Detention structures will also trap sediments, reducing the supply of sediment to the downstream channel, which can create either a beneficial or adverse impact.

The principal benefit of a detention pond as part of a naturalistic arroyo design is that flood peaks and resulting flood water levels and velocities can be reduced. Since the channel size and shape are a function of the channel forming discharge, the reduction of peak discharge achieved with these structures can reduce lateral and vertical erosion in the arroyo. A problem with detention ponds is the ongoing maintenance required to clean the ponds after floods to keep the structures from filling with sediment. Design criteria for detention ponds are available from AMAFCA. A method for estimating trap efficiency of a detention pond is presented in the following section.

5.5.2 Detention Pond Sediment Trap Efficiency. The design life and/or maintenance requirements for a detention pond depends in part on the amount of sediment that deposits in the pond during flow events. In addition, it is necessary to estimate the amount of sediment that will be trapped by the detention facility to determine the sediment supply to downstream reaches for sediment continuity and equilibrium slope calculations. This section presents a method that can be used to estimate the trap efficiency of a detention pond in response to a specific storm hydrograph.

Trap efficiency calculations for engineering works normally rely on one of two general types of procedures. One type (e.g., Brune, 1953; Churchill, 1948; Lara, 1962) applies to large reservoirs where the incoming sediment load consists primarily of fine silt and clay-sized particles. The other type (e.g., Metcalf and Eddy, Inc., 1979) applies to settling basin design for wastewater treatment which is based on relatively low sediment concentrations with low velocities and regularly shaped, lined channels. Both types of procedures assume that the pool area is full at all times. They do not, therefore, apply to relatively small ponds on ephemeral channels where the incoming sediment load is very large and contains a high concentration of sand and coarser material, the incoming flow has high velocity and is very turbulent, and the reservoir pool area is often dry at the beginning of the storm event.

The method presented here accounts for the variable flow-through velocities in the detention pond, the highly turbulent nature of the flow and the effect of high sediment concentration on the fall velocity of the individual particles. The method is based on a statistical random walk model presented by Li and Shen (1975), which relies on the observation that solid particle settlement in turbulent flows is a random phenomenon. The model assumes that the turbulent fluctuations are normally distributed. By superimposing the turbulent fluctuations on the longitudinal velocity and fall velocity of the particles, they derived a relationship for the percentage of particles of a specific size that will settle in a given length of pond. The relationship requires knowledge of the mean velocity through the pond, the average settling depth in the pond, and the size distribution of the incoming sediment load. The original model assumed relatively low concentrations of sediment such that individual particles do not interfere with each other during the settling process. The model presented here has been revised to account for the effect of high sediment concentrations on the settling velocity of the individual particles. The modification is based on the following relationship, proposed by Richardson and Zaki (1954):

$$W_p = w_p(1-C_w)^{2.35} \qquad (5.1)$$

where $W_p$ = the fall velocity of the particle in the water-sediment mixture
$w_p$ = the fall velocity of the particle in clear water
$C_w$ = the **total** sediment concentration by weight

A computer program is available from AMAFCA to perform these calculations. See Appendix E for a description of input data for the program.

To compute the trap efficiency of a pond in response to a given storm hydrograph, use the following procedure:

1. Estimate the clear-water inflow hydrograph using the rainfall-runoff procedures in Section 22.2 Hydrology of the Development Process Manual (City of Albuquerque, 1993) as discussed in Chapter 2 of this Design Guide.

2. Estimate the sediment concentration and particle size distribution in the inflow hydrograph using the procedures presented in Section 2.2 and Section 3.3. It is important to recognize that the inflowing load consists of the fine sediment delivered from the watershed areas (wash load) as well as the coarser bed material load from the upstream arroyo. As discussed in Chapter 2, the wash-load size distribution can be assumed to be approximately the same as the surface soil material in the watershed. Methods for estimating the watershed sediment yield presented in Chapter 2 provide an average concentration for the storm hydrograph. Since the wash load is not controlled by the hydraulic conditions in the arroyo, it is usually reasonable, for computational purposes, to assume that the wash load concentration will not vary significantly during the hydrograph. The variation in bed material load is obtained by applying an appropriate bed material transport equation as discussed in Section 3.3.

3. Bulk the inflow hydrograph to include the **total** sediment load derived in the previous step by adding the sediment discharge to the clear-water hydrograph (see Section 3.3.5).

4. Route the bulked hydrograph through the detention pond using an appropriate reservoir routing routine.

5. Estimate the average velocity and settling depth for each time increment of the hydrograph (use the hydrograph discretization procedure discussed in Section 4.6).

   In detention ponds that are relatively wide in comparison to the upstream and outlet channels, it may be necessary to estimate an effective flow area to determine the average flow velocity through the pond. Based on the work of Wright (1977), it is reasonable to assume that the effective flow area will expand at a maximum angle of about 12-1/2° both horizontally and vertically. Contraction of the flow through the outlet will occur at about 45°. **Figure 5.3** illustrates the above assumption. To determine the average velocity through the pond, compute the average velocity of the inlet expansion zone (zone 1) based on the inflow discharge and the average velocity of the outlet contraction zone (zone 2) using the outflow discharge. The average velocity of zone 1 is computed from:

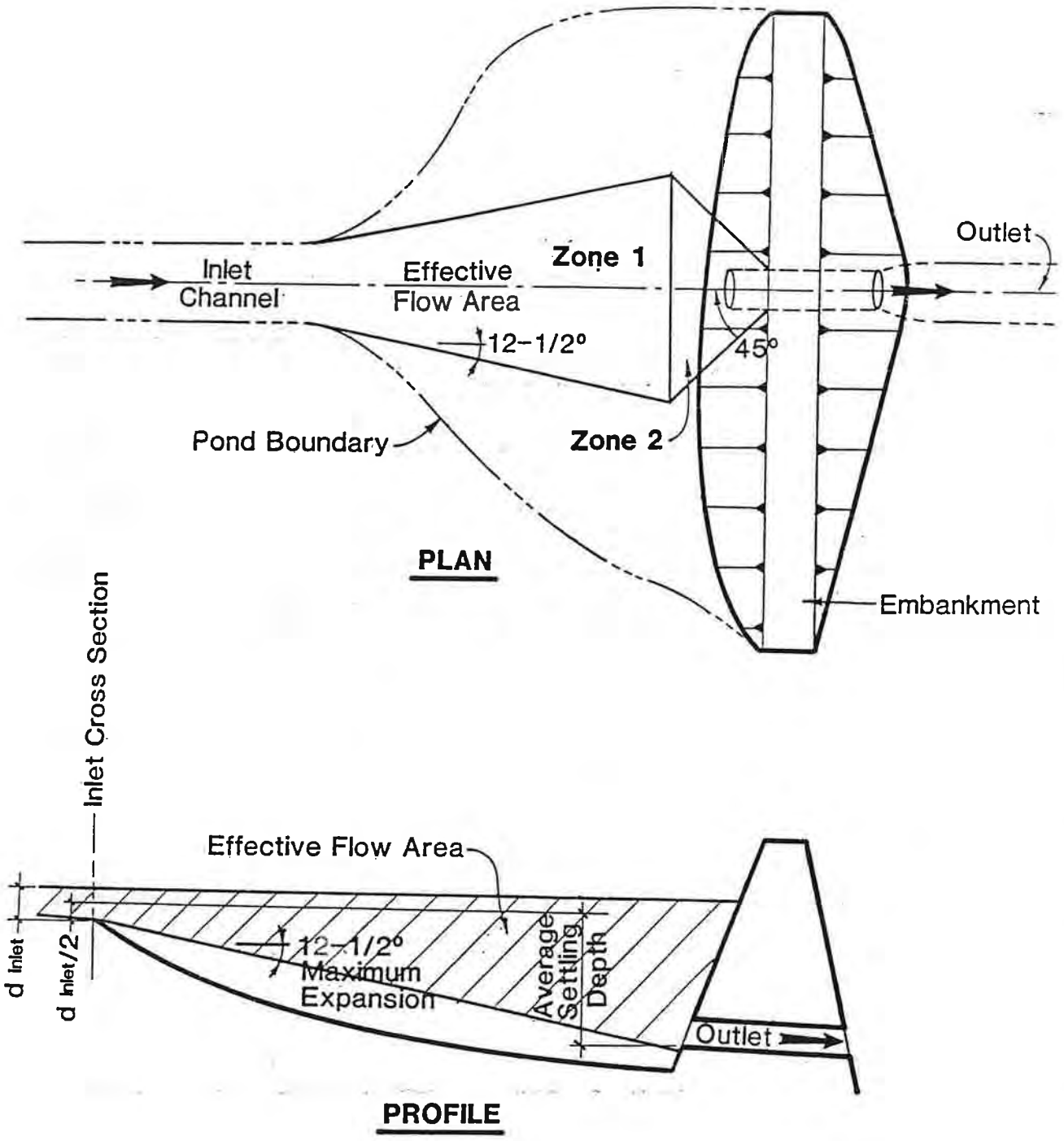


Figure 5.3. Detention pond effective flow area.

$$\bar{V}_1 = \frac{Q_{inlet}}{\bar{A}_1} \qquad (5.2)$$

In Equation 5.2, $\bar{A}_1$ is the average cross-sectional area in zone 1 given by:

$$\bar{A}_1 = \frac{V_1}{L_1} \qquad (5.3)$$

Where $V_1$ is the total volume of zone 1, $A_1$ is the length at zone 1. The average velocity in zone 2 is computed using the same relationships with the outlet discharge volume and length of zone 2. If the average velocities in the two zones are significantly different and/or the length of zone 1 is large compared to the length of zone 2, it may be necessary to perform the calculations from each zone separately with the sediment inflow to zone 2 based on the amount passing through zone 1. If the length of zone 1 exceed about 4 times the width of the inlet channel, it may be necessary to further refine the computation by breaking zone 1 into 2 or more segments. In general, greater accuracy is obtained by increasing the number of segments considered in the computation with the minimum length of any given segment no **less than** the width of the inlet channel. The average velocity through the pond can then be estimated as the mean of the velocities through the inlet expansion zone and outlet contraction zones.

For highly turbulent, high concentration flows, the average settling depth can be assumed to be the distance between the elevation of the vertical mid-point of the inflow to the pond and the invert of the outlet works (see **Figure 5.3**).

6. Compute the trap efficiency of the pond for each time increment for the range and percentage of particle sizes anticipated in the flow using the model discussed above. The gradation of the bed material can be used to approximate the gradation of the transported sand and gravel sizes. The wash load size can be approximated based on the gradation of the silts and clays in the watershed soils which, for the Albuquerque area, can be determined from SCS (1977).

7. Based on the trap efficiency results in Step 6, compute the cumulative volume of sediment trapped in the pond and released with the outflow discharge during the storm by accumulating the total amount trapped during each time step. When the amount of sediment trapped in the pond is of sufficient quantity to significantly affect the storage capacity, it may be necessary to refine the results by repeating the reservoir routing and trap efficiency calculations in an iterative manner. This can be accomplished by using the results of the initial calculations to adjust the storage-elevation curves and the geometry of the effective flow area through the pond.

## 5.6 Riprap

One of the most effective and versatile erosion control countermeasures is riprap. Riprap can be used to control lateral migration of channel banks and vertical degradation of channel beds, as well as mitigation of local scour at spurs, abutments, guide banks, grade control structures, and/or channel drops.

An advantage to the use of riprap is that this countermeasure is somewhat flexible and porous, allowing the stones to shift if there is subsidence. Riprap can prevent buildup of pore water pressure in the soil, which can cause more rigid stabilization measures such as concrete pavement to fail. Local failures of the riprap protection can be easily repaired by placement of more stone. Additionally, riprap can be aesthetically pleasing, and over a period of time, vegetation can establish itself between the stones, increasing the stability of this countermeasure.

A riprap design guide is also available from AMAFCA (1983). This guide discusses placement and filter requirements for protection of channel banks, channel bottoms, and locations of local scour such as drop structures, baffled aprons and grade control structures. In addition, the Federal Highway Administration recently (March 1989) published Hydraulic Engineering Circular No. 11, "Design of Riprap Revetment" (HEC-11), which provides an excellent supplemental source of design guidelines for use of riprap and other materials for bankline protection (Brown and Clyde, 1989). Also, the U.S. Army Corps of Engineers Engineering Manual EM 1110-2-1601, "Hydraulic Design of Flood Control Channels" (COE, 1991) contains a chapter and numerous plates to guide riprap design.

If suitable sizes of riprap are not available, wire baskets filled with smaller stones (gabions) can be utilized in much the same fashion as riprap. This countermeasure is suitable for bankline stabilization, protection of approach embankments, and can be used to form grade control or drop structures. It is important to note that the wire baskets are subject to clipping if coarse material (gravel sizes and larger) is transported by the flows in the channel. Furthermore, gabions are more vulnerable to vandalism and are not as flexible as riprap. As a result, they can withstand less settlement than riprap.

As with riprap, care must be exercised in the design to prevent piping of subgrade material from under the gabion mattresses. Suitable filter material must be placed under these structures, and edges must be tied into existing ground to prevent undermining and outflanking by the flow. HEC-11 (Brown and Clyde, 1989) provides detailed design guidelines for use of wire enclosed rock, including gabions, as bank protection (see **Figures 5.4 and 5.5**). Gabion manufacturers also provide guidelines and technical advisories on their particular products.

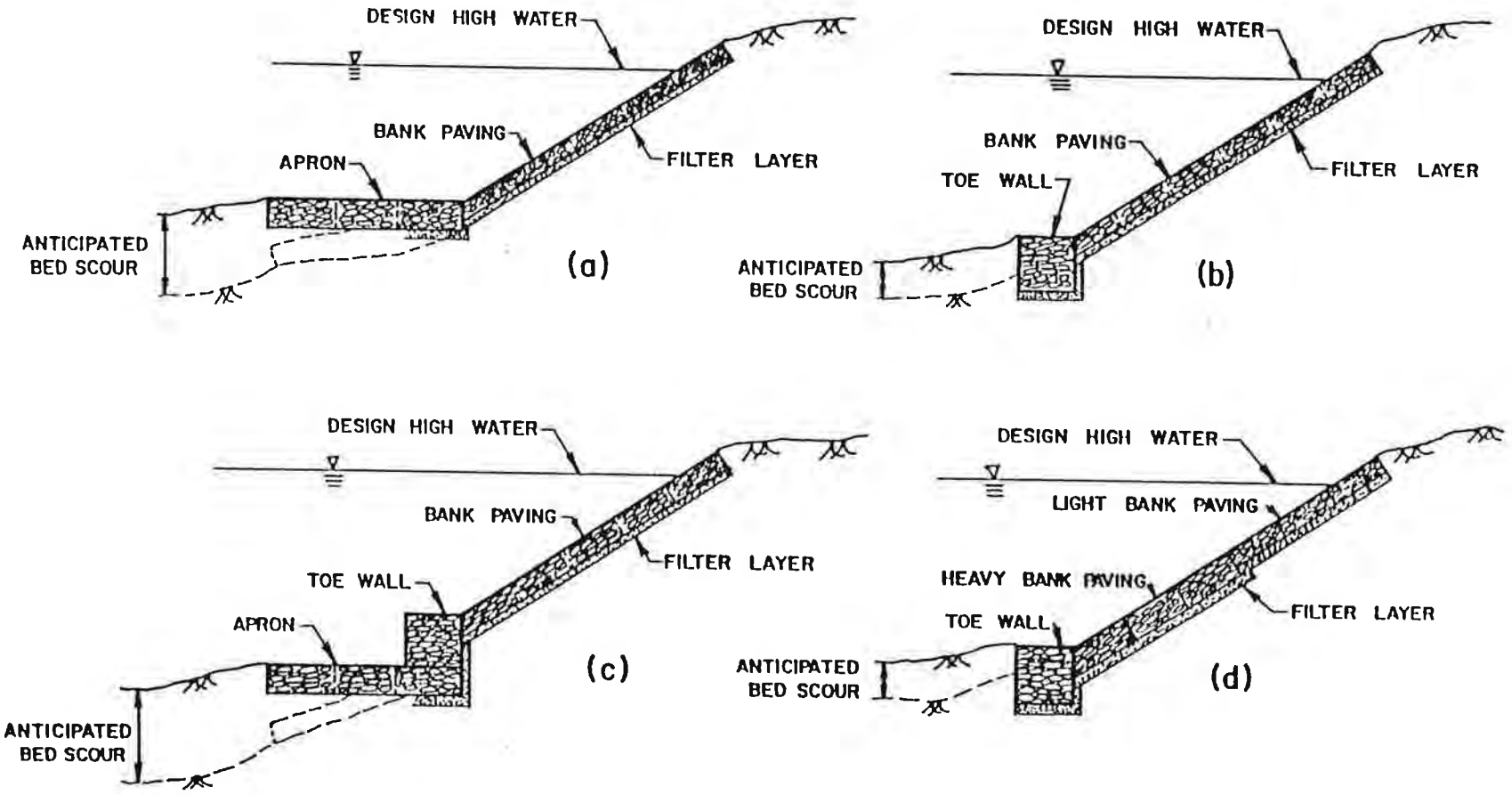


Figure 5.4. Rock and wire mattress configurations: (a) mattress with toe apron; (b) mattress with toe wall; (c) mattress with toe wall; (d) mattress of variable thickness (after Brown and Clyde, 1989).

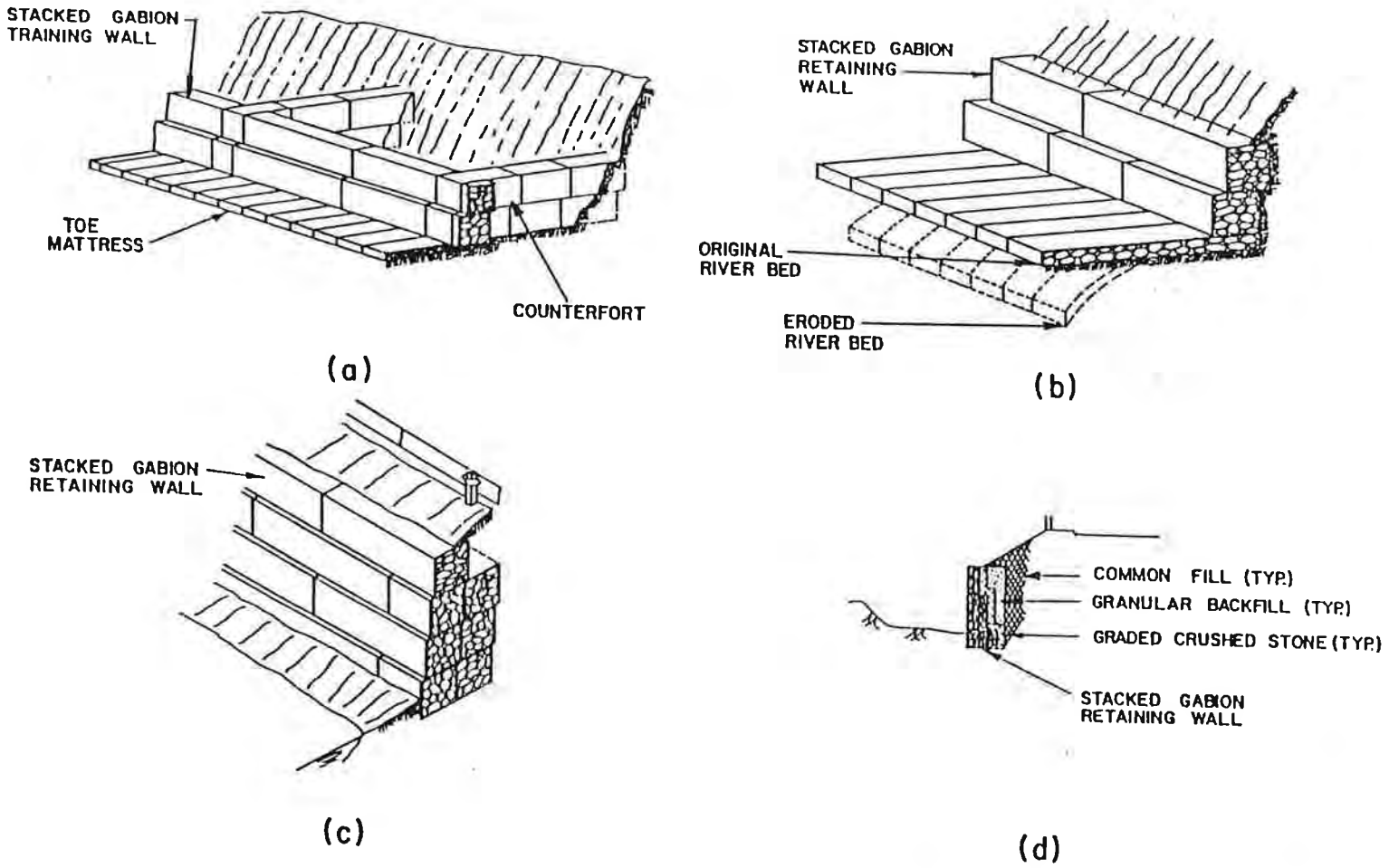


Figure 5.5. Typical stacked block gabion revetment details: (a) training wall with counterforts; (b) stepped back low retaining wall with apron; (c) high retaining wall, stepped-back configuration; (d) high retaining wall, batter type (after Brown and Clyde, 1989).

## 5.7 Soil Cement

Soil cement can also be used for a wide range of stability problems in arroyos. Soil cement can be used to stabilize access roads, grade control structures, and channel banks. A unique advantage of soil cement for channel protection and grade control is that a large mass of material can be provided relatively cost effectively to counter erosion forces. As with any rigid countermeasure, soil cement installations must be protected against degradation and outflanking. Since soil cement is relatively impervious it is not recommended for areas where pore water pressure in the underlying soil could cause failure. AMAFCA is currently developing guidelines for the use of soil cement. Specifications for use are available from AMAFCA.

A stair-step soil cement construction is recommended on channel banks with relatively steep slopes. Best results have been achieved on slopes no steeper than 3:1 as shown in **Figure 5.6.** However, in the arid southwest a steeper slope up to 1:1 can be used for stair-stepped soil cement. The material is placed in 6- to 12-inch lifts similar to compacted earth. Special care should be exercised to prevent raw soil seams between successive layers of soil cement. A sheepsfoot roller should be used on the last layer at the end of a day to provide an interlock for the next layer. The completed soil-cement installation must be protected from drying out for a 7-day hydration period. After completion, the material has sufficient strength to serve as a roadway along the embankment. Procedures for constructing soil-cement slope protection by the stair step method can be found in Portland Cement Association (PCA, 1984a and 1984b).

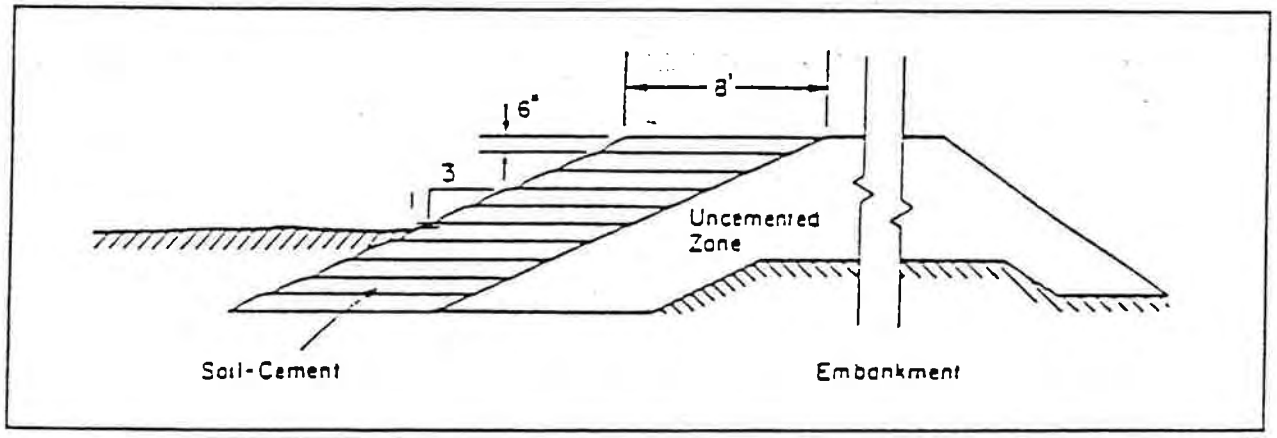


Figure 5.6. Typical soil-cement bank protection (after Richardson et al., 1990)

Precautions must be taken to prevent undermining at the toe and ends for any soil-cement installation. Protection at the toe can be provided by extending the installation below estimated scour depth, by a riprap launching apron, or by a concrete or sheet pile cutoff-wall extending to bedrock or well below the anticipated scour elevation. Weep holes or subsurface drains for relief of hydrostatic pressure are required for some situations.

## 5.8 Revetment and Bankline Stabilization

Revetments are either flexible or rigid structures placed longitudinally along a channel to protect banklines or to establish a new bankline in the arroyo. A comprehensive discussion of revetments is presented in FHWA's HEC-20 (Lagasse et al., 1991) and detailed design guidelines are available in FHWA's HEC-11 (Brown and CLyde, 1989).

5.8.1 Flexible Revetment. Dumped rock riprap and gabions are the most widely used flexible revetments (see Section 5.6).

5.8.2 Rigid Revetment. Rigid revetments include concrete pavement, sacked concrete, concrete-grouted riprap, concrete-filled fabric mat, and soil cement. Special precautions are warranted in the design to prevent undermining at the toe and termini as well as failure from unstable soils or hydrostatic pressures.

## 5.9 Spurs and Guide Banks

5.9.1 Spur Description. Spurs are pervious or impervious structures which project perpendicularly from the stream bank into the channel. Spurs deflect flowing water away from the bank, reducing velocities and mitigating bank erosion. They can also be used to establish a more desirable channel alignment or width. Sediments carried by the flow can deposit in the low velocity area behind the spur, thus increasing the stability of the spur and bank protection. Local scour can occur at the nose of spurs and therefore must be protected with revetment material.

Spurs are generally used to halt meander migration at a bend. They are also used to channelize wide, poorly defined streams into well-defined channels. Spurs are classified based upon their permeability as retarder spurs, retarder/deflector spurs, or deflector spurs. The permeability of spurs is defined simply as the percentage of the spur surface area facing the streamflow that is open. Deflector spurs are impermeable spurs (< 30 percent permeability) which function by diverting the primary flow currents away from the bank. Retarder/deflector spurs are moderately permeable and function by retarding flow velocities at the bank and diverting flow away from the bank. Retarder spurs are more permeable (> 70 percent permeability) and function by retarding flow velocities near the bank. Spurs can be constructed using rock and wire basket (gabion) techniques or rock riprap (see **Figures 5.7 and 5.8**) or soil cement.

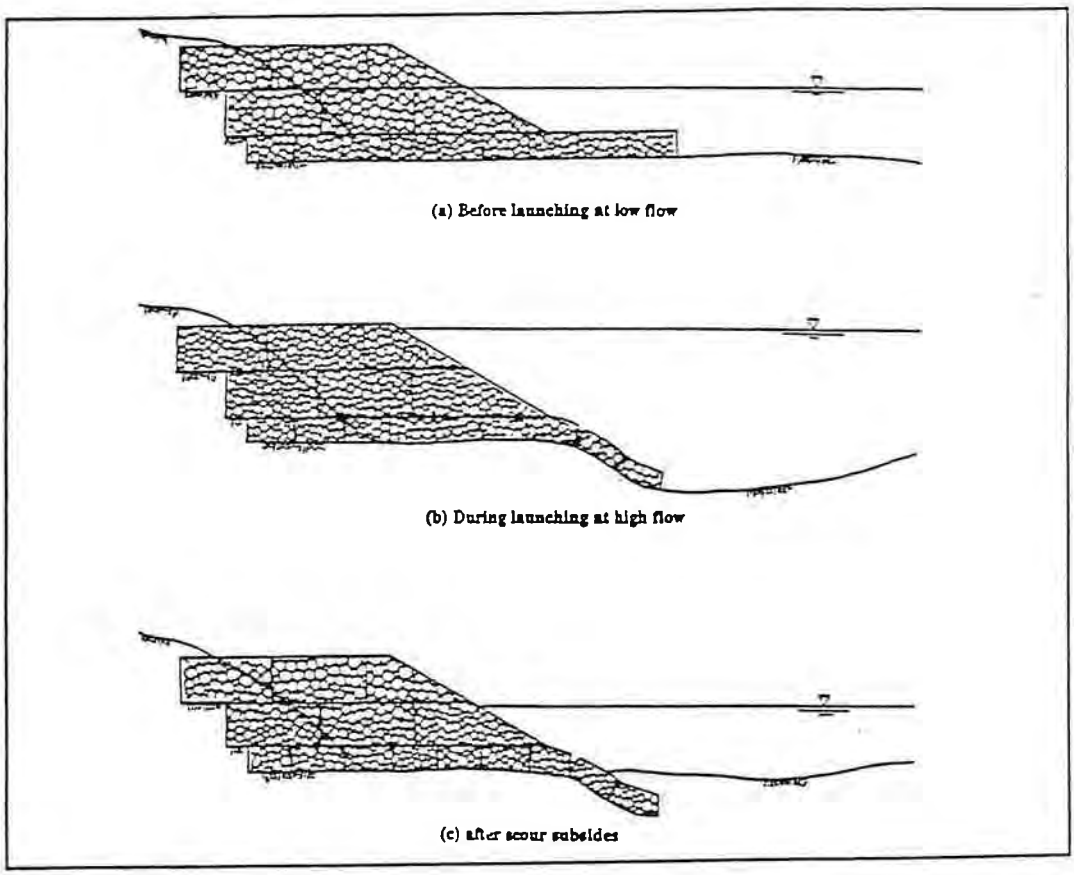


Figure 5.7. Gabion spur illustrating flexible mat tip protection: (a) before launching at low flow, (b) during launching at high flow, and (c) after scour subsides (after Brown, 1985).

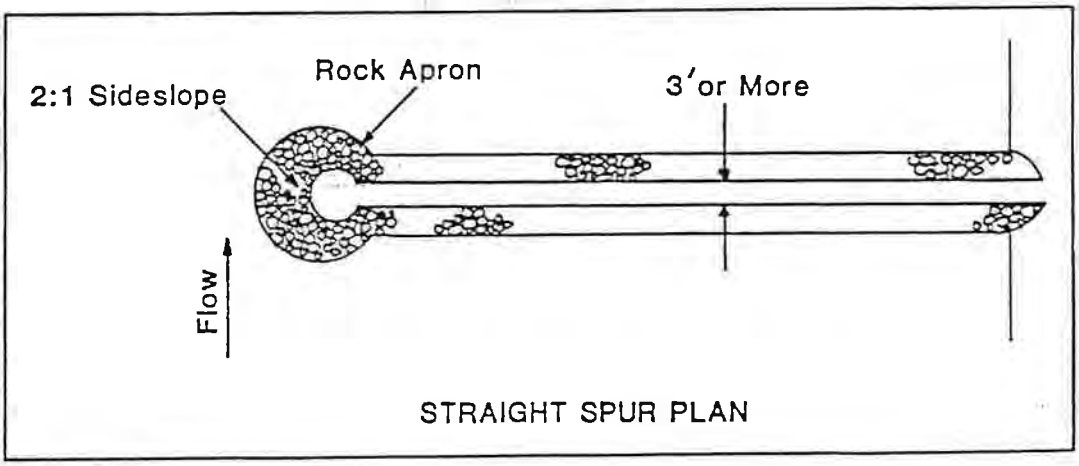


Figure 5.8. Typical straight, round nose spur (Lagasse et al., 1991).

5.9.2 Spur Design Considerations. Spur design includes setting the limits of bank protection required, selection of the spur type to be used, and design of the spur installation including spur length, orientation, permeability, height, profile, and spacing. Defining the limits of bank protection is subjective and very little quantitative guidance, particularly for arroyo applications, is available. As a minimum, the length of spur field should be equal to the observed or expected length of erosion or bank instability. Evaluation of installations in meandering streams suggests that the protection often extends too far upstream and not far enough downstream, which is valuable insight for any spur field design.

Spur Length. Spur length is the projected length of the spur from the bankline normal to the main flow direction. When the bankline is irregular, spur length should be adjusted to provide for a curvilinear flow path. If the spur length is too great, relative to channel width, erosion of the opposite bankline can occur. Generally, impermeable spur length should be less than 15 percent of the channel width, and permeable spurs less than 25 percent of the channel width.

Spur Orientation. Spur orientation, relative to the main flow direction, can affect spur spacing, the degree of flow control achieved and the scour depth at the tip of the spur. However, most evidence indicates that spurs normal to the bankline perform adequately and are most cost effective. Only the spur furthest upstream should be angled downstream to provide a smoother transition into the spur field and minimize scour at the nose of the leading spur.

Spur Height. The height of impermeable spurs should not exceed the bank height to minimize scour in the overbank and potential outflanking at high stream stages. When the design water surface is equal or greater than the bank height, impermeable spurs should equal the bank height. When the water surface is lower than the bank height, impermeable spurs should be designed so that overtopping will not occur. Permeable spurs are typically designed so that debris can pass over the top of the spur.

Scour Potential. Spur permeability influences scour potential at the streambank and spur tip. Impermeable spurs, in particular, can create erosion of the streambank at the spur root if the spur becomes overtopped, while such erosion is less likely for permeable spurs. Similarly, more scour at the spur tip would be expected for impermeable spurs. Scour depths at spur tips for permeabilities up to about 35 percent are given by **Figure 5.9**. For design purposes, the same figure will provide conservative results for spurs with permeabilities greater than 35 percent.

Spur Spacing. Spur spacing is a function of spur length, spur angle, permeability, and the degree of curvature of the bend. For smaller watercourses, such as the arroyos in the Albuquerque area, the spur spacing is also a function of the shape of the meander flow path as described in Section 3.4.5. The flow expansion angle, or the angle at which flow expands toward the bank downstream of a spur, is a function of spur permeability and the ratio of spur length to channel width. The shape of the meander flow path is a function of the dominant discharge, dominant channel width and channel sinuosity. Spur spacing is determined by the following steps:

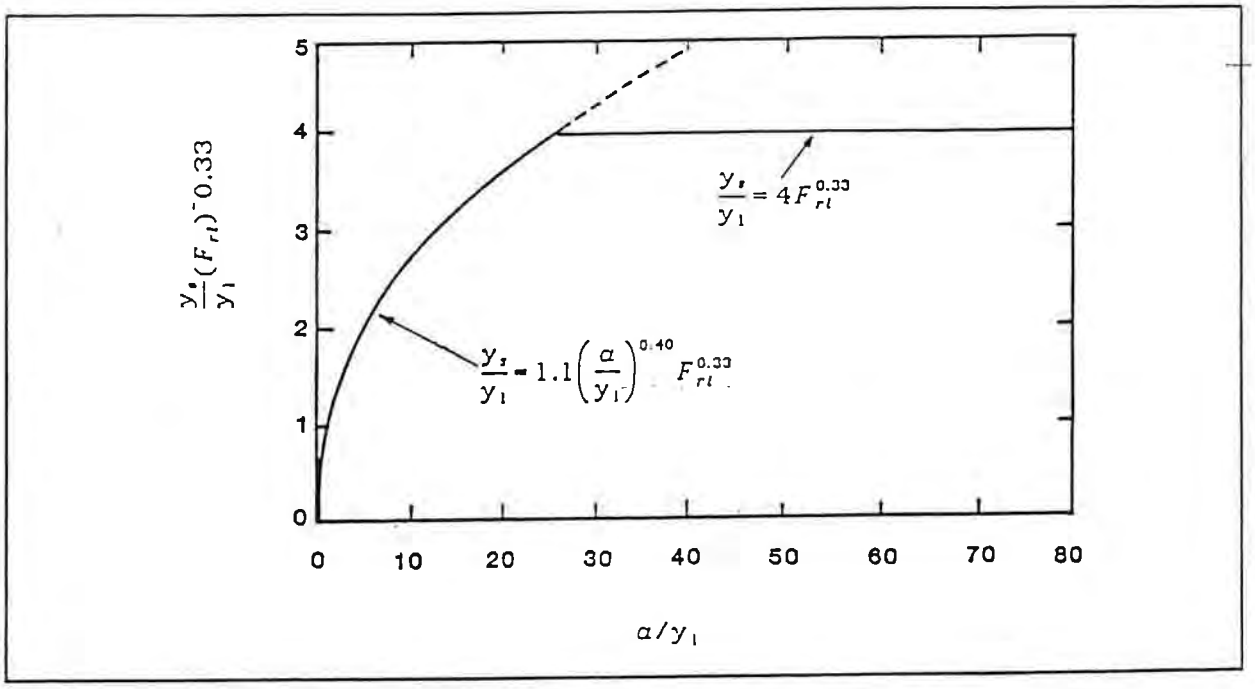


Figure 5.9. Recommended prediction curves for scour at the end of spurs with permeability up to about 35 percent (Lagasse et al., 1991). See Section 3.5.3 for a definition of terms.

1. Sketch the desired thalweg or flow alignment. Based on the up- and downstream flow conditions, sketch the desired flow lines with smooth transitions to up- and downstream conditions.

2. Sketch the desired bankline and alignment of the spur tips. Based on the desired flow lines and the general guidelines on spur length, sketch the alignment of the toe of the spur tips and desired bankline. Note that typically spur length is measured from the desired bankline.

3. Locate the first spur. Locate the most downstream spur so that the flow expansion angle, as defined in **Figure 5.10** and determined from **Figure 5.11** will intersect the downstream bankline at the desired location. If spurs are designed to provide erosion protection for the prudent line, the bank end of the first spur should extend to the prudent line.

4. Locate remaining spurs. The remaining spurs are located based on the following:

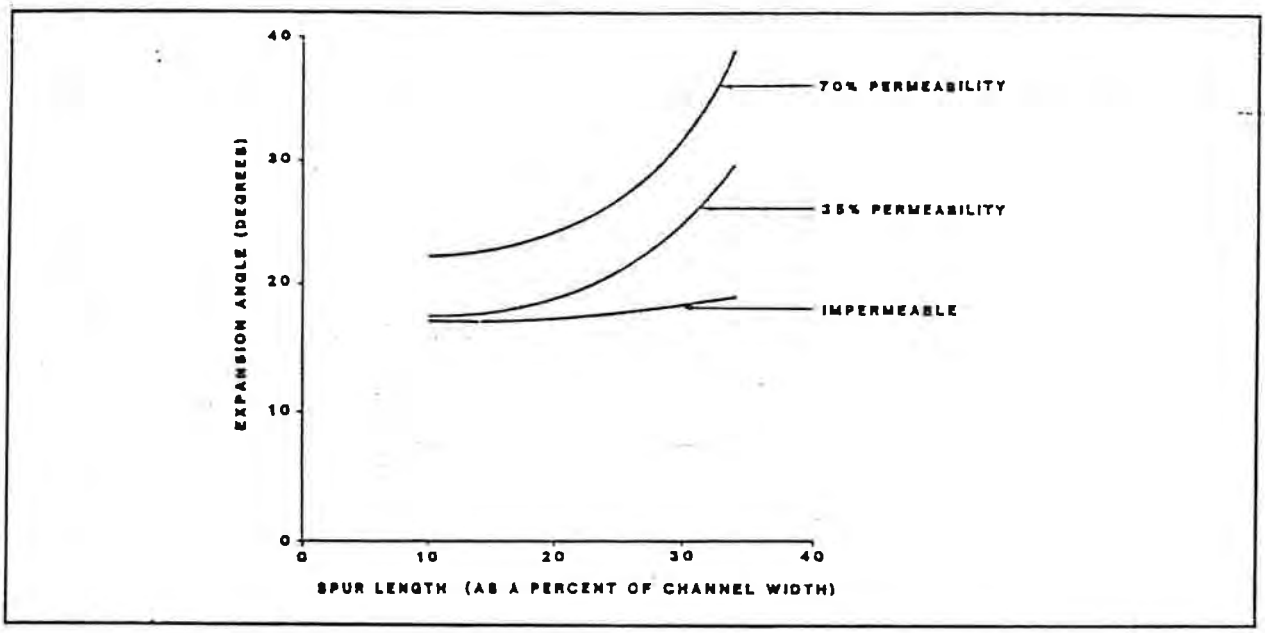


Figure 5.10. Relationship between spur length and expansion angle for several spur permeabilities (after Brown, 1985).

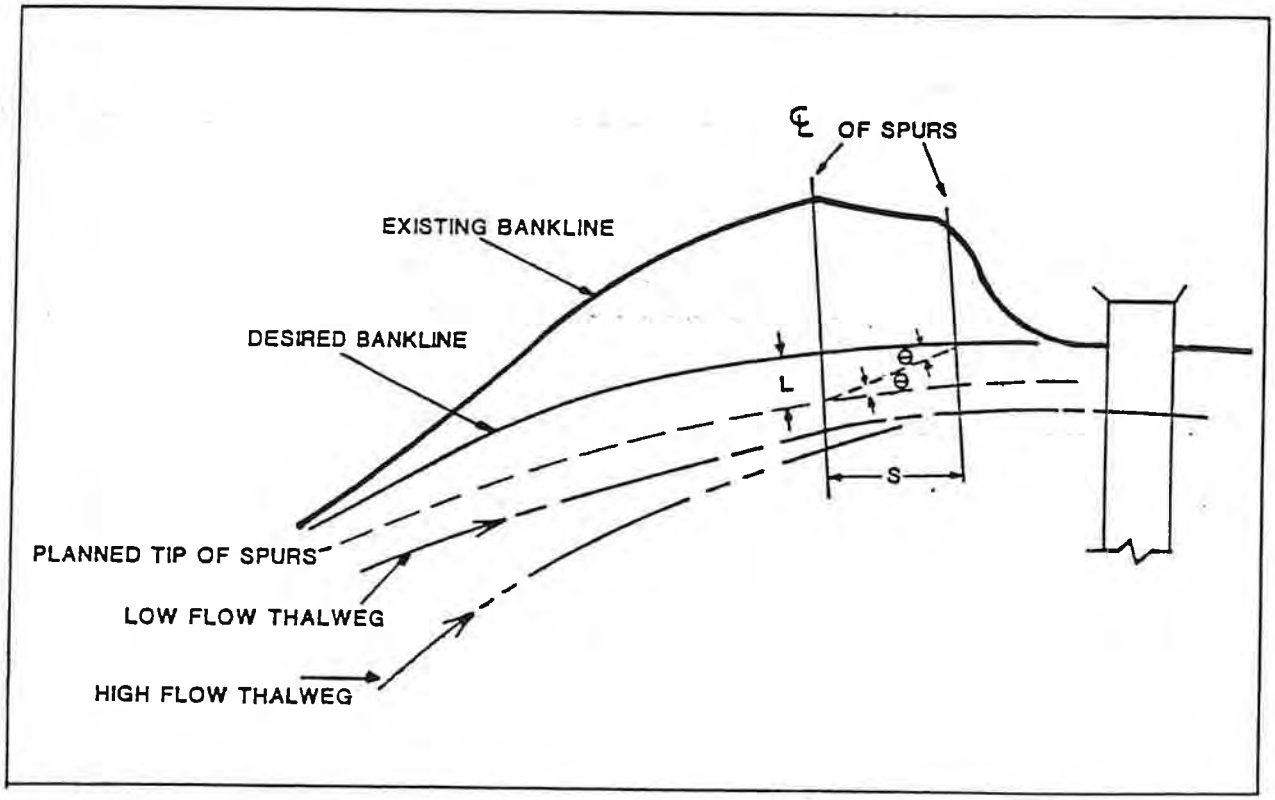


Figure 5.11: Spur spacing in a meander bend (after Brown, 1985).

a. Use the following equation to determine the minimum flow expansion angle:

$$S = L \cot(\theta) \quad (5.4)$$

where S = spacing between spurs at the toe, ft
L = effective length of spur, or the distance between arcs describing the toe of spurs and the desired bankline, ft
θ = expansion angle downstream of spur tips, degrees.

b. Use Figure 3.24 and the procedures to compute channel widths for dominant discharge ($W_D$) to compute the maximum offset from the channel bank, assumed to be at the channel end of the spurs.

The length of spur (L) must be greater than the maximum offset, but not less than (L) used in Equation 5.4.

Example. An example of spur field design, as well as more detailed discussion of spur design, are provided in FHWA's HEC-20 (Lagasse et al., 1991). This example does not include the adjustment for meander flow path that is recommended by this Design Guide.

5.9.3 Kellner Jetty. The steel jack (Kellner Jetty) system is a special case of the retarder spur concept that has been used extensively in the Southwest, particularly along the Rio Grande, and which may have limited application on the larger arroyos in the Albuquerque area. Because of environmental, aesthetic and safety concerns with the use of steel jetties in an urban setting, they are discussed here primarily for reference purposes. The purpose of a jetty field is to add roughness to a channel or overbank area to train the main stream along a selected path. The added roughness along the bank reduces the velocity and protects the bank from erosion. Jetty fields are usually made up of steel jacks (**Figure 5.12**) tied together with cables. Both lateral and longitudinal rows of jacks are used to make up the jetty field as shown in **Figure 5.13**.

The lateral rows are usually angled about 45 to 70 degrees downstream from the bank. The spacing varies, depending upon the debris and sediment content in the stream, and may be 50 to 250 feet apart. A jetty field can be designed as a permeable spur field using the techniques outlined above. Jetty fields are effective only if there is a significant amount of debris carried by the stream and the suspended sediment concentration is high. They are most effective on mild bends and in wide, shallow channels which carry a large sediment load. These conditions may be met on some of the larger arroyos in the Albuquerque area, but are probably not met on smaller arroyos.

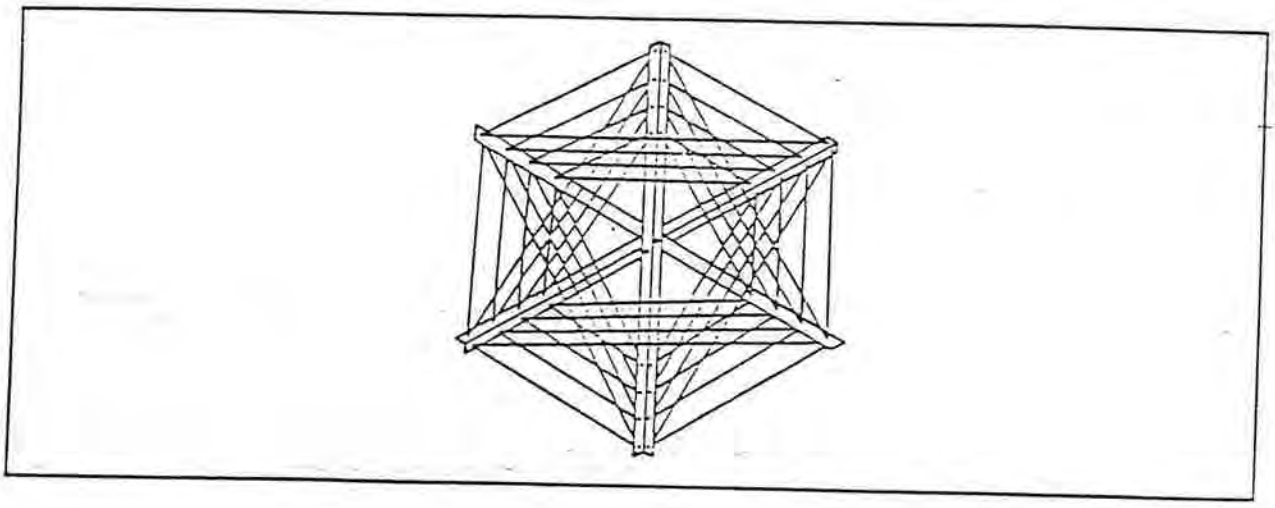

Figure 5.12. Typical jack unit (after Brown, 1985).

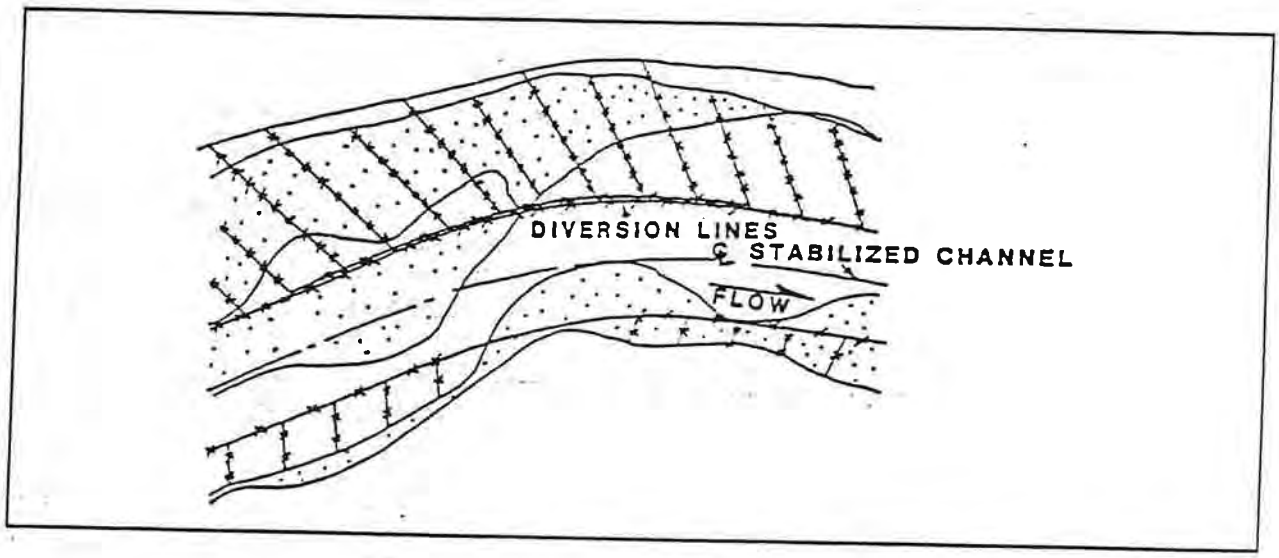


Figure 5.13. Retarder field schematic (after Richardson et al., 1990).

5.9.4 Guide Banks. Guide banks can be used at bridges or culverts whenever there is overbank flow which must return to a bridge opening or when road-approach embankments encroach into the channel (see **Figure 5.14**). The function of guide banks (in older references these are referred to as spur dikes) is to provide a more streamlined flow through the bridge or culvert by reducing separation of the flow which must return to the constricted bridge or culvert opening upstream of the crossing. The guidebank will

minimize local scour at abutments by transferring the local scour upstream to the nose of the guide bank. Guide banks can be constructed with rock revetment or embankment material. Since local scour can occur at the upstream nose of the guide bank, protection in the form of revetment, needs to be considered. The design and layout of guide banks are discussed in FHWA's HEC-20 (Lagasse et al., 1991).

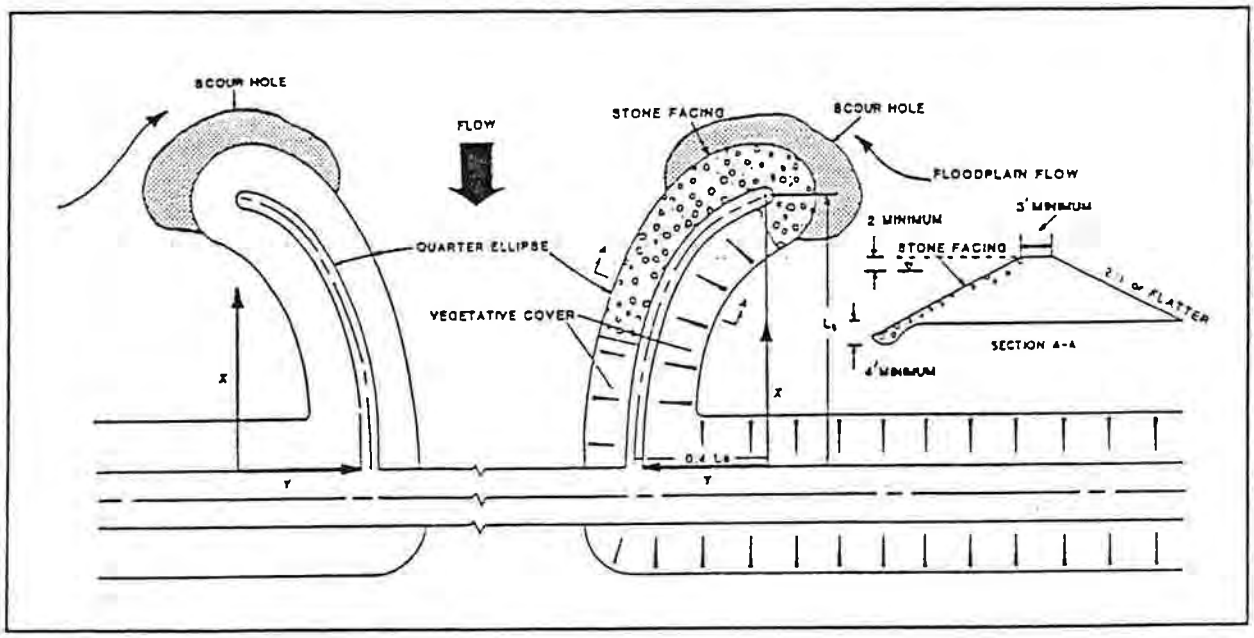


Figure 5.14. Typical guide bank (modified from Bradley, 1978).

## 5.10 Drop Structures

Drop structures are used to provide vertical control of the channel bed. For small drops, vertical or sloping drops may be adequate; for larger drop heights the use of gabion drops or baffled drops may be required. Guidance for the type of drop structure to use is given in AMAFCA's Design Guide for Riprap-Lined Flood Control Channels (1983). A method to estimate the depth of scour below a vertical drop structure is presented in Section 3.6.2. Care must be exercised in the design to prevent outflanking or undermining by the flow, and to mitigate lateral bank erosion downstream of the drop structure.

## 5.11 Case Histories of Countermeasure Performance

The Federal Highway Administration has assembled a collection of case histories of hydraulic problems at bridge sites. These case histories provide insight on the performance of a variety of countermeasures and are summarized in this section to provide information on the relative success of the various countermeasures that can be used to stabilize streams. All case histories are taken from Brice et al. (1978a, b); Brice (1984), and Brown et al. (1980). Site data are from Report No. FHWA-RD-78-163 (Brice

et al., 1978a, b). This compilation of case histories at 224 bridge sites in various geographic regions is recommended reference material for those responsible for selecting countermeasures for stream instability. Additional information regarding experience with various countermeasures in the Albuquerque area is provided, where available.

### 5.11.1 Flexible Revetment

#### Rock Riprap

Dumped rock riprap is the most widely used revetment in the United States. Its effectiveness has been well established where it is of adequate size, of suitable size gradation, and properly installed. Brice et al. (1978a, b) documented the use of rock riprap at 110 sites. They rated the performance at 58 sites and found satisfactory performance at 34 sites, partially satisfactory performance at 12 sites, and failure to perform satisfactorily at 12 sites. Keeley (1971) concluded that riprap used in Oklahoma performed without significant failure and provides basic and efficient bank control on the meandering streams in Oklahoma.

A review of the causes of failure at the sites studied by Brice et al. (1978a, b) is instructive. They found the absence of a filter blanket clearly the cause of the failure at one site. The riprap was placed on a fill of sand and fine gravel which eroded through the interstices of the riprap. Internal slope failure was the cause of failure of riprap at the abutment of bridges at two sites. Inadequate rock size and size gradation were given as the causes of failure at eight sites. All of these sites are complex, and it is difficult to assign failure to one cause, but rock size was definitely a factor.

Channel degradation accounted for failure at three sites in Mississippi. Channel degradation at these sites is due to channel straightening and clearing by the Soil Conservation Service and U.S. Army Corps of Engineers. Riprap installations on the streambanks, at bridge abutments and in the streambed have failed to stop lateral erosion. At one site, riprap placed on the banks and bed of the stream resulted in severe bed scour and bank erosion downstream of the riprap.

Failure of riprap at one site was attributed to the steep slope on which the riprap was placed. At this site, rock riprap failed to stop slumping of the steep banks downstream of a check dam in a degrading stream.

Successful rock riprap installations at bends were found at five sites. Bank erosion was controlled at these sites by rock riprap alone. Installations rated as failing were damaged at the toe and upstream end, indicating inadequate design and/or construction, and damage to an installation of rounded boulders, indicating inadequate attention to riprap specifications. Other successful rock riprap study sites were sites where bank revetment was used in conjunction with other countermeasures, such as spurs or retards.

The success of these installations was attributed more to the spurs or retards, but the contribution of the bank revetment was not discounted.

Broken Concrete

Broken concrete is commonly used in emergencies and where rock is unavailable or very expensive. No specifications were found for its use. Performance was found to be more or less unsatisfactory at three sites. AMAFCA discourages the use of broken concrete as riprap for a number of reasons: the appearance is generally unsatisfactory and can attract subsequent dumping, the slab shape of most broken concrete does not provide the interlocking or gradation characteristics of properly designed riprap, and finally, the durability is generally not satisfactory.

Rock-and-Wire Mattress and Gabions

The distinction made between rock-and-wire mattress and gabions is in the dimensions of the devices. Rock-and-wire mattress is usually one foot or less in thickness and a gabion is thicker and nearly equidimensional. The economic use of rock-and-wire mattress is favored by an arid climate, availability of stones of cobble size, and unavailability of rock for dumped rock riprap. Corrosion of wire mesh is slow in arid climates, and ephemeral streams do not subject the wire to continuous abrasion. Where large rock is not available, the use of rock-and-wire mattress may be advantageous in spite of eventual corrosion or abrasion of the wire.

Rock-and-wire mattress performance was found to be generally satisfactory although local failure of the wire mesh and spilling out of the rock was not uncommon. Mattresses are held in place against the bank by railroad rails at sites in New Mexico and Arizona where good performance was documented. This is known locally as "railbank protection." The steel rail supported rock-and-wire mattress stays in place better than dumped rock riprap on the unstable vertical banks found on the ephemeral streams of this area. Mattress held in place by stakes has been found to be effective in Wyoming.

The use of rock-and-wire mattress has diminished in California because of the questionable service of wire mesh, the high cost of labor for installation, and the efficiency of modern methods of excavating for dumped riprap toe protection. The Los Angeles Flood Control District, however, has had installations in-place for 15 years or more with no evidence of wire corrosion. On the other hand, Montana and Maryland reported abrasion damage of wire. These experiences illustrate that economic use of countermeasures is dependent on the availability of materials, costs, and the stream environment in which the measure is placed.

Several sites were identified where gabions were installed, but the countermeasures had been tested by floods at only one site where gabions placed on the downstream slope of a roadway overflow section performed satisfactorily.

In the Albuquerque area, performance of gabions for bank protection and grade control has generally been satisfactory. Performance problems have related more to the proper design of the filter between the gabion and the in-situ material, rather than with broken or corroded gabion wire. In other urban settings such as Denver, Colorado, vandalism and the use of gabion installations as a source of landscaping materials have been reported as significant problems and the local flood control authority discourages their use.

Other Flexible Revetment

Favorable performance of precast-concrete blocks at bridges was reported in Louisiana. Vegetation is reported to grow between blocks and contribute to appearance and stability. Vegetation apparently is seldom used alone at bridges. Iowa relies on sod protection of spur dikes, but Arkansas reported failure of sod as bank protection.

5.11.2 Rigid Revetments. Failure of rigid revetment tends to be progressive; therefore, special precautions to prevent undermining at the toe and termini and failure from unstable soils or hydrostatic pressure are warranted.

Concrete Pavement

Well-designed concrete paving is satisfactory as fill slope revetment, as revetment on streams having low gradients, and in other circumstances where it is well protected against undermining at the toe and ends. The case histories include at least one location where riprap launching aprons were successful in preventing undermining at the toe from damaging the concrete pavement revetment. Weep holes for relief of hydrostatic pressure are required for many situations.

Documented causes of failure in the case histories are: undermining at the toe (six sites), erosion at termini (five sites), eddy action at downstream end (two sites), channel degradation (two sites), high water velocities (two sites), overtopping (two sites), and hydrostatic pressure (one site). Good success is reported with concrete slope paving in Florida, Illinois, and Texas.

Sacked Concrete

No highway agency reported a general use of sacked concrete as revetment. California was reported to regard this as an expensive revetment almost never used unless satisfactory riprap was not available. Sacked concrete revetment failures were reported from undermining of the toe (two sites), erosion at termini (one site), channel degradation (two sites), and wave action (one site).

Concrete-Grouted Riprap

Concrete-grouted riprap permits the use of smaller rock, a lesser thickness, and more latitude in gradation of rock than in dumped rock riprap. No failures of grouted riprap were documented in the case histories, but it is subject to the same types of failures as other impermeable, rigid revetments. This is particularly true since grouted riprap has little or no tensile strength and is subject to failure due to the buildup of pore water pressure underneath or by undercutting. In the Albuquerque area, over grouting is a common problem which can produce a much smoother surface than ungrouted riprap. This can adversely affect hydraulic parameters such as roughness and velocity.

Concrete-Filled Fabric Mat

Concrete-filled fabric mat is a patented product (Fabriform) consisting of porous, pre-assembled nylon fabric forms which are placed on the surface to be protected and then filled with high-strength mortar by injection. Variations of Fabriform and Fabricast consist of nylon bags similarly filled. Successful installations were reported by the manufacturer of Fabriform in Iowa, and North Dakota reported successful installations.

Soil Cement

In areas where any type of riprap is scarce, use of in-place soil combined with cement provides a practical alternative. The resulting mixture, soil cement, has been successfully used as bank protection in many areas of the Southwest. Unlike other types of bank revetment, where milder side slopes are desirable, soil cement in a stairstep construction can be used on steeper slopes (i.e., typically one to one), which reduces channel excavation costs. For many applications, soil cement can be more aesthetically pleasing than other types of revetment.

5.11.3 Bulkheads (Erosion Barrier Walls). A bulkhead is a steep or vertical wall used to support a slope and/or protect it from erosion. Bulkheads usually project above ground, although the distinction between bulkheads and cutoff walls is not always sharp. Most bulkhead applications were found at bridge abutments. They were found to be most useful at the following locations: (1) on braided streams with erodible sandy banks, (2) where banks or abutment fill slopes have failed by slumping, and (3) where stream alignment with the bridge opening was poor, to provide a transition between stream banks and the bridge opening. It was not clear what caused failures at five sites summarized in Brice et al. (1978a, b), but in each case, the probable cause was undermining.

5.11.4 Spurs. Spurs are permeable or impermeable structures which project from the bank into the channel. Spurs may be used to alter flow direction, induce deposition, or reduce flow velocity. A combination of these purposes is generally served. Where spurs project from embankments to decrease flow along the embankment, they are called

embankment spurs. These may project into the floodplain rather than the channel, and thus function as spurs only during overbank flow. According to a summary prepared by Richardson and Simons (1984), spurs may protect a stream bank at less cost than riprap revetment. By deflecting current away from the bank and causing deposition, they may more effectively protect banks from erosion than revetment. Uses other than bank protection include the constriction of long reaches of wide, braided streams to establish a stable channel, constriction of short reaches to establish a desired flow path and to increase sediment transport capacity, and control of flow at a bend. Where used to constrict a braided stream to a narrow flow channel, the structure may be more correctly referred to as a dike or a retard in some locations.

Several factors enter into the performance of spurs, such as permeability, orientation, spacing, height, shape, length, construction materials, and the stream environment in which the spur is placed.

Impermeable Spurs

The case histories show good success with well-designed impermeable spurs at bends and at crossings of braided stream channels (eight sites). At one site, hardpoints barely projecting into the stream and spaced at about 100 to 150 feet failed to stop bank erosion at a severe bend. At another site, spurs projecting 40 feet into the channel, spaced at 100 feet, and constructed of rock with a maximum diameter of 1.5 feet experienced erosion between spurs and erosion of the spurs. At a third site, spurs constructed of timber piling filled with rock were destroyed. Failure was attributed to the inability to get enough penetration in the sand-bed channel with timber piles and the unstable wide channel in which the thalweg wanders unpredictably. Spurs (or other countermeasures) are not likely to be effective over the long term in such an unstable channel unless well-designed, well-built, and deployed over a substantial reach of stream.

Permeable Spurs

A wide variety of permeable spur designs were also shown to successfully control bank erosion by the case histories. Failures were experienced at a site which is highly unstable with rapid lateral migration, abundant debris, and extreme scour depths. Bank revetments of riprap and car bodies and debris deflectors at bridge piers, as well as bridges, have also failed at this site. At another site, steel H-pile spurs with wire mesh have partially failed on a degrading stream.

5.11.5 Retardance Structures. A retardance structure (retard) is a permeable or impermeable linear structure in a channel, parallel with and usually at the toe of the bank. The purposes of retardance structures are to reduce flow velocity, induce deposition, or to maintain an existing flow alignment. They may be constructed of earth, rock, timber pile, sheet pile, or steel pile, and steel jacks or tetrahedrons (see below) are also used.

Most retardance structures are permeable and most have good performance records. They have proved to be useful in the following situations: (1) for alignment problems very near a bridge or roadway embankment, particularly those involving rather sharp channel bends and direct impingement of flow against a bank (ten sites), and (2) for other bank erosion problems that occur very near a bridge, particularly on streams that have a wandering thalweg or very unstable banks (seven sites).

The case histories include a site where a rock retardance structure similar to a rock toe dike was successful in protecting a bank on a highly unstable channel where spurs had failed. There were, however, deficiencies in the design and construction of the spur installation. At another site, a rock retardance structure similar to a rock toe-dike has reversed bank erosion at a bend in a degrading stream. The U. S. Army Corps of Engineers reported that longitudinal rock toe dikes were the most effective bank stabilization measure studied for channels having very dynamic and/or actively degrading beds.

5.11.6 Dikes. Dikes are impermeable linear structures for the control or containment of overbank flow. Most are in floodplains, but they may be within channels, as in braided streams or on alluvial fans. Dikes at study sites were used to prevent floodwater from bypassing a bridge at four sites, or to confine channel width and maintain channel alignment at two sites. Performance of dikes at study sites was judged generally satisfactory.

5.11.7 Guide Banks (Spur Dikes). The major use of guide banks (or spur dikes) in the United States is to prevent erosion by eddy action at bridge abutments or piers where concentrated flood flow travelling along the upstream side of an approach embankment enters the main flow at the bridge. By establishing smooth parallel streamlines in the approaching flow, guide banks improve flow conditions in the bridge waterway. Scour, if it occurs, is near the upstream end of the dike away from the bridge. A guide bank differs from dikes described above in that a dike is intended to contain overbank flow while a guide bank only seeks to align overbank flow with flow through the bridge opening. An extension of the usual concept of the purpose for guide banks, but not in conflict with that concept, is the use of guide banks and highway fill to constrict braided channels to one channel. At three sites studied Brice et al. (1978a, b), guide banks only or guide banks plus revetment on the highway fill were used to constrict wide braided channels rather severely, and the installations have performed well.

5.11.8 Check Dams. A check dam is a low weir or dam across a channel for the control of water stage or velocity, or to stop degradation from progressing upstream. They may be constructed of concrete, rock, sheet pile, rock-and-wire mattress, gabions, or concrete-filled fabric mat. They are usually used to stop degradation in a channel. At one site, however, a check dam was apparently used to inhibit contraction scour in a bridge waterway. The problem with vertical scour was resolved, but lateral scour became a problem and riprap revetment on the streambanks failed (Brice et al., 1978a, b).

Scour downstream of check dams was found to be a problem at two sites, especially lateral erosion of the channel banks. Riprap placed on the streambanks at the scour holes also failed, at least in part because of the steep slopes on which the riprap was placed. At the time of the study, lateral erosion threatened damage to bridge abutments and highway fills. At another site, a check dam placed at the mouth of a tributary stream failed to stop degradation in the tributary and the delivery of damaging volumes of sediment to the main stream.

No structural failure of check dams was documented. Failures are known to have occurred, however, and the absence of documented failures should not be given undue weight. Failure can occur by bank erosion around the ends of the structure resulting in outflanking; by seepage or piping under or around the structure resulting in undermining and structural or functional failure; by overturning, especially after degradation of the channel downstream of the structure; by bending of sheet pile; by erosion and abrasion of wire fabric in gabions or rock-and-wire mattress; or by any number of structural causes for failure.

5.11.9 Jack or Tetrahedron Fields. Jacks and tetrahedrons function as flow control measures by reducing the water velocity along a bank, which in turn results in an accumulation of sediment and the establishment of vegetation. Steel jacks, or Kellner jacks which consist of six mutually perpendicular arms rigidly fixed at the midpoints and strung with wire are the most commonly used. Jacks are usually deployed in fields consisting of rows of jacks tied together with cables.

Four sites where steel jack fields were used are included in the case histories (Brice et al., 1978a, b). At two sites, the jack fields performed satisfactorily. Jacks were buried in the streambed and rendered ineffective at one site, and jacks were damaged by ice at one site, but apparently continued to perform satisfactorily. From Keeley's observations (1971) of the performance of jack fields used in Oklahoma and findings of the study of countermeasures by Brice et al. (1978a, b), the following conclusions were reached regarding performance:

1. The probability of satisfactory performance of jack fields is greatly enhanced if the stream transports small floating debris and sediment load in sufficient quantity to form accumulations during the first few years after construction.

2. Jack fields may serve to protect an existing bank line, or to alter the course of a stream if the stream course is realigned and the former channel backfilled before the jack field is installed.

3. On wide shallow channels, which are commonly braided, jack fields may serve to shift the bankline channelward if jacks of large dimensions are used.

Steel jetties have performed very well in New Mexico along the mainstem Rio Grande, which meets the requirements of high suspended sediment concentrations and significant debris loads (Lagasse, 1980). Attempts to use steel jetties in smaller arroyos in New Mexico have generally produced less than satisfactory results (Lagasse et al., 1982).

## 6.0 BIBLIOGRAPHY


Agricultural Research Service, 1964, "Summary of Reservoir Sediment Deposition Surveys Made in the United States Through 1960," Miscellaneous Publication 964.

Albuquerque Metropolitan Arroyo Flood Control Authority, 1983, "Design Guide for Riprap-Lined Flood Control Channels."

American Geological Institute, 1972, "Glossary of Geology," Washington D.C.

Anderson, C.E. 1994, "AHYMO Computer Program Users Manual" Version 194, Albuquerque Metropolitan Arroyo Flood Control Authority, New Mexico.

Anderson, C.E. 1992, "Prediction of Sediment Deposition in the La Cueva Tributary Arroyo Using HEC-6," Albuquerque Metropolitan Arroyo Flood Control Authority, New Mexico.

Anderson, G.K., A.S. Paintall, and J.T. Davenport, 1970, "Tentative Design Procedure for Riprap-Lined Channels," Highway Research Bord, NCHRP Report Number 108.

Arcement, G.K. and V.R. Schneider, 1984, "Guide for Selecting Manning's Roughness Coefficients for Natural Channels and Floodplains," USGS Water Supply Paper 2339.

Bachman, G.O. and H.H. Mehnert, 1978, "New K-Ar Dates and the Late Pliocene to Holocene Geomorphic History of the Central Rio Grande Region, New Mexico," Geological Society of America, Bulletin, v. 89, no. 2, pp. 283-292.

Bagnold, R.A., 1960, "Some Aspects of the Shape of River Meanders," USGS Professional Paper 282-E.

Bajorunas, L., Discussion of 1952, "River Channel Roughness," by H.A. Einstein and N.L. Barbarossa, Transactions, ASCE, v. 117, pp. 1140-1142.

Baker, V.R., 1977, "Stream Channel Response to Floods, with Examples from Central Texas," Geologist Society of America Bulletin, v. 86, pp. 1057-1071.

Begin, Z.B., 1981, "Stream Curvature and Bank Erosion: A Model Based on the Momentum Equation," Journal of Geology, v. 89.

Begin, Z.B., 1979, "Aspects of Degradation of Alluvial Stream in Response to Base-Level Lowering," Ph.D. Dissertation, Colorado State University, Fort Collins, Colorado.

Begin, Z.B. and S.A. Schumm, 1984, "Gradational Thresholds and Landform Singularity," Significance for Quaternary Studies, Quaternary Research, v. 21, pp. 267-274.

Begin, Z.B., D.F. Meyer, and S.A. Schumm, 1980, "Sediment Production of Alluvial Channels in Response to Baseload Lowering," Trans. Amer. Soc, Agric. Engr. no. 23.

Beverage, J.P. and J.K. Culbertson, 1964, "Hyperconcentrations of Suspended Sediment," Journal of Hydraulic Engineering, ASCE, v. 90, HY6, pp. 117-128.

Biedenharn, D.S., P.G. Combs, M.D. Harvey, C.D. Little, and C.C. Watson, 1991, "Systems Design Approach in Northern Mississippi," in Proc. 5th Federal Interagency Sedimentation Conference, Las Vegas, NV, Shou-Shan Fan and Yung-Huang Ko (eds.), pp. 3.8-3.15.

Blair, T.C., 1987, "Sedimentary Processes, Vertical Stratification Sequences and Geomorphology of the Roaring River Alluvial Fan, Rocky Mountain National Park, Colorado," Journal of Sedimentary Petrology, v. 57, no. 1, pp. 1-18.

Bohannan-Huston, Inc., 1991, "Draft, Ladera Dam #15 Hydrology and Sediment Issues," prepared for the Albuquerque Metropolitan Arroyo Flood Control District, New Mexico.

Bohannan-Huston, Inc., 1990, "Black Arroyo Sediment Issues," prepared for the Albuquerque Metropolitan Arroyo Flood Control District, New Mexico.

Bohannan-Huston, Inc., 1982, "Preliminary Flood Insurance Study, City of Albuquerque, Bernalillo County, New Mexico," prepared for the Federal Emergency Management Agency.

Bondurant, D.C., 1951, "Sedimentation Studies at Conchas Reservoir in New Mexico," Trans. ASCE, v. 116.

Bradford, J.M. and R.F. Piest, 1980, "Erosional Development of Valley-Bottom Gullies in the Upper Midwestern United States," in Thresholds in Geomorphology, D.R. Coats and J.D. Vitak (Eds.), pp. 75-101.

Bradley, J.N., 1978, "Hydraulics of Bridge Waterways," Hydraulic Design Series No. 1, U. S. Department of Transportation, Federal Highway Administration, Washington, D.C.

Brice, J.C., 1984, "Assessment of Channel Stability at Bridge Sites," Transportation Research Record, v. 2, no. 950. Available from the Transportation Research Board, 2101 Constitution Avenue, Washington, D.C. 20418.

Brice, J.C. and J.C. Blodgett, 1978a, "Countermeasures for Hydraulic Problems at Bridges, v. 1, Analysis and Assessment," FHWA/RD-78-162, Federal Highway Administration, Washington, DC. Available from the National Technical Information Service, 5285 Port Royal Road, Springfield, Virginia 22161. Available from the NTIS.

Brice, J.C. and J.C. Blodgett, 1978b, "Countermeasures for Hydraulic Problems at Bridges, v. 2., Case Histories for Sites 1-283," FHWA/RD-78-163, Federal Highway Administration, Washington, D.C. Available from the NTIS.

Brown, S.A., 1985a, "Streambank Stabilization Measures for Highway Engineers," FHWA/RD-84.100, Federal Highway Administration, McLean, Virginia.

Brown, S.A., 1985b, "Streambank Stabilization Measures for Highway Stream Crossings--Executive Summary," FHWA/RD-84/099, Federal Highway Administration, Washington, D.C. Available from the NTIS.

Brown, S.A., 1985c, "Design of Spur-Type Streambank Stabilization Structures, Final Report," FHWA/RD-84-101, Federal Highway Administration, Washington, D.C., available from the NTIS.

Brown, S.A. and E.S. Clyde, 1989, "Design of Riprap Revetment," Hydraulic Engineering Circular No. 11, FHWA-IP-89-016, prepared for the Federal Highway Administration, Washington, D.C.

Brown, S.A., R.S. McQuivey, and T.N. Keefer, 1980, "Stream Channel Degradation and Aggradation: Analysis of Impacts to Highway Crossings," FHWA/RD-80-159, Federal Highway Administration, Washington, D.C. Available from the NTIS.

Brownlie, W.R., 1983, "Flow Depth in Sand-Bed Channels," ASCE, Journal of Hydrologic Engineering, v. 109, no. HY7, pp. 959-990.

Brune, G.M., 1953, "Trap Efficiency of Reservoirs," Transactions of American Geophysical Union, v. 34, no. 3.

Bryan, K., 1938, "Geology and Ground-Water Conditions of the Rio Grande Depression in Colorado and New Mexico," U.S. Natural Resources Planning Board, Washington D.C., prepared for the The Rio Grande Joint Investigations in the Upper Rio Grande Basin, v. 1, pt. 2, pp. 196-225.

Bryan, K. and F.T. McCann, 1937, "The Ceja del Rio Puerco--A Border Feature of the Basin and Range Province in New Mexico, Part I, Stratigraphy and Structure," Journal of Geology, v. 45, pp. 801-828.

Bull, W.B., 1977, "The Alluvial-Fan Environment," Progress in Physical Geography, v. 1, p. 222.

Bull, W.B., 1964a, "Alluvial Fans and Near-Surface Subsidence in Western Fresno County, California," USGS Professional Paper 437-A, pp. A1-A71.

Bull, W.B., 1964b, "Geomorphology of Segmented Alluvial Fans in Western Fresno County, California," USGS Professional Paper 532-F, pp. 79-129.

Burkham, D.E. and D.R. Dawdy, 1976, "Resistance Equation for Alluvial Channel Flow," Journal of the Hydraulics Division, American Society of Civil Engineers, pp. 1479-1489.

Carey, W.C., 1969, "Formation of Floodplain Lands," ASCE Journal of Hydraulic Engineering, v. 95.

Chang, H.H., 1988, Fluvial Processes in River Engineering, San Diego State University, San Diego, California. A Wiley-Interscience Publication, John Wiley & Sons, New York.

Chein, N. and Z. Wan, 1965, "The Effect of Sediment Concentration Gradient on the Characteristics of Flow and Sediment Motion," Journal of Hydraulic Engineering, Beijing, China (in Chinese).

Chow, V.T., 1959, Open-Channel Hydraulics, McGraw-Hill, Civil Engineering Series.

Churchill, M.A., 1948, discussion of "Analysis and Use of Reservoir Sedimentation Data," by L.C. Gottschalk, Proceedings of Federal Inter-Agency Sedimentation Conference, Denver, Colorado, pp. 139-140.

City of Albuquerque, 1993, "Development Process Manual, Section 22.2, Hydrology," v. 2, Design Criteria, prepared by the D.P.M. Drainage Design Criteria Committee.

Colby, B.R., 1964, "Practical Computations of Bed-Material Discharge," Journal of the Hydraulics Division, ASCE, v. 90, no. HY2.

Cooke, R.U. and R.W. Reeves, 1976, "Arroyos and Environmental Change in the American Southwest," Oxford Res. Studies in Geog., Clarendon Press, Oxford, England.

Costa, J.E., 1988, Rheologic, Geomorphic and Sedimentologic Differentiation of Water Floods, Hyperconcentrated Flows and Debris Flows, Flood Geomorphology, John Wiley & Sons, Inc., New York.

Curtis, N.M., 1976, "Erosion and Sediment Yield in New Mexico," proceedings of the Third Federal Inter-Agency Sedimentation Conference, prepared by the Sedimentation Committee of the Water Resources Council, March 22-25.

Davidian, J. and D.I. Cahal, 1963, "Distribution of Shear Stresses in Rectangular Channels," USGS Professional Paper No. 475-C, Article 113.

Denny, C.S., 1965, "Alluvial Fans in the Death Valley Region, California and Nevada," USGS Professional Paper 466.

Doehring, D.O, 1970, "Discrimination of Pediments and Alluvial Fans from Topographic Maps," Geological Society of America Bulletin, v. 81, pp. 3109-3115.

Drury, G.H., 1964, "Principles of Underfit Streams," USGS Professional Paper 452-A, 67 pp.

Eckis, R., 1928, "Alluvial Fans of the Cucamonga District, Southern California," Journal of Geology, v. 36, p. 225-247.

Einstein, H.A., 1950, "The Bed-Load Function for Sediment Transportation in Open Channel Flows," Technical Bulletin No. 1026, USDA, Soil Conservation Service, Washington, D.C.

Einstein, H.A. and N. Chien, 1955, "Effects of Heavy Sediment Concentration near the Bed on Velocity and Sediment Distribution," University of California, Institute of Engineering Research and U.S. Army Corps of Engineers, Missouri River Division, MRD Series No. 8.

Elliott, J.G., 1979, "Evolution of Large Arroyos, the Rio Puerco of New Mexico" Unpubl. MS Thesis, Colorado State University, Fort Collins, Colorado, 106 p.

Fairbridge, R.W., Ed., 1968, The Encyclopedia of Geomorphology, Encyclopedia of Earth Science Series, v. III, Reinhold Book Corp., New York, New York.

Federal Emergency Management Agency, 1991, "Flood Insurance Study, Guidelines and Specifications for Study Contractors," FEMA 37.

Federal Highway Administration, 1992, "HYDRAIN Integrated Drainage Design Computer System: Version 4.0," Final Report No. FHWA-RD-92-061.

Federal Highway Administration, 1985, "Hydraulic Design of Highway Culverts," U.S. Department of Transportation, Hydraulic Design Series No. 5.

Federal Highway Administration, 1983, "Hydraulic Design of Energy Dissipators for Culverts and Channels," Hydraulic Engineering Circular No. 14.

Fischer, K.J. and M.D. Harvey, 1990, "Geomorphic and Stratigraphic Evidence for Sediment Transport Processes on a Valley Fan, Southern Utah," in Proc. Symposium on Hydrology and Hydraulics of Arid Lands, ASCE, San Diego, California, R.H. French (ed.), pp. 602-607.

Gellis, A., R. Hereford, S.A. Schumm, and B.R. Hayes, 1991, "Channel Evolution and Hydrologic Variations in the Colorado River Basin: Factors Influencing Sediment and Salt Loads," Journal of Hydrology, v. 124, pp. 317-344.

Gessler, J., 1970a, "Beginning and Ceasing of Sediment Motion," in River Mechanics, by Shen.

Gessler, J., 1970b, "Self-Stabilizing Tendencies of Alluvial Channels," Journal of the Waterways and Harbors Division, ASCE, v. 96, no. WW2, pp. 235-249.

Graf, W.L., 1979, "Mining and Channel Response," Annals of the Association of American Geographers, v. 69, no. 2, pp. 262-275.

Graf, W.H., 1984, Hydraulics of Sediment Transport, Water Resources Publications, Littleton, Colorado, U.S. Library of Congress Catalog Number 79-128788.

Harvey, M.D. and R.C. MacArthur, 1991, "Estimating Sediment Delivery and Yield on Alluvial Fans," in Proc. 15th Annual ASFPM Meeting, Denver, Colorado, June 14-17 pp. 238-242.

Harvey, M.D. and C.C. Watson, 1986, "Fluvial Processes and Morphological Thresholds in Stream Channel Restoration," Water Resources Bulletin, v. 22, no. 3.

Harvey, M.D., C.C. Watson, and S.A. Schumm, 1985, "Gully Erosion," prepared for the Bureau of Land Management.

Hawley, J.W. (ed.), 1978, "Guidebook to the Rio Grande Rift in New Mexico and Colorado," New Mexico Bureau of Mines and Mineral Resources, Circular 163, 2 maps, pp. 241.

Heggen, R.J., 1983, "Arroyo Engineering in an Urban Environment," Journal of Urban Planning and Development, ASCE, v. 109, no. 1, pp. 1-6.

Henderson, F.M., 1966, Open Channel Flow, The Macmillan Company.

Hickin, E.J., 1975, "The Development of Meanders in Natural River-Channels," American Journal of Science, v. 274.

Hooke, R.L., 1968, "Model Geology: Prototype and Laboratory Streams," Discussion: Geological Society of America Bulletin, v. 79, pp. 391-394.

Hooke, R.L., 1967, "Processes on Arid-Region Alluvial Fans," Journal of Geology, v. 75, pp. 438-460.

Ippen, A.T. and P.A. Drinker, 1962, "Boundary Shear Stresses in Curved Trapezoidal Channels," Journal of the Hydraulics Division, ASCE, v. 88, no. HY5.

Julien, P.Y. and Y. Lan, 1991, "Rheology of Hyperconcentrations," ASCE Journal of Hydraulic Engineering, v. 117, no. 3.

Karim, F. and J.F. Kennedy, 1983, "Missouri River Computer-Based Predictors for Sediment Discharges and Friction Factors of Alluvial Streams," IHR Report No. 242, Iowa Institute of Hydraulic Research, University of Iowa.

Kartha, V.C. and H.J. Leutheusser, 1970, "Distribution of Tractive Force in Open Channels," Journal of the Hydraulics Division, ASCE, v. 96, no. HY7.

Keefer, T.N., R.S. McQuivey, and D.B. Simons, 1980, "Interim Report - Stream Channel Degradation and Aggradation: Causes and Consequences to Highways," FHWA/RD-80/038, Federal Highway Administration, Washington, D.C. Available from the NTIS.

Keeley, J.W., 1971, "Bank Protection and River Control in Oklahoma," Federal Highway Administration, Washington, D.C.

Kellerhals, R. and D.I. Bray, 1971, "Sampling Procedures for Coarse Fluvial Sediments," Journal of the Hydraulics Division, ASCE, v. 97, no. HY8, pp. 1165-1179.

Kelley, V.C., 1977, "Geology of Albuquerque Basin, New Mexico," New Mexico Bureau of Mines and Mineral Resources, Mem. 33, p. 59.

Kelley, V.C., 1974, "Albuquerque: Its Mountains, Valleys, Water and Volcanoes, Scenic Trips to the Geologic Past, No. 9," New Mexico Bureau of Mines and Mineral Resources, p. 106.

Kennedy, J.F., 1963, "Mechanics of Dunes and Antidunes in Erodible-Bed Channels," Journal of Fluid Mechanics, v. 16, pt. 4, pp. 521-544.

Knox, J.C., 1972, "Valley Alluviation in Southwestern Wisconsin," Annals of the Association of American Geographers, v. 62, no. 3, pp. 401-410.

Kochel, R.C. and R.A. Johnson, 1984, "Geomorphology and Sedimentology of Humid-Temperate Alluvial Fans, Central Virginia," in Sedimentology of Gravel and Conglomerates, E.H. Koster and R.J. Steel (eds.), Canadian Society of Petroleum Geologists Memoir 10, pp. 109-122.

Lagasse, P.F., 1980, "An Assessment of the Response of the Rio Grande to Dam Construction," Technical Report for the U.S. Army Engineer District, Corps of Engineers, Albuquerque, New Mexico.

Lagasse, P.F., J.D. Schall, and K.G. Eggert, 1982, "Erosion Study at Chaco Culture National Historic Park, New Mexico," Simons, Li & Associates, Inc. for the USDI National Park Service, Southwest Region, Santa Fe, New Mexico.

Lagasse, P.F., J.D. Schall, and M.R. Peterson, 1985, "Erosion Risk Analysis for a Southwestern Arroyo," ASCE, Journal of Urban Planning and Development, v. 111, no. 1, pp. 10-44.

Lagasse, P.F., J.D. Schall, F. Johnson, E.V. Richardson, J.R. Richardson, and F. Chang, 1991, "Stream Stability at Highway Structures," Hydraulic Engineering Circular No. 20, U.S. Department of Transportation, FHWA, Turner Fairbanks Highway Research Center, McLean, Virginia.

Lambert, P.W., 1968, "Quaternary Stratigraphy of the Albuquerque Area, New Mexico," Ph.D. Dissertation, University of New Mexico.

Lane, E.W., 1974, "Notes on Limits of Sediment Concentration," J. Sedimentary Petrology, v. 10, no. 2, pp. 95-96.

Lane, E.W., 1955, "The Importance of Fluvial Morphology in Hydraulic Engineering," Proceedings of the American Society of Civil Engineers, 8 (745).

Langbein, W.B. and L.B. Leopold, 1966, "River Meanders - Theory of Minimum Variance," USGS Professional Paper 422-H.

Lara, J.M., 1962, "Revision of the Procedure to Compute Sediment Distribution in Large Reservoirs," Bureau of Reclamation, Denver, Colorado.

Laursen, E.M., 1960, "Scour at Bridge Crossings," Journal of the Hydraulics Division, ASCE, v. 92, HY3.

Lavelle, J.W. and W.C. Thacker, 1978, "Effects of Hindered Settling on Sediment Concentration Profiles," Journal of Hydraulic Research, 16(4).

Lecce, S.A., 1990, "The Alluvial Fan Problem," in Alluvial Fans: A Field Approach, A.H. Rachocki and M. Church (eds.), John Wiley & Sons, New York, New York, pp. 3-24.

Leopold, L.B. and J.P. Miller, 1956, "Ephemeral Streams - Hydraulic Factors and Their Relation to the Drainage Net," Physiographic and Hydraulic Studies of Rivers, USGS Professional Paper 282-A.

Leopold, L.B. and M.G. Wolman, 1960, "River Meanders," Geologic Society of America Bulletin, v. 32, p. 769-794.

Leopold, L.B., W.W. Emmett, and R.M. Myrick, 1966, "Channel and Hillslope Processes in a Semiarid Area, New Mexico," USGS Professional Paper 352-G, Washington, D.C.

Leopold, L.B., M.G. Wolman, and J.P. Miller, 1964, "Fluvial Processes in Geomorphology," Freeman Co., San Francisco, California.

Li, R.M. and H.W. Shen, 1975, "Solid Particle Settlement in Open-Channel Flow," ASCE, Journal of Hydraulic Engineering, v. 101, no. HY7, pp. 917-931.

Limerinos, J.T., 1970, "Determination of the Manning Coefficient From Measured Bed Roughness in Natural Channels," USGS Water Supply Paper 1898-B.

Little, W.D., C.R. Thorne, and J.B. Murphey, 1982, "Mass Bank Failure Analysis of Selected Yazoo Basin Streams," Trans. of the ASAE, v. 25, no. 5, pp. 1321-1328.

Lohnes, R. and R.L. Handy, 1968, "Slope Angles in Friable Loess," Journal of Geology 76, pp. 247-258.

Love, D.W., 1979, "Quaternary Fluvial Geomorphic Adjustments in Chaco Canyon, New Mexico," in Adjustment of the Fluvial System, D.D. Rhodes and G.P. Williams (eds.), Kendall-Hunt, Dubuque, Iowa, pp. 277-280.

Lustig, L.K., 1965, "Clastic Sedimentation in Deep Springs Valley, California," USGS Professional Paper 352 F, pp. 131-192.

Maude, A.D. and R.L. Whitmore, 1958, "A Generalized Theory of Sedimentation," British Journal of Applied, Physics, Bristol, England, v. 9.

Metcalf & Eddy, Inc., 1979, Wastewater Engineering Treatment, Disposal, Reuse, McGraw-Hill, Inc.

Meyer-Peter, E. and R. Muller, 1948, "Formulas for Bed-Load Transport," Proceedings, Third Meeting of International Association, Hydraulic Research, Stockholm, pp. 39-64.

Molinas, A., 1993, User's Manual for BRI-STARS (BRIdge Stream Tube Model for Alluvial River Simulation), National Cooperative Highway Research Program, Project No. HR15-11.

Nanson G.C. and E.J. Hickin, 1983, "Channel Migration and Incision on the Beatton River," ASCE Journal of Hydraulic Engineering, v. 109.

Nordin, C.F., 1963, "A Preliminary Study of Sediment Transport Parameters, Rio Puerco Near Bernardo, New Mexico," USGS Professional Paper 462-C.

Norman, V.W., 1968, "Trends of Suspended Sediments in the Upper Rio Grande Basin in New Mexico."

O'Brien, J.S., 1986, "Physical Processes, Rheology and Modeling of Mud Flows," Ph.D. Dissertation, Colorado State University, Fort Collins, Colorado.

O'Brien, J.S. and P.Y. Julien, 1989, "Laboratory Analysis of Mudflow Properties," ASCE Journal of Hydraulic Engineering, v. 114, no. 8.

Odgaard, A.J., 1987, "Streambank Erosion along Two Rivers in Iowa," Water Resources Research, v. 23, n. 7.

Olsen, O.J. and Q.L. Florey, 1952, "Sedimentation Studies in Open Channels - Boundary Shear and Velocity Distribution by Membrane Analogy, Analytical and Finite Difference Methods," Laboratory Report No. SP34, U.S. Bureau of Reclamation.

Ordonez-C., N.A., 1970, "The Absolute Concentration Distribution of Suspended Sediment in Turbulent Streams," Ph.D. Dissertation, M.I.T., R.M. Parsons Lab. for Water Resources and Hydrodynamics.

Osman, A.M. and C.R. Thorne, 1988, "Riverbank Stability Analysis I: Theory," Journal of Hydraulic Engineering, ASCE, HY2, v. 114, pp. 134-150.

Pacific Southwest Interagency Committee (PSIAC), 1968, "Factors Affecting Sediment Yield in the Pacific Southwest Areas," Water Management Subcommittee Sediment Task Force.

Page, K. and G.C. Nanson, 1982, "Concave Bank Benches and Associated Floodplain Formation," Earth Surface Processes and Landforms, v. 7.

Patton, P.C. and S.A. Schumm, 1975, "Gully Erosion, Northern Colorado," A Threshold Phenomenon: Geology, v. 3, pp. 88-90.

Pemberton, E.L. and J.M. Lara, 1984, "Computing Degradation and Local Scour," Technical Guidelines for Bureau of Reclamation, Engineering Research Center, Denver, Colorado.

Pickup, G., 1977, "Simulation Modeling of River Channel Erosion," in River Channel Changes, K.G. Gregory (Ed.), Wiley and Sous, 47-60.

Ponce, V.M., 1978, "Generalized Stability Analysis of Channel Banks," Journal of the Irrigation and Drainage Division, ASCE, v. 104, no. 1R4, pp. 343-350.

Portland Cement Association, 1984a, "Soil-Cement for Facing Slopes and Lining Channels, Reservoirs, and Lagoons," PCA Publication IS126.05W, Skokie, Illinois.

Portland Cement Association, 1984b, "Soil-Cement Slope Protection for Embankments: Planning and Design," PCA Publication IS173.02W, Skokie, Illinois.

Rajaratnam, N. and D. Muralidhar, 1969, "Boundary Shear Stress Distribution in Rectangular Open Channels," LaHouille Blanche, v. 24, no. 6.

Reading, H.G., 1978, Sedimentary Environments and Facies, Elsevier-North-Holland, New York, New York.

Renard, K.G., 1980, "Estimating Erosion and Sediment Yield from Rangelands," Proceedings of ASCE Symposium on Watershed Management, pp. 164-175.

Replogle, J.A. and V.T. Chow, 1966, "Tractive Force Distribution in Open Channels," Journal of the Hydraulics Division, ASCE, v. 92, no. HY2.

Resource Consultants, Inc., 1989, "Unser Bridge/Calabacillas Arroyo Detention Basin," prepared for Albuquerque Metropolitan Arroyo Flood Control Authority, New Mexico.

Resource Consultants & Engineers, Inc., 1994, "Prudent Line Analysis, La Cueva Arroyo Tributary between Tennyson Street and Modesto Avenue," prepared for Albuquerque Metropolitan Arroyo Flood Control Authority, New Mexico.

Resource Consultants & Engineers, Inc., 1993, "Geomorphic and Sediment Yield Analysis for Albuquerque Arroyos," prepared for U.S. Army Engineer Waterways Experiment Station, Reston, Virginia.

Richardson, E.V. and D.B. Simons, 1984, "Use of Spurs and Guidebanks for Highway Crossings," Transportation Research Board, v. 950, no. 2, Washington, D.C., pp. 184-193.

Richardson, E.V., L.J. Harrison, and S.R. Davis, 1991, "Evaluating Scour at Bridges," Hydraulic Engineering Circular No. 18, U.S. Department of Transportation, FHWA, Turner Fairbanks Highway Research Center, McLean, Virginia.

Richardson, E.V., D.B. Simons, and P.Y. Julien, 1990, "Highways in the River Environment," prepared for the Federal Highway Administration, Washington, D.C. by the Department of Civil Engineering, Colorado State University, Fort Collins, Colorado.

Richardson, J.F. and W.N., Zaki, 1954, "Sedimentation and Fluidization, Part I," Transactions, Institute of Chemical Engineers, 32, p. 35-53.

Riecker, R.E. (ed.), 1979, "Rio Grande Rift: Tectonics and Magnetism," Journal of the American Geophysical Union, p. 438.

Rouse, H., 1937, "Modern Conceptions of the Mechanics of Fluid Turbulence," Transactions of the American Society of Civil Engineers, v. 102.

Schall, J.D., 1979, "Spatial and Temporal Distribution of Boundary Shear Stress in Open Channel Flows," Master Thesis, Colorado State University, Fort Collins, Colorado.

Schumm, S.A., 1977, The Fluvial System, A Wiley-Interscience Publication, John Wiley & Sons, New York.

Schumm, S.A., 1973, "Geomorphic Thresholds and Complex Response of Drainage Systems," in Fluvial Geomorphology, SUNY, Binghampton Pub. in Geomorphology, pp. 299-310.

Schumm, S.A. and A. Gellis, 1989, "Sediment Yield Variations as a Function of Incised Channel Evolution," in Taming the Yellow River: Silt and Floods, L.M. Brush et al. (eds.), Kluwer Academic Publishers, pp. 99-109.

Schumm, S.A. and R.F. Hadley, 1957, "Arroyos and the Semiarid Cycle of Erosion," American Journal of Science, v. 255, pp. 161-174.

Schumm, S.A. and R.S. Parker, 1973, "Implications of Complex Response of Drainage Systems for Quaternary Alluvial Stratigraphy," Nat. Phys. Sci., v. 243, pp. 99-100.

Schumm, S.A., M.D. Harvey, and C.C. Watson, 1984, "Incised Channels: Morphology, Dynamics and Control," Water Resources Publications, Littleton, Colorado.

Schumm, S.A., M.D. Harvey, and C.C. Watson, 1981, "Yazoo Basin Geomorphology," prepared for the Soil Conservation Service, USDA Report, Project SCS-23-MS-80.

Schumm, S.A., M.P. Mosley, and W.E. Weaver, 1987, Experimental Fluvial Geomorphology, Wiley Interscience, New York, New York.

Shearman, J.D., 1990, "User's Manual for WSPRO - A Computer Model for Water Surface Profile Computations," U.S. Department of Transportation, Federal Highway Administration, Publication No. FHWA-IP-89-027, Hydraulic Computer Program HY-7.

Shearman, J.O., 1989, "Design of Riprap Revetment," Hydraulic Engineering Circular No. 11, Federal Highway Administration, McLean, Virginia.

Shen, H.W., S.A. Schumm, J.D. Nelson, D.O. Doehring, and M.M. Skinner, 1981, "Methods for Assessment of Stream-Related Hazards to Highways and Bridges," FHWA/RD-80/160, Federal Highway Administration, Washington, D.C. Available from the NTIS.

Shown, L., 1970, "Evaluation of a Method for Estimating Sediment Yield," USGS Professional Paper 700-B, pp. 245-249.

Simon, A., W.J. Wolfe, and A. Molinas, 1991, "Mass-Wasting Algorithms in an Alluvial Channel Model," in Proc. 5th Federal Interagency Sedimentation Conference, Las Vegas, Nevada, pp. 8.22-8.29.

Simons, D.B. and E.V. Richardson, 1966, "Resistance to Flow in Alluvial Channels," USGS Professional Paper 422-J.

Simons, D.B. and F. Senturk, 1976, Sediment Transport Technology, Water Resources Publication, Fort Collins, Colorado.

Simons, Li & Associates, Inc. 1985, "Design Manual for Engineering Analysis of Fluvial Systems," prepared for the Arizona Department of Water Resources.

Simons, Li & Associates, Inc., 1983, "Erosion Study to Determine Boundaries for Adjacent Development - Calabacillas Arroyo, Bernalillo County, New Mexico," prepared for the Albuquerque Metropolitan Arroyo and Flood Control Authority, Albuquerque, New Mexico.

Simons, Li & Associates, Inc., 1982a, "Engineering Analysis of Fluvial Systems," Fort Collins, Colorado. Available from BookCrafters, Inc., Chelsea, Michigan.

Simons, Li & Associates, Inc., 1982b, "Erosion Study of Chaco Culture National Historical Park," prepared for the USDI, National Park Service, Southwest Region, Santa Fe, New Mexico.

Taylor, R.H., Jr. and N.H. Brooks, 1962, "Resistance to Flow in Alluvial Channels," discussion by D.B. Simons and E.V. Richardson, Transactions, ASCE, v. 127, pt. I, pp. 982-992.

Thorne, C.R., 1982, "Processes and Mechanisms of River Bank Erosion," in Proc. of the International Workshop on Engineering Problems in the Management of Gravel-Bed Rivers, R.D. Hey, J.C. Bathurst and C.R. Thorne (eds.), Greynog, Wales, June 23-28, 1980, John Wiley & Sons, London, United Kingdom.

Thorne, C.R., 1981, "Field Measurements of Rate of Bank Erosion and Bank Material Strength, Erosion and Sediment Transport Measurement," Proc., Florence Symp., International Association for Hydraulic Science Pub. no. 133, Florence, Italy.

Thornes, J.B., 1976, "Semi-Arid Erosional Systems," London School of Economics, Geographical Paper no. 7.

Trieste, D.J., 1992, "Evaluation of Supercritical/Subcritical Flows in High-Gradient Channel," Journal of Hydraulic Engineering, ASCE, v. 118, no. 8, pp. 1107-1118.

U.S. Army Corps of Engineers, 1991, "HEC-6, Scour and Deposition in Rivers and Reservoirs, Users Manual," Hydrologic Engineering Center, Water Resources Support Center, Davis, California.

U.S. Army Corps of Engineers (Headquarters), 1991, "Hydraulic Design of Flood Control Channels," Engineer Manual 1110-2-1601, July.

U.S. Army Corps of Engineers, 1982, "HEC-2, Water Surface Profiles, Users Manual," Hydrologic Engineering Center, Water Resources Support Center, Davis, California.

U.S. Army Corps of Engineers, 1981, "The Streambank Erosion Control Evaluation and Demonstration Act of 1974," Final Report to Congress, Executive Summary and Conclusions.

U.S. Army Corps of Engineers, 1970a, "Hydraulic Design of Flood Control Channels," EM 1110-2-1601.

U.S. Army Corps of Engineers, 1970b, "Laboratory Soil Testing," EM 1110-2-1906.

U.S. Bureau of Reclamation, 1984, "Computing Degradation and Local Scour," Technical Guideline for Bureau of Reclamation, prepared by E.L. Pemberton and J.M. Lara.

U.S. Bureau of Reclamation, Department of the Interior, 1977, "Design of Small Dams," a Water Resources Technical Publication, U.S. Government Printing Office, Washington, D.C.

U.S. Bureau of Reclamation, 1960, "Investigation of Meyer-Peter, Muller Bed Load Formulas," Department of the Interior, Sedimentation Section, Hydrology Branch, Denver, Colorado.

U.S. Geological Survey, 1989, "Summary and Use of Selected Fluvial Sediment-Discharge Formulas," Water Resources Investigations Report 89-4026 by H. H. Stevens and C.T. Yang.

U.S. Geological Survey, 1982, "Characteristics of Suspended Sediment in the San Juan River near Bluff," Utah, Water Resources Investigations 82-4104, Salt Lake City, Utah.

U.S. Geological Survey, 1952, "Sedimentation Rates in Small Reservoirs in the Little Colorado Basin," Water Supply Paper 1110-D by C.F. Humes, D.M. Van Sickle and H.V. Peterson.

U.S. Soil Conservation Service, 1992, "Physical and Chemical Properties of the Soils, Bernalillo County and Parts of Sandoval and Valencia Counties, New Mexico," unpublished table.

U.S. Soil Conservation Service, 1978, "Predictions of Rainfall Erosion Losses," Agriculture Handbook Number 537.

U.S. Soil Conservation Service, 1977, "Soil Survey for Bernallilo and Parts of Sandoval and Valencia Counties, New Mexico."

U.S. Soil Conservation Service, 1936, "Silting of Reservoirs," Technical Bulletin No. 524.

U.S. Water Resources Council, 1979, "A Unified National Program for Flood Plain Management," U.S. Government Printing Office, Washington, D.C.

Vanoni, V.A., 1977, "Sedimentation Engineering, ASCE Manuals and Reports on Engineering Practice - No. 54," prepared by the ASCE Task Committee for the Preparation of the Manual on Sedimentation of the Sedimentation Committee of the Hydraulics Division.

van Rijn, L.C., 1984, "Sediment Transport: Suspended Load Transport," Journal of Hydraulic Engineering, ASCE, v. 110, no. HY11.

Watson, C.C., M.D. Harvey, and J.S. Garbrecht, 1986, "Geomorphic-Hydraulic Simulation of Channel Evolution," Proceedings of 4th Federal Inter-Agency Sedimentation Conference, v. II, pp. 5.21-5.30

Watson, C.C., M.D. Harvey, D.S. Biedenharn, and P.G. Combs, 1988a, "Geotechnical and Hydraulic Stability Numbers for Channel Rehabilitation: Part I, The Approach," ASCE, Hydraulic Division, National Conf. Proc., S.R. Abt and J. Gessler (eds.), pp. 120-125.

Watson, C.C., M.D. Harvey, D.S. Biedenharn, and P.G. Combs, 1988b, "Geotechnical and Hydraulic Stability Numbers for Channel Rehabilitation: Part II, Application," ASCE, Hydraulic Division, National Conf. Proc., S.R. Abt and J. Gessler (eds.), pp. 126-131.

Williams, J.R. and H.D. Berndt, 1972, "Sediment Yields Computed with Universal Equation," Journal of Hydraulics, ASCE, v. 102 no. HY9, pp. 1241-1253.

Wilson, K.V., 1973, "Changes in Flood-Flow Characteristics of a Rectified Channel Caused by Vegetation, Jackson, Mississippi," Journal of Research of the USGS, v. 1, pp. 621-625.

Wischmeier, W.H. and D.D. Smith, 1978, "Predicting Rainfall Erosion Losses," Agricultural Handbook 537, Science and Education Administration, USDA.

Wischmeier, W.H. and D.D. Smith, 1965, "Predicting Rainfall-Erosion Losses for Cropland East of the Rocky Mountains," Agricultural Handbook no. 282, ARS, USDA, Washington D.C.

Wolman, M.G., 1954, "A Method of Sampling Coarse River-Bed Material," American Geophysical Union Transactions, v. 35, no. 6, pp. 951-956.

Wolman, M.G. and J.P. Miller, 1960, "Magnitude and Frequency of Forces in Geomorphic Processes," Journal of Geology, v. 68, pp. 54-75.

Woo, H.S., 1985, "Sediment Transport in Hyperconcentrated Flows," Ph.D. Dissertation, Colorado State University, Fort Collins, Colorado.

Woo, H.S., P.Y. Julien, and E.V. Richardson, 1988, "Suspension of Large Concentrations of Sands," Journal of the Hydraulics Division, ASCE, v. 114, no. HY8.

Wright, C.D., 1977, "Sediment Transport and Deposition in River Mouths," GSA Bulletin no. 88, pp. 857-868.

Yang, C.T., 1972, "Unit Stream Power and Sediment Transport," ASCE, Journal of Hydraulic Engineering, v. 98, no. HY10, pp. 1805-1826.

Zeller, M.E. and W.T. Fullerton, 1983, "A Theoretically Derived Sediment Transport Equation for Sand-Bed Channels in Arid Regions," Proceedings of the D.B. Simons Symposium on Erosion and Sedimentation, R.M. Li and P.F. Lagasse, eds.

# APPENDIX A

## Pacific Southwest Inter-Agency Committee (PSIAC) Method for Predicting Watershed Soil Loss

# APPENDIX A

PACIFIC SOUTHWEST INTER-AGENCY COMMITTEE (PSIAC)
METHOD FOR PREDICTING WATERSHED SOIL LOSS

Note: The information presented in APPENDIX A is from the following source: "Pacific Southwest Inter-Agency Committee, Report of the Water Management Subcommittee on Factors Affecting Sediment Yield in the Pacific Southwest Area and Selection and Evaluation of Measures for Reduction of Erosion and Sediment Yield," October, 1968.

## Introduction

The material that follows is suggested for use in the evaluation of sediment yield in the Pacific Southwest. It is intended as an aid to the estimation of sediment yield for the variety of conditions encountered in this area.

The classifications and companion guide material are intended for broad planning purposes only, rather than for specific projects where more intensive investigations of sediment yield would be required. For these purposes it is recommended that map delineations be for areas no smaller than 10 square miles.

It is suggested that actual measurements of sediment yield be used to the fullest extent possible. This descriptive material and the related numerical evaluation system would best serve its purpose as a means of delineating boundaries between sediment yield areas and in extrapolation of existing data to areas where none is available.

This may involve a plotting of known sediment yield data on work maps. Prepared materials such as geologic and soil maps, topographic, climatic, vegetative type and other references would be used as aids in delineation of boundaries separating yield classifications. A study of the general relationships between known sediment yield rates and the watershed conditions that produce them would be of substantial benefit in projecting data to areas without information.

## Sediment Yield Classification

It is recommended that sediment yields in the Pacific Southwest area be divided into five classes of average annual yield in acre-feet per square mile. These are as follows:

| | | | |
|---|---|---|---|
| Classification | 1 | > 3.0 | acre-feet/square mile |
| | 2 | 1.0 - 3.0 | " " |
| | 3 | 0.5 - 1.0 | " " |
| | 4 | 0.2 - 0.5 | " " |
| | 5 | < 0.2 | " " |

Nine factors are recommended for consideration in determining the sediment yield classification. These are geology, soils, climate, runoff, topography, ground cover, land use, upland erosion, and channel erosion and sediment transport.

Characteristics of each of the nine factors which give that factor high, moderate, or low sediment yield level are shown on Table A-1. The sediment yield characteristic of each factor is assigned a numerical value representing its relative significance in the yield rating. The yield rating is the sum of values for the appropriate characteristics for each of the nine factors. Conversion to yield classes should be as follows:

| Rating | Class |
|---|---|
| > 100 | 1 |
| 75 - 100 | 2 |
| 50 - 75 | 3 |
| 25 - 50 | 4 |
| 0 - 25 | 5 |

Guidelines which accompany the table are an integral part of the procedure. They describe the characteristics of factors which influence sediment yield and these are summarized in the space provided on the table.

The factors are generally described, for purposes of avoiding complexity, as independently influencing the amount of sediment yield. The variable impact of any one factor is the result of influence by the others. To account for this variable influence in any one area would require much more intensive investigational procedures than are available for broad planning purposes.

To briefly indicate the interdependence of the factors discussed separately, ground cover is used as an example. If there is no vegetation, litter or rock fragments protecting the surface, the rock, soil, and topography express their uniqueness on erosion and sediment yield. If the surface is very well protected by cover, the characteristics of the other factors are obscured by this circumstance. In similar vein, an arid region has a high potential for erosion and sediment yield because of little or no ground cover, sensitive soils and rugged topography. Given very low intensity rainfall and rare intervals of runoff, the sediment yield could be quite low.

Each of the 9 factors shown on Table A-1 are paired influences with the exception of topography. That is, geology and soils are directly related as are climate and runoff, ground cover and land use, and upland and channel erosion. Ground cover and land use have a negative influence under average or better conditions. Their impact on sediment yield is therefore indicated as a negative influence when affording better protection than this average.

It is recommended that the observer follow a feedback process whereby he checks the sum of the values on the table from A through G with the sum of H and I. In most instances high values in the former should correspond to high values in the latter. If they do not, either special erosion conditions exist or the A through G factors should be re-evaluated.

Although only the high, moderate and low sediment yield levels are shown on the attached table, interpolation between these levels may be made.

Surface Geology

Over much of the southwest area, the effect of surface geology on erosion is readily apparent. The weaker and softer rocks are more easily eroded and generally yield more sediment than do the harder more resistant types. Sandstones and similar coarse-textured rocks that disintegrate to form permeable soils erode less than shales and related mudstones and siltstones under the same conditions of precipitation. On the other hand, because of the absence of cementing agents in some soils derived from sandstone, large storms may produce some of the highest sediment yields known.

The widely distributed marine shales, such as the Mancos and shale members of the Moenkopi Formation, constitute a group of highly erodible formations. The very large areal extent of the shales and their outwash deposits

gives them a rank of special importance in relation to erosion. Few of the shale areas are free from erosion. Occasionally, because of slope or cover conditions, metamorphic rocks and highly fractured and deeply weathered granites and granodiorites produce high sediment yield. Limestone and volcanic outcrop areas are among the most stable found within the western lands. The principal reason for this appears to be the excellent infiltration characteristics, which allow most precipitation to percolate into the underlying rocks.

In some areas, all geologic formations are covered with alluvial or colluvial material which may have no relation to the underlying geology. In such areas the geologic factor would have no influence and should be assigned a value of 0 in the rating.

Soils

Soil formation in the Pacific Southwest generally has not had climatic conditions conducive to rapid development. Therefore, the soils are in an immature stage of development and consist essentially of physically weathered rock materials. The presence of sodium carbonate (black alkali) in a soil tends to cause the soil particles to disperse and renders such a soil susceptible to erosion.

There are essentially three inorganic properties--sand, silt, and clay--which may in any combination give soil its physical characteristics. Organic substances plus clay provide the binding material which tends to hold the soil separates together and form aggregates. Aggregate formation and stability of these aggregates are the resistant properties of soil against erosion. Unstable aggregates or single grain soil materials can be very erodible.

Climate and living organisms acting on parent material, as conditioned by relief or topography over a period of time, are the essential factors for soil development. Any one of these factors may overshadow or depress another in a given area and cause a difference in soil formation. For instance, climate determines what type of vegetation and animal population will be present in an area, and this will have a definite influence or determine the type of soil that evolves. As an example, soils developing under a forest canopy are much different from soils developing in a grassland community.

The raw, shaley type areas (marine shales) of the Pacific Southwest have very little, if any, solid development. Colluvial-alluvial fan type areas are

usually present at the lower extremities of the steeper sloping shale areas. Infiltration and percolation are usually minimal on these areas due to the fine textured nature of the soil material. This material is easily dispersed and probably has a high shrink-swell capacity. Vegetation is generally sparse, and consists of a salt desert shrub type.

There are areas that contain soils with definite profile development, and also, stony soils that contain few fines, which constitutes an improved physical condition for infiltration and plant growth over the fine textured shaley areas. These areas usually occur at higher and more moist elevations where bare, hard crystalline rocks provide the soil parent material. Vegetation and other ground cover, under these circumstances, provide adequate protection against the erosive forces and thus low sediment yield results.

In arid and semi-arid areas, an accumulation of rock fragments (desert pavement) or calcareous material (caliche) is not uncommon. These layers can offer substantial resistance to erosion processes.

The two extreme conditions of sediment yield areas have been described. Intermediate situations would contain some features of the two extremes. One such situation might be an area of predominately good soil development that contains small areas of badlands. This combination would possibly result in an intermediate classification.

Climate and Runoff

Climatic factors are paramount in soil and vegetal development and determine the quantity and discharge rate of runoff. The same factors constitute the forces that cause erosion and the resultant sediment yield. Likewise, temperature, precipitation, and particularly the distribution of precipitation during the growing season, affect the quantity and quality of the ground cover as well as soil development. The quantity and intensity of precipitation determine the amount and discharge rates of runoff and resultant detachment of soil and the transport media for sediment yield. The intensity of prevailing and seasonal winds affects precipitation pattern, snow accumulation and evaporation rate.

Snow appears to have a minor effect on upland slope erosion since raindrop impact is absent and runoff associated with snow melt is generally in resistant mountain systems.

Frontal storms in which periods of moderate to high intensity precipitation occur can produce the highest sediment yields within the Southwest. In humid and subhumid areas the impact of frontal storms on sediment may be greatest on upland slopes and unstable geologic areas where slides and other downhill soil movement can readily occur.

Convective thunderstorm activity in the Southwest has its greatest influence on eroison (sic) and sedimentation in Arizona and New Mexico and portions of the adjoining states. High rainfall intensities on low density cover or easily dispersed soils produces high sediment yields. The average annual sediment yield is usually kept within moderate bounds by infrequent occurrence of thunderstorms in any one locality.

High runoff of rare frequency may cause an impact on average annual sediment yield for a long period of time in a watershed that is sensitive to erosion, or it may have little effect in an insensitive watershed. For example, sediment that has been collecting in the bottom of a canyon and on side slopes for many years of low and moderate flows may be swept out during the rare event, creating a large change in the indicated sediment yield rate for the period of record.

In some areas the action of freezing and thawing becomes important in the erosion process. Impermeable ice usually forms in areas of fine textured soils where a supply of moisture is available before the advent of cold weather. Under these conditions the ice often persists throughout the winter and is still present when the spring thaw occurs. In some instances water tends to run over the surface of the ice and not detach soil particles, but it is possible for the ice in a surface layer to thaw during a warm period and create a very erodible situation. Spring rains with ice at shallow depth may wash away the loose material on the surface.

In some areas of the Pacific Southwest, particularly those underlain by marine shale, freezing and thawing alters the texture of soil near the surface, and thus changes the infiltration characteristics. These areas generally do not receive enough snow or have cold enough temperatures to build a snow pack for spring melt. Later in the year soil in a loosened condition is able to absorb a large part of the early rainfall. As rains occur during the summer, the soil becomes compacted on the surface, thus allowing more water to run off and affording a greater chance for erosion.

Topography

Watershed slopes, relief, floodplain development, drainage patterns, orientation and size are basic items to consider in connection with topography. However, their influence is closely associated with geology, soils, and cover.

Generally, steep slopes result in rapid runoff. The rimrock and badlands, common in portions of the Pacific Southwest, consist of steep slopes of soft shales usually maintained by the presence of overlying cap rock. As the soft material is eroded, the cap rock is undercut and falls, exposing more soft shales to be carried away in a continuing process. However, high sediment yields from these areas are often modified by the temporary deposition of sediment on the intermediate floodplains.

The high mountain ranges, although having steep slopes, produce varying quantities of sediment depending upon the type of parent materials, soil development, and cover which directly affect the erosion processes.

Southerly exposed slopes generally erode more rapidly than do the northerly exposed slopes due to greater fluctuation of air and soil temperatures, more frequent freezing and thawing cycles, and usually less ground cover.

The size of the watershed may or may not materially affect the sediment yield per unit area. Generally, the sediment yield is inversely related to the watershed size because the larger areas usually have less overall slope, smaller proportions of upland sediment sources, and more opportunity for the deposition of upstream derived sediments on floodplains and fans. In addition, large watersheds are less affected by small convective type storms. However, under other conditions, the sediment yield may not decrease as the watershed size increases. There is little change in mountainous areas of relatively uniform terrain. There may be an increase of sediment yield as the watershed size increases if downstream watersheds or channels are more susceptible to erosion than upstream areas.

Ground Cover

Ground cover is described as anything on or above the surface of the ground which alters the effect of precipitation on the soil surface and profile. Included in this factor are vegetation, litter, and rock fragments. A

good ground cover dissipates the energy of rainfall before it strikes the soil surface, delivers water to the soil at a relatively uniform rate, impedes the flow of water, and promotes infiltration by the action of roots within the soil. Conversely, the absence of ground cover, whether through natural growth habits or the effect of overgrazing or fire, leave the land surface open to the worst effects of storms.

In certain areas, small rocks or rock fragments may be so numerous on the surface of the ground that they afford excellent protection for any underlying fine material. These rocks absorb the energy of falling rain and are resistant enough to prevent cutting by flowing water.

The Pacific Southwest is made up of land with all classes of ground cover. The high mountain areas generally have the most vegetation, while many areas in the desert regions have practically none. The abundance of vegetation is related in a large degree to precipitation. If vegetative ground cover is destroyed in areas where precipitation is high, abnormally high erosion rates may be experienced.

Differences in vegetative type have a variable effect on erosion and sediment yield, even though percentages of total ground cover may be the same. For instance, in areas of pinyon-juniper forest having the same percentage of ground cover as an area of grass, the absence of understory in some of the pinyon-juniper stands would allow a higher erosion rate than in the area of grass.

Land Use

The use of land has a widely variable impact on sediment yield, depending largely on the susceptibility of the soil and rock to erosion, the amount of stress exerted by climatic factors and the type and intensity of use. Factors other than the latter have been discussed in appropriate places in this guide.

In almost all instances, use either removes or reduces the amount of natural vegetative cover which reflects the varied relationships within the environment. Activities which remove all vegetation for parts of each year for several years, or permanently, are cultivation, urban development, and road construction. Grazing, logging, mining, and fires artifically (sic) induce permanent or temporary reduction in cover density.

High erosion hazard sites, because of the geology, soils, climate, etc., are also of high hazard from the standpoint of type and intensity of use. For

example, any use which reduces cover density on a steep slope with erodible soils and severe climatic conditions will strongly affect sediment yield. The extent of this effect will depend on the area and intensity of use relative to the availability of sediment from other causes. Construction of road or urban development with numerous cut and fill slopes through a large area of widespread sheet or gully erosion will probably not cause a change in sediment yield classification. Similar contruction (sic) and continued disturbance in an area of good vegetative response to a favorable climate can raise yield by one or more classifications.

Use of the land has its greatest potential impact on sediment yield where a delicate balance exists under natural conditions. Alluvial valleys of fine, easily dispersed soils from shales and sandstones are highly vulnerable to erosion where intensive grazing and trailing by livestock have occurred. Valley trenching has developed in many of these valleys and provides a large part of the sediment in high yield classes from these areas.

A decline in vegetative density is not the only effect of livestock on erosion and sediment yield. Studies at Badger Wash, Colorado, which is underlain by Mancos shale, have indicated that sediment yield from ungrazed watersheds is appreciably less than from those that are grazed. This difference is attributed to the absence of soil trampling in the ungrazed areas, since the density of vegetation has not noticeably changed since exclusion began.

Areas in the arid and semi-arid portions of the Southwest that are surfaced by desert pavement are much less sensitive to grazing and other use, since the pavement affords a substitute for vegetative cover.

In certain instances the loss or deterioration of vegetative cover may have little noticeable on-site impact but may increase off-site erosion by acceleration of runoff. This could be particularly evident below urbanized areas where accelerated runoff from pavement and rooftops has increased the stress on downstream channels. Widespread destruction of cover by poor logging practices or by brush and timber fires frequently increases channel erosion as well as that on the directly affected watershed slopes. On the other hand, cover disturbances under favorable conditions, such as a cool, moist climate, frequently result in a healing of erosion sources within a few years.

Upland Slope Erosion

This erosion form occurs on sloping watershed lands beyond the confines of valleys. Sheet erosion, which involves the removal of a thin layer of soil over an extensive area, is usually not visible to the eye. This erosion form is evidenced by the formation of rills. Experience indicates that soil loss from rill erosion can be seen if it amounts to about 5 tons or more per acre. This is equivalent in volume per square mile to aproximately (sic)2 acre-feet.

Wind erosion from upland slopes and the deposition of the eroded material in stream channels may be a significant factor. The material so deposited in channels is readily moved by subsequent runoff.

Downslope soil movement due to creep can be an important factor in sediment yield on steep slopes underlain by unstable geologic formations.

Significant gully erosion as a sediment contributor is evidenced by the presence of numerous raw cuts along the hill slopes. Deep soils on moderately steep to steep slopes usually provide an environment for gully development.

Processes of slope erosion must be considered in the light of factors which contribute to its development. These have been discussed in previous sections.

Channel Erosion and Sediment Transport

If a stream is ephemeral, runoff that traverses the dry alluvial bed may be drastically reduced by transmission losses (absorption by channel alluvium). This decrease in the volume of flow results in a decreased potential to move sediment. Sediment may be deposited in the streambed from one or a series of relatively small flows only to be picked up and moved on in a subsequent larger flow. Sediment concentrations, determined from field measurements at consecutive stations, have generally been shown to increase many fold for instances of no tributary inflow. Thus, although water yield per unit area will decrease with increasing drainage area, the sediment yield per unit area may remain nearly constant or may even increase with increasing drainage area.

In instances of convective precipitation in a watershed with perennial flow, the role of transmission losses is not as significant as in watersheds with ephemeral flow, but other channel factors, such as the shape of the channel, may be important.

For frontal storm runoff, the flow durations are generally much longer than for convective storms, and runoff is often generated from the entire basin. In such instances, sediment removed from the land surfaces is generally carried out of the area by the runoff. Stream channel degradation and/or aggradation must be considered in such cases, as well as bank scour. Because many of the stream beds in the Pacific Southwest are composed of fine-grained alluvium in well defined channels, the potential for sediment transport is limited only by the amount and duration of runoff. Large volumes of sediment may thus be moved by these frontal storms because of the longer flow durations.

The combination of frontal storms of long duration with high intensity and limited areal-extent convective activity will generally be in the highest class for sediment movement in the channels. Storms of this type generally produce both the high peak flows and the long durations necessary for maximum sediment transport.

Sediment yield may be substantially affected by the degree of channel development in a watershed. This development can be described by the channel cross sections, as well as by geomorphic parameters such as drainage density, channel gradients and width-depth ratio. The effect of these geomorphic parameters is difficult to evaluate, primarily because of the scarcity of sediment transport data in the Pacific Southwest.

If the cross section of a stream is such as to keep the flow within defined banks, then the sediment from an upstream point is generally transported to a downstream point without significant losses. Confinement of the flow within alluvial banks can result in a high erosional capability of a flood flow, especially the flows with long return periods. In most channels with wide floodplains, deposition on the floodplain during floods is often significant, and the transport is thus less than that for a within bank flow. The effect of this transport capability can be explained in terms of tractive force which signifies the hydraulic stress exerted by the flow on the bed of the stream. This average bed-shear stress is obtained as the product of the specific weight of the fluid, hydraulic radius, and energy gradient slope. Thus, greater depth results in a greater bed shear and a greater potential for moving sediment. By the same reasoning, steep slopes (the energy slope and bed slope are assumed to be equivalent) also result in high bed-shear stress.

The boundary between sediment yield classifications in much of the Pacific Southwest may be at the mountain front, with the highest yield

designation on the alluvial plain if there is extensive channel erosion. In contrast, many mountain streams emerge from canyon reaches and then spread over fans or valley flats. Here water depths can decrease from many feet to only a few inches in short distances with a resultant loss of the capacity to transport sediment. Sediment yield of the highest classification can thus drop to the lowest in such a transition from a confined channel to one that has no definition.

Channel bank and bed composition may greatly influence the sediment yield of a watershed. In many areas within the Pacific Southwest, the channels in valleys dissect unconsolidated material which may contribute significantly to the stream sediment load. Bank sloughing during periods of flow, as well as during dry periods, piping, and bank scour generally add greatly to the sediment load of the stream and often change upward the sediment yield classification of the watershed. Field examination for areas of head cutting, aggradation or degradation, and bank cutting are generally necessary prior to classification of the transport expectancy of a stream. Geology plays a significant role in such an evaluation. Geologic controls in channels can greatly affect the stream regimen by limiting degradation and headcuts. Thus, the transport capacity may be present, but the supply of sediment from this source is limited.

Man-made structures can also greatly affect the transport characteristics of the stream. For example, channel straightening can temporarily upset the channel equilibrium and cause an increase in channel gradient and an increase in the stream velocity and the shear stress. Thus, the sediment transport capacity of the stream may be temporarily increased. Structures such as debris darns, lined channels, drop spillways, and detention dams may drastically reduce the sediment transport.

AN EXPLANATION OF THE USE OF THE RATING CHART (TABLE A-1) FOR EVALUATING FACTORS AFFECTING SEDIMENT YIELD IN THE PACIFIC SOUTHWEST FOLLOWS

# Table A.1. Factors Affecting Sediment Yield in the Pacific Southwest

PSIAC - Table A-1

| Sediment Yield Levels | A SURFACE GEOLOGY (10)* | B SOILS (10) | C CLIMATE (10) | D RUNOFF (10) | E TOPOGRAPHY (20) | F GROUND COVER (10) | G LAND USE (10) | H UPLAND EROSION (25) | I CHANNEL EROSION & SEDIMENT TRANSPORT (25) |
|---|---|---|---|---|---|---|---|---|---|
| High | a. Marine shales and related mudstones and siltstones. | a. Fine textured easily dispersed; saline-alkaline; high shrink-swell characteristics<br>b. Single grain silts and fine sands | a. Storms of several days' duration with short periods of intense rainfall<br>b. Frequent intense convective storms<br>c. Freeze-thaw occurrence | a. High peak flows per unit area<br>b. Large volume of flow per unit area | a. Steep upland slopes (in excess of 30%) High relief; little or no floodplain development | Ground cover does not exceed 20%<br>a. Vegetation sparse; little or no litter<br>b. No rock in surface soil | a. More than 50% cultivated<br>b. Almost all of area intensively grazed<br>c. All of area recently burned | a. More than 50% of the area characterized by rill and gully or landslide erosion | a. Eroding banks continuously or at frequent intervals with large depths and long flow duration<br>b. Active headcuts and degradation in tributary channels |
| ** | | | | | | | | | |
| Moderate | (5)<br>a. Rocks of medium hardness<br>b. Moderately weathered<br>c. Moderately fractured | (5)<br>a. Medium textured soil<br>b. Occasional rock fragments<br>c. Caliche layers | (5)<br>a. Storms of moderate duration and intensity<br>b. Infrequent convective storms | (5)<br>a. Moderate peak flows<br>b. Moderate volume of flow per unit area | (10)<br>a. Moderate upland slopes (less than 20%)<br>b. Moderate fan or floodplain development | (10)<br>Cover not exceeding 40%<br>a. Noticeable litter<br>b. If trees present understory not well developed | (0)<br>a. Less than 25% cultivated<br>b. 50% or less recently logged<br>c. Less than 50% intensively grazed<br>d. Ordinary road and other construction | (10)<br>a. About 25% of the area characterized by rill and gully or landslide erosion<br>b. Wind erosion with deposition in stream channels | (10)<br>a. Moderate flow depths, medium flow duration with occasionally eroding banks or bed |
| ** | | | | | | | | | |
| Low | (0)<br>a. Massive, hard formations | (0)<br>a. High percentage of rock fragments<br>b. Aggregated clays<br>c. High in organic matter | (0)<br>a. Humid climate with rainfall of low intensity<br>b. Precipitation in form of snow<br>c. Arid climate, low intensity storms<br>d. Arid climate; rare convective storms | (0)<br>a. Low peak flows per unit area<br>b. Low volume of runoff per unit area<br>c. Rare runoff events | (0)<br>a. Gentle upland slopes (less than 5%)<br>b. Extensive alluvial plains | (-10)<br>a. Area completely protected by vegetation, rock fragments, litter. Little opportunity for rainfall to reach erodible material | (-10)<br>a. No cultivation<br>b. No recent logging<br>c. Low intensity grazing | (0)<br>a. No apparent signs of erosion | (0)<br>a. Wide shallow channels with flat gradients, short flow duration<br>b. Channels in massive rock, large boulders or well vegetated<br>c. Artificially controlled channels |

* THE NUMBERS IN SPECIFIC BOXES INDICATE VALUES TO BE ASSIGNED APPROPRIATE CHARACTERISTICS.
THE SMALL LETTERS, a, b, c, REFER TO INDEPENDENT CHARACTERISTICS TO WHICH FULL VALUE MAY BE ASSIGNED.

** IF EXPERIENCE SO INDICATES, INTERPOLATION BETWEEN THE 3 SEDIMENT YIELD LEVELS MAY BE MADE.

## Use of the Rating Chart of Factors Affecting Sediment Yield in the Pacific Southwest

The following is a summary of the sediment yield classification presented for this methodology.

| Classification | Rating | Sediment Yield AF/sq. ml. |
|---|---|---|
| 1 | > 100 | 3.0 |
| 2 | 75 - 100 | 1.0 - 3.0 |
| 3 | 50 - 75 | 0.5 - 1.0 |
| 4 | 25 - 50 | 0.2 - 0.5 |
| 5 | 0 - 25 | < 0.2 |

In most instances, high values for the A through G factors should correspond to high values for the H and/or I factors.

An example of the use of the rating chart is as follows:

A watershed of 15 square miles in western Colorado has the following characteristics and sediment yield levels:

| Factors | Sediment Yield Levels | Rating |
|---|---|---|
| A Surface geology | Marine Shales | 10 |
| B Soils | Easily dispersed, high shrink-swell characteristics | 10 |
| C Climate | Infrequent convective storms, freeze-thaw occurrence | 7 |
| D Runoff | High peak flows; low volumes | 5 |
| E Topography | Moderate slopes | 10 |
| F Ground cover | Sparse, little or no litter | 10 |
| G Land use | Intensively grazed | 10 |
| H Upland erosion | More than 50% rill and gully erosion | 25 |
| I Channel erosion | Occasionally eroding banks and bed but short flow duration | 5 |
| | TOTAL | 92 |

This total rating of 92 would indicate that the sediment yield is in Classification 2. This compares with a sediment yield of 1.96 acre-feet per square mile as the average of a number of measurements in this area.

# APPENDIX B

## Modified Universal Soil Loss Equation for Predicting Watershed Soil Loss

## APPENDIX B

### MODIFIED UNIVERSAL SOIL LOSS EQUATION FOR PREDICTING WATERSHED SOIL LOSS

The Modified Universal Soil Loss Equation (MUSLE) described by Williams (1975) is an empirically derived methodology for predicting watershed sediment yield on a per-storm basis. The MUSLE is:

$$Y_S = R_W K LS C P \tag{B.1}$$

where $Y_S$ is sediment yield in tons for the storm event, $R_W$ is a storm runoff energy factor, K is the soil erodibility factor, LS is the topographic factor representing the combination of slope length and slope gradient, C is the cover and management factor and P is the erosion control practice factor. Factors K, LS, C and P are as defined for the Universal Soil Loss Equation (USLE) as described in the USDA Soil Conservation Service, Agriculture Handbook Number 537 "Predicting Rainfall Erosion Losses" (1978), and as reviewed in later paragraphs, Smith and Wischmeier, 1975; Wischmeier, 1960; and Wischmeier and Smith, 1978, provide detailed descriptions of the USLE factors and their values.

The storm runoff energy factor $R_W$ in Equation B.1 represents the modification of the USLE where $R_W$ is given by:

$$R_W = \alpha(Vq_p)^{\beta} \tag{B.2}$$

In Equation B.2, V is the storm event runoff volume in acre-feet, $q_p$ is the storm event peak flow rate in cfs, and $\alpha$ and $\beta$ are coefficients. Utilization of a storm runoff factor makes the MUSLE applicable to semiarid regions of the West where short-duration, high-intensity storms are dominant. For watersheds having measured sediment data, values for the coefficients $\alpha$ and $\beta$ of 95 and 0.56, respectively, for experimental watersheds in Texas and Nebraska. For the Albuquerque area, it is recommended that the formula be used only to establish wash load (silts and clays), and that values of $\alpha$ and $\beta$ of 285 and 0.56, respectively, be used.

Recommended values for the soil erodibility factor, K, based on USDA soil texture, are given in USDA SCS-New Mexico Conservation Agronomy Technical Note No. 28 (1981). These values are shown as **Table B.1**. A nomograph to determine factor K based on percent of silt and coarse sand permeability, soil structure and percent organic matter is found in the SCS Agriculture Handbook Number 537 (1978). **Figure B.1** is a guide to determine the textural classification of soil based on the percentage of clay, silt, and sand.

| Table B.1. Soil Erodibility Factor K Based on USDA Texture. | | | | |
|---|---|---|---|---|
| | Estimated K Factor[1] | | | |
| USDA Texture | Normal[2] | Gravelly[2] | Very Gravelly[2] | Extremely Gravelly[2] |
| Coarse Sand | 0.10 | 0.05 | 0.02 | 0.02 |
| Sand | 0.10 | 0.05 | 0.02 | 0.02 |
| Fine Sand | 0.17 | 0.10 | 0.05 | 0.02 |
| Very Coarse Sand | 0.10 | 0.05 | 0.02 | 0.02 |
| Loamy Coarse Sand | 0.15 | 0.10 | 0.05 | 0.02 |
| Loamy Sand | 0.17 | 0.10 | 0.05 | 0.02 |
| Loamy Fine Sand | 0.20 | 0.10 | 0.05 | 0.02 |
| Loamy Very Fine Sand | 0.49 | 0.28 | 0.15 | 0.05 |
| Coarse Sandy Loam | 0.20 | 0.10 | 0.05 | 0.02 |
| Sandy Loam | 0.24 | 0.15 | 0.10 | 0.05 |
| Fine Sandy Loam | 0.28 | 0.15 | 0.10 | 0.05 |
| Very Fine Sandy Loam | 0.55 | 0.28 | 0.17 | 0.10 |
| Loam | 0.37 | 0.20 | 0.10 | 0.05 |
| Silt Loam | 0.43 | 0.24 | 0.15 | 0.05 |
| Silt | 0.64 | 0.37 | 0.20 | 0.10 |
| Sandy Clay Loam | 0.32 | 0.15 | 0.10 | 0.05 |
| Clay Loam | 0.32 | 0.15 | 0.10 | 0.05 |
| Silty Clay Loam | 0.37 | 0.20 | 0.10 | 0.05 |
| Sandy Clay | 0.32 | 0.15 | 0.10 | 0.05 |
| Silty Clay | 0.24 | 0.15 | 0.10 | 0.05 |
| Clay | 0.20 | 0.10 | 0.05 | 0.02 |

[1]Where a Soils Survey Interpretation Sheet, SOILS-5, is available for a soil, the K Factor listed will be more accurate than the factor provided by this table.

[2]Total rock fragments are included in these figures, not just gravel. Normal = 0-15 percent, gravelly = 15-35 percent, very gravelly = 35-60 percent, and extremely gravelly = over 60 percent.

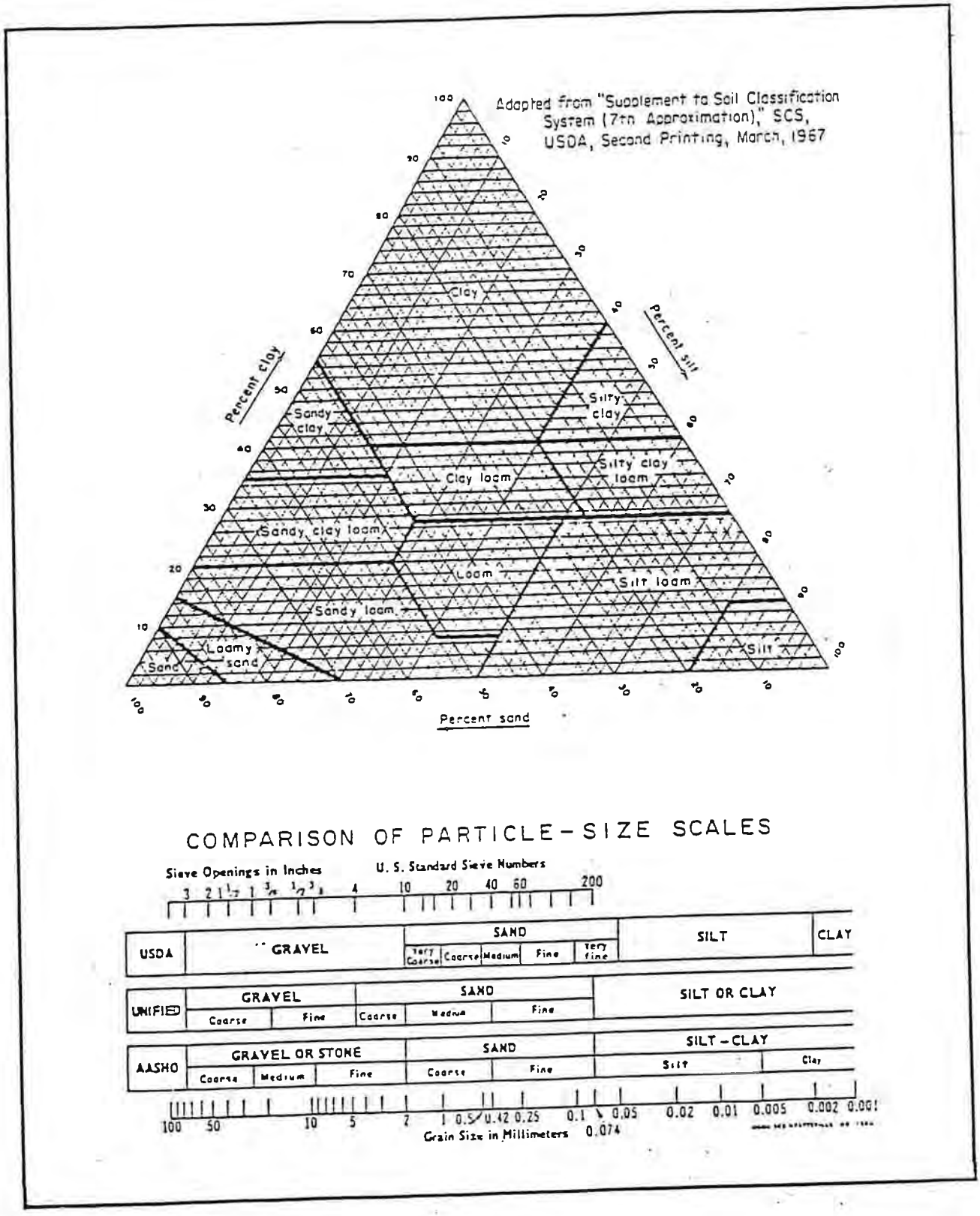


Figure B.1. Guide for the textural classification of soil.

SCS Agriculture Handbook Number 537 (1978) also presents a table to determine the Cover and Management Factor (Cropping management factor, C) for pasture, range, idle land, and grazed woodland. This table is reproduced as **Table B.2**. A table with identical values is contained in SCS-New Mexico Technical Note 28 (1981). The Cover and Management Factors, L, for cropland and fallow areas not described in **Table B.2** are continued in SCS Agriculture Handbook Number 537 and SCS-New Mexico Technical Note 28 (1981).

The topographic factor LS is defined as the ratio of soil loss from any slope and length to soil loss from a 72.6-foot plot length at a nine percent slope, with all other conditions the same. Slope length is defined as the distance from the point of overland flow origin to the point where either slope decreases to the extent that deposition begins or runoff water enters a well-defined channel (Smith and Wischmeier, 1975). Effect of slope length on soil loss is primarily a result of increased potential due to greater accumulation of runoff on the longer slopes. Based on data for slopes between three and 20 percent and with lengths up to 400 feet, Wischmeier and Smith (1965) proposed the topographic factor be computed as:

$$LS = \left(\frac{\lambda}{72.6}\right)^n (0.065 + 0.0454\ S + 0.0065\ S^2) \qquad \text{(B.3)}$$

where $\lambda$ is slope length, S is percent slope, and n is an exponent depending upon slope. The exponent n is given by:

n = 0.3 for slope $\leq$ 3 percent
n = 0.4 for slope = 4 percent
n = 0.5 for slope $\geq$ 5 percent

SCS New Mexico Technical Note 28 (1981) has extended Equation B.3 to slopes between 0.2 and 60 percent and to lengths up to 2,000 feet. However, for lengths exceeding 400 feet and slopes greater than 24 percent, soil loss estimates are speculative as these values are beyond the range of research data. The LS data from SCS New Mexico Technical Note 28 are included as **Table B.3**.

Erosion-control practice factor P accounts for the effect of conservation practices such as contouring, strip cropping, and terracing on erosion. It is defined as the ratio of soil loss using one of these practices to the loss using straight row farming up and down the slope. Terracing is generally the most effective conservation practice for decreasing soil erosion. This factor has no significance for range and wild-land areas and can be set at 1.0.

When estimating sediment yield using the MUSLE, a useful computation is to express sediment yield in terms of an average concentration (ppm) based on the total water and sediment yields. This value can be compared with measured stream data in the area, if available. Annual sediment yield from the land surface can be estimated using the MUSLE in combination with the probability-weighting procedure described in Section 4.6.3.

Table B.2. Cover and Management Factor C for Permanent Pasture, Range, and Idle Land.[1]

| Vegetative Canopy | | Cover that contacts the soil surface | | | | | | |
|---|---|---|---|---|---|---|---|---|
| Type and Height[2] | Percent Cover[3] | Type[4] | Percent ground cover | | | | | |
| | | | 0 | 20 | 40 | 60 | 80 | 95+ |
| No appreciable canopy | | G | 0.45 | 0.20 | 0.10 | 0.042 | 0.013 | 0.003 |
| | | W | 0.45 | 0.24 | 0.15 | 0.091 | 0.043 | 0.011 |
| Tall weeds or short brush with average drop fall height of 20 inches | 25 | G | 0.36 | 0.17 | 0.09 | 0.038 | 0.013 | 0.003 |
| | | W | 0.36 | 0.20 | 0.13 | 0.083 | 0.041 | 0.011 |
| | 75 | G | 0.26 | 0.13 | 0.07 | 0.035 | 0.012 | 0.003 |
| | | W | 0.26 | 0.16 | 0.11 | 0.076 | 0.039 | 0.011 |
| Appreciable brush or brushes with average drop fall height of 6-1/2 ft | 25 | G | 0.40 | 0.18 | 0.09 | 0.040 | 0.13 | 0.003 |
| | | W | 0.40 | 0.22 | 0.14 | 0.087 | 0.42 | 0.011 |
| | 50 | G | 0.34 | 0.16 | 0.08 | 0.038 | 0.012 | 0.003 |
| | | W | 0.34 | 0.19 | 0.13 | 0.082 | 0.041 | 0.011 |
| | 75 | G | 0.28 | 0.14 | 0.08 | 0.036 | 0.012 | 0.003 |
| | | W | 0.28 | 0.17 | 0.12 | 0.078 | 0.040 | 0.011 |
| Trees, but no appreciable low brush. Average drop fall height of 13 ft | 25 | G | 0.42 | 0.19 | 0.10 | 0.041 | 0.013 | 0.003 |
| | | W | 0.42 | 0.23 | 0.14 | 0.089 | 0.042 | 0.011 |
| | 50 | G | 0.39 | 0.18 | 0.09 | 0.040 | 0.013 | 0.003 |
| | | W | 0.39 | 0.21 | 0.14 | 0.087 | 0.042 | 0.011 |
| | 75 | G | 0.36 | 0.17 | 0.09 | 0.039 | 0.012 | 0.003 |
| | | W | 0.36 | 0.20 | 0.13 | 0.084 | 0.041 | 0.011 |

[1]The listed C values assumes that the vegetation and mulch are randomly distributed over the entire area.

[2]Canopy height is measured as the average fall height of water drops falling from the canopy to the ground. Canopy effect is inversely proportional to drop fall height and is negligible is fall height exceeds 33 ft.

[3]Portion of total-area surface that would be hidden from view by canopy in a vertical projection (a bird's eye view).

[4]G = Cover at surface is grass, grasslike plants, decaying compacted duff, or liter 2 in. deep. W = Cover at surface is mostly broadleft herbaceaous plants (as weeds with little lateral-root network near the surface) or undecayed residues or both.

# Table B.3. Slope-Length and Slope-Steepness Factor LS (Topographic Factor).

| Length of Slope (L) 2/ | SOIL LOSS RATIO (LS) 1/ Percent of Slope 2/ | | | | | | | | | | | | | | | | | | | | |
|---|---|---|---|---|---|---|---|---|---|---|---|---|---|---|---|---|---|---|---|---|---|
| | 0.2 | 0.3 | 0.4 | 0.5 | 1.0 | 2.0 | 3.0 | 4.0 | 5.0 | 6.0 | 8.0 | 10.0 | 12.0 | 14.0 | 16.0 | 18.0 | 20.0 | 25.0 | 30.0 | 40.0 | 50.0 | 60.0 |
| 20 | .05 | .05 | .06 | .06 | .08 | .12 | .18 | .21 | .24 | .30 | .44 | .61 | .81 | 1.0 | 1.2 | 1.6 | 1.8 | 2.6 | 3.5 | 5.5 | 8 | 10 |
| 40 | .06 | .07 | .07 | .08 | .10 | .15 | .22 | .28 | .34 | .43 | .63 | .87 | 1.2 | 1.4 | 1.8 | 2.2 | 2.6 | 3.5 | 5.0 | 8 | 11 | 15 |
| 60 | .07 | .08 | .08 | .08 | .11 | .17 | .25 | .33 | .41 | .52 | .77 | 1.0 | 1.4 | 1.8 | 2.2 | 2.6 | 3.0 | 4.5 | 6.0 | 10 | 14 | 18 |
| 80 | .08 | .08 | .09 | .09 | .12 | .19 | .27 | .37 | .48 | .60 | .89 | 1.2 | 1.6 | 2.0 | 2.6 | 3.0 | 3.5 | 5.5 | 7 | 11 | 16 | 21 |
| 100 | .08 | .09 | .09 | .10 | .13 | .20 | .29 | .40 | .54 | .67 | .99 | 1.4 | 1.8 | 2.3 | 2.8 | 3.4 | 4.1 | 6.0 | 8 | 13 | 18 | 23 |
| 110 | .08 | .09 | .10 | .10 | .13 | .21 | .30 | .42 | .56 | .71 | 1.0 | 1.4 | 1.8 | 2.4 | 3.0 | 3.5 | 4.5 | 6.0 | 8 | 13 | 19 | 24 |
| 120 | .09 | .09 | .10 | .10 | .14 | .21 | .30 | .43 | .59 | .74 | 1.0 | 1.6 | 2.0 | 2.6 | 3.0 | 4.0 | 4.5 | 6.0 | 9 | 14 | 20 | 25 |
| 130 | .09 | .09 | .10 | .10 | .14 | .22 | .31 | .44 | .61 | .77 | 1.2 | 1.6 | 2.0 | 2.6 | 3.0 | 4.0 | 4.5 | 7 | 9 | 14 | 20 | 26 |
| 140 | .09 | .10 | .10 | .10 | .14 | .22 | .32 | .46 | .63 | .80 | 1.2 | 1.6 | 2.2 | 2.8 | 3.5 | 4.0 | 5.0 | 7 | 9 | 15 | 21 | 27 |
| 150 | .09 | .10 | .10 | .10 | .15 | .23 | .32 | .47 | .66 | .82 | 1.2 | 1.7 | 2.2 | 2.8 | 3.5 | 4.2 | 5.0 | 7 | 10 | 15 | 22 | 28 |
| 160 | .09 | .10 | .11 | .11 | .15 | .23 | .33 | .48 | .68 | .85 | 1.2 | 1.8 | 2.2 | 3.0 | 3.5 | 4.5 | 5.0 | 7 | 10 | 16 | 23 | 29 |
| 180 | .10 | .10 | .11 | .11 | .15 | .24 | .34 | .51 | .72 | .90 | 1.4 | 1.8 | 2.4 | 3.0 | 4.0 | 4.5 | 5.5 | 8 | 11 | 17 | 24 | 31 |
| 200 | .10 | .10 | .11 | .11 | .16 | .25 | .35 | .53 | .76 | .95 | 1.4 | 1.9 | 2.6 | 3.2 | 4.0 | 5.0 | 5.8 | 8 | 11 | 18 | 25 | 33 |
| 300 | .10 | .11 | .12 | .12 | .18 | .28 | .40 | .62 | .93 | 1.2 | 1.7 | 2.4 | 3.1 | 4.0 | 4.9 | 6.0 | 7.1 | 10 | 14 | 22 | 31 | 40 |
| 400 | .11 | .12 | .13 | .13 | .20 | .31 | .44 | .70 | 1.1 | 1.4 | 2.0 | 2.7 | 3.6 | 4.6 | 5.7 | 6.9 | 8.2 | 12 | 16 | 25 | 36 | 46 |
| 500 | .11 | .12 | .13 | .13 | .21 | .33 | .47 | .76 | 1.2 | 1.5 | 2.2 | 3.1 | 4.0 | 5.1 | 6.4 | 7.7 | 9.1 | 13 | 18 | 28 | 40 | 52 |
| 600 | .11 | .12 | .13 | .14 | .22 | .34 | .49 | .82 | 1.3 | 1.6 | 2.4 | 3.4 | 4.4 | 5.6 | 7 | 8.4 | 10 | 14 | 19 | 31 | 44 | 57 |
| 700 | .12 | .13 | .14 | .14 | .23 | .36 | .52 | .87 | 1.4 | 1.8 | 2.6 | 3.5 | 5.0 | 6.0 | 8 | 9 | 11 | 16 | 21 | 33 | 47 | 61 |
| 800 | .12 | .13 | .14 | .15 | .24 | .38 | .54 | .92 | 1.5 | 1.9 | 2.8 | 3.9 | 5.1 | 6.5 | 8 | 9.7 | 11.5 | 17 | 22 | 36 | 50 | 65 |
| 900 | .12 | .13 | .14 | .15 | .25 | .39 | .56 | .96 | 1.6 | 2.0 | 3.0 | 4.0 | 5.5 | 7 | 9 | 10 | 12 | 18 | 24 | 38 | 53 | 69 |
| 1000 | .13 | .14 | .15 | .15 | .26 | .40 | .57 | 1.0 | 1.7 | 2.1 | 3.1 | 4.3 | 5.7 | 7.3 | 9 | 10.9 | 12.9 | 19 | 25 | 40 | 56 | 73 |
| 1100 | .17 | .18 | .19 | .20 | .27 | .41 | .59 | 1.0 | 1.8 | 2.2 | 3.5 | 4.5 | 6.0 | 8 | 9 | 11 | 14 | 20 | 26 | 42 | 59 | 77 |
| 1200 | .17 | .18 | .20 | .21 | .27 | .42 | .61 | 1.0 | 1.8 | 2.4 | 3.5 | 4.5 | 6.0 | 8 | 10 | 12 | 14 | 20 | 28 | 44 | 62 | 80 |
| 1300 | .18 | .19 | .20 | .21 | .28 | .43 | .62 | 1.2 | 2.0 | 2.4 | 3.5 | 5.0 | 7 | 8 | 10 | 12 | 15 | 21 | 29 | 46 | 64 | 83 |
| 1400 | .18 | .19 | .21 | .22 | .29 | .44 | .63 | 1.2 | 2.0 | 2.6 | 3.5 | 5.0 | 7 | 9 | 11 | 13 | 15 | 22 | 30 | 47 | 67 | 87 |
| 1500 | .19 | .20 | .21 | .22 | .29 | .45 | .65 | 1.2 | 2.0 | 2.6 | 4.0 | 5.5 | 7 | 9 | 11 | 13 | 16 | 23 | 31 | 49 | 69 | 90 |
| 1600 | .19 | .20 | .21 | .23 | .30 | .46 | .66 | 1.2 | 2.2 | 2.6 | 4.0 | 5.5 | 7 | 9 | 11 | 14 | 16 | 24 | 32 | 51 | 71 | 93 |
| 1700 | .19 | .21 | .22 | .23 | .30 | .47 | .67 | 1.2 | 2.2 | 2.8 | 4.0 | 5.5 | 7 | 9 | 12 | 14 | 17 | 24 | 33 | 52 | 73 | 95 |
| 2000 | .20 | .22 | .23 | .24 | .32 | .49 | .71 | 1.4 | 2.4 | 3.0 | 4.5 | 6.0 | 8 | 10 | 13 | 15 | 18 | 26 | 36 | 57 | 80 | 104 |

1/ From USDA Ag. Handbook No. 537, December 1978.

2/ When the length of slope exceeds 400 feet and (or) percent of slope exceeds 24 percent, soil loss estimates are speculative as these values are beyond the range of research data.

April 1981

# APPENDIX C

## Hydraulic Calculations

## APPENDIX C

### C.1. Normal Depth Calculations

Manning's equation can be written for discharge as:

$$Q = \frac{1.486}{n} AR^{\frac{2}{3}} S^{\frac{1}{2}} \qquad \text{(C.1)}$$

Area and wetted perimeter for trapezoidal channel may be expressed as a function of depth as follows:

$$A = zy^2 + by \qquad \text{(C.2)}$$

where z = sideslope
b = bottom width
y = depth

Wetted perimeter is given by:

$$P = b + 2y(1 + z)\frac{1}{2} \qquad \text{(C.3)}$$

Therefore, the discharge for a normal depth $y_o$, is:

$$Q = \frac{1.486}{n} \frac{(z\, y_o^2 + by_o)^{\frac{5}{3}} S^{\frac{1}{2}}}{[b + 2y_o\,(1 + z)^{\frac{1}{2}}]^{\frac{2}{3}}} \qquad \text{(C.4)}$$

For a known discharge this equation may be solved for normal depth $y_o$ in terms of the other known parameters by use of an iterative technique such as Newton's iterative method. The equation actually solved, in this case for $y_o$, would be:

$$\frac{Qn}{1.486\, S^{\frac{1}{2}}} = \frac{[zy_u^{2_o} + by_o]^{\frac{5}{3}}}{[b + 2y_o\,(1 + z)^{\frac{1}{2}}]^{\frac{2}{3}}} \qquad \text{(C.5)}$$

## C.2. Normal Depth Calculations for Natural Channels

Using data taken at a given cross section, wetter perimeter P is often related to cross-sectional flow area A by regression. The resulting expression is usually a power function of the form:

$$P = a_1 A^{b_1} \tag{C.6}$$

Similarly, flow area may be related to flow depth as:

$$A = a_2 y^{b_2} \tag{C.7}$$

Here, $a_1$, $a_2$, $b_1$, and $b_2$ are statisticaly fitted coefficients and exponents. By using these expressions, hydraulic radius R in Equation C.1 may be expressed as a function of y as follows:

$$R = \frac{A}{P} = \frac{a_2 y^{b_2}}{a_1 (a_2 y^{b_2})^{b_1}} = \frac{a_2}{a_1 a_2^{b_1}} y^{(b_2 - b_2 b_1)} \tag{C.8}$$

Therefore, Equation C.1 may be rewritten in terms of depth of flow in a natural channel as:

$$Q = \frac{1.486}{n} a_2 y_o^{b_2} \left[ \frac{a_2}{a_1 a_2^{b_1}} y_o^{(b_2 - b_2 b_1)} \right]^{\frac{2}{3}} S_o^{\frac{1}{2}} \tag{C.9}$$

This equation may be solved directly for $y_o$, resulting in:

$$y_o = \left[ \left( \frac{Qn}{1.486\, S_o^{\frac{1}{2}}} \right)^{\frac{3}{2}} \left( \frac{a_1}{a_2^{\left(\frac{5}{2} - b^2\right)}} \right) \right]^{\left( \frac{2}{5b_2 - 2b_1 b_2} \right)} \tag{C.10}$$

## C.3. Critical and Supercritical Flow Calculations

$$\text{Froude Number} = F_r = \frac{V}{\sqrt{gy}} = \frac{Q}{A\sqrt{gA/w}} \qquad \text{(C.11)}$$

where
- V = velocity
- g = acceleration of gravity (≈ 32.2 ft/sec)
- y = depth
- A = area of section
- w = width
- Q = flow rate

$$\text{Critical depth (Rectangular Section)} = y_c = \sqrt[3]{\frac{Q^2}{gb^2}} = \sqrt[3]{\frac{q^2}{g}} \qquad \text{(C.12)}$$

$$\text{Critical velocity} = V_c = \sqrt{g\,y_c} \qquad \text{(C.13)}$$

Critical discharge ($Q_c$):

| Channel Section | Equation | |
|---|---|---|
| *Rectangular* | $Q_c = \sqrt{g}\,y^{1.5}$ | (C.14) |
| *Trapezoidal* | $Q_c = \frac{\sqrt{g}\,[(b + Zy)\,y]^{1.5}}{(b + 2Zy)^{0.5}}$ | (C.15) |
| *Circular* | $Q_c = \frac{0.251(\theta - \sin\theta)^{1.5}}{(\sin 1/2\,\theta)^{0.5}} d_o^{2.5}$ | (C.16) |

- y = depth
- b = bottom width
- z = sideslope
- $d_o$ = diameter

$$\Theta = 2\,COS^{-1}\left(\frac{d_o/2 - y}{d_o}\right) \qquad \text{(C.17)}$$

Sequent depth (at hydraulic jump)

$$\frac{y_2}{y_1} = 1/2\ (\sqrt{1 + 8\ F_r^2}\ -1) \qquad \text{(C.18)}$$

where $Y_1$ = depth before hydraulic jump
$Y_2$ = depth after hydraulic jump

or

$$Y_2 = Y_1 + 0.5 * \left(\frac{A}{w}\right) (\sqrt{1 + 8F_r^2}\ -3) \qquad \text{(C.19)}$$

# APPENDIX D

## Computer Program for Estimating Lateral Migration Rates and Distances (CURVCALC)

# APPENDIX D

## CURVCALC

### A computer Program for Estimating Lateral Migration Rates

### D.1. General

This program computes the rate of lateral migration for channels that are either degradational or vertically stable. **It should not be used for aggrading channels.** The computational procedure and assumptions used in the program are discussed in Section 3.4.5 (pages 3-74 through 3-78). (Other background information is presented in the preceding portion of Section 3.4.5.)

This program is intended to automate the computational procedure for estimating lateral migration rates. The basic procedure is believed to reasonably represent the important physical processes that cause lateral erosion of arroyos. The program uses an idealized bend geometry and approximate relations for bank erosion rate as a function of bend geometry. Comparison and calibration of results from the program with field data in the specific area to which it is applied is strongly recommended. A calibration factor is provided in the input file that can be used to adjust the predicted erosion rates to match observed erosion rates in a particular area. It is the responsibility of the user to insure that the procedure and assumptions are applicable to their specific problem; Resource Consultants & Engineers, Inc. makes no warranty, expressed or implied, as to the accuracy of the procedure for a specific application or the acceptability of the results obtained therefrom and accepts no liability of any type related to the program or its use.

## D.2. Input Data

Input data for the program consists of necessary data to describe the initial conditions (geometry, bed gradient, channel size) in the bend being analyzed and the coefficients of the power function sediment transport capacity relationship (See Section 3.3.4, pages 3-32 through 3-38). The input file is organized as follows:

| | | | | | | | | | | |
|---|---|---|---|---|---|---|---|---|---|---|
| Line 1 | Title (up to 60 characters) | | | | | | | | | |
| Line G1 | $L_{b0}$ | $L_v$ | $W_D$ | $\lambda/W_D$ | $H_0$ | $H_c$ | $S_0$ | K | $L_c$ | Bkslp |
| Line G2 | a | b | c | $\eta_{Bed}$ | $\eta_{Bank}$ | | | | | |
| Line V1 | $V_{ss\,1}$ | $V_{sc\,1}$ | | | | | | | | |
| Line V2 | $V_{ss\,2}$ | $V_{sc\,2}$ | | | | | | | | |
| . | . | . | . | | | | | | | |
| . | . | . | . | | | | | | | |
| . | . | . | . | | | | | | | |
| Line $V_3$ | $V_{ss\,n}$ | $V_{sc\,n}$ | | | | | | | | |

where $L_{b0}$ = Initial length of the bend (feet)

$L_v$ = Average downvalley length through the bend (feet)

$W_D$ = Dominant width of the arroyo (See Section 3.4.5, page 3-71, Equations 3.78 and 3.79)

$\lambda/W_D$ = Ratio of meander wavelength to dominant width of the channel (see Equation 3.74, p. 3-69)

$H_0$ = Initial average bank height through the bend (feet)

$H_c$ = Critical bank height (feet) (See 3.4.5, pages 3-58 through 3-64, Figure 3.20)

$S_0$ = Initial bed slope

K = Calibration factor for erosion rate (default = 1.00). Use a calibration factor of 1.0, unless erosion rate data is available from a field calibration study to substantiate a different factor. At the time of preparation of this Design Guide, no field calibration studies are available for the Albuquerque area.

$L_c$ = Spacing of lateral controls (feet) (input -1 if $L_c > 7W_D$)

Bkslp = Average slope of overbank perpendicular to the channel (Horizontal distance/vertical distance)

$a,b,c$ = Coefficient and exponents for the bed material sediment transport capacity relationship given by (See Section 3.3.4, pages 3-32 through 3-38)

$$q_s = a\ V^b Y^c$$

$$a = a'[1 - (C_t/10^6)]^d$$

$\eta_{Bed}$ = Average poposity of bed material

$\eta_{Bank}$ = Average porosity of overbank material

$V_{ss\ i}$ = Unbulked volume of sediment supplied to the reach during the i-th time increment ($ft^3$)

$V_{sc\ i}$ = Unbulked volume of bed material that would be transported through the reach during the i-th time increment based on the existing capacity ($ft^3$) bed material transport

The accompanying diskette contains the executable program (CURVCALC.EXE), the FORTRAN source code (CURVCALC.FOR), two test input files (TESTCURV.IN and TESTCCG1.IN) and two test output files (TESTCURV.OUT and TESTCCG1.OUT). It is recommended that the program be run using the test data input files and the results compared with the test data output files contained on the disk to insure that the program executes properly on the user's computer.

# APPENDIX E

## Computer Program for Estimating Sediment Basin Trap Efficiency (TRAPMIX)

# APPENDIX E

## TRAPMIX

## A Computer Program for Estimating Trap Efficiency

### E.1. General

This program computes the trap efficiency of a sediment mixture given the average velocity, settling depth, and settling length. The procedure is based on the turbulent settling depth as presented in "Solid Particle Settlement in Open-Channel Flow", (Li and Shen, 1975, ASCE J. Hydraulics, HY7, pp 917-931). The effect of high suspended sediment concentrations is accounted for using the following relationship, proposed by Richardson and Zaki (1954):

$$W_p = w_p \, (1 - C_w)^{2.35}$$

where $W_p$ = settling velocity of the particle in the water/sediment mixture
$w_p$ = settling velocity of that particle in clear water
$C_w$ = total sediment concentration in the water/sediment mixture

Please note that this approach is one of many available for computing trap efficiency. It is important to understand that, while this approach is believed to overcome may of the weaknesses of other available methods, it is relatively untested. Comparison of results from the program with field data in the specific area to which it is applied would be very desirable. The user should be aware that there are a number of assumptions inherent in the model, which are spelled out in Li and Shen (1975) and/or in Section 5.5 of this Design Guide. It is the responsibility of the user to insure that the procedure and assumptions are applicable to their specific problem; Resource Consultants & Engineers, Inc. makes no warranty, expressed or implied, as to the accuracy of the procedure for a specific application or the acceptability of the results obtained therefrom and accepts no liability of any type related to the program or its use.

## E.2. Input Data

Input data for the program consists of the gradation of the inflowing sediment mixture, and the average velocity, settling depth, settling length and inflowing sediment concentration. Each line of input, as specified below, can be unformatted or comma-delimited. The input file is organized as follows:

| | | | | |
|---|---|---|---|---|
| Line 1 | Title (up to 60 characters) | | | |
| Line 2 | n | | | |
| Line $S_1$ | $D_{g\,1}$ | $\Delta_1$ | | |
| Line $S_2$ | $D_{g\,2}$ | $\Delta_2$ | | |
| . | . | . | | |
| . | . | . | | |
| . | . | . | | |
| Line $S_n$ | $D_{g\,n}$ | $\Delta_n$ | | |
| Line $H_1$ | $V_{avg\,1}$ | $D_{avg\,1}$ | $L_{s\,1}$ | $C_{s\,1}$ |
| Line $H_2$ | $V_{avg\,2}$ | $D_{avg\,2}$ | $L_{s\,2}$ | $C_{s\,2}$ |
| . | . | . | . | . |
| . | . | . | . | . |
| . | . | . | . | . |
| Line $H_m$ | $V_{avg\,m}$ | $D_{avg\,m}$ | $L_{s\,m}$ | $C_{s\,m}$ |

where n = number of sediment size ranges

$D_{g\,i}$ = geometric mean size of the i-th size range in mm
$= \sqrt{(D_i D_{i+1})}$

$\Delta_i$ = Percentage of material in the i-th size range

m = number of hydraulic data sets to be evaluated

$V_{avg}$ = Average velocity (fps)

$D_{avg}$ = Average settling depth (feet)

$L_s$ = Settling length (feet)

$C_s$ = Total inflowing sediment concentration (decimal fraction by weight)

The accompanying diskette contains the executable program (TRAPMIX.EXE), the FORTRAN source code (TRAPMIX.FOR), and an input (TESTTRAP.IN) and output file (TESTTRAP.OUT) for the test data set. Note that the test data contains a sediment gradation with 12 size ranges and 36 separate hydraulic data sets. It is recommended that the program be run using the test data input file and the results compared with the test data output file contained on the disk to insure that the program executes properly on the users computer.

# APPENDIX F

## LaCueva Tributary Prudent Line Report

# APPENDIX F

A prudent line evaluation of a tributary to LaCueva Arroyo between Tennyson Street and Modesto Avenue was performed by for AMAFCA by RCE in 1992. This study illustrates the application of many of the procedures presented in this Design Guide to an actual problem. The accompanying paper, which was presented at the Arid West Conference of the Association of State Floodplain Managers held in Las Vegas, Nevada, in December 1992, summarizes the important aspects of the study. The complete study report, including backup calculations, can be reviewed by contacting AMAFCA.

# DELINEATION OF EROSION AND FLOODING LIMITS ALONG ARROYOS IN URBANIZING AREAS

Robert A. Mussetter
Resource Consultants & Engineers, Inc.

Michael D. Harvey
Resource Consultants & Engineers, Inc.

Clifford E. Anderson
Albuquerque Metropolitan Arroyo Flood Control District

## Introduction

Urbanization along ephemeral flow arroyos in the arid southwest frequently poses difficult and complex problems for planning and regulatory agencies, developers and design engineers. Runoff producing storm events in this environment occur relatively infrequently, but when they do occur, hydraulic and sediment transport conditions in the arroyos are very intense, often resulting in significant lateral and vertical adjustment of the channels and damage to adjacent property by flooding and erosion. Due to the dynamic nature of arroyos, it is imperative that appropriate steps be taken to protect adjacent property from damage during such storm events. Lining of the arroyos with non-erosive or erosion resistant material historically has been the method of choice to prevent such damage. While this approach may maximize the land area available for development and minimize the risk of damage, the cost, in terms of construction and maintenance, as well as degradation of the natural environment may be unacceptable.

To balance the need to protect public safety with the growing public desire to maintain a natural environment, the Albuquerque Metropolitan Arroyo Flood Control Authority (AMAFCA) has recognized that some arroyos within their area of concern should remain in a natural or naturalistic condition to protect public safety during storm events, safeguard the local environment and meet the policy goals of other governmental agencies. In many cases, these goals can be accomplished by use of setbacks and installation of selective stabilization measures to maintain a naturalistic environment while also protecting adjacent property.

In 1991, Resource Consultants & Engineers, Inc. (RCE) was retained by AMAFCA to develop a manual to guide local agencies and consultants in the analysis of arroyos in the Albuquerque metropolitan area. Specific concerns in the evaluation include the potential for flooding and erosion damage during storm events and, where appropriate, establishment of an erosion limit line within which it would not be prudent to develop. The manual also provides guidance on the use of selective

stabilization measures that can reduce the width of the corridor within the erosion limit line while maintaining the desired naturalistic environment. The Prudent Line concept was discussed in detail in Lagasse, et al. (1985) and previously presented to the ASFPM by Lagasse and Schall (1988). At present, AMAFCA defines the erosion limit line as a boundary along an unlined arroyo that would have a low possibility of being disturbed by flooding or erosion by any storm up to and including the 100-year storm occurring at any time during a thirty year period.

As originally applied, the prudent line concept emphasized the erosion processes associated with incised arroyos where the potential for erosion damage rather than flooding was the primary concern. In certain portions of the Albuquerque metropolitan area, however, the arroyos are aggradational which creates channel capacity problems and the potential for avulsion during flood events. In this case, the Prudent Line is defined, not by the potential limit of channel erosion but rather, by the limits of overbank flooding, and hence is very similar to the alluvial fan flooding problem. In either case, the expected response of the arroyo to flood flows is governed by the relative balance between the capacity of the arroyo to transport sediment in relation to the supply of sediment from upstream.

The purpose of this paper is to demonstrate the methodologies outlined in the manual for evaluating flooding and erosion concerns by applying them to a reach of a tributary to La Cueva Arroyo.

## Description of the Study Area

The area of concern in this study was an approximately 1,000 foot long unincised reach of a tributary of La Cueva Arroyo, located in a rapidly urbanizing region of the Ceja Pediment, northeast of metropolitan Albuquerque (**Figure 1**). The watershed area upstream of the study reach drains approximately 380 acres of the western face of the Sandia Mountains. Limited development of the watershed includes low-density residential lots and some commercial development. Several roads cross the arroyo upstream of the study reach with flow conveyance structures varying from one or more relatively small CMP pipes to a double 6 foot by 6 foot box culvert connected to a 72" reinforced concrete pipe which delivers water from the upstream side of Tramway Boulevard to the upstream end of the study reach west of Tennyson Street. Through the study reach, the arroyo crosses several residential lots with houses located from 25 to 50 feet from the existing active channel.

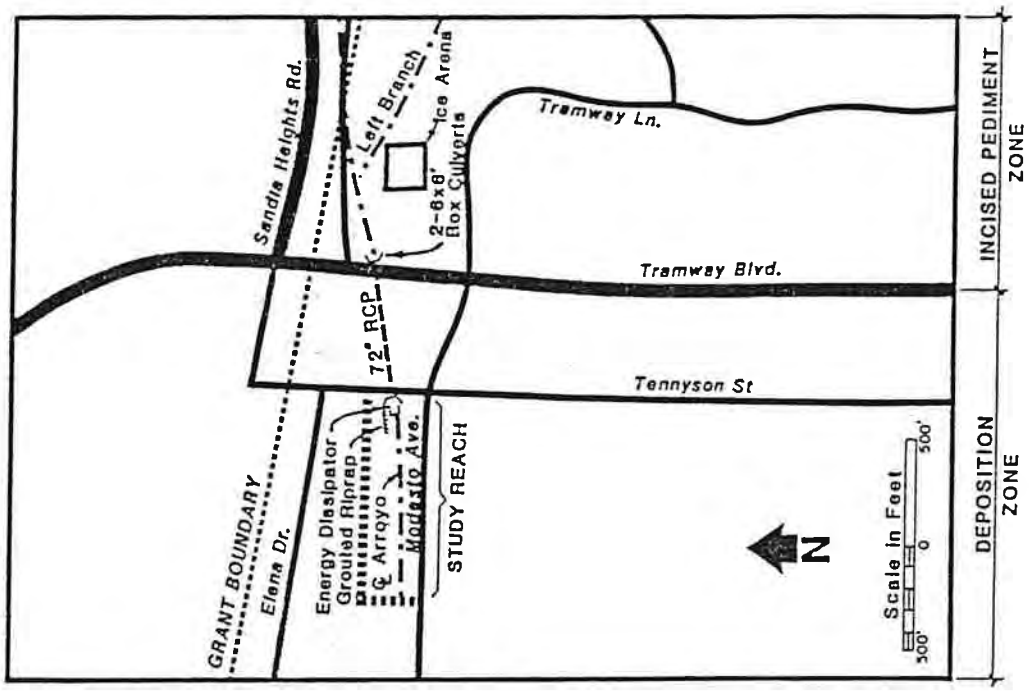


Figure 1. Schematic showing general vicinity of study reach.

## Study Approach

Evaluation of the erosion and flooding limits along the study reach was based on the geomorphic characteristics of the arroyo, the estimated clear water discharge in the arroyo upstream and within the study reach for the 2- through 100-year storm events, the estimated sediment yield from the upstream watershed area, and the sediment transport capacity of the arroyo both upstream and within the study reach. An important factor in the analysis was the impact of the upstream road crossings on both the amount and timing of water and sediment input to the study reach.

## Geology and Geomorphology of the Study Area

The Albuquerque basin can be divided informally into four quadrants on the basis of landscape components, channel characteristics and underlying geology. A convenient north-south line is the Rio Grande River and the east-west dividing line is Interstate 40 on the west side of the river and Tijeras Arroyo on the east side (RCE, 1991). The drainage basin of the La Cueva tributary is located in the Northeast Quadrant. The quadrant is included within a landscape unit that is referred to as the East Mesa, a pediment surface which is underlain by the Santa Fe Formation. The quadrant can be further

subdivided into three roughly parallel, north-south trending geomorphic subunits, west of the granitic Sandia Mountains. These subunits, from the Sandia Mountain front westward, are an alluvial fan zone, an incised pediment zone and a depositional zone.

The reach of concern in this study is located just downstream of Tennyson Street at the approximate eastern boundary of the depositional zone (Figure 1). The arroyo is characteristically braided and the active channel is actually perched above the surrounding overbank areas. The depositional nature of the arroyo in this area has created a convexity in the longitudinal profile. Comparison of historical thalweg profiles indicates a slight degradational trend in the study reach since 1973. Due to the braided nature of the arroyo in this area, however, this apparent trend may be due to shifting of the thalweg during storm events rather than the result of degradation due to a deficit in the sediment supply.

Bed material sediment in the arroyo channel consists primarily of coarse sand (D50~1.9 mm) with some fine gravel and relatively small amounts (<5 percent) of silt and clay (**Figure 2**). The gradation of the bank material is roughly the same as the bed material, however, it contains somewhat greater amounts (~10 percent) of silt and clay. The curve labelled "detrital apron" in Figure 2 was developed from a sediment sample taken from the detrital wedge at the toe of a bank just upstream of the detailed study reach and is representative of the bank material in this area. The bulk of the sediments exposed in the channel bed and banks are horizontally bedded which is characteristic of fluvial sediment transport under upper regime flow conditions. The presence of the horizontal bedding indicates that sediment concentrations lie within the range of water floods (<20 percent by volume). Within some of the sedimentary deposits, there is no stratification and the coarser sediments are interspersed among the finer sediments, a characteristic of mud flood (hyperconcentrated flow with solid concentrations up to ~40 percent by volume) deposits.

## Hydrology

Clear water hydrographs for the study reach were developed for the 2- through 100-year return period storm events using the AHYMO computer program (AMAFCA, 1992). The analysis was performed using AMAFCA's recommended storm distribution and considered the precipitation/runoff characteristics of the watershed and the routing characteristics of the arroyo channel resulting from in-channel flows and ponding upstream of the road crossings. The clear water peak discharges at the upstream end of the study reach ranged from 168 cfs for the 2-year storm to 1045 cfs for the 100-year storm. Runoff volumes ranged from 7.1 acre-feet to 40.2 acre-feet for the two storms, respectively.

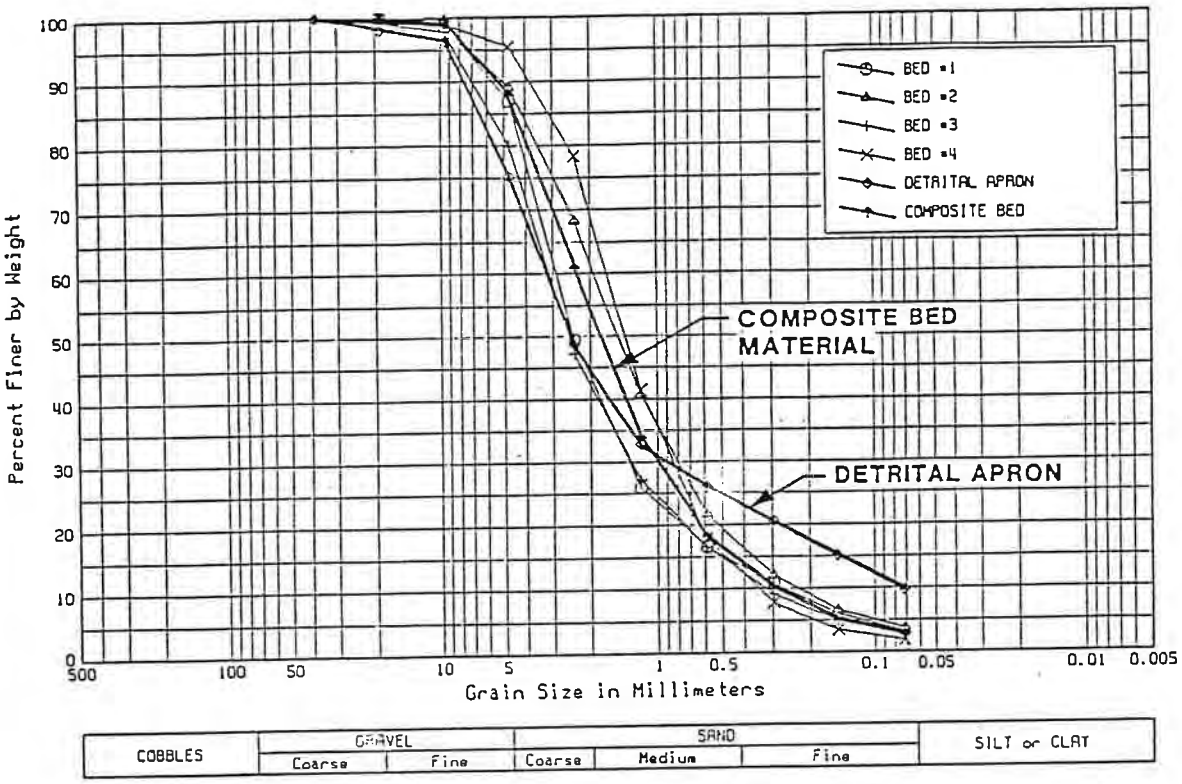


Figure 2. La Cueva tributary bed material gradations.

## Hydraulic and Sediment Transport Analysis

The hydraulic analysis was performed using the Corps of Engineers HEC-2 computer program (COE, 1991) to define the limits of flooding for the peak flood discharges and to estimate the flow velocities, depths and widths for use in the sediment transport analysis. The analysis was complicated by several factors including: (1) the steepness of the reach (~3.5 percent) (The HEC-2 model indicated supercritical flow under rigid boundary conditions), (2) the highly erodible nature of the sediments in the arroyo, (3) the wide range of hydraulic roughness due to the presence of chamisa and other vegetation, sedimentary bars and debris within the channel, (4) the ill-defined flow paths within this characteristically braided reach of arroyo, and (5) the presence of the box culverts and 72" RCP which deliver water from the arroyo upstream of Tramway Road to the study reach.

The fifth factor presented a particularly difficult problem in defining the quantity and timing of water and sediment delivery to the detailed study reach since the double 6 foot by 6 foot box culvert creates a backwater condition at discharges greater than approximately 50 cfs with flow overtopping the left bank at approximately 325 cfs. Overbank flows leaving the channel at this location spill across

Tramway Boulevard, flow overland and re-enter the arroyo downstream of Tennyson Street (Figure 1). The presence of the backwater normally would lead to the conclusion that significant sediment trapping would occur upstream of the box culvert inlet, resulting in a deficit of sediment to the study reach and consequent channel degradation.

The interactions among the first four factors create a problem that is very similar to that encountered in flood analysis on alluvial fans. The 100-year flood profile, upon which the finished floor elevations for the residents along the arroyo were based, was established using the results of a supercritical HEC-2 flow analysis for clear water conditions. There is considerable doubt that supercritical flow conditions will persist in an alluvial channel for more than a very short distance due to the interaction between the flowing water and the channel boundary and the effects of obstructions (Chang, 1988, Trieste, 1992). In fact, the alluvial fan flooding procedure used by FEMA is based on the assumption of critical flow conditions. In natural channels with steep slopes, energy is dissipated by a variety of factors to reduce the erosive nature of the flow. This most often occurs through the formation of bed forms (antidunes or chutes and pools in sand bed streams and step-pool structure in cobble and boulder bed streams (Grant and Mizuyama, 1991) and the presence of obstructions. In most cases, in steep channels the flow is characterized by alternating short reaches of supercritical and subcritical flow with hydraulic jumps forming the transition between the super- and subcritical condition. The appropriateness of clear water, supercritical flow analysis for establishing regulatory flood profiles and flood hazard boundaries is, therefore, questionable, at best.

The sediment transport analysis involved estimation of the bed material transport capacity of the arroyo upstream and through the detailed study reach. Although the amount of fine sediment (silt and clay) in the watershed soils is relatively small, it is sufficient to increase the fine sediment load in the flood flows which can significantly increase the bed material transport capacity due to its effect on fluid viscosity and turbulence. Fine sediment loading to the arroyo during storm flows was estimated using the MUSLE equation (Williams and Berndt, 1972), with the values of the variables estimated from topographic mapping of the watershed, data from the Bernallilo County soil survey (SCS, 1977). field observations and the results of the hydrologic analysis. The coefficient of the MUSLE equation was adjusted based on available data for the Albuquerque area.

The bed material transport capacity of the arroyo was computed using the Meyer-Peter, Muller bed load equation and Einstein integral for the suspended bed material concentration (Simons, Li & Associates, Inc., 1982). The basic computed capacity was adjusted for the presence of fine sediment using the Colby procedure (Colby, 1964) and the result was adjusted by a calibration factor to obtain a reasonable total sediment yield for the individual storms and on a mean annual basis.

The sediment transport analysis results indicated a maximum sediment concentration by weight of approximately 130,000 parts per million which would increase the 100-year peak discharge by approximately 6 percent above the clear water discharge from the AHYMO analysis. The resulting total sediment yields varied from -1.8 tons per acre for the 2-year flood to -16.6 tons per acre for the 100-year flood with an average annual yield of -2.9 tons per acre based on integration of the flood flow frequency curve.

The flood profiles for the 100-year event were reanalyzed using the bulked discharge to account for the effect of sediment transport on the volume of the fluid/sediment matrix. The increase in water-surface elevation above the clear water analysis result was approximately 0.1 feet at most locations. The computed bed material transport capacities were also used to perform a continuity analysis to evaluate the vertical stability of the arroyo within the study reach. The continuity analysis showed that the study reach was slightly aggradational under existing conditions, assuming that all of the sediment carried by the arroyo upstream of Tramway Boulevard is delivered to the study reach through the box culverts and 72" RCP. Trapping of sediment upstream of Tramway Boulevard will result in a degradational tendency and channel incision.

## Discussion

### Degradation Potential

A detailed analysis of the hydraulic conditions at the box culvert inlet upstream of the study reach indicated that, while a significant portion of the flow during floods larger than the 5-year event will flow overland rather than through the culverts and RCP pipe, the effect on the downstream clear water hydrograph was insignificant (**Figure 3**). The initial sediment continuity analysis for this location indicated that a significant amount of bed material sediment should be trapped in the backwater area upstream of the box culvert, thereby creating a sediment deficit to the study reach. Field observations and available survey data, however, show that, in spite of several runoff events in recent years, including a 1991 storm that is believed to have been in excess of the 5-year event, the channel upstream of the box culverts has actually degraded slightly and the expected degradation in the study reach has not occurred. From a detailed evaluation of the hydraulic conditions at the culvert inlet during the passage of a flood hydrograph, it was determined that a positive feedback mechanism would occur between the sediment deposition and the energy gradient (and thus sediment transport capacity). As the depositional sediment wedge begins to develop, the local energy gradient steepens, increasing the sediment transport capacity and removing the deposited sediment, thus the expected net deposition in the culvert backwater does not occur. Additionally, a relatively constant channel width is maintained

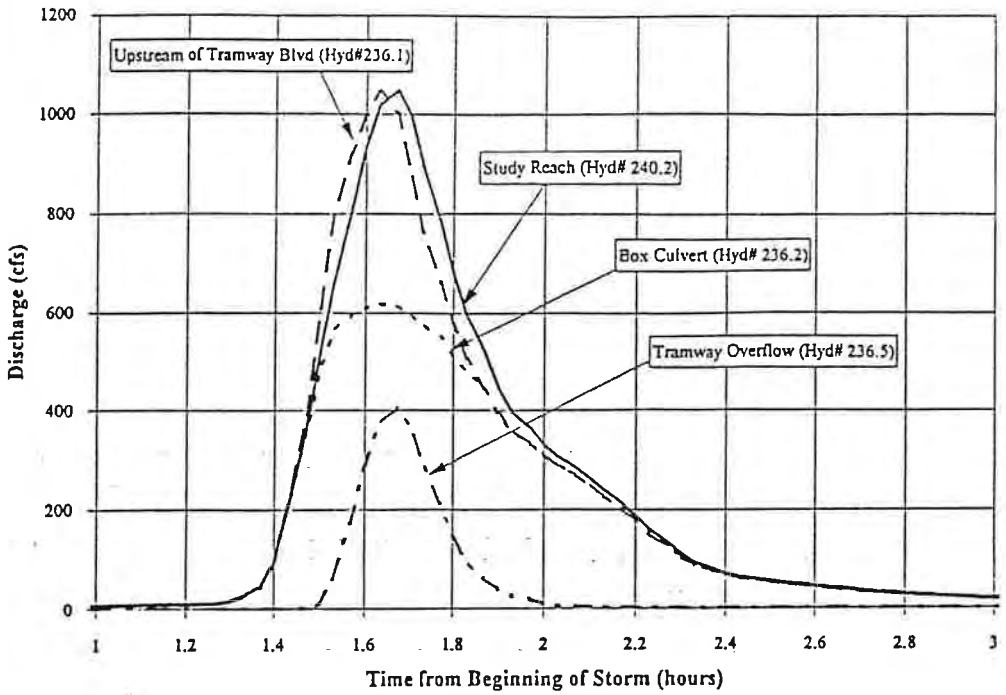


Figure 3. 100-year storm hydrographs.

from the upstream arroyo into the box culvert which confines the flow and helps to maintain the flow velocity through the inlet region. As a result, the majority of the sediment delivered from upstream during previous floods has passed through the culverts, maintaining the supply of sediment to the downstream study reach. For these conditions, the continuity analysis indicates that the study reach is slightly aggradational for the range of storms considered in the analysis.

Maintenance of sediment transport through the culvert is related primarily to the relatively large capacity of the box culvert inlet and confined channel upstream of Tramway Boulevard. Although a backwater condition develops due to energy losses at the culvert inlet, the opening is sufficiently large to allow adjustment of local energy gradient and removal of the deposited sediment before the inlet becomes plugged. The relatively large opening also reduces the possibility of plugging with debris during the storm. Although debris blockage at the culvert inlet apparently has not occurred during previous storms, it is a distinct possibility given the amount of tumbleweeds and other debris that tends to build up in the arroyo during long periods of little or no flow. This possibility should not be overlooked when evaluating the potential response of the arroyo to future flood flow. To account for this possibility, two scenarios were analyzed, assuming that 50 percent and 75 percent of the bed material supply would be trapped upstream of the culverts, respectively. Under both scenarios, the expected response of the upstream half of the study reach changed from slightly aggradational to strongly degradational. If this were to occur, rapid incision of the arroyo would result.

Flooding Potential

The limits of flooding that could be expected for the 100-year flood were evaluated using the HEC-2 model and supplemental calculations. Since the model considers only rigid boundary conditions, additional analyses are necessary to obtain realistic maximum water surface profiles. This was accomplished by developing the supercritical flood profile for rigid boundary conditions with the HEC-2 model and using the results to estimate the subcritical flow depth that could occur through a hydraulic jump (the sequent depth) for the given flow condition. The subcritical depth was computed using the hydraulic jump equation found in most open-channel flow texts (e.g., Chow, 1959; Henderson, 1966). This depth is believed to be a realistic representation of the maximum depth that could occur and is recommended for use in establishing the water surface elevations and flood protection boundaries under upper regime, chute and pool conditions likely during the peak of a flood.

**Figure 4** shows a typical cross section of the arroyo near the middle of the detailed study reach with the supercritical and subcritical (conjugate) water-surface elevations, the energy gradeline elevation and the location and finished floor elevation of the residence at that cross section. The conditions at this cross section illustrate the potential effect of basing the flood elevation on the supercritical water-surface elevation rather than the corresponding subcritical elevation. Using the supercritical elevation, the residence would be safe from flooding during the 100-year storm. The conjugate depth, however, indicates that the house would be subject to flooding during that event.

Lateral Erosion Potential

It is important to emphasize that the above discussion of flow depths is based on a rigid boundary analysis. Using the assumption that all of the sediment delivered from upstream will pass through the box culvert, the channel is slightly aggradational. The average bed elevation will, therefore, remain relatively stable. Deposition within the active channel may cause lateral erosion of the relatively low banks. Due to the overbank topography, however, the flood limits rather than an erosion setback distance from the existing channel banks will define the boundary within which it would not be prudent to develop.

Based on the scenarios assuming blockage of the culvert inlet and trapping of sediment upstream of Tramway Boulevard, this conclusion would be invalid. Under these conditions, rapid incision of the arroyo would occur, consolidating the existing multiple flow paths into a single channel and most likely increasing the in-channel capacity for flood flows. The stability of the banks would, however, decrease and lateral erosion of the channel would become the primary concern. Evolution of the arroyo from the initial state of disequilibrium to a new state of dynamic equilibrium would occur, following the incised channel evolution model (ICEM) (Schumm et al., 1984). A discussion of this model is included in the Design Guide (RCE, 1991).

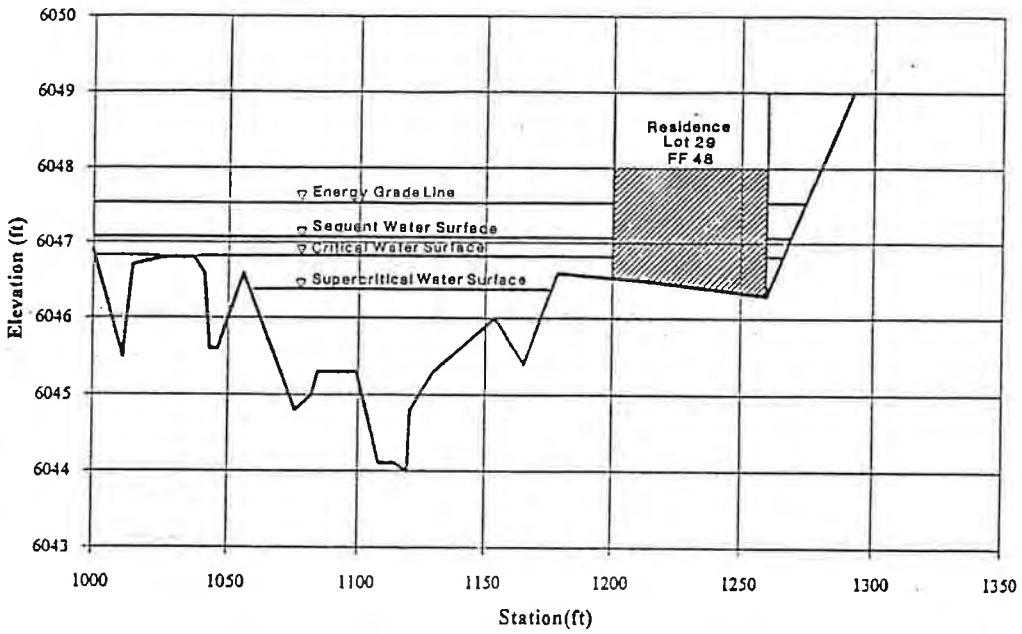


Figure 4. Cross section at Lot #29 showing water surface elevations for 100-year flood and finished floor elevation. (Drainage Management Plan and lot design based on supercritical water surface elevations).

According to the ICEM, the arroyo will initially incise very rapidly until the critical bank height is exceeded (based on geotechnical considerations). At this point, the dominant bank erosion process will change from grain-by-grain erosion to mass failure. When this condition is reached, a period of channel widening, with moderate to slight incision will ensue. Eventually, the channel geometry and gradient within the incision will adjust to achieve a state of dynamic equilibrium with the upstream supply of water and sediment. During the period of adjustment, severe bank erosion will occur in the absence of stabilization measures. Establishment of an erosion limit line would, therefore, be based on the expected lateral erosion distance resulting from the mass bank failures and removal of the failed material by fluvial transport. Although the lateral erosion process is essentially a sediment continuity problem, precise quantification of the lateral erosion distance is difficult due to the complexity of the erosion mechanism. (Procedures for estimating the lateral erosion distance are also discussed in the Design Guide (RCE, 1991)). As a general rule-of-thumb, it can be reasonably assumed that the maximum lateral erosion distance within one wavelength of channel would be about 2.5 channel widths, based on the minimum radius of curvature that could develop before channel avulsion or cutoff of the bend would occur.

## Conclusions

This analysis illustrates that the concept of the prudent line should not be interpreted to represent only an erosion boundary. For a relatively shallow arroyo in a vertically stable or aggradational condition, the limits of flooding may be significantly wider than the potential erosion limits. The analysis also illustrates the precarious balance between the sediment supply and sediment transport capacity in the arroyo environment. For the case considered here, debris blockage at the box culvert upstream of the study reach is a very distinct possibility which would probably cause incision of the arroyo within the study reach. In the area of the incision, the flood carrying capacity of the arroyo would increase but the possibility of lateral erosion will increase due to the increased bank height. The erosion limits would thus become the controlling factor for protection of adjacent property. The incision would result in a temporary increase in sediment transport and probable increased aggradation in the next downstream reach, with the associated flooding and channel stability problems. This process can be observed in several locations in the vicinity of the study reach on this and other arroyos where undersized culverts, unconfined channels leading to the culvert inlet and/or severe backwater have caused trapping of sediment. As a consequence, the downstream channel has rapidly incised to depths of greater than 10 feet.

# REFERENCES


Albuquerque Metropolitan Arroyo Flood Control Authority (AMFCA), 1992. "AHYMO, AMAFCA Hydrologic Model Users Manual."

Chang, H.H., 1988. "Fluvial Processes in River Engineering," San Diego State University, San Diego, California. A Wiley-Interscience Publication, John Wiley & Sons, New York.

Chow, V.T., 1959. "Open-Channel Hydraulics," McGraw-Hill Civil Engineering Series.

Colby, B.R., 1964. "Practical Computations of Bed-Material Discharge," Journal of the Hydraulics Division, ASCE, v. 90, no. HY2.

Grant, Gordon E., Mizuyama, T., 1991. "Origin of Step-Pool Sequences in High Gradient Streams: A Flume Experiment," Japan-U.S. Workshop on Snow Avalanche, Landslide, Debris Flow Prediction and Control.

Henderson, F.M., 1966. "Open Channel Flow," The Macmillan Company.

Lagasse, P.F., Schall, J.D., and Peterson, M.R., 1985. "Erosion Risk Analysis for a Southwestern Arroyo," ASCE, Journal of Urban Planning and Development, v. 111, no. 1, pp. 10-44.

Lagasse, P.F. and Schall, J.D., 1988. "Delineation of a Flooding and Erosion Buffer for a Southwestern Arroyo," Association of State Floodplain Managers, Proceedings of the Conference on Arid West Floodplain Management Issues.

Resource Consultants & Engineers, Inc., 1991. "Sediment and Erosion Design Guide," prepared for Albuquerque Metropolitan Arroyo Flood Control Authority.

Schumm, S.A., Harvey, M.D., and Watson, C.C., 1984. "Incised Channels: Morphology, Dynamics and Control," Water Resources Publications, Littleton, Colorado.

Simons, Li & Associates, Inc., 1982a. "Engineering Analysis of Fluvial Systems," Fort Collins, Colorado. Available from BookCrafters, Inc., Chelsea, Michigan.

Soil Conservation Service, 1977. "Soil Survey of Bernallilo and Parts of Sandoval and Valencia Counties, New Mexico."

Trieste, Douglas J., 1992. "Evaluation of Supercritical/Subcritical Flows in High-Gradient Channel", Journal of the Hydraulics Division, ASCE, v. 188, No. HY8, pp 1107-1118.

U.S. Army Corps of Engineers, 1990. HEC-2 Water Surface Profiles User's Manual.

Williams and Berndt, 1972. "Sediment Yields Computed with Universal Equation," J. Hydraulics, ASCE, v. 102, no. HY9, pp. 1241-1253.

# APPENDIX G

## Example Problems

# APPENDIX G

# EXAMPLE PROBLEMS

Given an arroyo with the following characteristics:

- Relatively flat bottom with minor cross section irregularity, gradual variation in cross section shape,
- Negligible obstructions (small vegetation),
- Vertical banks ~ 3 ft high,
- Sparse vegetation within the active channel,
- Minor sinuosity,
- 100-year Peak Discharge = 1,045 cfs,
- Channel width (W) = 39 ft,
- Bed slope ($S_0$) = 4%,
- Bed material size $D_{50}$ = 1.9 mm, $D_{84}$ = 4.2 mm, $D_{16}$ = 0.48 mm, and
- Channel thalweg (minimum bed) elevation = 6,000 ft MSL.

## I. HYDRAULICS

1. Compute normal depth, velocity and Froude Number for the peak of the 100-year storm.

   Use Manning's equation assuming wide rectangular channel to compute normal depth:

$$q = \frac{1.49}{n} y^{5/3} \sqrt{S_e} \qquad (3.3)$$

   From continuity $q = Q/W_d = 1045/39 = 26.8$ cfs/ft

   Estimate Manning's n using Brownlie's equation for the base n-value ($n_b$) and Equation 3.11 to adjust $n_b$ for channel irregularities, etc. Due to the steepness of the arroyo, upper regime flow is expected; therefore, use Equation 3.13 for $n_b$:

$$n_b = [1.0213\ (R/D_{50})^{0.0662}\ S_0^{0.0395}\ G^{0.1282}]\ 0.034\ D_{50}^{0.167} \qquad (3.13)$$

$$G = \frac{1}{2}\left(\frac{D_{84}}{D_{50}} + \frac{D_{50}}{D_{16}}\right) = \frac{1}{2}\left(\frac{4.2}{1.9} + \frac{1.9}{.48}\right) = 3.1$$

Assume R = 2 ft

$$n_b = \left[1.0213 \left\{\frac{2}{(1.9/304.8)}\right\}^{0.0662} (0.04)^{.0395} (3.1)^{.1282}\right] 0.034 \left(\frac{1.9}{304.8}\right)^{0.167} = 0.022$$

From Equation 3.11 and Table 3.2:

$$n = (n_b + n_1 + n_2 + n_3 + n_4)\ m \qquad (3.11)$$

Rearrange Equation 3.3:

$$n = (0.022 + .004 + 0 + .002 + .007)\ 1.0 = .035$$

$$y = \left[\frac{qn}{1.486\sqrt{S_o}}\right]^{\frac{3}{5}} = \left[\frac{(26.8)(.035)}{1.486\sqrt{.04}}\right]^{\frac{3}{5}} = 2.0\ ft$$

By continuity:

$$v = \frac{q}{y} = \frac{26.8}{2.0} = 13.4\ fps$$

$$A = \frac{Q}{v} = \frac{1045}{13.4} = 78.0\ ft^2$$

$$F_r = \frac{v}{\sqrt{gy_n}} = \frac{13.4}{\sqrt{g\ (2.0)}} = 1.67 \qquad (3.24)$$

2. Compute normal depth water surface elevation.

$$WSEL_n = Z + Y_n = 6000 + 2.0 = 6002.0\ ft\ MSL$$

3. Compute energy gradeline elevation.

$$EGL = Z + Y_n + \frac{V^2}{2g} = 6000 + 2.0 + \frac{13.4^2}{2g} = 6004.8\ ft\ MSL$$

4. Compute critical depth ($y_c$) and critical water surface elevation ($CWSEL_{crit}$).

By continuity and Equation 3.24:

$$y_c = \sqrt[3]{\frac{q^2}{g}}$$

$$y_c = \sqrt[3]{\frac{26.8^2}{g}} = 2.8 \text{ ft}$$

$$CWSEL_{crit} = Z + Y_c = 6002.8$$

5. Compute conjugate (or sequent) depth and water surface elevation. (This is the expected high-water condition for natural channels. Bank protection and protection of structures will require appropriate freeboard.)

$$CWSEL_{seq} = CWSEL + 0.5\,(A/W)\,(\sqrt{1 + 8\,F_r^2} - 3 \qquad (3.23)$$

$$CWSEL_{seq} = 6002 + 0.5\left(\frac{78}{39}\right)(\sqrt{1 + 8(1.67)^2} = 6002 + 1.83$$

$$= 6003.83 \text{ ft MSL}$$

## II. SUPERELEVATION ON A CURVE

At one location, the arroyo in the previous problem makes a bend. From available mapping, the radius of curvature of the bend ($r_c$) is estimated to be 195 feet.

1. Compute the superelevation on the outside of the curve for normal depth, at the peak of the 100-year storm.

$$\Delta Z = C \frac{v^2 W}{g r_c} \qquad (3.22)$$

From Table 3.3, with rapid flow, rectangular channel, and circular curve, C = 1.0.

$$\Delta Z = 1.0 \frac{(13.4)^2 (39)}{g(195)} = 1.1 \ \textit{feet}$$

2. Compute the expected water surface elevation on the outside of the bend.

$$CWSEL_{Bend} = Z + y_n + \Delta Z$$

$$= 6000 + 2.0 + 1.1$$

$$= 6003.1 \ \textit{ft MSL}$$

## III. SHEAR STRESS

Determine if the bed material is mobile at the peak of the 100-year flood.

1. Compute total average shear stress in the channel.

$$\tau_0 = \gamma\ RS \approx \gamma\ y_n\ S = (62.4)\ (2.0)\ (0.04) = 5.0\ psf \qquad (3.8)$$

2. Compute grain shear stress ($\tau'_o$).

   Use Equation 3.26 where $k_s = 3.5\ D_{84}$

$$\tau_0 = \frac{\rho V^2}{[5.75\ \log(12.27\ \frac{y_n}{k_s})]^2} = \frac{(1.94)\ (13.4)^2}{\{5.75\ \log[12.27\ \frac{2}{(3.5)(4.2/304.8)}]\}^2} = 1.44\ psf \qquad (3.26)$$

   This result represents the grain roughness rather than the total roughness. The grain roughness is more realistic for determining bed material transport than the total shear.

3. Using the grain shear from the previous calculation, determine the critical grain size.

$$D_c = \frac{\tau_0}{0.047\ (\gamma_s - \gamma)} \qquad (3.25)$$

$$= \frac{1.44}{.047[(2.65)\ (62.4)\ -62.4]} = 0.30\ feet = 90.7mm >> 4.2mm$$

   Is the bed mobile at the given discharge? Yes.

   Is there potential for armoring? No, since $D_c >> D_{84}$ (and probably $D_{100}$).

## IV. FINE SEDIMENT YIELD

The watershed upstream of the location analyzed in the previous problems has the following characteristics:

- Drainage area = 370 acres
- Watershed soil type: 52% Rock outcrop, Orthids Complex (ROF)
  48% Tesajo-Millett (Te)
- Percent impervious (roads, roofs, etc.) = 9.5%
- Average overland slope = 9.45%
- Average slope length = 100 ft
- Rangeland, grass-like plants, 10% ground cover, no canopy
- 100-year storm runoff volume = 40.2 ac-ft

1. Compute fine sediment yield from the watershed using MUSLE:

$$Y_s = C\ 95\ (V_w\ Q_p)^{0.56}\ K\ LS\ C\ P \qquad \text{(B.1 \& B.2)}$$

where C is a calibration factor (for the Albuquerque area, use 3.0, unless data are available indicating a more appropriate value).

Estimate K value from Table B.1 (see also SCS, 1992):

for Te use 0.1 - gravelly, sandy loam and loamy sand
for ROF use 0.0 (Rock outcrop 40%, Orthids 30%)

Compute weighted K:

$$K' = \frac{(A_{ROF}\ K_{ROF} + A_{Te}\ K_{Te})}{A_{total}} = \frac{0.52(0) + 0.48(0.1)}{1.0} = 0.048$$

Estimate C value from Table B.2:

C = 0.32

P = 1.0 (no terracing)

Estimate LS using Equation B.3, page B-4:

$$LS = \left(\frac{\lambda}{72.6}\right)^{n} (0.065 + 0.0454S + 0.0065S^2) \qquad (B.3)$$

$$= \left(\frac{100}{72.6}\right)^{0.5} [0.065 + 0.0454(9.45) + 0.0065(9.45)^2]$$

$$= 1.26$$

As discussed above, use a calibration factor (C) of 3.

$Y_s$ = (3) (95) $[(40.5)\ (1045)]^{0.56}$ (0.048) (1.26) (0.32) (1.0)

= 2150 *tons fine sediment*

This result assumes 100% of the watershed is pervious. Adjust for given percent impervious:

$Y_s'$ = (1 - % impervious) $Y_s$ = (1 - 0.095) (2150) = 1946 tons

2. Compute average fine sediment concentration from watershed for the 100-year storm:

$$C_f\ (ppm) = 10^6 \frac{W_s}{W_w + W_s} \qquad (3.43)$$

$$= 10^6 \frac{1946\ (2000)}{[(40.5)\ (43560)\ (62.4) + (1946)\ (2000)]}$$

$$= 34{,}147\ ppm\text{-}w$$

## V. BED MATERIAL AND TOTAL SEDIMENT LOAD

Compute the bed material transport capacity, total sediment load and bulking factors for the peak of the 100-year storm, for the arroyo in the previous problems.

1. Compute bed material transport capacity at $Q_{100}$ = 1,045 cfs using Equation 3.41.

From Figure 3.10:

$a' = 1.5 \times 10^{-6}$
$b = 5.8$
$c = -0.7$
$d = -1.9$

From hydraulics example problem:

$V_{100} = 13.4$ fps
$y_{100} = 2.0$ ft
$W = 39$ ft

Assume constant fine sediment yield throughout the storm:

$C_f = 34{,}147$ ppm-w

Apply Equation 3.41:

$$q_s = a' V^b y^c (1 - C_f/10^6)^d \qquad (3.41)$$

$$= 1.5 \times 10^{-6} (13.4)^{5.8} (2.0)^{-0.7} \left(1 - \frac{34{,}147}{10^6}\right)^{-1.9} = 3.40 \text{ cfs/ft}$$

$$Q_s = q_s W$$

$$= (3.40)(39) = 132.6 \text{ cfs}$$

2. Compute the bed material concentration.

From Equation 3.43:

$$C_s = \frac{2.65 \times 10^6 \, Q_s}{(Q + 2.65 \, Q_s)} \qquad (3.43)$$

$$= \frac{2.65 \times 10^6 (132.6)}{1045 + 2.65(132.6)} = 251{,}642 \; ppm\text{-}w$$

3. Compute the total sediment load.

Compute the wash load discharge $(Q_f)$:

$$Q_f = \left(\frac{Q}{2.65}\right)\left(\frac{C_f}{10^6 - C_f}\right) \qquad \text{(rearranging 3.43)}$$

$$= \left(\frac{1045}{2.65}\right)\left(\frac{34{,}147}{10^6 - 34{,}147}\right) = 13.9 \; cfs$$

$$Q_{s_{Total}} = Q_s + Q_f$$

$$= 132.6 + 13.9 = 146.5 \; cfs$$

4. Compute the total sediment concentration, bulking factor, and bulked peak discharge.

$$C_{s_{Total}} = \frac{2.65 \times 10^6 \, Q_{s_{Total}}}{(Q + 2.65 \, Q_{s_{Total}})}$$

$$= \frac{2.65 \times 10^6 \, (146.5)}{1045 + 2.65 \, (146.5)}$$

$$= 270{,}875 \; ppm\text{-}w$$

$$BF = \frac{1}{1 - \dfrac{C_{s_{Total}}/10^6}{2.65 - (C_{s_{Total}}/10^6)(S-1)}} \qquad (3.53)$$

$$= \frac{1}{1 - \dfrac{270{,}875 \,/\, 10^6}{2.65 - \dfrac{270{,}875}{10^6}(2.65 - 1)}} = 1.14$$

$$Q_{p_{bulked}} = BF\, Q_p$$

$$= (1.14)\ (1045) = 1191\ cfs$$

## VI. ANNUAL SEDIMENT YIELD

The following total sediment yield results were obtained by integrating the bed material transport capacity (from Equation 3.41) and adding the fine sediment for each storm.

| Return Period (years) | Water Yield (ac-ft) | Total Sediment Yield (tons) | Unit Sediment Yield (tons/acre) |
|---|---|---|---|
| 100 | 40.2 | 6142 | 16.6 |
| 50 | 33.8 | 4863 | 13.1 |
| 25 | 27.5 | 3774 | 10.2 |
| 10 | 19.4 | 2413 | 6.5 |
| 5 | 13.7 | 1559 | 4.2 |
| 2 | 7.1 | 668 | 1.8 |

Compute the mean annual water and sediment yields.

From Equation 1.1:

$$Y_{x\,Annual} = 0.015\ Y_{x\,100} + 0.015\ Y_{x\,50} + 0.04\ Y_{x\,25} + 0.08\ Y_{x\,10} + 0.20\ Y_{x\,5} + 0.40\ Y_{x\,2} \quad (1.1)$$

where x = Either the total sediment or water yield.

(1) Water yield:

$$Y_{w\,a} = 0.015\ (40.2) + 0.015\ (33.8) + 0.04\ (27.5) + 0.08\ (19.4) + 0.2\ (13.7) + 0.4\ (7.1)$$

$$= 9.34\ ac\text{-}ft$$

Sediment yield:

$$Y_{s\,a} = .015\ (6142) + 0.015\ (4863) + 0.04\ (3774) + 0.08\ (2413) + 0.2\ (1559) + 0.4\ (668)$$

$$= 1088\ \textit{tons}$$

Unit sediment yield:

$$Y_{s\,a} = \frac{1088}{370} = 2.94\ \textit{tons/acre}$$

$$= 2.94/3.4^{*} = 0.86\ \textit{ac-ft/mi}^2$$

(*assuming bulked unit weight of 100 pcf, see Constants and Conversions, Page xiv)

## VII. EQUILIBRIUM SLOPE

For the given arroyo, estimate the equilibrium slope for the dominant discharge.

1. Estimate the dominant discharge ($Q_D$) from Equation 3.77:

$$Q_D = 0.2\ Q_{100} = (.2)\ (1045) = 209\ cfs$$

2. Estimate the hydraulic conditions for $Q_D$. Using procedures in the hydraulic example problem, the following results are obtained:

Velocity = 7.1 fps
Hydraulic depth = 0.76 ft

3. If the bed material supply at this discharge is 3.2 cfs (from similar analysis of the supply reach) estimate the equilibrium slope.

**Method 1** - Use Equation 3.56:

$$S_{eq} = \left(\frac{a}{q_{s\ supply}}\right)^{\frac{10}{3(c-b)}} q^{\frac{2(2b+3c)}{3(c-b)}} \left(\frac{n}{1.486}\right)^2 \qquad (3.56)$$

where a, b, c are given by Equation 3.41:

$$Q_s = a'\ V^b\ Y^c\ (1 - (C_f / 10^6))^d \qquad (3.41)$$

a' = $1.5 \times 10^{-6}$
b = 5.8
c = -0.7
d = -1.9

$$q = Q/W = 210/39 = 5.38 \ cfs/ft$$

$$q_{s\,supply} = Q_{s\,supply}/W = \frac{3.2}{39} = 0.082 \ cfs/ft$$

If the fine sediment concentration for ($C_f$) $Q_d$ is 10,000 ppm

$$a = a' \left(1 - (C_f/10^6)\right)^d = 1.5 \times 10^6 \left(1 - \frac{10{,}000}{10^6}\right)^{-1.9} = 1.53 \times 10^{-6}$$

$$S_{eq} = \left(\frac{1.53 \times 10^{-6}}{0.082}\right)^{\frac{10}{3\,(-0.7\,-\,5.8)}} (5.38)^{\frac{[2\,(2(5.8)\,+\,3(-0.7))]}{3(-0.7\,-\,5.8)}} \left(\frac{0.035}{1.486}\right)^2$$

$$= 0.029$$

**Method 2** - Use Equation 3.57

$$S_{eq} = S_{existing} \left(\frac{Q_{s\ Supply}}{Q_{s\ Existing}}\right)^{\left(\frac{2}{(b\,-x)}\right)} \qquad (3.57)$$

where

$$x = \left(\frac{3}{5}\right)\left(\frac{2b}{3} + c\right) = \left(\frac{3}{5}\right)\left[\frac{2(5.8)}{3} + (-0.7)\right] = 1.9$$

$$Q_{s\ Existing} = a' V^b Y^c \left(1 - (C_f/10^6)\right)^d W$$

$$= (1.5 \times 10^{-6})\ (7.1)^{5.8}\ (.76)^{-0.7} \left(1 - \frac{10{,}000}{10^6}\right)^{-1.9} (39) = 6.25 \ cfs$$

$$S_{eq} = 0.04 \left(\frac{3.2}{6.25}\right)^{\left(\frac{2}{(5.8 - 1.9)}\right)} = 0.028$$

What is the required spacing (L) of a series of grade control structures if the maximum drop height over on structure is 3 feet?

$$L = \frac{H_{max}}{\Delta S}$$

$$= \frac{3}{(0.04 - 0.028)} = 250 \textit{ feet}$$

## VIII. CONTINUITY ANALYSIS

For the given arroyo, the bed material supply to the study reach during the 100-year storm is 4,685 tons and the existing bed material transport capacity is 4,107 tons [of the total yield of 6,142 (see Part VI)].

1. If the study reach is 470 ft long, estimate the average change in bed elevation that would be expected during the 100-year storm:

   Convert bed material load to solid volume:

$$V_s = \frac{2000}{2.65\gamma} Y_s$$

   Supply:

$$V_s = \frac{2000}{2.65\gamma} (4685) = 56{,}664 \ ft^3$$

   Transport capacity:

$$V_s = \frac{2000}{2.65\gamma} (4107) = 49{,}673 \ ft^3$$

   Apply continuity equation

$$\Delta V_s = V_{s\ Inflow} - V_{s\ Outflow} \qquad (3.54)$$

$$= 56{,}664 - 49{,}673 = 6{,}991 \ ft^3$$

   Estimate average change in bed elevation from Equation 3.55, assuming porosity ($\eta$) = 0.4 (equivalent to in-situ unit weight of ~100 pcf)

$$\Delta Z = \frac{\Delta V_s}{WL\,(1-\eta)} = \frac{6991}{(39)(470)(1-0.4)} = 0.64 \text{ feet (i.e., ~0.6 of aggradation)} \quad (3.55)$$

2. Assume that a culvert upstream of the study reach is partially blocked such that half of the bed material supply is trapped with no significant change in the hydrograph in the study reach. Recompute the average change in bed elevation.

$$\Delta V_s = \frac{1}{2}(56{,}664) - 49{,}673$$

$$= -21{,}341 \text{ ft}^3$$

$$\Delta Z = \frac{-21{,}341}{(39)\,(470)\,(1-0.4)} = -1.94 \text{ ft (i.e., ~1.9 feet of degradation)}$$

## IX. LATERAL EROSION

In the equilibrium slope example, it was determined that approximately 1.2 feet of degradation per 100 feet of channel length will occur under the given conditions (i.e., $\Delta Z/100 = (0.4 - .028)\ 100 = 1.2$). Assume the arroyo in the study reach has an average bank height of approximately 3 feet; the in-situ overbank soils have a cohesion of ~200 psf, an internal friction angle of ~30°, and a porosity of 0.30; and the channel bed material has a porosity of 0.40.

1. Compute the required spacing of a series of grade control structures to avoid exceeding the critical bank height.

   Estimate the critical bank height from Figure 3.20:

   $$H_c = 9.2\ ft$$

   Compute the maximum allowable degradation.

   $$\Delta Z_{max} = H_c - H_0 = 9.2 - 3.0 = 6.2\ ft$$

   Compute the maximum spacing of the structures.

   $$L = \Delta Z_{max}/\Delta S = 6.2/(0.04 - 0.028) = 517\ ft$$

2. Estimate the maximum lateral erosion distance ($\Delta_{max}$) that can be expected for the given arroyo based on an optimal bend shape. See Section 3.4.5.

   Estimate the meander wavelength and unconstrained bend length from Equation 3.74b:

   $$\lambda/W_D = 0.8 + 4 \log Q_D \qquad (3.74b)$$

   $$= 0.8 + 4 \log (290) = 10.1$$

   Compute the dominant channel width.

   Estimate the critical slope from Equation 3.80:

$$S_c = 0.037\ Q_d^{-0.133} = 0.018 < S_o = 0.04 \quad (3.80)$$

Since $S_0 > S_c$ use Equation 3.78 to compute $W_D$:

$$W_D = 4.6\ Q_D^{0.4} = 39\ \textit{feet} \quad (3.78)$$

$$\lambda = 10.1(39) = 394\ \textit{feet}$$

$$L_{BU} = \lambda/2 = 197\ \textit{feet}$$

From Equation 3.75b:

$$\Delta_{max} = [0.2 + \log Q_D]\ W_D \quad (3.75b)$$

$$= [0.2 + \log (209)]\ (39) = 98.4\ \textit{feet} \quad (3.81b)$$

or, alternatively, from Equation 3.81b:

$$\Delta_{max} = [0.92 + 4.6 \log Q_D]\ Q_D^{0.4}$$

$$= [0.92 + 4.6 \log (209)]\ (209)^{0.4} = 98.4\ \textit{feet} \quad (3.81b)$$

For this example, $\Delta_{max}$ represents the bankline setback (BSB). The centerline setback (CSB) is BSB + $W_D/2$ = 117.9. Use a calibration factor for erosion rate (K) of 1.0, unless erosion rate data from a field calibration study is available to substantiate a different value.

3. The limits of the erosion envelope can be reduced by constructing lateral controls at intervals less than the unconstrained bend length. Assuming that the desired distance of the erosion envelope from the centerline of the downvalley direction is 50 feet, what is the required spacing of the lateral controls ($L_s$)?

Compute the ratio of maximum offset to unconstrained offset.

$\Delta_{max} / \Delta_{max\ u} = 50/98.4 = 0.51$

From Figure 3.24:

$L_s / (\lambda/2) = 0.72$

$L_s = L_{BU}\ (0.72) = (197)\ (0.72) = 142$ ft

With the supply reduced to half the existing capacity, the channel is initially nearly straight and the average slope of the overbank perpendicular to the arroyo is 3H:1V. Estimate the amount of lateral migration that would occur over a 30 year period based on the average annual sediment yield. How much additional lateral migration is likely if the 100-year storm occurred at the end of the 30 year period?

Use the CURVCALC computer program to perform the computations. The input and output files for the given data are shown in Tables G.1 and G.2, respectively. (The existing average annual bed material capacity is estimated to be 725 tons).

$$Y_{s\,a}\ (\textit{existng capacity, unbulked}) = 725\ \textit{tons}\left(\frac{2000}{(62.4)(2.65)}\right) = 8{,}770\ ft^3$$

$$Y_{s\,a}\ (\textit{supply}) = 0.5\ Y_{s\,a}\ (\textit{existing capacity, unbulked}) = 4385\ ft^3$$

$$Y_{s_{100}}\ (\textit{existing capacity, unbulked}) = 4107\ \textit{tons}\left(\frac{2000}{(62.4)(2.65)}\right) = 49{,}673\ ft^3$$

$$Y_{s_{100}}\ (\textit{supply}) = 0.5\ (49{,}673) = 24{,}837\ ft^3$$

From Table G.2, the estimated lateral migration at the end of 30 years, based on the average annual transport is 38.9 ft. An additional 11.4 ft of migration is estimated if the 100-year flood occurred at the end of this period. The estimated total migration for the 30-year period plus the 10-year shown is thus 50.3 ft. (Note that the approximate maximum erosion distance based on optimal bend shape is 98.4 ft.)

## Table G.1. CURVCALC Input File for Lateral Erosion Example Problem

```
Test data set for CURVCALC  (Input Data File: EXPROB.IN)
197     197     39      10.1    3  9.2    0.04    1       -1      3
1.53E-06        5.8    -0.7   0.4  0.3
4385. 8770.
4385. 8770.
4385. 8770.
4385. 8770.
4385. 8770.
4385. 8770
4385. 8770.
4385. 8770.
4385. 8770.
4385. 8770.
4385. 8770.
4385. 8770.
4385. 8770.
4385. 8770.
4385. 8770.
4385. 8770.
4385. 8770.
4385. 8770.
4385. 8770.
4385. 8770.
4385. 8770.
4385. 8770.
4385. 8770.
4385. 8770.
4385. 8770.
4385. 8770.
4385. 8770.
4385. 8770.
4385. 8770.
4385. 8770.
24837. 49673.
```

## Table G.2. CURVCALC Output File for Lateral Erosion Example Problem (Page 1 of 3)

```
Test data set for CURVCALC  (Input Data File: EXPROB.IN)

  11-17-1994  23:14

Input File:  EXPROB.IN


 ** THIS IS A TEST VERSION OF CURVCALC (10/7/94).
    IT MAY STILL CONTAIN BUGS AND/OR ERRORS IN LOGIC.
    If you encounter such problems in using the program,
    please contact Bob Mussetter at (303)224-4612 or
                  RCE at (303)223-5556.


 CURVCALC (Version 1.2) - Copyright, 1994
 Resource Consultants & Engineers, Inc. (RCE)

 The computational procedure used in this program was
 developed by Bob Mussetter at RCE using concepts presented
 in the Erosion and Sediment Design Guide prepared for AMAFCA.
 RCE accepts no liability or responsibility for the
 consequences of any actions resulting from the use of this
 program.
 Use of results obtained from this program and determination of
 their applicability to a specific problem is entirely the
 responsibility of the user.

 Using this software indicates your acceptance of
 these terms and conditions.


 Initial Sinousity =                          1.001
 Initial Slope =                               .04000
 Equilibrium Slope =                           .02803
 Initial Bank Height (ft) =                   3.00
 Channel Width (ft) =                        39.00
 Bank Erosion Calibration Factor =            1.00
 Average Overbank Slope (Horiz./Vert.)=       3.00
 Uncontrolled Bend Length (ft) =            197.1
 Bed Porosity =                                .40
 Overbank Porosity=                            .30
 Initial offset from downvalley direction =   4.03
 Maximum additional erosion distance =       94.44
```

Table G.2. CURVCALC Output File for Lateral Erosion Example Problem (Page 2 of 3)

| step | Vssup | Vscap | Leros | dzmax | Savg | Lbend | R/W | dlatm | Tlatm | Ymax | Tlatw | Hbavg |
|---|---|---|---|---|---|---|---|---|---|---|---|---|
| 1 | 4385. | 5849. | 127.8 | 1.5 | .03225 | 197.2 | 21.2 | .7 | .7 | .1 | .0 | 3.6 |
| 2 | 4385. | 5269. | 155.7 | 1.9 | .03055 | 197.3 | 19.8 | .3 | 1.0 | .1 | .0 | 3.9 |
| 3 | 4385. | 4951. | 170.6 | 2.0 | .02965 | 197.3 | 18.9 | .2 | 1.3 | .1 | .0 | 4.1 |
| 4 | 4385. | 4767. | 179.6 | 2.1 | .02911 | 197.3 | 18.3 | .2 | 1.5 | .1 | .0 | 4.3 |
| 5 | 4385. | 4656. | 185.5 | 2.2 | .02875 | 197.4 | 17.5 | .3 | 1.8 | .1 | .0 | 4.4 |
| 6 | 4385. | 4606. | 189.7 | 2.3 | .02850 | 197.4 | 17.0 | .4 | 2.2 | .2 | .1 | 4.5 |
| 7 | 4385. | 4528. | 192.4 | 2.3 | .02834 | 197.5 | 16.0 | .3 | 2.5 | .2 | .1 | 4.6 |
| 8 | 4385. | 4479. | 194.2 | 2.3 | .02824 | 197.6 | 15.2 | .4 | 2.9 | .2 | .1 | 4.7 |
| 9 | 4385. | 4448. | 195.3 | 2.3 | .02818 | 197.6 | 14.1 | .5 | 3.4 | .2 | .1 | 4.9 |
| 10 | 4385. | 4428. | 196.1 | 2.3 | .02813 | 197.7 | 13.2 | .5 | 3.9 | .2 | .1 | 5.0 |
| 11 | 4385. | 4415. | 196.6 | 2.4 | .02811 | 197.9 | 12.3 | .6 | 4.5 | .2 | .1 | 5.1 |
| 12 | 4385. | 4407. | 197.1 | 2.4 | .02809 | 198.0 | 11.5 | .7 | 5.2 | .2 | .1 | 5.3 |
| 13 | 4385. | 4403. | 197.4 | 2.4 | .02808 | 198.2 | 10.7 | .8 | 6.0 | .3 | .2 | 5.5 |
| 14 | 4385. | 4400. | 197.6 | 2.4 | .02808 | 198.4 | 9.9 | .9 | 6.9 | .3 | .2 | 5.7 |
| 15 | 4385. | 4399. | 197.9 | 2.4 | .02808 | 198.7 | 9.1 | 1.0 | 7.9 | .3 | .2 | 5.9 |
| 16 | 4385. | 4400. | 198.2 | 2.4 | .02809 | 199.1 | 8.3 | 1.2 | 9.1 | .3 | .2 | 6.2 |
| 17 | 4385. | 4402. | 198.5 | 2.4 | .02810 | 199.5 | 7.6 | 1.3 | 10.4 | .4 | .3 | 6.5 |
| 18 | 4385. | 4404. | 198.8 | 2.4 | .02811 | 200.1 | 6.9 | 1.5 | 11.9 | .4 | .3 | 6.9 |
| 19 | 4385. | 4408. | 199.2 | 2.4 | .02813 | 200.8 | 6.3 | 1.7 | 13.6 | .5 | .3 | 7.3 |
| 20 | 4385. | 4413. | 199.7 | 2.4 | .02815 | 201.6 | 5.7 | 1.8 | 15.4 | .5 | .4 | 7.8 |
| 21 | 4385. | 4419. | 200.4 | 2.4 | .02817 | 202.7 | 5.2 | 2.0 | 17.4 | .6 | .4 | 8.3 |
| 22 | 4385. | 4427. | 201.1 | 2.4 | .02820 | 203.9 | 4.8 | 2.2 | 19.6 | .6 | .5 | 8.8 |
| 23 | 4385. | 4435. | 202.0 | 2.4 | .02822 | 205.2 | 4.4 | 2.3 | 21.9 | .7 | .6 | 9.4 |
| 24 | 4385. | 4443. | 203.0 | 2.4 | .02825 | 206.8 | 4.0 | 2.4 | 24.3 | .7 | .6 | 10.1 |
| 25 | 4385. | 4452. | 203.0 | 2.4 | .02835 | 208.5 | 3.7 | 2.4 | 26.7 | .8 | .7 | 10.7 |
| 26 | 4385. | 4482. | 203.0 | 2.4 | .02846 | 210.4 | 3.5 | 2.5 | 29.2 | .9 | .7 | 11.4 |
| 27 | 4385. | 4514. | 203.0 | 2.4 | .02857 | 212.5 | 3.3 | 2.5 | 31.6 | .9 | .8 | 12.1 |
| 28 | 4385. | 4549. | 203.0 | 2.4 | .02868 | 214.6 | 3.1 | 2.5 | 34.1 | 1.0 | .9 | 12.8 |
| 29 | 4385. | 4584. | 203.0 | 2.4 | .02880 | 216.8 | 3.0 | 2.4 | 36.5 | 1.0 | .9 | 13.4 |
| 30 | 4385. | 4640. | 203.0 | 2.4 | .02892 | 219.2 | 2.8 | 2.4 | 38.9 | 1.1 | 1.0 | 14.5 |
| 31 | 24837. | 26939. | 203.0 | 2.4 | .02952 | 231.7 | 2.5 | 11.3 | 50.3 | 1.4 | 1.3 | 16.7 |

## Table G.2. CURVCALC Output File for Lateral Erosion Example Problem (Page 3 of 3)

```
Definition of variables in output table.
   step = time step
   Vssup = sediment supply to the bend (ft^3)
   Vscap = transport capacity of channel through bend (ft^3)
   Leros = length of degradational wedge (feet)
   dzmax = maximum degradation depth (feet)
   Savg = average slope through bend
   Lbend = length of bend (feet)
   R/W = Ratio of radius of curvature to width
   dlatm = incremental lateral migration distance at apex of
           bend for this time step (feet)
   Tlatm = cumulative lateral migration distance (feet)
   Ymax = ratio of cumulative lateral migration offset from
          downvalley direction to channel width
   Tlatw = ratio of cumulative lateral migration distance from
           initial condition to width
   Hbavg = average bank height through the bend

   ****** NOTE:  Maximum degradation depth is limited to the
                 critical bank height less the initial
                 bank height. **************
```

# X. CHECK DAMS (DROPS)

A. Check dams are used to mitigate vertical instability problems.

- Used to maintain a stable bed elevation.
- Arrest head cuts.

B. Design considerations.

- Scour depth downstream of drop;
- Number of drop structures;
- Bank erosion.

C. Design problem.

Given:

| | | |
|---|---|---|
| Design Discharge | Q | = 1000 $ft^3/s$ |
| Channel Width | B | = 40 ft |
| Mean Water Depth* | $d_m$ | = 2.7 ft |
| Unit Discharge | q | = 25 $ft^3/s/ft$ |
| Mean Velocity* | V | = 9.26 ft/s |
| Total Drop Height | h | = 5 ft |
| Maximum Allowable Scour Depth | $d_s$ | = 7 ft |

*For this example, the depth and velocity is the same upstream and downstream.

From Energy Equation: $Z_u - Z_d = H_T$ = drop height

See Figure 3.29 for definition of variables.

1. Determine the maximum scour depth (single check dam).

Use Equation 3.86

$$d_s = 1.32\ H_t^{0.225}\ q^{0.54} - d_m$$

$$= 1.32\ (5.0)^{0.225}\ (25)^{0.54} - 2.7$$

$$= 8.08\ ft$$

2. Use multiple drops if scour is too deep.

   Decrease drop height and use more drops.

   Estimate drop for scour depth of 7 feet:

$$7 = 1.32\ H_{max}^{0.225}\ (25)^{0.54} - 2.7$$

$$H_{max} = 3.12\ ft$$

   Re-compute scour depth.

   Number of equally spaced drops required = 2

   Drop height per drop = 2.50 ft

$$d_s = (1.32)\ (2.5)^{0.225}\ (25)^{0.54} - 2.7 = 6.5\ ft < 7'$$

   Scour depth per drop, $d_s$ = 6.5 ft < 7' (given)

3. Adequately protect banks downstream of check dam.

   a. Briefly discuss extent of riprap protection.

      5 to 10 times $d_s$ in downstream direction

   b. Briefly discuss any other considerations which must be specified in the design.

      Use equilibrium slope to determine spacing of drops and the total drop height (see previous example).

# XI. CONTRACTION SCOUR EXAMPLE

Given:

- $Q_{100}$ = 500 cfs
- Channel is a sand bed arroyo, relatively flat bottom, vertical banks ~2' high, sparce vegetation within the active channel.
- Bed Slope ($S_0$) = 2.2 percent
- Channel width = 29 feet
- Normal Depth = 1.6'
- Velocity = 10.8
- $D_{50}$ = 1.9 mm
- Temp = 60°F
- Lateral encroachment for floodwall = 12'

Estimate Contraction Scour

Use Laursen (1960) live-bed equation (Equation 3.62)

$$\frac{y_2}{y_1} = \left(\frac{Q_2}{Q_1}\right)^{6/7} \left(\frac{W_1}{W_2}\right)^{k_1} \qquad (3.62)$$

$V_{*c} = (g_1\ y_1\ S_1)^{0.5} = [(32.2)\ (1.6)\ (.022)]^{0.5} = 1.06\ fps$

From Figure 3.13, with $D_{50}$ = 1.9 mm and Temp = 60°F

$\omega = 0.9\ fps$ (Figure 3.13)

From Table 3.8

$$\frac{V_{*c}}{\omega} = \left(\frac{1.06}{.9}\right) = 1.18$$

$$K_1 = .69$$

$$Y_2 = (1.6)\left(\frac{29}{29-12}\right)^{0.69} ft = 2.3\ ft$$

$$Y_s = Y_2 - Y_1 = (2.3) - (1.6) = 0.7\ ft$$

## XII. LOCAL SCOUR AT FLOOD WALL

A flood wall will be constructed along one side of the given arroyo to limit the lateral erosion potential. The unconstrained valley width after construction of the wall will be 82 feet. Estimate the scour depth along the wall at the peak of the 100-year flood.

Estimate the dominant arroyo width ($W_D$):

$$Q_D = 0.2 * Q_{100} = (0.2)\ (500) = 100\ cfs$$

Check critical slope ($S_c$):

$$S_c = 0.037 * Q_D^{-0.133}$$

$$S_c = 0.037(100)^{-0.133} = 0.02 < S_0 = 0.022$$

Since $S_0 > S_c$,

$$W_D = 4.6\ Q^{0.4}$$

$$W_D = (4.6)\ (100)^{0.4} = 29.0\ feet$$

Estimate the ratio of unconstrained valley width to channel width:

$$W_v / W_D = 82/29 = 2.83$$

Determine the Froude number for the 100-year flood peak:

Find the normal depth from Manning's equation:

$$y = \left[ \frac{(\frac{Q}{W})n}{1.486\sqrt{S_0}} \right]^{3/5}$$

$y = [(500/29)*0.035/1.486/\sqrt{0.022}]^{3/5} = 1.83$ *feet*

$V = Q/W/y$

$V = 500/29/1.83 = 9.42$ *fps*

$F_r = V/\sqrt{gy}$

$F_r = (9.42)/\sqrt{(g)(1.83)} = 1.23$

From Figure 3.31:

$D_{sc}/y = 4.4$

$D_{sc} = (4.4)(1.83) = 8.0$ *feet*

# SUPPLEMENT

## Additional information from AMAFCA

# SUPPLEMENT TO

# SEDIMENT AND EROSION DESIGN GUIDE

prepared by
Clifford E. Anderson
for
AMAFCA
November 15, 1994

The following information is intended to supplement the recommendations of AMAFCA's *Sediment and Erosion Design Guide* by Resource Consultants and Engineers, Inc. (November, 1994), and to provide additional guidance to users of the guide. It is anticipated that this supplement will be revised periodically to address engineering issues and clarify information in response to questions from Design Guide users.

## 1. Manning's Roughness for Concrete Lined Channels

Figure 3.4 of the Design Guide shows a schematic of sediment conveyed in a concrete channel. Section 3.2.3 of the Design Guide states "When the channel carries a significant sediment load, the bed roughness may increase to values consistent with an alluvial channel... As the sediment approaches the transport capacity, a layer of sediment will deposit and move along the bed which will impact channel roughness similar to an alluvial channel."

The Design Guide does not define a level at which the sediment load is "significant", and does not provide a specific recommendation on the adjustment of Manning's n value when sediment load is somewhat less than the sediment transport capacity. The following table contains guidance on recommended adjustments to the roughness coefficient:

| Ratio (Sediment Load/Transport Capacity) | Manning's n value |
|---|---|
| 0 to 0.3 | Use value for concrete channel (generally 0.013) |
| 0.3 to 1.0 | Uniform transition from value for concrete to value for bed material |
| $\geq$ 1.0 | Use bed material roughness |

For concrete trapezoidal channels, the bed material will only impact the bottom of the concrete section. Use Equation 3.20 or 3.20a to compute the composite n-value. It is anticipated that the above table will be revised when additional research becomes available.

2. Arroyo Avulsions

Section 4.3.4 of the Design Guide (1 paragraph at page 4-15) contains information on potential channel avulsion, and outlines general procedures for further consideration of these features. Richard J. Heggen has recently prepared for AMAFCA a "Draft Interim Procedure, Determination and Use of Avulsion Probabilities on Alluvial Fans" that provides further guidance on determination of flow rates at avulsions. This procedure uses risk assessment and return period probabilities in a manor similar to the FEMA alluvial fan procedures, but the avulsion procedure described has not yet been endorsed by FEMA. This avulsion procedure provides a method to quantify specific flow rates at arroyos downstream of avulsion areas. It is anticipated that this procedure will be further refined and clarified through further application and technical review. A copy of the procedure developed by Dr. Heggen is enclosed with this supplement.

# Draft Interim Procedure

# Determination and Use of Avulsion Probabilities on Alluvial Fans

Richard J. Heggen
Department of Civil Engineering
University of New Mexico

April 6, 1994

This report summarizes three issues associated with risk assessment in alluvial fan flood plain mapping:

1) Risk vs. return period. Why 100-year channel design may use other than 100-year rainfall.

2) Avulsion probabilities. How avulsion direction may be quantified.

3) Active Channel Correction. Why risk should be assumed for discharge that might avulse from an historic path and flow toward a site. Why risk should not be decreased for a site along a historic path when an upstream avulsion might send the discharge elsewhere.

Each issue has a subjective aspect. The methods discussed are conservative approaches appropriate to the Albuquerque region.

## 1) Risk vs. Return Period

### Terms

Development at site along a channel is to be protected from a specified annual risk. Care must be taken to distinguish between,

$T_i$, the return period of rainfall at watershed i,

$R_j$, the level of risk for site j,0.01 being a common standard,

$p(Q_{ij})$, the probability of flow from watershed i to site j,

$p(Q_f/Q)$, the conditional probability of flow in avulsion path f, given flow to avulsion,

$p(Q_k/Q)$, the conditional probability of flow in reach k, given flow to top of reach)

$p(Q_{ij}/W_i)$, the conditional $p(Q_{ij})$, given rainfall at i,

$p(Q_{gij}/Q_{ij})$, the conditional $p(Q_{ij})$, given flow from i to j, and

$p(W_i)$, the probability of rainfall at watershed i.

In All Cases

As all runoff must flow out of the basin, for a control area with I watersheds and m sites of exiting flow,

$$\sum_{j=1}^{m} p(Q_{ij}/W_i) = 1.00, i = 1, \ldots I \quad (1)$$

Return period is,

$$T_i = \frac{1}{p(W_i)} \quad (2)$$

From conditional probability,

$$p(Q_{ij}) = p(Q_{ij}/W_i)\, p(W_i) \quad (3)$$

Substituting (2) into (3),

$$p(Q_{ij}) = p(Q_{ij}/W_i) \frac{1}{T_i} \quad (4)$$

$$T_i = \frac{p(Q_{ij}/W_i)}{p(Q_{ij})} \quad (5)$$

To determine the discharge having $R_j$ at a site, apply the appropriate rainfall at every upstream watershed such that the probability of flow of that rainfall to j is $R_j$.

$$p(Q_{ij}) = R_j, i = 1, \ldots I \quad (6)$$

The Case of No Avulsions

Where channels remain fixed, $p(Q_{ij}/W_i)$ is 1.00. Rainfall return period for watershed i, is,

$$T_i = \frac{1}{R_j} \quad (7)$$

Example 1.

Avulsions do not occur. For runoff to have a 0.01 annual risk, find the upstream design rainfall return period.

$$T = \frac{1.00}{0.01} = 100 \text{ years}$$

The Case of Avulsion, Single Watershed to Single Site

If upstream discharge may avulse to and not flow to site i, $p(Q_{ij}/W_i)$ is less than 1.00.

Example 2.

Upstream flow has a 20 percent chance of diverting out of the channel. For a 0.01 site risk, find the design rainfall return period for the watershed.

$$T = \frac{0.80}{0.01} = 80 \text{ years}$$

Where avulsions may occur in more than one upstream channel reach, the conditional probability of flow from i to j, given rainfall in i, is,

$$p(Q_{ij}/W_i) = \prod_{k=1}^{n} (Q_k/Q) \qquad (8)$$

where $(Q_k/Q)$ is the conditional probability for flow in reach k, given flow to top of k, and n is the number of reaches between i and j.

Example 3.

The flow path from a watershed has two reaches. Flow has a 30 percent conditional probability of diverting from the channel in reach 1 and a 10 percent chance of diverting in reach 2. Determine the appropriate rainfall return period for a 0.01 risk below these potential avulsions.

$(0.70)(0.90) = 0.63$

$$T = \frac{0.63}{0.01} = 63 \text{ years}$$

A channel site may receive runoff from one watershed by more than one path, *i.e.*, a channel may take more than one path to the same destination. If so, the combined $p(Q_{gij}/Qij)$ by all h paths is,

$$\sum_{g=1}^{h} p(Q_{gij}/Q_{ij}) = 1.00 \qquad (9)$$

Example 4.

The flow path from a watershed had a 30 percent conditional probability of diversion from the channel. If diverted, the conditional probability is 40 percent that the lost flow will return to the channel downstream.

Determine the appropriate rainfall return period for a 0.01 risk below this potential confluence.

$0.70 + (0.30)(0.40) = 0.82$

$$T = \frac{0.82}{0.01} = 82 \text{ years}$$

The Case of Avulsion, Multiple Watersheds to Single Site

Example 5.

A site receives flow from two upstream watersheds. The flow path from watershed 1 is fixed. The flow path from watershed 2 has a 40 percent conditional probability of flowing to the site. Determine the appropriate rainfall return periods for a 0.01 risk at the site.

$$T_1 = \frac{1.00}{0.01} = 100 \text{ years}$$

$$T_2 = \frac{0.40}{0.01} = 40 \text{ years}$$

The Case of Avulsion, Multiple Watersheds to Multiple Sites

Combine the above techniques for complex basins where several watersheds may potentially discharge to several sites.

Example 6.

Three sites receive flow from two upstream watersheds as shown in Fig. 1. Conditional $p(Q_f/Q)$'s are indicated at the bifurcations. Determine the appropriate return periods for 0.01 risk at each site.

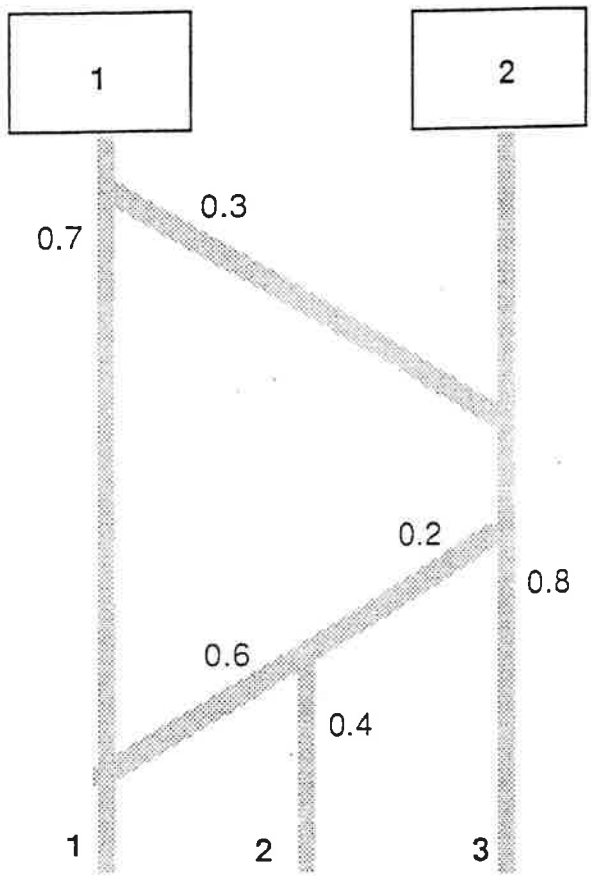


Figure 1. Alluvial Fan Schematic

$$p(Q_{11}/W_1) = p(Q_{111}/W_1) + p(Q_{211}/W_1)$$
$$= p(Q_{111}/W_1) + p(Q_1/Q)\ p(Q_2/Q)\ p(Q_3/Q)$$
$$= 0.7 + (0.3)(0.2)(0.6) = 0.736$$

$$p(Q_{21}/W_2) = p(Q_1/Q)\ p(Q_2/Q$$
$$= (0.2)(0.6) = 0.120$$

$$p(Q_{12}/W_1) = (0.3)(0.2)(0.4) = 0.024$$

$$p(Q_{22}/W_2) = (0.2)(0.4) = 0.080$$

$$p(Q_{13}/W_1) = (0.3)(0.8) = 0.240$$

$$p(Q_{23}/W_2) = 0.8 = 0.800$$

Note that, per Eq. 1,

$$\sum_{i=1}^{3} p(Q_{i1}/W_1) = 0.736 + 0.240 + 0.024 = 1.000$$

and,

$$\sum_{i=1}^{3} p(Q_{i2}/W_2) = 0.120 + 0.080 + 0.800 = 1.000$$

Table 1. Return Periods, Example 6

| Watershed i | Site j | $p(Q_{ij}/Wi)$ | $T_i$ (yr) |
|---|---|---|---|
| 1 | 1 | 0.736 | 73.6 |
| 2 | 1 | 0.120 | 12 |
| 1 | 2 | 0.024 | 2.4 |
| 2 | 2 | 0.080 | 8 |
| 1 | 3 | 0.240 | 24 |
| 2 | 3 | 0.800 | 80 |

Site 1 needs 73.6 and 12-year upstream events. Site 2 needs 2.4 and 8-year events. Site 3 needs 24 and 80-year events.

In a complex alluvial fan with multiple avulsion possibilities, a site near the fan's toe protected at the 0.01 risk level may have to be designed for a simultaneous 100-year storm in one watershed, a 40-year storm in another watershed, a 75-year storm in another watershed, etc.

Such analysis becomes unduly complex with many sites. If appropriate, relate the design runoff for a typical site to the runoff from 100-year rainfall at all watersheds. Apply that ratio to similar sites.

Example 7.

Site 2 receives discharge from upstream avulsions similar to those above site 1, that of Example 5. Determine the appropriate 100-year discharge at site 2.

$Q_1$, the combined discharge from 100-year precipitation in watershed 1 and 40-year rainfall in watershed 2 (Example 5), is 150 cfs. If watersheds 1 and 2 have 100-year precipitation, $Q_1$ is 200 cfs. Rather than adjusting the upstream precipitation to equalize probabilities for site 2 (*i.e.*, another Example 5), assume 100-year rainfall upstream of site 2 and multiply the resultant discharge by 150/200 to account for the similar avulsions.

## 2) Avulsion Probabilities

The $p(Q_k/Q)$ conditional probability term is a key in the determination of $T_i$ and $R_j$. Several options exist for the probability assignment. Three methods are proposed.

Method 1, Radial Distribution

A method suggested by FEMA literature is that of radial dispersion. From an apex, an avulsion has equal probability of flowing in any down-fan direction. If a fan is 100° wide, the conditional probability is 0.01 that flow will flow down any 1° segment. Assign conditional probabilities proportionately to the radial width of avulsion arcs.

Example 8 illustrates the use of this method.

Example 8

Fig. 2 shows discharge down a 120° fan that may avulse to the left or right of a rock outcrop. The arc length to the left to the outcrop is 90°. The arc length to the right is 30°. Flow to the left of the enters the left channel. Flow to the right enters the right channel. Assign avulsion conditional probabilities.

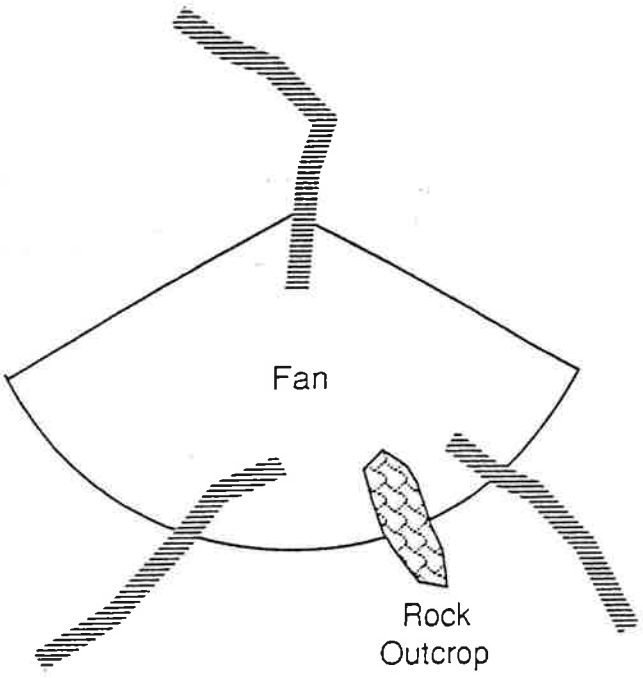


Figure 2. Radial Distribution

$p(Q_{left}/Q) = 90/120 = 0.75$

$p(Q_{right}/Q) = 30/120 = 0.25$

Method 2, Conveyance Capacity

The relative conveyance capacities of the alternative channels may indicate propensity to avulse. Assign conditional probabilities proportionately to the capacities.

Example 9

Discharge may avulse to one of three channels. Channel 1 capacity from the avulsion is 100 cfs. Channel 2 capacity is 200 cfs. Channel 3 capacity is 700 cfs. Assign avulsion conditional probabilities.

$p(Q_1/Q) = 100/1000 = 0.10$

$p(Q_2/Q) = 200/1000 = 0.20$

$p(Q_3/Q) = 700/1000 = 0.70$

Method 3, Scour and Deposition Expectation

Avulsions occur under conditions of channel scour or deposition. Assign conditional probabilities by weighting the conditional probabilities of flow in alternative channels with the respective probabilities of scour and deposition.

Example 10

Discharge may avulse to one of two channels. Channel 1 has a 10 percent conditional probability of capturing the flow if deposition occurs and a 70 percent chance if scour occurs. Channel 2 has a 90 percent conditional probability of capturing the flow if deposition occurs and a 30 percent chance if scour occurs. Given that change occurs, the conditional probability of deposition is 0.40 and of scour is 0.60. Assign avulsion conditional probabilities.

$p(Q_1/Q) = (0.1)(0.4) + (0.7)(0.6) = 0.46$

$p(Q_2/Q) = (0.9)(0.4) + (0.3)(0.6) = 0.54$

Of the three methods, use the one that best matches understanding of the physical process. In the same basin, different methods might be appropriate for different avulsions.

## 3) Active Channel Correction

In a random system, an avulsion has a 100 percent conditional probability of following one of its directions (Examples 7, 8 and 9).

$$\sum_{f=1}^{0} p(Q_f/Q) = 1.00 \qquad (10)$$

Unfortunately, the summation to 1.00 may lead to underdesign for some downstream sites. Example 11 demonstrates the problem.

Example 11

Fig. 3 shows a multiple site basin. All the flow emanates from watershed 1 at the apex. Sites are indicated by number. The active channel (the one currently conveying runoff) is the dark line. Three potential avulsions have $p(Q_i/Q)$ as shown. All sites are to be protected at the 0.01 level.

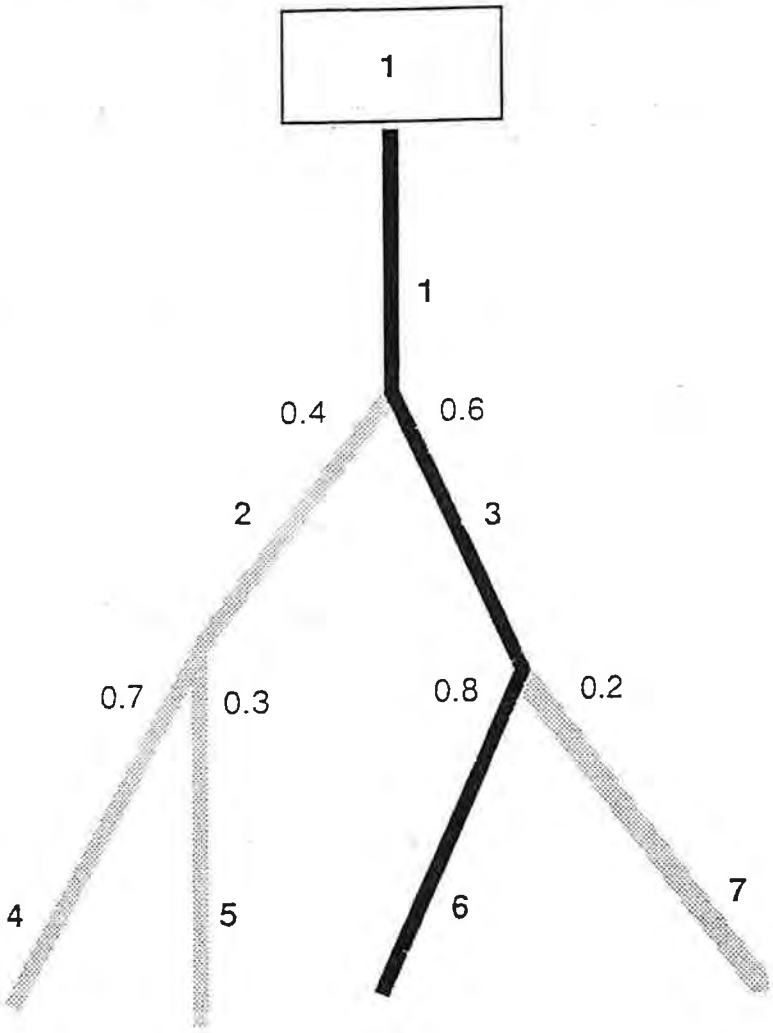


Figure 3. Alluvial Fan Schematic

Table 2. Return Periods, Example 11, Eq. 10

| Site j | $p(Q_{1j}/W_1)$ | | $T_1$ (yr) |
|---|---|---|---|
| 1 | 1.0 | = 1.00 | 100 |
| 2 | (1.0)(0.4) | = 0.40 | 40 |
| 3 | (1.0)(0.6) | = 0.60 | 60 |
| 4 | (0.4)(0.7) | = 0.28 | 28 |
| 5 | (0.4)(0.3) | = 0.12 | 12 |
| 6 | (0.6)(0.8) | = 0.48 | 48 |
| 7 | (0.6)(0.2) | = 0.12 | 12 |

Because flow might leave the active channel and go elsewhere, site 3 need only be protected from a 60-year storm. Further down the active channel, site 6 needs protection from the 48-year storm.

Sites 3 and 6 should not be protected from runoff less than that required for site 1, in essence crediting sites 3 and 6 with an avulsion benefit. If the active channel is well maintained, as it should be, the most likely route for flow is from site 1 to 3 to 6. An avulsion site might be a road crossing where a plugged culvert could send flow to an adjacent basin. Were downstream sites along the active channel built for only the reduced conditional probability and the crossing then upgraded, those sites would be then underprotected. Sites 1, 3 and 6 merit equal protection.

The active channel correction is as follows:

| For active channels, $p(Q_f/Q)$ is 1.00, regardless of avulsion possibility. |
|---|

For an avulsion location on an active channel, Eq. 10 is not valid, as the sum exceeds 1.00. Table 3 illustrates the result of the active channel correction for Example 11.

Table 3. Return Periods, Example 11, Active Channel Correction

| Site j | $p(Q_{1j}/W_1)$ | | $T_1$ (yr) |
|---|---|---|---|
| 1 | 1.0 | = 1.00 | 100 |
| 2 | (1.0)(0.4) | = 0.40 | 40 |
| 3 | 1.0 | = 1.00 | 100 |
| 4 | (0.4)(0.7) | = 0.28 | 28 |
| 5 | (0.4)(0.3) | = 0.12 | 12 |
| 6 | 1.0 | = 1.00 | 100 |
| 7 | (0.6)(0.2) | = 0.12 | 12 |

Site 1 faces full conditional probability and needs protection from the 100-year storm. Sites 3, 4, 5 and 7, not on the active channel, have less than full

conditional probability and should have some protection, but less than 100-year. To this point, Eq. 10 and the active channel correction agree. By the active channel correction, however, sites 3 and 6 merit protection from the 100-year storm, not the 60 and 48-year storms, because on the active channel they have full conditional probability.

Example 12

Fig. 4 illustrates a modification of Example 11 where channels rejoin.

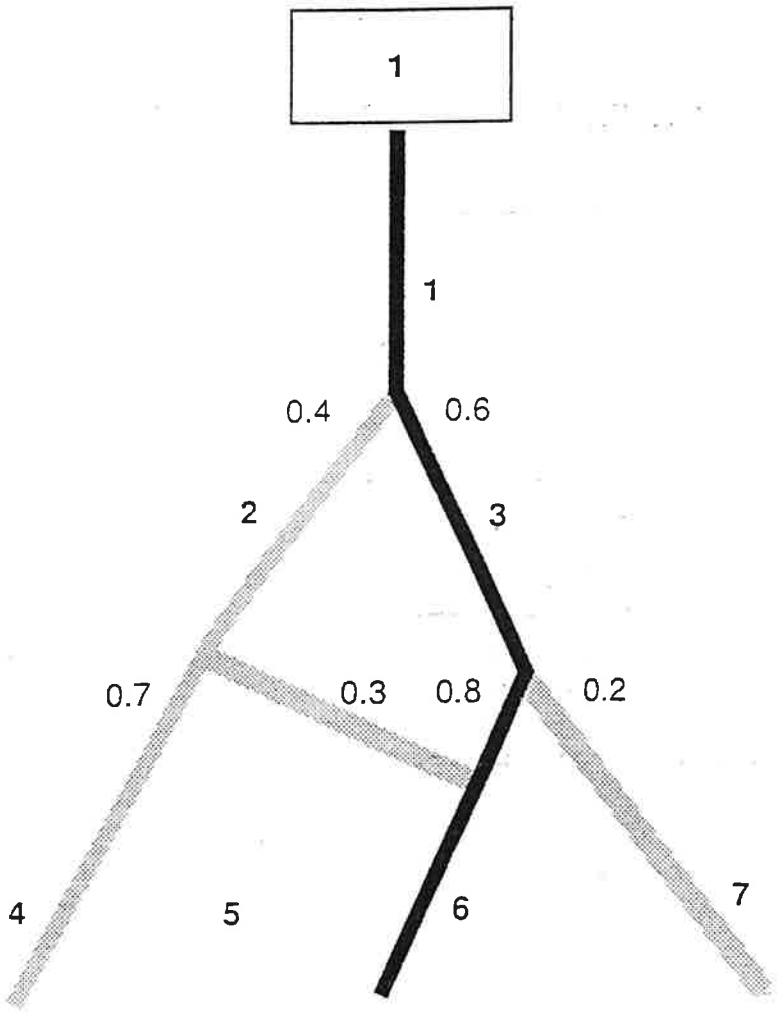


Figure 4. Alluvial fan schematic, channel confluence

Table 4. Return Periods, Example 12, Eq. 10

| Site j | $p(Q_{1j}/W_1)$ | | $T_1$ (yr) |
|---|---|---|---|
| 1 | 1.0 | = 1.00 | 100 |
| 2 | (1.0)(0.4) | = 0.40 | 40 |
| 3 | 0.6 | = 0.60 | 60 |
| 4 | (0.4)(0.7) | = 0.28 | 28 |
| 5 | 0 | = 0 | 0 |
| 6 | (0.4)(0.3) | =0.12 | |
| | (0.6)(0.8) | = 0.48 | |
| | | 0.60 | 60 |
| 7 | (0.6)(0.2 | = 0.12 | 12 |

Table 5. Return Periods, Example 12, Active Channel Correction

| Site j | $p(Q_{1j}/W_1)$ | | $T_1$ (yr) |
|---|---|---|---|
| 1 | 1.0 | = 1.00 | 100 |
| 2 | (1.0)(0.4) | = 0.40 | 40 |
| 3 | 1.0 | = 1.00 | 100 |
| 4 | (0.4)(0.7) | = 0.28 | 28 |
| 5 | 0 | = 0 | 0 |
| 6 | 1.0 | = 1.00 | 100 |
| 7 | (0.6)(0.2) | = 0.12 | 12 |

Site 5 is risk free by either method. With Eq. 10, the channel confluence exposes site 6 to more conditional probability than in Example 11, 0.60 vs. 0.48 (Table 2 vs. Table 4), but still not 1.00. With the active channel correction, site 6 conditional probability becomes 1.00 (Table 5).

The examples can be extended. Let the Example 12 active channel be the far right branch, passing through site 7. Conditional probabilities at 6 and 7, Eq. 10, would be 0.60 and 0.12, unchanged from Table 4. Conditional probabilities at 6 and 7, active channel correction, would be 0.60 and 1.00, shifting full conditional probability from site 6 to site 7.

## Notation

| | |
|---|---|
| f | Avulsion direction |
| g | Channel path between i and j |
| h | Number of channel paths from i to j, g = 1, ... h |
| i | Watershed |
| j | Channel site |
| k | Channel reach |
| l | Number of watersheds, i = 1, ... l |
| m | Number of channel sites, j = 1, ... m |
| n | Number of channel reaches in path g, k = 1, ... n |
| o | Number of avulsion directions from a given channel point, f = 1, ... o |
| $p(Q_{ij})$ | Probability (flow from watershed i to site j) |
| $p(Q_f/Q)$ | Conditional probability (flow in avulsion direction f, given flow to avulsion) |
| $p(Q_k/Q)$ | Conditional probability (flow in reach k, given flow to top of k) |
| $p(Q_{gij}/Q_{ij})$ | Conditional probability (flow from i to j taking path g, given flow from i to j) |
| $p(Q_{ij}/Wi)$ | Conditional probability (flow from i to j, given precipitation at i) |
| $p(W_i)$ | Probability (precipitation at i) |
| $R_j$ | Level of risk for j |
| $T_i$ | Return period of rainfall at i |

# INDEX

# INDEX